DISSERTATION

THE SUSTAINABILITY OF ATOLL ISLANDS FRESHWATER LENSES UNDER NON-STATIONARY CLIMATIC AND ANTHROPOGENIC STRESSES

Submitted by

Abdullah Ahmad Alsumaiei

Department of Civil and Environmental Engineering

In partial fulfillment of the requirements

For the Degree of Doctor of Philosophy

Colorado State University

Fort Collins, Colorado

Spring 2017

Doctoral Committee:

Advisor: Ryan Bailey

Neil Grigg
Thomas Sale
Michael Ronayne

ABSTRACT

THE SUSTAINABILITY OF ATOLL ISLANDS FRESHWATER LENSES UNDER NON-STATIONARY CLIMATIC AND ANTHROPOGENIC STRESSES

Atolls consist of small low carbonate islands and fringing reefs that enclose a shallow seawater central lagoon. A lens of fresh groundwater forms at shallow depths within the subsurface of atoll islands, with thickness and volume of the lens dependent on island size, aquifer hydraulic conductivity, depth and frequency of recharge events, and the depth to the solution conformity that separates the upper sand aquifer from an underlying limestone aquifer. The freshwater supply on atoll islands is very fragile and is under continual threat due to the general small geographic size of the islands and from climatic and anthropogenic stresses such as changing rainfall patterns, sea-level rise, wave over-wash events, and population growth.

In the Republic of Maldives, groundwater resources are a vulnerable freshwater natural resource, and an accurate estimate of current and future quantity of available freshwater is necessary for efficient water management. Of major concern is the quantity of water to be available in the coming decades under the influence of variable rainfall patterns, rising sea level, environmental conditions, and expected population growth that depends on groundwater resource.

The objective of this dissertation is to evaluate the reliability of the freshwater supplies on the Maldivian atolls. A numerical modeling approach is used to estimate the flow dynamics of the freshwater lens and to determine the fluctuation of lens thickness and volume of islands of the Maldives in response to long-term changes in rainfall, sea level rise, and anthropogenic stresses such as groundwater pumping, and short-term impacts from tsunami-induced marine

over-wash events. Specifically, this study estimates the quantity of fresh groundwater for selected islands of the Maldives under current and future climate and population stresses. System stresses (rainfall, sea level rise, pumping, and over-wash) are analyzed separately and in combination to quantify their respective influence on groundwater availability. As such, the vulnerability of each island's groundwater resources to these stresses is quantified.

Future rainfall through 2050 is extracted from general circulation models contributing to the CMIP5 framework, with the effects of sea level rise, wave over-wash events, and the influence of a growing population (i.e. groundwater pumping) assessed within this future context. Four islands have been selected for groundwater analysis that span the geographic and climatic regions of the Maldives: N. Holhudhoo and N. Velidhoo in the Northern, climatic region of the Republic of Maldives, and GDh. Thinadhoo and L. Gan in the wetter Southern climatic region. Three dimensional numerical simulations were conducted using the USGS modeling code SEAWAT to analyze the flow and salt transport dynamics of the aquifer system. Model results are tested against groundwater status data from these four islands, as well as previous numerical modeling efforts dedicated to the climate and geology of the Maldives.

The major goal of this study is to provide an overall analysis for the fresh groundwater resources of selected atoll islands in the Republic of Maldives, and to provide water resource managers with valuable data for consideration in water security measures to appraise alternatives for water sector reform and help them to establish appropriate water management plans. As the geologic structure of atoll island aquifers generally is similar across geographic regions, the methods used in this dissertation can be applied to other atoll nations throughout the Pacific and Indian Oceans.

Results indicate that groundwater, in terms of freshwater lens volume, can contribute to water resources planning for the Maldives in the coming decades, although groundwater for small islands is more vulnerable to climatic and environmental stresses. Freshwater lenses in small atoll islands (area < 0.6 km^2) are shown to have a strong variability trends in the upcoming decades with expected reduction in lens volume sea level rise between 11-36%. On the other hand, freshwater lenses in larger atoll islands (area > 1.0 km^2) are shown to have less variability to changing patterns with expected reduction in lens volume due to sea level rise between 8-27%. Results can provide water resource managers with valuable findings for consideration in water security measures. It is shown that there is a linear relation between average lens volumes predicted by different RCP models and island area. Moreover, Results for post-overwash lens recovery showed instant damage of freshwater lens in all islands. Freshwater reserves depleted to critical levels in small islands especially in severe overwash events simulations as seawater inundated as high as one third of islands land area. Larger islands showed relatively slower recovery patterns, where percentages for the recovered freshwater lenses after two years following the storms were lower than percentages in smaller islands (up to 30%). Mitigated emission climate change models showed that freshwater lenses may recover quicker in both climatic regions studied, while other RCPs scenarios did not show any variability in freshwater lens recovery in comparison to historical averages. The effect of pumping caused a lag in freshwater lens recovery (between 5-15%) especially in smaller islands under severe overwash events scenarios. Overall, salinization is more widespread on small islands (< 1 km^2), but recovery is more rapid than for large islands. Between 50% and 90% of lens recovery occurs after two years for small islands (< 1 km^2), whereas only 35% and 55% for large islands. Imposing pumping rates required to sustain the local population lengthened the recovery time

between 5% and 15%, with higher percentage for the smaller islands. Also, it is concluded from 3D simulations for the freshwater lens recovery that there is relation between the pre overwash lens volume and the percentage at which the lens is recovered after 2 years (using historical recharge rates for recovery) is inversely proportional on a semi-logarithmic scale. The results of this research can be used to estimate the sustainability of the freshwater lens in other atoll islands aquifers as atoll islands aquifers share the same hydrogeological settings.

ACKNOWLEDGEMENTS

First and Foremost I am thankful to ALLAH for providing me with health, patience, and strength to complete my graduate studies in the United States. Secondly, I would like to thank my Mother, Salwa Nasser Alazemi. Without her, I would not be in this position. Whenever I was down, you were able to bring me strong again. My wife Sarah Alrashdan, my PhD journey was not possible to complete without your love, endless support, patience, faith and encouragement. I am also grateful to my advisor, Dr. Ryan T. Bailey. I am glad that I had such a great opportunity to work with such an outstanding advisor, and mentor. His directions, and continuous help were always available. My doctoral committee members: Prof. Neil Grigg, Dr. Thomas Sale, and Dr. Michel Ronayne, thank you for accepting to serve in my doctoral committee. Also, I would say thank you to all of my friends in Fort Collins. I would like to thank my country for trusting me and giving me the opportunity to complete my graduate studies. Without the financial support from Kuwait University, the completion of the PhD degree was not possible.

DEDICATION

To

My parents Salwa, and Ahmad

My wife Sarah

My Sons Saud, and Ahmad

TABLE OF CONTENTS

LIST OF TABLES

LIST OF FIGURES

CHAPTER 1. INTRODUCTION

In this chapter, the main research goals of the dissertation are presented. An overview of the study area and a brief description of the modeling tool using to accomplish the research objectives also are presented.

1.1 Research Scope and Problem Statement

Groundwater is an important water resource for communities residing on small coral islands, particularly during times of drought. However, this resource is under continual threat of depletion or contamination due to intense El Niño-induced droughts, over-extraction, surface pollution and leaching, marine overwash due to storm-surge or tsunamis, and long-term sea level rise (SLR). Furthermore, communities on small islands are some of the most vulnerable worldwide in terms of freshwater scarcity and depletion of water resources due to small land surface area, low elevations, geographic remoteness, and expected changes in climate, population, and land use (White et al., 2007; White and Falkland, 2010). In particular, atoll islands have consistently been identified as the natural systems most at risk from climate change (Houghton, 1995; Watson et al., 1998; McCarthy, 2001; Barnett and Adger, 2003). Determining the impact of future climate change, such as changing rainfall patterns and long-term sea level rise, on groundwater resources of atoll islands is vital for water resources planning and management and may indicate when these islands no longer are habitable. Parry et al. (2007) predict that several island nations, including Tuvalu and the Republic of Maldives, may require abandonment during the 21st century due to SLR.

Groundwater resources of atoll islands in the coming decades are strongly dependent on rainfall patterns and SLR, as rainfall determines the amount of recharge to the freshwater lens

and island width and surface area control the thickness of the freshwater lens. In climate scenarios provided by the Intergovernmental Panel on Climate Change (IPCC), significant impacts are predicted for small islands in both the Pacific and Indian Oceans (Parry et al., 2007; Nicholls and Cazenave, 2010). Estimates of future rainfall are dependent on geographic region, ranging from -64% to -22% of current averages. A recent water balance study in the Pacific Ocean basin (De Freitas et al.; 2013) considering future rainfall and temperature estimates highlight the sensitivity of island water resources to a changing climate. Rainfall models indicate that the Western Indian Ocean is particularly affected by future climate, with an estimated decrease of up to 30% in groundwater recharge (Doll, 2009). For atolls in the Indian Ocean, data sets of historical temperature and precipitation for five nations in the Western Indian Ocean (Comoros, Madagascar, Maldives, Mauritius, and Seychelles) shows significant variations in trends, including extreme droughts (Ragoonaden et al., 2006).

The effect of SLR on atoll island groundwater resources is expected to be as severe as that of future rainfall (Ketabchi et al., 2014). As sea level rises, and depending on beach slope, which typically ranges from 0.5% to 2% (Tysban et al., 1990), seawater will inundate beachfronts leading to beach shoreline recession, also termed “land-surface inundation” (LSI) in island studies (Mahmoodzadeh et al., 2014; Morgan and Werner, 2014), which can be significant even for a small rise of sea level. Shoreline recession can be significant even for a small rise in sea level. For example, a 1 m rise in sea level will result in 80% loss of surface area of Majuro Atoll, the capital island of the Marshall Islands in the western Pacific, due to the extreme low topography (2-3 m) of the islands (Burns, 2000).

In particular, small islands are under serious threat due to a naturally thin lens (Falkland, 1991; Bricker and Hughes, 2007). Furthermore, the study performed by Storlazzi et al. (2015)

shows that the effect on low islands can be even more significant due to the interaction between higher-energy waves and SLR, leading to more inundation than expected. Recent studies predict that sea level will rise between 0.5 m and 1 m by the year 2100 (Raper and Braithwaite, 2006; Rahmstorf, 2007; Parry et al., 2007; Pfeffer et al., 2008; Dickinson, 2009), and studies considered by the IPCC (Church et al., 2013) estimate a rise of approximately 0.4 m to 0.7 m by the year 2100. Combined with El Niño-induced severe droughts that can cause rapid depletion of fresh groundwater for atolls (Peterson, 1990; White et al., 2007; White and Falkland, 2010). The impact of SLR and the thinning of the lens poses serious threats to the inhabitability of atoll islands in the coming decades and centuries. Moreover, due to the small surface area, and relatively flat beach slope, with maximum election of few meters above mean sea level (Wheatcraft and Buddemeier, 1981), islands might be inundated by seawater either partially or completely due to overwash events can occur. Seawater flooding coastal area will percolate through the high-hydraulic conductivity soil profile causing salinization to the shallow groundwater. After overwash events, freshwater recharge will recover the damaged freshwater lens and rebuild the freshwater lens again. Depending on overwash events intensity, rainfall patterns, and other geologic characteristics, the time required for the freshwater lens to restore its pre-overwash status is determined (Chui and Terry, 2012; Bailey and Jenson, 2013).

In the Republic of Maldives, atoll islands aquifers are important sources for securing freshwater supply for domestic and industrial uses. The fresh groundwater occurs in the shape of a water lens floating on the top of seawater in the sub-surface. Several climatic and anthropogenic stresses, such as variable precipitation patterns, sea level rise, rapidly growing urban population for many of the islands, limited rainfall harvesting capacity, and saltwater intrusion contamination, storm surge events (Woodroffe, 2007; Barthibanet et al., 2012), and

intensive pumping rates put the freshwater sources under serious threats. These threats are particularly severe for groundwater resources due to the small island surface area and low elevation of each island (Bailey et al., 2015). In this research, the groundwater resources of atoll islands' aquifers in the Republic of Maldives is addressed to assess the sustainability of the freshwater lens as it is fragile and very dependent on various parameters (including: hydraulic conductivity, recharge rates, and island geometry). An assessment of the sustainability groundwater resources in atoll islands aquifers of the Republic Maldives is urgent to help water managers in atoll islands nations in analyzing future water security measures and to appraise alternatives for water sector reform and help them to establish appropriate water management plans. Methodology presented in this dissertation is applicable to any coral island or group of islands. Results provide not only quantified results of impacts on groundwater, but also important implications for long-term water resources management. Research findings can help atoll island nations in analyzing future water security.

1.2 Research Objectives

The overall objective of this dissertation is to quantify the general hydrologic response of atoll island aquifer systems in the Republic of Maldives to various climatic and anthropogenic stresses. The assessment will be fulfilled by applying the public domain, three-dimensional, variable-density, transient groundwater flow numerical model SEAWAT (Langevin et al., 2007), to selected islands of the Maldives for simulating saltwater intrusion and available fresh groundwater volume. The following tasks will be carried out to accomplish this objective:

1) Apply three dimensional groundwater flow and solute transport models for selected islands in the Republic of Maldives that are capable of simulating the available fresh groundwater volume
2) Calibrate these models to reproduce the actual observed fresh groundwater volumes that have been measured in the field
3) Assess the impact of future climate scenarios (variable rainfall from Global Circulation Models (GCMs), and sea level rise)
4) Assess the impact of anthropogenic stresses (pumping, increase in population) within the context of climate change (rainfall, and sea level rise)
5) Assess the impact of marine overwash events on the freshwater lens (with and without the effect of future climate change)
6) Assess each island ability to meet future freshwater demand under environmental and anthropogenic stresses.

1.3 Research Importance

This research is seeking to contextualize its findings within atoll islands communities to help in managing their available water resources effectively in cases of severe droughts or in case of catastrophic tsunami events. Also, this research seeks to provide baseline for future research in the field of groundwater engineering and water resources planning and management to further understand the sustainability and fresh groundwater lens development in atoll islands aquifers.

1.4 Study Area Overview

1.4.1 Geography, Population, and Land Use

The Republic of Maldives lies southwest of India and Sri Lanka in the Indian Ocean, consisting of about 200 inhabited small coral atoll islands (out of approximately 2000 coral islands) that stretch from Ihavandhippolhu atoll in the North to the Addu atoll in the South. Encompassing a total land area spread over 90,000 km^2, the islands have a total population of approximately 330,000 (Sobir et al., 2014). As a community on tropical islands, the Maldivians are considered among the most threatened nations worldwide in terms of fresh groundwater lens scarcity and reduction in water resources due to small land surface, low elevations, sea level rise, ever-present anthropogenic stresses, and potential climate change (Watson et al., 1997; White and Falkland, 2010). Figure 1A shows the location of the Republic of Maldives in the world, while Figure 1B shows a zoom in map for the atolls and the location of capital, Male.

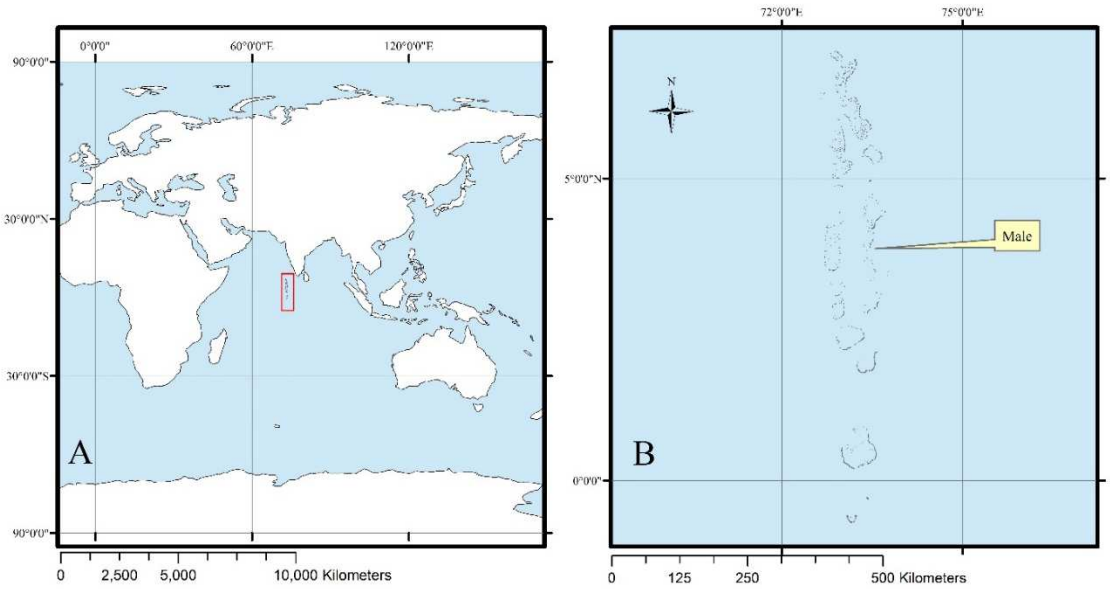

Figure 1: **1A** Location of Republic of Maldives in the world, **1B** a zoom in map for the Maldivian atolls showing the location of the capital city, Male.

According to the State of Environment report published by Maldivian Ministry of Environment and Energy in 2011 (Latheefa et al., 2011), it is estimated that only 300 km^2 out 90,000 km^2 is the total actual land area of the Maldives). Land use categories are: 10% occupied by agricultural cultivated land, 3% by forested land, 3% by pastures, and 84% by miscellaneous infrastructure and native vegetation (Bailey et al., 2014). Geographically, The Republic of Maldives is composed of 26 atolls which vary enormously in size and shape with Huvadhu atoll being the largest atoll and Thoddo atoll being the smallest atoll with land areas of 2800 km^2 and 5.4 km^2 respectively (Latheefa et al., 2011).

1.4.2 Climate

The climate in the Maldives is described as warm and tropical year round, with average annual temperature and average relative humidity of 28.0 C^o and 80% respectively (Bailey et al. 2014). The southern provinces of the Maldives receive higher precipitation with annual average of approximately 2350 mm/yr, while lower precipitation rates in the Northern provinces, with annual average of approximately 1700 mm/yr (Bailey et al., 2014). The precipitation pattern is seasonal with January-April being the dry season while the remaining months typically receive evenly distributed amounts of rainfall (see Figure 2).

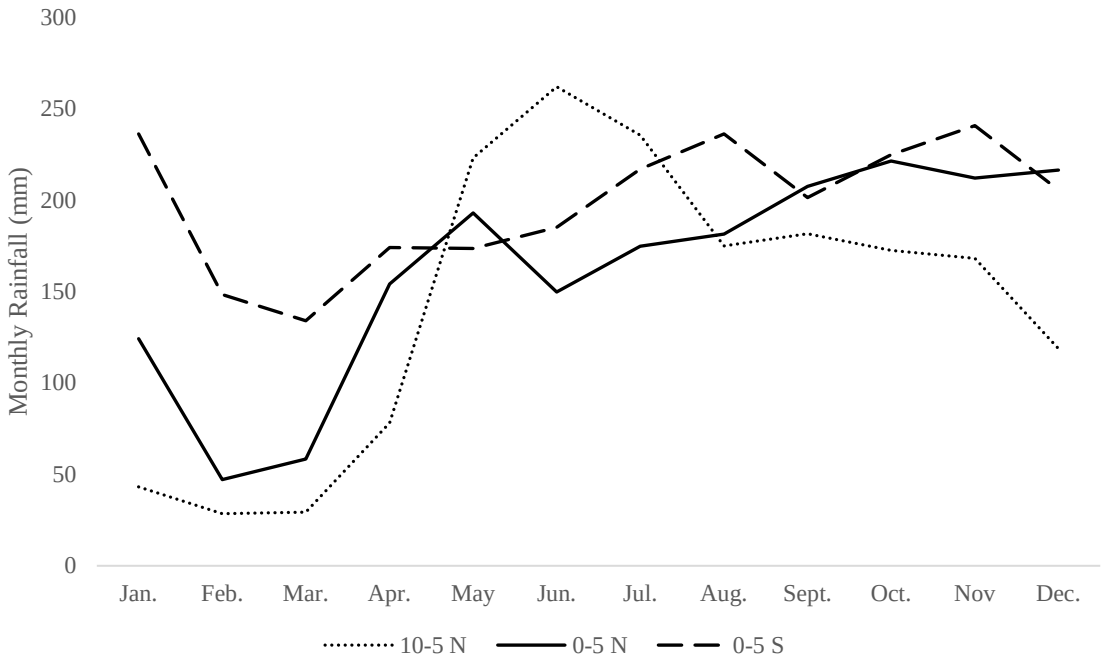

Figure 2 Average monthly rainfall for different regions in the Republic of Maldives.

1.4.3 Water Resources

The community in the Maldivian atolls depends on a combination of rainwater harvesting systems, desalinized seawater, and groundwater extraction from the freshwater lens to meet freshwater demands for domestic and industrial uses. Surface water bodies such as streams and lakes do not exist due to limited surface area and high permeability of surface deposits (Urish, 1974), consequently, sub-surface groundwater storage in the form of fresh groundwater lens is the only way for natural water storage. Aside from freshwater resources, seawater desalination is used typically in intensively populated islands such the capital Male. National Maldivian census of 2006 states that 35% of the Maldivian population have access to desalinated water, where desalinated water is provided to households via piped distribution systems. Table 1 shows the desalinated water volume in the Male area from 2004 to 2009 (Latheefa et al., 2011).

Table 1 Desalinated seawater volume in thousands metric tons in Male area from Latheefa et al. (2011).

Location	2004	2005	2006	2007	2008	2009
Male	1667.7	1969.4	2147.4	2444.5	2880.6	3275
Villingilli	-	-	87.61	94.64	132.75	153.44
Hulhumale	-	-	63.95	63.95	79.81	138.17

In the outer atoll islands, where desalination technology is not available, rainwater is captured using individual household or communal rain water catchment systems and is used as the primary source of drinking water, while groundwater is pumped and is typically used for secondary purposes including bathing, washing, and toilet flushing. This pattern of water usage and water availability is similar to other atoll islands communities such as: the Republic of Kiribati (White et al., 1999).

1.5 The Numerical Model

1.5.1 Simulation Code Selection

For the sake of modeling and analyzing the available groundwater resources of the Maldivian atolls, the three-dimensional, variable-density, transient groundwater flow numerical model (SEAWAT), which is developed by the United States Geological Survey (USGS), is selected. The selection of an appropriate saltwater intrusion model is an important and difficult stage in the modeling process. Several factors should be considered by the modeler which makes the model selection not an easy step. The model should be able to simulate and predict the desired hydrological target based on mass balance principle, which is in this research the available fresh groundwater volume, at the appropriate temporal and spatial scales. In this context, the SEAWAT model was selected for several reasons:

1) It can simulate the saltwater intrusion problem by coupling the USGS ground flow model (MODFLOW) and the solute transport, multi-species model (MT3DMS)
2) It can simulate saltwater intrusion problem based on transition zone approach, rather than sharp interface approach, where seawater and groundwater transition area is represented by a transition zone where water fluid density is changing gradually rather than representing the transition zone as two fluids separated by too narrow zone
3) It is a public domain code, and has been applied and tested on many applications of saltwater intrusion problems.

1.5.2 Graphical User Interfaces

There are many commercial, and non-commercial graphical interfaces programs to SEAWAT. These programs facilitate the input of data for creating SEAWAT input files. In addition to that, they aid in visualizing results and preparing color coded maps for the results. In this modeling study, Groundwater Vistas (Rumbaugh and Rumbaugh, 2011) is utilized for the sake of preparing inputs files for running the SEAWAT code. Groundwater Vistas is a windows platform graphical user interface developed by Environmental Simulations Incorporated. Model Viewer, a computer program for three-dimensional visualization of groundwater model results developed by the USGS, is utilized for the sake of reading and visualizing output files after running a SEAWAT simulation. The SEAWAT modeling code (in FORTRAN) was modified to output salt concentrations for each cell and for each layer for specified output times. Data were processed to calculate lens thickness for each column of grid cells and the total volume of freshwater in the aquifer is recorded.

1.6 Available Data

Previous groundwater investigations were undertaken by Bangladesh Ltd. Consultation Company (Tony Falkland on behalf of Bangladesh Consultants 2010a; 2010b; 2010c; 2010d) to collect data regarding observed groundwater conditions, estimating hydraulic conductivity via field tests, and collecting historical daily rainfall data. Other data regarding sea level rise rates, and data required for accurate groundwater analysis were collected from published literature (see Table 5). These data are required for the sake of modeling the fresh groundwater lens as they give estimates for model inputs such; recharge rates or assigning hydraulic parameters like hydraulic conductivity which will lead to accurate assessments of fresh groundwater lens sustainability for the islands of the Republic of Maldives.

Data regarding the observed freshwater lens thickness of atoll islands and associated groundwater volumes in the Maldives have been collected by the consulting company and analyzed using geophysical surveys utilizing Geonics EM34-3 electromagnetic induction (EM) equipment. These data were extracted from the reports of (Falkland, 2000; Falkland, 2001), and Bangladesh Consultants groundwater investigation reports (Tony Falkland 2010a; b; c; d), and were employed to calibrate the saltwater intrusion models. The Geonics EM34-3 equipment is composed of a transmitter with a transmitter coil connected to it, and a receiver connected to a receiver coil. Operators hold the two coils which linked with a cable. The coils are spaced apart by a distinct distance of 10m, 20m, or 40m (inter-coil spacing). The coils can be placed either vertically or horizontally. When switched on, the transmitter sends via the transmitter coils an alternating current which generates a primary magnetic field. The primary magnetic field induces small electrical currents in the ground which eventually induces a secondary magnetic field. This secondary magnetic field is dependent on: coils spacing, operating frequency, and the ground

conductivity. The receivers senses both magnetic field via the receiver coil and a reading for apparent ground conductivity is recorded (EM conductivity) according to the ratio of the secondary to the primary magnetic fields.

The groundwater lens volume is estimated from EM conductivities reading by using empirical equations. Several EM readings are conducted in multiple locations in each island using different coils spacing and a single groundwater lens volume is averaged for each island. The depth of contact between the upper Holocene aquifer and the lower Pleistocene aquifer (Thurber Discontinuity) was observed by the field done in multiple islands in the Republic of Maldives by (Falkland 2000; Falkland 2001; Tony Falkland 2010a; 2010b; 2010c; 2010d). It is estimated that the depth of contacted in the Maldivian atoll islands is ranging between 10-15 meters. For the study islands, the lens base will have a shallow (i.e. lens base will be always in the upper Holocene aquifer, and will not be significantly affected by the Thurber Discontinuity location. Borehole logging indicates that the hydraulic conductivity in the Maldivian atoll islands range between 5-50 m/day (Falkland 2000; Falkland 2001).

Daily precipitation data were collected from TRMM (Tropical Rainfall Measuring Mission) open access database website in tabular form for the geographic region of the Maldives. Two geographic regions are targeted: the geographic region between the latitudes of 5^{o}N to 10^{o} N, and the region between 0^{o} and 5^{o}N, with each region between the longitudes of 71^{o}E and 74^{o}E. Precipitation data were employed to calculate recharge forcing to the SEAWAT models.

1.7 Dissertation Organization

The remainder of this dissertation is organized as follows:

- The second chapter gives a brief overview and exploration of the literature regarding atoll islands hydrology and previous efforts in modeling saltwater intrusion in atoll islands aquifers
- The third chapter, demonstrates the development of SEAWAT models for the four selected islands in the Republic of Maldives, and the calibration procedure used to match observed and simulated fresh groundwater volumes
- The fourth chapter presents methods and simulations results for fresh groundwater lens volume under future variable rainfall
- The fifth chapter, presents methods and simulations results for fresh groundwater lens volume under projected sea level rise rates
- The sixth chapter, presents methods and simulations results for fresh groundwater lens volume under potential overwash and storm surges events
- The seventh chapter, presents an analysis of the impact of anthropogenic stresses (pumping, increase in population) within the context of climate change (rainfall, sea level rise, and overwash events), and provide estimates for future available freshwater quantities for domestic consumption
- The eighth chapter, presents a summary of the major findings and conclusions of this dissertation and discusses potential future research challenges and requirements.

CHAPTER 2. ATOLL ISLANDS HYDROLOGY AND MODELING

In this chapter, a brief overview and exploration of the literature regarding atoll islands hydrology and previous efforts in modeling saltwater intrusion in atoll islands aquifers are presented.

2.1 Atoll Islands Formation

Atoll islands have long been an interesting field of research to scholars of a variety of research fields due to their extreme geographic isolation, vegetation, unique subsurface geologic structure, and fragile groundwater resources. Typically, atolls consist of small low carbonate islands (islets) and fringing reefs that vary in size enclosing a shallow seawater central lagoon (Petreson, 1991). The size of the carbonate reef platform determines the width of these small islets and their elevation, which is not more than 3 meters above mean sea level. Infiltrating rainfall forms a body of fresh groundwater termed a “freshwater lens” that floats atop seawater within the aquifer sediments. The amount and the size of this freshwater lens are strongly dependent on the amount of rainfall and the surface area of the island. Typically, larger islands of widths greater than 500 meters are inhabited by humans as they are adequate in terms of size for fresh groundwater lens development (Spennemann, 2006).

The enclosed central seawater lagoon size is variable in width and depth; however, most of the lagoons have interior enclosed area of less than 1000 km^2, with small islets scattered around the perimeter of the lagoon. Atolls often are grouped in a large geographic region, with several nations composed solely of atoll islands. The Republic of Maldives, the Republic of the Marshall Islands, and the Federated States of Micronesia are examples of many nations whose populations inhabit exclusively or almost exclusively atoll islands.

Charles Darwin was the first scientist who proposed a theory regarding atoll islands development. His theory was published in 1842, entitled “The structure and distribution of coral reef” (Darwin, 1842). Darwin hypothesized that atolls are situated above carbonate platforms built above subsided volcanic edifices. These carbonate reef platforms were eroded in the early Holocene era as sea level subsided. The sea level subsiding promotes the deposition of sand and other fine sediments as suitable environment was found (Darwin, 1842). Consequently, the subsurface lithology of atolls consists of Holocene deposits (termed the Holocene aquifer) resting on top of older Pleistocene limestone foundation, forming what generally is called the “Dual Aquifer System” of atoll islands (Dickinson, 2004; Presley, 2005; Dickinson, 2009). Most of the sediments in the upper Holocene layer are gravels and unconsolidated sand. In his paper, Spennemann (2006) points out that this dual aquifer geological setting allows fresh groundwater zone to develop beneath atoll islands in the shape of floating fresh lens over seawater. Figure 3 shows the geological setting of atoll islands aquifers based on “Dual Aquifer System.”

The island position relative to dominant wind blowing direction has a strong effect on Holocene aquifer deposits hydraulic conductivity (Anthony, 2004). Coarser sediments are disposed in the wind bearing islands (Windward Islands) as a result of the blowing winds high energy. Also, Windward Islands are exposed to stronger waves which will tend to wash out fine sediments and this will eventually lead to removal of fine sediments. On the other side, and unlike the Windward Islands, Leeward Islands tend to have finer sediments, and to be larger in size than Windward Islands as they are partially protected from erosional force of prevailing winds and waves (Bailey et al., 2010). Numerical simulations for fresh groundwater lens volume on atoll islands of Federated States of Micronesia conducted by Bailey et al. (2009) estimated hydraulic conductivity values of Leeward and Windward islands to be 50 and 400 m/day

respectively. It is worth mentioning in this context that variability of blowing winds energy and patterns on atolls, will result in variability in the range of hydraulic conductivities values. Moreover, numerical simulations results conducted by Bailey et al. (2009) revealed that lower hydraulic conductivity values will promote the development of thicker fresh groundwater lenses. Figure 4 illustrates Windward and Leeward Islands relative to the direction of prevailing winds.

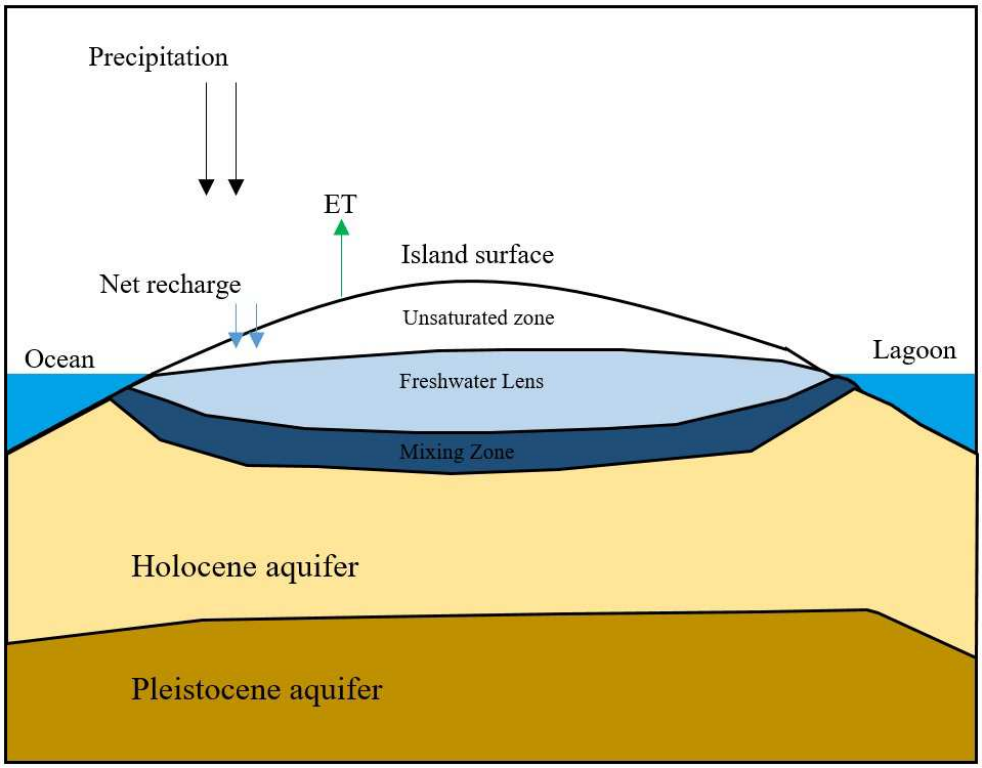

Figure 3 Simplified schematic diagram for the geological structure of atoll islands aquifers based on "Dual Aquifer System" vertical scale is highly exaggerated.

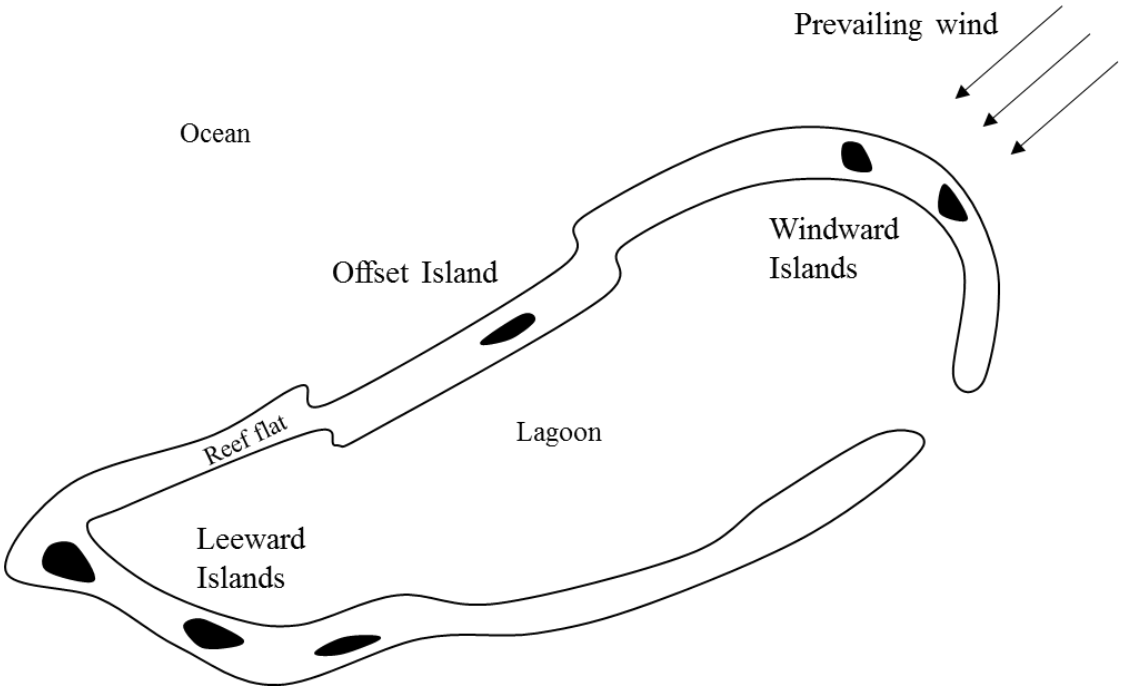

Figure 4 Schematic diagram illustrating the location of Windward and Leeward Islands relative to the prevailing wind direction.

2.2 Integrated Freshwater Management Need in Atolls Islands Communities

Due to the lack of surface water bodies, atoll islands people depend on rainwater harvesting and extracting groundwater from subsurface freshwater storage. Mainly, atoll islands communities consume water for domestic uses due to fresh groundwater lenses fragile nature. However, water drawn from ground is rarely used for agricultural or rising livestock. A paper published by White et al. (2007) concludes that the main management challenges facing fresh water supply in coral islands are the following:

- Limited freshwater resources
- Lack of people's knowledge in managing their water resources
- Conflicting interests between stakeholders
- Deteriorating water resources due to anthropogenic stresses
- Limited surface area and isolated geography

As listed above, we can conclude that water scarcity problems in such developing communities in Atoll Islands Nations could be resolved just by managing the available resources effectively by encouraging collective actions between conflicting parties and teaching people how important their available water resources are.

Using inappropriate methods in groundwater extraction and over pumping represent serious threats and could salinize groundwater in atolls (White et al., 2007). Moreover, groundwater could be contaminated with biological and chemical pollutants caused by sewerage, pigs, crop production, spillage of petroleum products, and seepage from waste dumps (White et al., 2007). Sanitation systems and lack of effective management of human waste in atoll islands communities can threaten groundwater resources also. In many low density islands communities, defecation on the beach is practiced, while in higher density populated islands, pit latrines are used. Sanitation systems improper site selection can introduce faecal contaminants to groundwater. Also, people are consuming up to 40% of their water supply for flushing toilets (Falkland, 2000). Lack of maintenance and cultural barriers can also contribute to groundwater contamination. Crennan and Berry (2002) stated that Majuro in the Marshalls and South Tarawa in Kiribati had leaked saltwater sewerage while elsewhere composting toilets are used. Cultural barriers are preventing community from adapting the upgraded sanitation system.

As discussed above, adverse practices contribute to reducing and contaminating available fresh groundwater resources in atoll islands communities. To mitigate the effects of these practices impact on expediting the reduction available freshwater volumes, integrated water resource management practices should be implemented.

2.3 Environmental Threats on Freshwater Resources on Atolls

2.3.1 Climate Variability and Severe Droughts

Drought events and climate variability are significant threats that affect freshwater availability in atoll islands. A study by Ragoonaden et al. (2006) discussed the climate change effects on the current status and future expectations on freshwater resources on atolls in the Indian Ocean. They analyzed short datasets of temperature, precipitation, and sea level rise measurements for five nations in the Western Indian oceans (including Republic of Maldives). It is concluded that data sets have shown meaningful variation in trends on the annual scale. Extreme droughts were noticed in the data, causing complete depletion of groundwater storage and thereby placing the atoll islands nations under serious threats.

Another study conducted by White et al. (1999), showed that atolls in the Pacific Ocean are exposed to severe droughts affected by the El Niño Southern Oscillation (ENSO) events, where variation in sea surface temperature is highly correlated to the amount of rainfall. Reduced rainfall amounts will eventually lead to drastic reduction in recharge to the subsurface groundwater storage. Another study by Peterson (1990) points out that if drought events lasted over prolonged periods, the subsurface groundwater storage is greatly reduced and the volume of extractable freshwater is seriously exhausted. During drought periods, atoll islands communities may have to look for alternative water resources to remedy the drought situation.

2.3.2 Sea Level Rise

The position of mean sea level also affects freshwater lens thickness and available extractable water. As sea level rises, and depending on beach slope, seawater will inundate beachfronts leading to beach shoreline recession. Consequently, total land surface area and cross-

section width will be decreased. The available fresh groundwater volume is dependent on island width, and hence, as island's width decreases due to sea level rise, available fresh groundwater volume will be reduced. Depending on the beach slope, shorelines recession could be significant. Beach slopes range from 0.5% (gentle slope) to 2% (steep slope). According to a general rule of thumb of estimating shoreline recession for sandy beaches on average slope is 100:1 (i.e. a shoreline recession of 100 m for every 1 m rise in sea-level) (Tsyban et al. , 1990).

Global sea level rise rates during the twentieth century was reported by Douglas (1997) to be 1.8 mm/yr. with accelerated rates of 4 mm/yr. during the first decade of the 21st century impacted by the large scale of climate change (Beckley et al., 2007). Other studies predict that sea level will rise between 0.5 m and 1 m by the year 2100 (Raper and Braithwaite, 2006; Rahmstorf, 2007; Meier et al., 2007; Pfeffer et al., 2008; Dickinson, 2009). Considering various rates of sea level rise, seawater may inundate up to 200 m of beach fronts (considering a beach slope of 0.5% and sea level increase of 1 m by 2100).

Regarding the study area in the Republic of Maldives, sea level rise predictions are variable. While conservative forecasts predict sea level to rise at a rate of 1.0 mm/yr (Church et al., 2006), aggressive forecasts expect that sea level is rising at higher rates of 6.5 mm/yr (Woodworth et al., 2002). A paper published by Nicholls and Cazenave (2010) points out that the Indian Ocean small atoll islands are among communities vulnerable to coastal flooding by future relative, or climate induced sea level rise.

2.3.3 Marine Overwash Events

Marine overwash events are considered among destructive threats to freshwater resources in atoll islands communities. As they may occur suddenly, overwash events are induced by

various causes such as: tsunamis, storm surge, rogue waves, and the combination of simultaneous multiple climatic factors such as strong wave setup from strong prevailing winds, extreme local high tide, and high regional sea level (White et al., 2007; Bricker and Hughes, 2007; Yamano et al., 2007; Terry and Falkland, 2010). Overwash events could significantly alter the amount of stored fresh groundwater in atoll aquifers.

Because of the small land area of atolls and low-lying elevations above mean sea level (White and Falkland, 2010; Wheatcraft and Buddemeier, 1981), atoll islands could be partially or completely inundated with sea water during over wash events. The seawater inundation will salinize the fresh groundwater lens as seawater percolates through shallow and highly conductive soil profile. Depending on the overwash event intensity, frequency, and shallow soil profile characteristics, recovery time of the fresh groundwater lens will vary between few months to 1-2 years (Chui and Terry, 2012; Bailey and Jenson, 2013).

2.4 Atoll Islands Hydrological Modeling

To assist water managers and officials in small atoll islands communities in making appropriate management decisions, and to further understand freshwater resources dynamics and sustainability, several efforts have been conducted by researchers to quantify atoll islands groundwater resources analytically, empirically, and numerically. In the following sub sections, an exploration of these efforts is demonstrated.

2.4.1 Analytical and Empirical Models

Following the Dupuit assumption of horizontal groundwater flow in unconfined aquifers, several scholars have analytically approximated the freshwater/seawater interface location in

coastal aquifers (Henry, 1964; Fetter, 1972; Collins and Gelbar, 1971; Shamir and Dagan, 1971; Chapman, 1985). Among these efforts, the paper published by Fetter (1972) is noteworthy within this research. Fetter developed two analytical models for simulating position of the saline water interface beneath infinite strip oceanic island receiving constant amount of recharge at any distance from the shoreline, and beneath circular oceanic islands receiving constant amount of recharge at any radial distance from the center of the island.

For an infinite strip island:

$$h^2 = \frac{w\left[a^2 - (a-x)^2\right]}{K(1+G)} \qquad (2.1)$$

Where:

h is the fresh water level elevation above seawater/fresh water sharp interface (L)

w is constant fresh water recharge rate (L/T)

a is half of island width (L)

x is the distance from the shoreline in landward direction (L)

K is the hydraulic conductivity of island's sediments (L/T)

G is a dimensionless factor equal to 40

For circular islands:

$$h^2 = \frac{w(R^2 - r^2)}{2K(1+G)} \qquad (2.2)$$

Where:

R is the radius of the island (L)

r is the radial distance from the center of the island (L)

Equations (2.1), and (2.2) were derived by Fetter by combining the Ghyben-Herzberg principle, which assumes a sharp interface between fresh and saline groundwater, and Dupuit assumption to solve the following steady-state version of the groundwater flow equation subject to islands geometry boundary conditions for both infinite strip islands, and circular islands:

$$\frac{\partial^2 h}{\partial x^2} + \frac{\partial^2 h}{\partial y^2} = \frac{-2w}{K(1+G)} \qquad (2.3)$$

Though Fetter's analytical models generally produces valid results, the embedded Dupuit assumption can be invalid due to significant upward flow component in atoll islands aquifers. Moreover, the Ghyben-Herzberg principle assumes a sharp transition between fresh and saline water across which there is assumed to be no flow (Hubbert, 1940; Henry, 1964; Glover, 1964; Bear and Dagan, 1964; Rumer and Shiau, 1968), while in reality, the transition between the fresh and saline water is not sharp, but rather a broad transition zone of brackish water (Underwood,

1990). Recently, A two dimensional algebraic empirical model was developed by Bailey et al.(2008) to approximate the thickness of fresh groundwater lenses beneath atoll islands as a function of width of various cross-sections. The model was later extended to the estimation of fresh groundwater volume by estimating the freshwater lens thickness at different cross-sections across the island surface and interpolating between the cross-sections (Bailey et al., 2014). The model, however, does not simulate changes in lens thickness or lens volume through time.

2.4.2 Numerical Models

Numerical modeling efforts for atoll islands groundwater hydrology began in the seventies of the last century with the work of Lam in 1974 by assuming homogenous, and isotropic aquifer with uniformly horizontal flow. These early efforts were then extended with the work of Lloyd et al., (1980); and Falkland (1983). Buddemeier and Holladay (1977) were the first researchers modelling the dual aquifer system, where relatively low permeability layer from the Holocene age overlying an extremely high conductivity karstic limestone layer from the Pleistocene age.

Herman and Wheatcraft (1984) studied the factors affecting groundwater flow within atoll island aquifers using two dimensional finite element model FEMWATER by comparing simulation results with field data in Enjebi Island, Enewetak atoll in the Marshalls Islands (Herman and Wheatcraft, 1984). Other scholars employed the finite element based computer model, SUTRA (Saturated-Unsaturated Transport) (Voss and Provost, 2010) to investigate strategies for freshwater lens management in Laura Island in the Republic of Marshalls (Griggs and Peterson, 1993). They calibrated their model with observed salinity data and used the calibrated models to investigate freshwater lens dynamics. Underwood (1990) developed

conceptual and numerical models to characterize hypothetical atoll islands hydrogeology (Underwood, 1990). Two years later, Underwood's research was extended to investigate the contribution of the factors which affect the groundwater movement and the transition zone mixing (Underwood et al., 1992). They applied two dimensional SUTRA model on a hypothetical atoll island groundwater system. Moreover, many other scholars utilized computer models to simulate groundwater lens dynamics in atoll islands (Hogan, 1988; Griggs and Peterson, 1993; Bailey et al., 2009; Bailey et al., 2014).

The evolution of three dimensional computer packages to simulate solute transport in groundwater systems began in the late 1980s (e.g. HST3D model by Kipp (1987), and SALTFLOW model by Molson and Frind (1994)). Researchers have employed three dimensional groundwater models to simulate fresh groundwater lens dynamics in small atoll islands aquifers (e.g. Ghassemi et al., 1998; Lee, 2003; Comte et al., 2014). The sustainable yield of a small coral island located in the Indian Ocean named Home Island was examined by scholars (Ghassemi et al., 1998). They employed SALTFLOW model to estimate the acceptable water extraction rate that has no short term impacts on groundwater during average or better than average recharge conditions (Ghassemi et al., 1998). However, the researchers did not calibrate their model in a transient mode and did not account for future rainfall variability while estimating recharge rates. Another paper published by Lee (2003) utilized TOUGH2, which is a general purpose numerical simulator for multi-phase fluid and heat flow in fractured porous media, to investigate relations among lens responses, aquifer parameters, and boundary conditions for a generalized, rather than site specific, shallow atoll island. Other researchers (Comte et al., 2014) simulated groundwater salinity evolution of a low-lying coral island in the Western Indian Ocean named Grande Glorieuse using SEAWAT model. They focused on land

vegetation for Grande Glorieuse which is intensively covered by coconut palm trees, banyan trees, casuarina trees, and soldierbush trees. The study concluded that plantation in the study area contributes significantly to freshwater uptake from shallow groundwater lens. The paper concluded that the increase in groundwater salinity is especially due freshwater uptake by vegetation. Until now, no three-dimensional modeling study has been conducted to investigate fresh groundwater lens dynamics for small atoll islands in such a way that comprises multiple environmental and anthropogenic stresses to provide comparisons of the impacts of threats associated with environmental or anthropogenic stress as discussed in Section 2.3. Table 2 summarizes the previous work done in numerical modeling of atoll islands aquifers.

Table 2 Previous efforts summary in numerical modeling of atoll islands, FD = finite difference model; FE = finite element model.

Reference	**Island**	**Model type**	**Dim**	**Dual aquifer**	**Transient flow**	**Anisotropic *K***
Lam (1974)	Swains Island	FD	2D			
Lloyd et al. (1980)	Buota, Tarawa	FD	2D		x	
Falkland (1983)	Christmas Island	FD	2D		x	
Herman and Wheatcraft (1984)	Enjebi, Enewetak	FE-FEMWATER	2D	x	x	
Hogan (1988)	Enjebi, Enewetak	FE-SUTRA	2D	x	x	
Underwood (1990), and Underwood et al. (1992)	Hypothetical	FE-SUTRA	2D	x	x	
Griggs and Peterson	Laura, Majuro	FE-SUTRA	2D	x	x	

(1993)						
Bailey et al. (2009)	Selected islands in the Republic of Micronesia	FE-SUTRA	2D	x	x	x
Chui and Terry (2013)	Hypothetical	FE-SUTRA	2D	x	x	x
Bailey et al. (2014)	Selected islands in the Republic of Maldives	FE-SUTRA	2D	x	x	x
Ghassemi et al. (1998)	Home Island in the Cocos Islands	FE-SALTFLOW	3D	x	x	x
Lee (2003)	Hypothetical	FE-TOUGH2	3D	x	x	x
Comte et al. (2014)	Grande Glorieuse in the Indian Ocean	FD-SEAWAT	3D	x	x	x

2.4.3 SEWAT Assumptions and Governing Equations

As SEAWAT is the modeling code used to simulate density dependent groundwater flow in this dissertation, its methodology in model set-up and numerical solution of the flow and transport based on mass balance equations are explained in detail in this section. SEAWAT is a finite difference program which simulate three dimensional, variable density, transient groundwater flow in porous media (Langevin et al., 2007). The program couples two modeling codes into a single program to simulate density dependent groundwater flow in saturated media. The first is MODFLOW2000 which simulate groundwater flow in saturated porous media, and

the second is MT3DMS which simulates multi-species solute transport in saturated porous media. SEAWAT was tested with five popular benchmark problems to examine its validity. SEAWAT contains common assumptions which are well established in the field of hydrological modeling of groundwater flow and solute transport as follows:

- The flow is assumed to laminar (Darcy's equation is valid)
- The standard expression for specific storage in a confined aquifer is applicable
- The diffusive approach to dispersive approach based on Fick's law can be applied (dispersion can be modeled as a Fickian process), and isothermal conditions prevail
- The porous media is assumed to be fully saturated with water
- A single, fully miscible liquid phase of very small compressibility.

The flow equation in MODFLOW2000 has been modified to solve the variable density flow of water in saturated media as follows:

$$\frac{\partial}{\partial\alpha}\left[\rho K_{f\alpha}\left(\frac{\partial h_f}{\partial\alpha}+\frac{\rho-\rho_f}{\rho}.\frac{\partial Z}{\partial\alpha}\right)\right]+\frac{\partial}{\partial\beta}\left[\rho K_{f\beta}\left(\frac{\partial h_f}{\partial\beta}+\frac{\rho-\rho_f}{\rho}.\frac{\partial Z}{\partial\beta}\right)\right]+\frac{\partial}{\partial\gamma}\left[\rho K_{f\gamma}\left(\frac{\partial h_f}{\partial\gamma}+\frac{\rho-\rho_f}{\rho}.\frac{\partial Z}{\partial\gamma}\right)\right]$$
$$=\rho S_f.\frac{\partial h_f}{\partial t}+\theta.\frac{\partial\rho}{\partial C}.\frac{\partial C}{\partial t}-\rho_s q_s \qquad (2.4)$$

where

α,β,γ are the orthogonal coordinate axes, aligned with prinicipal directions permeability

h_f is the freshwater equivalent head (L)

K_f is freshwater hydraulic conductivty (L/T)

ρ_f is the freshwater density (M/L^3)

C is solute concentration (M/L^3)

S_f is the specific storage in terms of freshwater head (1/L)

q_s is the volumetric flow rate per unit volume of aquifer representing sources and sinks (1/T)

ρ is the density of q_s (M/L^3)

θ is the effective porosity

Z is the elevation above datum (L)

t is time (T)

Equation (2.4) is solved by MODFLOW2000 for the velocity field. The resulting velocities are used to solve for concentration in the following transport equation by MT3DMS:

$$\frac{\partial C}{\partial t} = \nabla \cdot \left(D \nabla C \right) - \nabla \cdot (\vec{v} C) - \frac{q_s}{\theta} . C_s + \sum_{k=1}^{N} R_k \qquad (2.5)$$

where

D is the hydrodynamic dispersion coefficient (L^2/T)

$\vec{v}$ is the fluid velocity (L/T)

C_s is the solute concentration of water entering from sources os sinks (M/L^3)

R_k $(k = 1, ..., N)$ is the rate of solute production or decay in reaction k of N different reactions (M/L^3/T)

After solving equations (2.4) and (2.5), the density in each grid cell is updated as follows:

$$\rho = \rho_f + E.C \qquad (2.6)$$

where

E is dimensionless number approximately equals 0.7143

The updated density calculated in equation (2.6) is used by MODFLOW2000 in the next time step. SEAWAT solves the partial differential equations using finite differences scheme. SEAWAT manual contains further exploitations regarding numerical solution procedures.

CHAPTER 3. FRESH GROUNDWATER LENS MODELS DEVELOPMENT AND CALIBRATION

In this chapter, the development of three dimensional SEAWAT models for selected islands in the Republic of Maldives, and the calibration procedure used to match observed fresh groundwater volumes are presented.

3.1 Islands Selection

Four different islands have been selected for the purpose estimating future groundwater supply in the Republic of Maldives. The selection of these islands is based on the following criteria to provide a comprehensive, and representative analysis:

1) Selected islands have to represent different climatic regions in the Republic of Maldives
2) Selected islands have to represent different island sizes
3) Selected islands have to have available hydrogeologic data for model construction and model testing.

Bangladesh Consultants Ltd. has undertaken groundwater status investigations field work on four islands in the Republic of Maldives as part of a project entitled “Detailed design and works supervision for the development of sewage systems for the islands of L. Gan, GDh.Thinadhoo, N.Velidhoo and N. Holhudhoo”. This field work was documented in four reports describing the groundwater status in each island. For the purpose of this research, these four islands were selected to model fresh groundwater resources dynamics in the Republic of Maldives atolls as they represent different climatic regions and different island sizes. In the following sub-sections, a brief overview for these four islands is presented. Bangladesh Consultants Ltd. field reports

were prepared by Tony Falkland (May, 2010) and are extensively cited in the following sub-sections.

3.1.1 N. Holhudhoo Island

N. Holhudhoo is a tiny island which is located in the south of Noonu atoll. It is located at latitude 5º45’18” and longitude 73º15'46” at a distance of approximately 175 km north of Malé (Figure 5 shows an aerial photo of the island). The island length is about 670 m and the maximum width is about 370 m. The island’s current area bounded by the beach, as surveyed by ArcMap, is reported as 19.9 hectares (ha). The Island population as reported by island office data was 2,063 in December 2009. The population has increased by 21 from 2,042 in December 2006 (Bangladesh Consultants Ltd. field report based on Local Island’s office data). According to 2006 official National census, N. Holhudhoo population was 1,527. According to the island office data in 2006 and 2009, the average annual population growth is estimated to be 0.34%. Island office data show that the total number of houses was 396 in December 2009. Water supply in the island is based on fresh groundwater extraction from wells, harvesting rain water from roofs and storing it in polythene (PE) tanks, and desalinated water which is supplied to five public taps.

3.1.2 N.Velidhoo Island

N. Velidhoo is a small size island which is located in the south of Noonu atoll. It is located at latitude 5º39’50” and longitude 73º16'28” at a distance of approximately 165 km north of Malé. (Figure 6 shows an aerial photo of the island). The island length of the island is about 1.0 KM and the maximum width is about 830 m. The island’s current area bounded by the beach

as surveyed by ArcMap is reported as 59.5 hectares (ha). Island population as reported by Island office data was 2,256 in December 2009. The population has increased by 76 from 2,180 in December 2006 (Bangladesh Consultants Ltd. field report based on Local Island's office data). According to 2006 Maldivian government population census, N.Velidhoo population was 1,716. According to island office data in 2006 and 2009, the average annual population growth is estimated to be 1.15%. Island office data show that the total number of houses was 357 in December 2009. Water supply in the island is based on fresh groundwater extraction from wells, harvesting rain water from roofs and storing it in polythene (PE) tanks, and desalinated water.

Figure 5 Aerial photo of N.Holhudhoo Island from Google Earth.

Figure 6 Aerial photo of N. Velidhoo Island from Google Earth.

3.1.3 GDh.Thinadhoo Island

GDh.Thinadhoo is a medium size island which is located in the western side of Gaafu Dhaalu atoll. It is located at latitude 0º31’ and longitude 72º59' at a distance of approximately 405 km south of Malé. (Figure 7 shows an aerial photo of the island). The island length of the island is about 1.5 KM and the maximum width is about 930 m. The island’s current area bounded by the beach as surveyed by ArcMap is reported as 147.2 hectares (ha). Island population as reported by island office data was 6,745 in November 2009. The population has increased from 6,498 in December 2006 (Bangladesh Consultants Ltd. field report based on Local Island’s office data). According to 2006 official Maldivian government population census, GDh.Thinadhoo population was 4,442. According Island office data in 2006 and 2009, the average annual population growth is estimated to be 1.25%. Island office data show that the total number of houses was 1,162 in November 2009. Water supply in the island is based on fresh

groundwater extraction from wells, harvesting rain water from roofs and storing it in polythene (PE) tanks.

Figure 7 Aerial photo of GDh. Thinadhoo Island from Google Earth.

3.1.4 L. Gan Island

L. Gan is a large size island which is located in the eastern side of Laamu atoll. It is located at latitude 1º55’ and longitude 73º32'30’ at a distance of approximately 250 km south of Malé. (Figure 8 shows an aerial photo of the island). The island length of the island is about 8.1 KM and the maximum width is about 1.6 KM. The island’s current area bounded by the beach as surveyed by ArcMap is reported as 1015.8 hectares (ha). There are three villages in the island, Thundee in the north, Mathimaradhoo in the center, and Mukurimagu in the south. Since 2005, the population of the island has significantly increased. According to island office (as mentioned

in the field reports) data, L. Gan population was 2,537 in December 2005. Island population was reported by island office data in October 2009 to be 4,208. According to island office data in 2005 and 2009, the average annual population growth is estimated to be 13.5%. Island office data show that the total number of houses was 691 in October 2009. Water supply in the island is based on fresh groundwater extraction from wells, harvesting rain water from roofs and storing it in polythene (PE) tanks, and from seawater desalination.

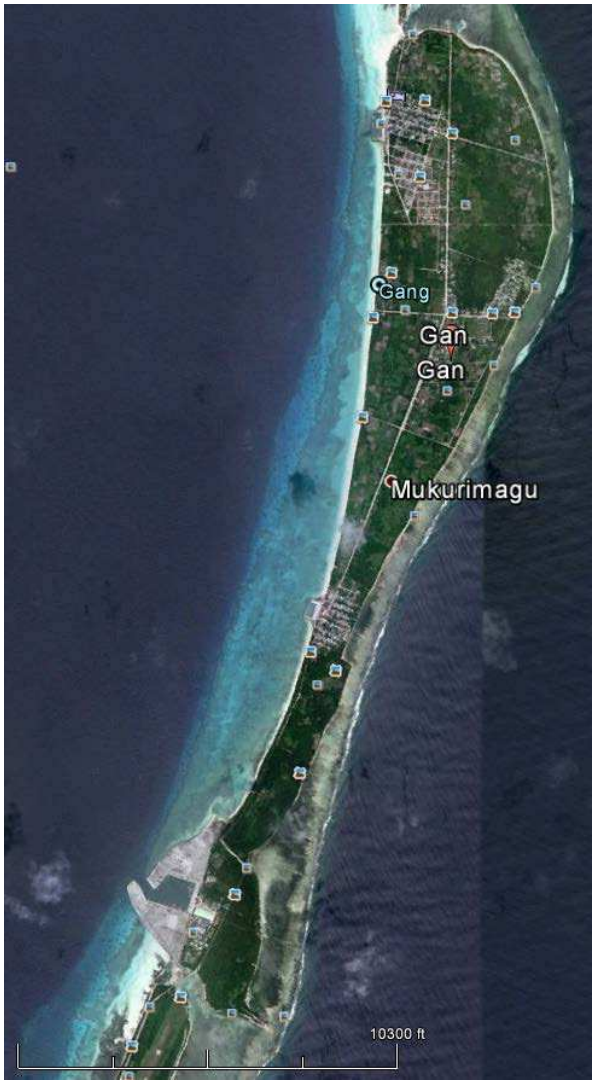

Figure 8 Aerial photo of L. Gan Island from Google Earth.

3.2 Islands' Hydrogeological Setting

According to the "Dual Aquifer System" theory discussed previously in Chapter 2 of this dissertation, atoll island aquifers consist of an upper aquifer of Holocene age deposits (Holocene aquifer) resting on top of older Pleistocene age limestone foundation (Pleistocene aquifer). The hydraulic conductivity of the Pleistocene aquifer has been estimated to be 1 to 2 orders of magnitude higher than that of the Holocene aquifer (Hunt and Peterson, 1980). The Holocene aquifer consists of sand and fine sediments and is typically 15-25 meters thick, while the lower Pleistocene aquifer is composed of highly conductive karstic limestone.

The fresh groundwater lenses in the Maldivian atolls form as rainfall that is not evaporated, intercepted by trees, transpired by vegetation, or captured by rooftop catchment systems, percolates through the unsaturated zone and recharges the freshwater lens at the water table (Wheatcraft and Buddemeier, 1981). Without continual recharge forcing, the fresh groundwater lens will be thin and dramatically deplete. The size of the fresh groundwater lens depends on the width of the island as larger islands provide adequate space to receive freshwater from rainfall and eventually developing larger fresh groundwater lens.

3.3 Models Development

3.3.1 Grid Discretization

3.3.1.1 Horizontal Discretization

The spatial scale of islands (Bangladesh Consultants Ltd. field report based on Local Island's office data) dictates whether a fine resolution grid or coarse resolution grid is needed. Moreover, the orientation of grid should be situated with respect to the general flow regime. To model the spatial scale of islands, uniform grid spacing is used. The very fine resolution of the

grid includes computational difficulties in terms of long simulations time. Google Earth was employed to delineate islands' boundaries to create KML files. These KML files were then imported and edited in ArcMap and a shape file for each island was created. Using the pre-processing graphical user interface for MODFLOW and MT3DMS, Groundwater Vistas, shapefiles were imported to the interface and were used to develop the grid for each island model. Groundwater Vistas allows for the creation of SEAWAT input files. The grid size was determined analytically by measuring the width and the height of each modeled island and dividing these measurements by a desired cell size. Once imported into Groundwater Vistas, the boundaries of the island shapefiles were traced to denote the models' active and inactive cells. Table 3 shows the horizontal grid design for the selected islands. Figure 9 shows the grid for N. Holhudhoo Island.

Table 3 Horizontal grid design for the selected islands

Island	**Island Area (ha)**	**No. of Rows**	**No. of Columns**	**Grid Size (m)**	**Total number of cells**
N. Holhudhoo	19.9	68	60	10	122,400
N. Veildhoo	59.5	98	110	10	323,400
GDh. Thinadhoo	147.2	85	70	20	178,500
L. Gan	1015.8	227	95	40	646,950

Figure 9 Horizontal grid design for Holhudhoo Island.

3.3.1.2 Vertical Discretization

The vertical discretization generally represents change in aquifer geology. As discussed earlier in section 3.2, the modeled groundwater system consists of two different aquifers: the Holocene upper aquifer, and the Pleistocene lower aquifer. Hence, two layers can be used at minimum, however, 30 layers were used to retain accuracy in representing vertical salinity profile and to model the variation in fresh groundwater lens adequately. Table 4 shows the vertical discretization that was used for island models.

Table 4 Vertical discretatizion used for all islands models.

Layer	Thickness (m)
1	0.250
2	0.250
3	0.250
4	0.250
5	0.250
6	0.250
7	0.250
8	0.250
9	0.250

10	0.250
11	2.500
12	2.500
13	2.500
14	2.500
15	2.500
16	2.500
17	2.500
18	5.000
19	5.000
20	5.000
21	5.000
22	5.000
23	5.000
24	10.000
25	10.000
26	10.000
27	10.000
28	10.000
29	10.000
30	10.000

3.3.2 Specified Head Boundary Conditions

The coastal line bounding each island model was specified to be zero head boundary with solute concentration, which is chloride, to be 1 (which means 100% seawater) to simulate seawater presence. The bottom of each model was designated as no flow boundary.

3.3.3 Aquifer Parameters

Aquifer parameters were assigned based on the published values in atoll islands modeling literature. The parameters described in this section are assigned to all models to establish baseline condition simulations. In the calibration process, as described in a later section, some of these parameters will be changed.

Bailey and others developed two dimensional vertical cross-section SUTRA models to simulate freshwater lens dynamics for generic islands within the Republic of Maldives (Bailey et al., 2014). Calibration to the hydraulic conductivity was performed to reproduce observed lens

thickness data. The calibrated hydraulic conductivity was found to be 75 m/day. This calibrated hydraulic found by the Bailey et al. (2014) has been used as initial hydraulic conductivity for selected islands. The specific yield of the upper Holocene aquifer, which determines the volume of available extractable fresh groundwater, was set at 0.20 (Griggs and Peterson, 1993). Other aquifer parameters are summarized in Table 5.

Table 5 Aquifer parameters assigned to all models in the baseline simulations stage

Parameter [units]	**Value**	**Source**
General aquifer properties		
Compressibility of porous matrix [m^2/N]	1×10^{-9}	Peterson and Gingerich, 1995
Specific yield [m^3/m^{-3}]	0.20	Griggs and Peterson, 1993
Longitudinal dispersivity, α_L [m]	6.0	
Transverse dispersivity, α_T [m]	0.05	Griggs and Peterson, 1993
Upper Holocene aquifer		
Porosity [m^3/m^{-3}]	0.2	Anthony, 1996
Thickness [m]	15	Hamlin and Anthony, 1987
Horizontal K [m/d]	75	Bailey et al., 2014
Vertical K [m/d]	15	Bailey et al., 2014
Lower Pleistocene aquifer		
Porosity [m^3/m^3]	0.3	Swartz, 1962
Thickness [m]	105	
Horizontal K [m/d]	5000	Oberdorfer et al., 1990
Vertical K [m/d]	1000	Oberdorfer et al., 1990

3.3.4 Baseline Simulations

Baseline simulations were run firstly to establish a baseline condition for fresh groundwater lens volume for each island. Using average annual precipitation for each climatic region at which each island is located, and based on the amount of actual recharge to the groundwater, monthly recharge stress periods were established, operating on daily time steps.

Historical annual recharges as reported by Bailey et al. (2014) for 5-10 N and 0-5 N regions ranges between 560 mm to 797 mm, and 458 mm to 1046 mm respectively. For the purpose of progressing toward stable condition, average daily recharge rates of 2 mm/day and 3 mm/day were assigned to 5-10 N region islands and 0-5 N region islands respectively. Recharge values were applied uniformly over the island surface. The transport simulations were allowed to run for 20 years until the simulated fresh groundwater volume stabilized. Table 6 and Figures 10-11 show baseline simulated fresh groundwater volume in each island.

3.4 Models Calibration

3.4.1 Transient Groundwater Recharge Calculation

Recharge represents the only freshwater source feeding the fresh groundwater lens. Daily recharge was calculated from Jan 1998 until Dec 2011 by Bailey et al. (2014) for different climatic regions in the Republic of Maldives using the water budget model of Falkland (1994), which accounts for interception storage by surface vegetation, evapotranspiration (ET), and soil water storage. The water budget model was not used in this research as it results in a lot of days with zero recharge, which will eventually lead to computational instability. Instead, the long term percentages of rainfall that recharges groundwater for two climatic regions were calculated by multiplying percentages shown in Table 7 by the average daily precipitation in each month. This approach was used to evenly distribute monthly precipitation amounts for each day where each day during monthly stress periods receives equal amount of recharge. The calculated recharges based constant percentages are plotted in Figure 12, and Figure 13. Table 7 shows the percentages of rainfall to become recharge in the selected islands based on the soil water balance model.

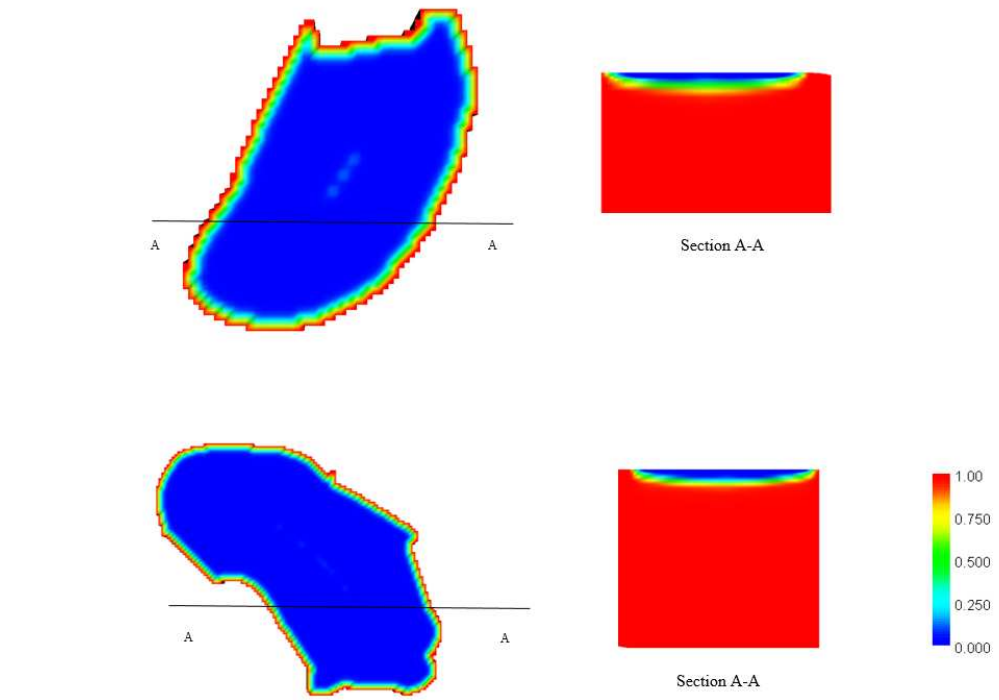

Figure 10 Baseline salinity profile for Holhudhoo, and GDh. Thinadhoo Islands (1.00 denotes 100% seawater) vertical scale is highly exaggerated.

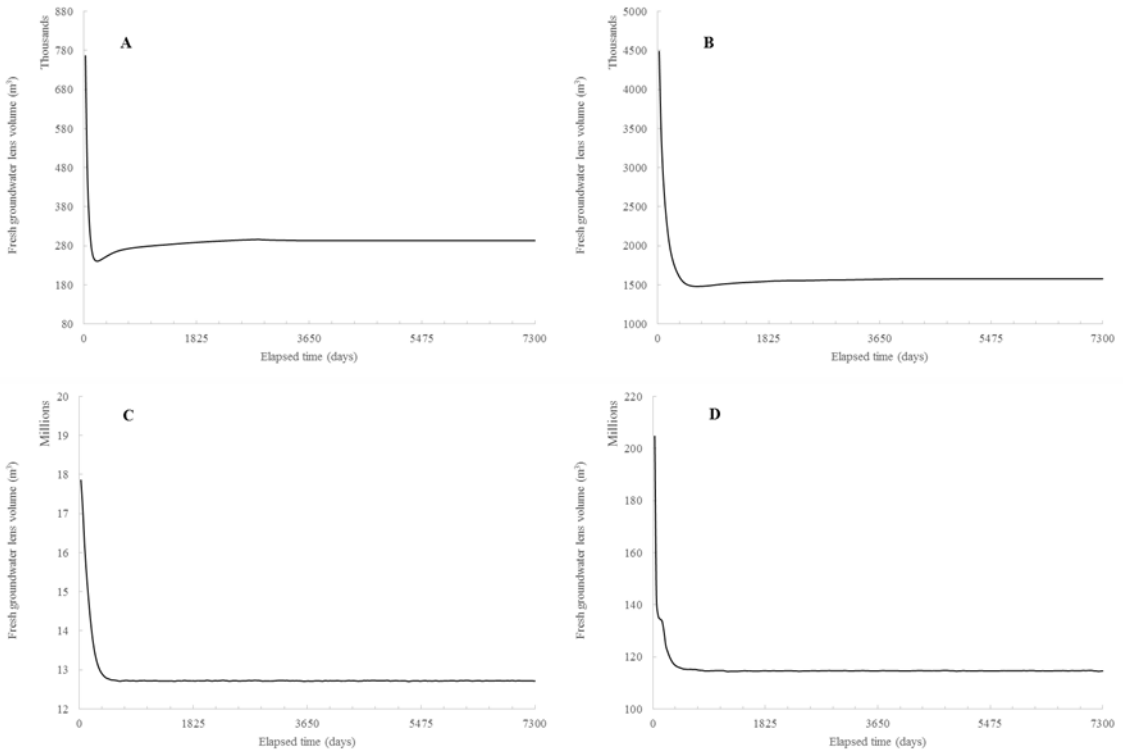

Figure 11 Baseline simulations results for: **A**. N Holhudhoo Island; **B**. N. Velidhoo Island; **C**. GDh. Thinadhoo Island; **D**. L. Gan Island.

Table 6 Baseline fresh groundwater lens volumes in modeled islands.

Island	Fresh Groundwater Lens Volume (m^3)
N. Holhudhoo	293,270
N. Velidhoo	1,577,852
GDh. Thinadhoo	1.271×10^7
L. Gan	1.146×10^8

Table 7 Percentage of rainfall to become groundwater recharge in modeled islands based on soil water balance model.

Climatic region	% of rainfall to become recharge	Islands included
5-10 N	48.9 %	N. Holhudhoo and N. Veildhoo
0-5 N	50.9%	GDh. Thinadhoo and L. Gan

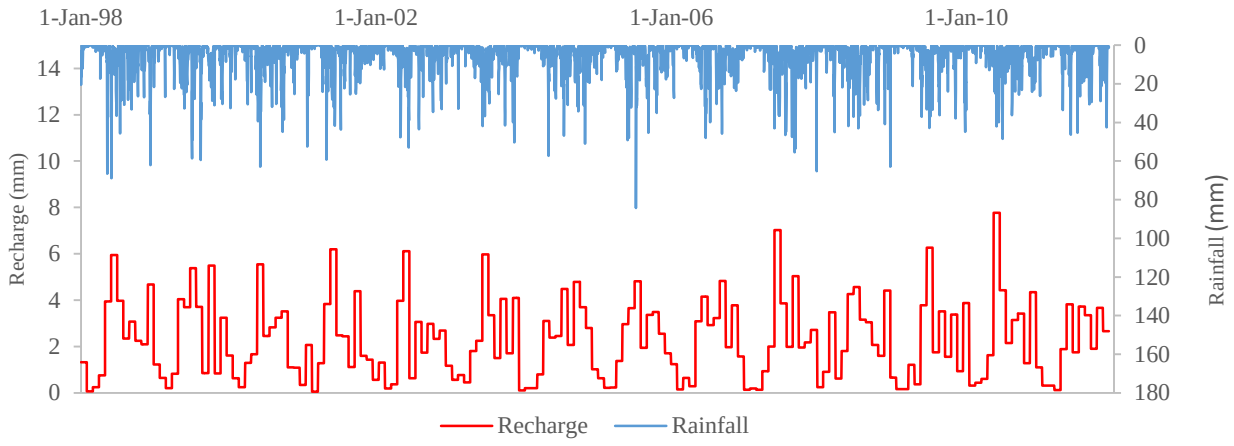

Figure 12 Daily rainfall and calculated recharges for 5-10 N climatic region.

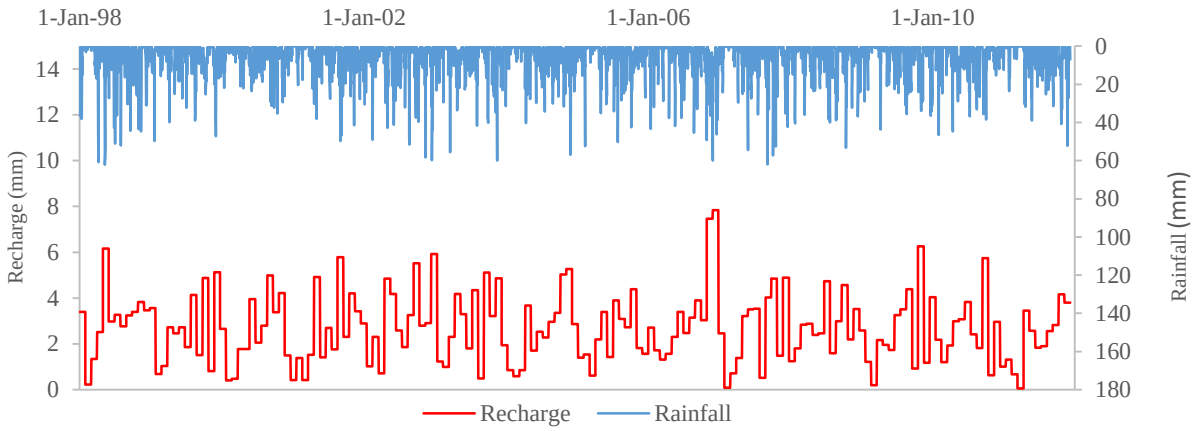

Figure 13 Daily rainfall and calculated recharges for 0-5 N climatic region.

3.4.2 Calibration Procedure

Once initial simulations have been performed to establish baseline fresh groundwater lens volumes, each model was calibrated using observed values of fresh groundwater lens volume. The objective of the calibration is to have simulated freshwater lens volumes match observed freshwater volumes with less than 1% volume discrepancy. The initial hydraulic conductivity used was 75 m/d as calibrated by Bailey et al. (2014) in a previous two dimensional modeling of islands in the Maldivian atolls using SUTRA. The hydraulic conductivity was adjusted until the freshwater lens volume estimated by the three-dimensional model matched the observed lens volumes for all islands. The depth of contact between the Holocene aquifer and the Pleistocene aquifer was not calibrated as it is concluded that it does not have a major influence on the lens volume Wallace (2015). Also, due to the limited observed fresh groundwater data (one observation in time), the calibration was constrained to one parameter.

Data regarding freshwater lens volumes in islands are available at only one time step, that is on April 2010 when the field investigations were undertaken, the transient models for each island was established with transient recharge data calculated from January 1st 1998 till

December 31st 2010. SEAWAT calculated salt concentrations on a daily basis for each island and the simulated groundwater lens volume values at the day when the data was measured compared to the recorded values of freshwater lens volumes reported by Tony Falkland in the field reports (2010) describing the groundwater status in each island. By changing the hydraulic conductivity of the upper aquifer for each island, several transient simulations were performed and sensitivity analysis for the influence of hydraulic conductivity of the upper aquifer on freshwater lens volume was conducted.

3.4.3 Sensitivity Analysis

Sensitivity analysis was performed for all modeled islands to investigate the effect of Holocene aquifer hydraulic conductivity on the development and size of the freshwater lens. Hydraulic conductivity values were varied across a range possible hydraulic conductivity values in an effort to bracket all potential values as reported by previous modeling studies for atoll islands. When changing horizontal hydraulic conductivity values, anisotropy ratio values were set to be 5 for all islands. Figures 14 through 17 show the sensitivity analysis plots for each island. Generally, The results of this analysis indicate that hydraulic conductivity has a significant influence on the thickness and volume of the freshwater lens where higher hydraulic conductivity values promote thinner freshwater lenses and vice versa.

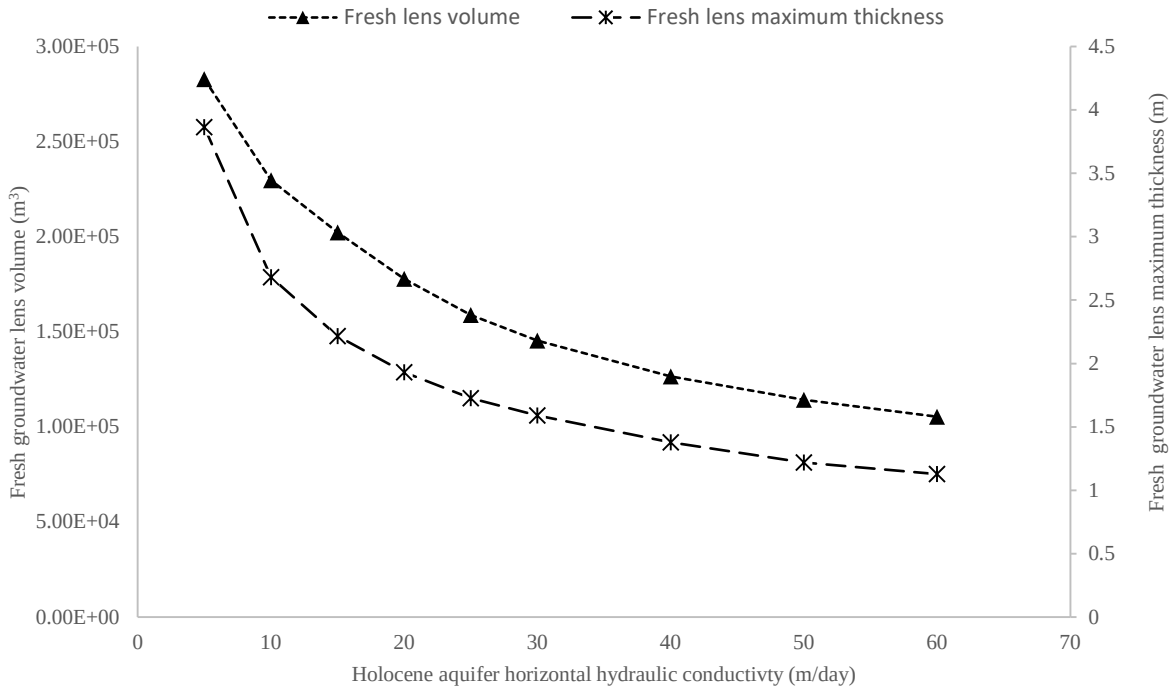

Figure 14 Horizontal hydraulic conductivity sensitivity analysis results for N. Holhudhoo Island.

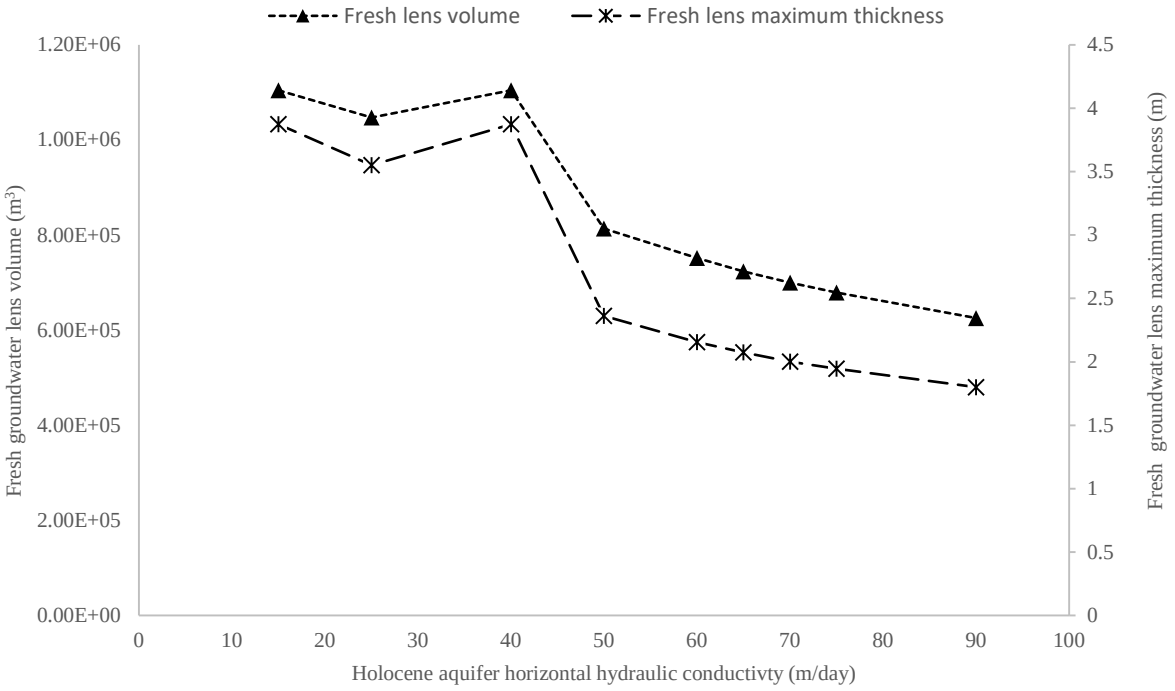

Figure 15 Horizontal hydraulic conductivity sensitivity analysis results for N. Velidhoo Island.

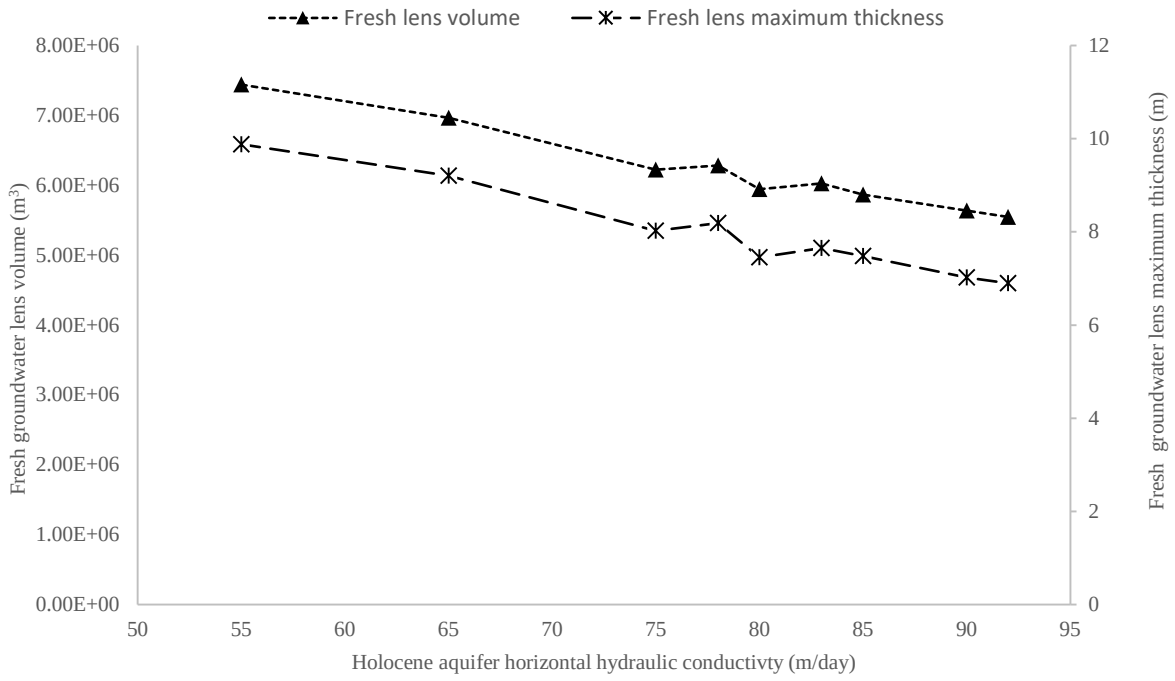

Figure 16 Horizontal hydraulic conductivity sensitivity analysis results for GDh. Thinadhoo Island.

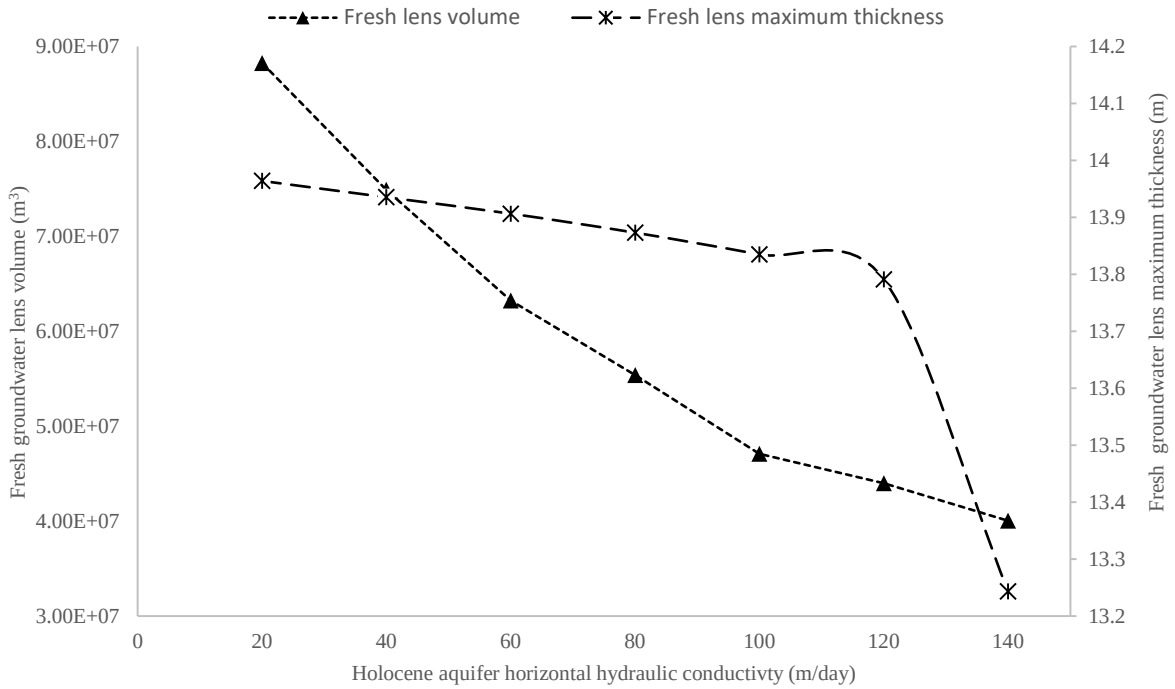

Figure 17 Horizontal hydraulic conductivity sensitivity analysis results for L. Gan Island.

3.4.4 Calibration Results

After running several simulations for modeled islands, horizontal hydraulic conductivity for the upper the Holocene aquifer was adjusted to match observed fresh groundwater volumes as reported by Tony Falkland (2010). Figure 19 and Table 8 show the observed and simulated volumes of the freshwater lens and the resulting calibrated values. Calibrated hydraulic conductivity values range from 15 m/day to 100 m/day, which is in the same order of magnitude for atoll islands hydraulic conductivity values (Bailey et al., 2009) and also within the range reported by Falkland (Falkland, 2000; Falkland, 2001).

A

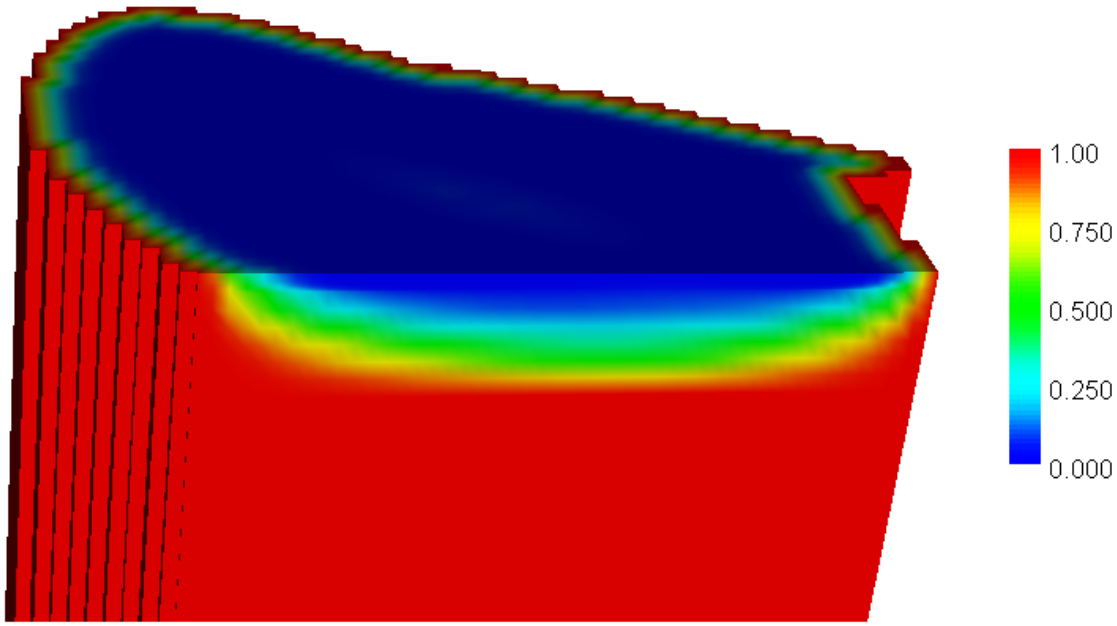

B

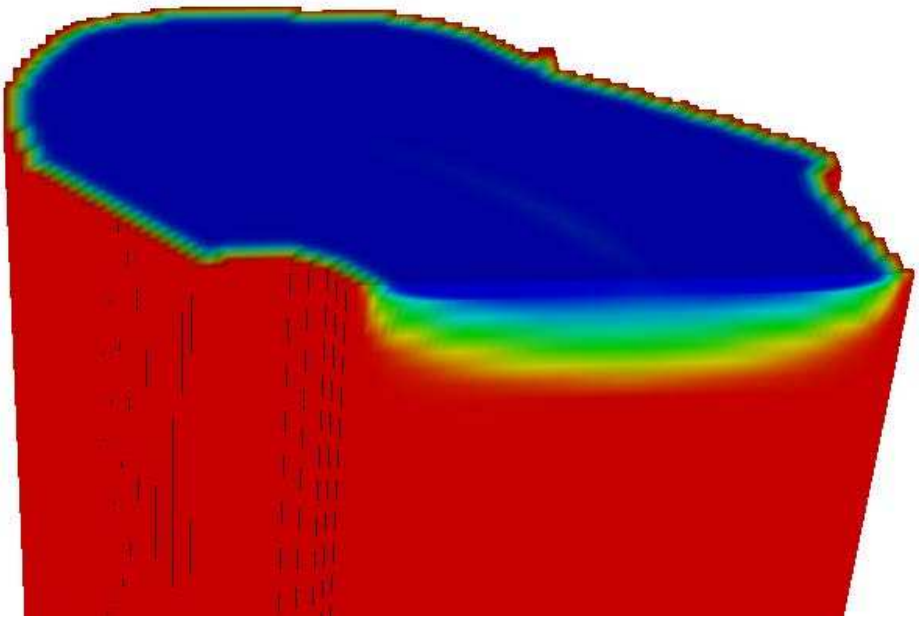

C

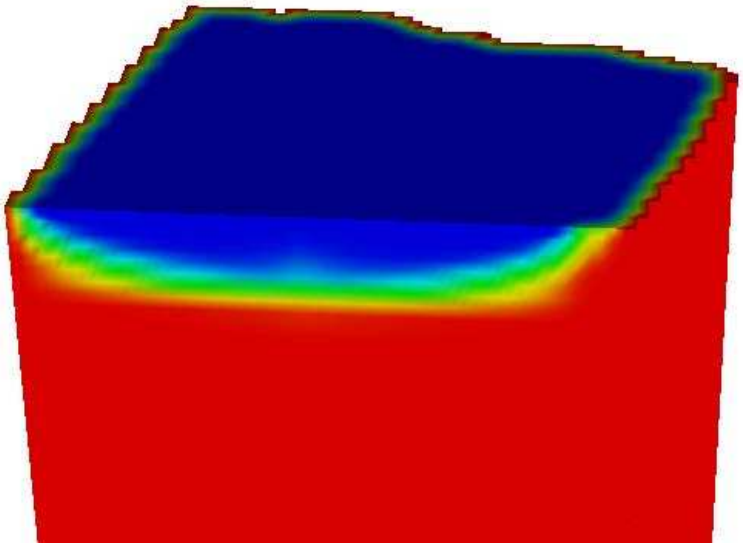

D

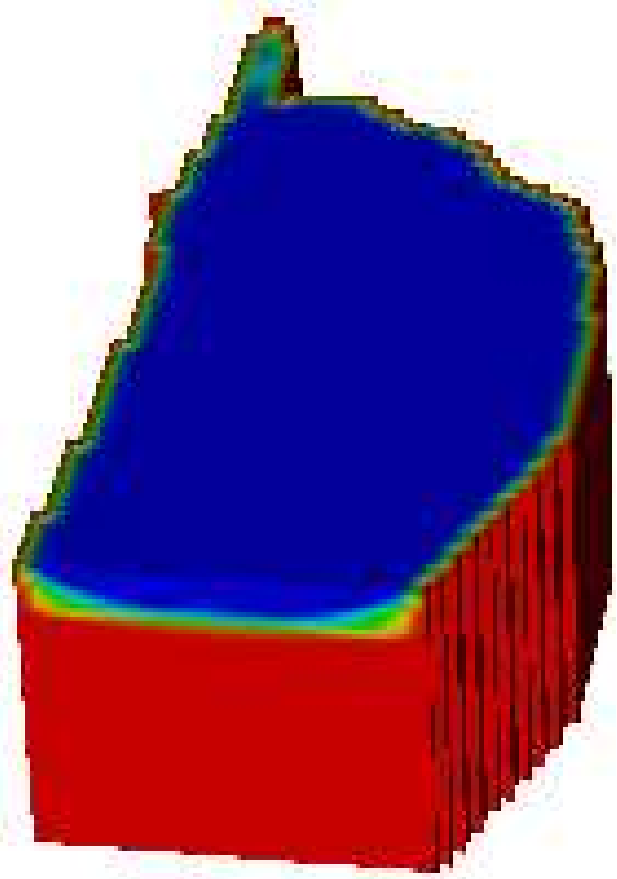

Figure 18 . Cross-sectional view of three-dimensional model of modeled Islands showing calibrated lens volume. Red indicates seawater salt concentration of 100% seawater and blue indicates freshwater concentration of salt near 0% seawater. A transitional zone is seen between the freshwater and seawater regions, **A**. N. Holhudhoo island; **B**. N. Velidhoo island; **C**. GDh. Thinadhoo island; **D**. L. Gan island (vertical scale is highly exaggerated).

Table 8 Calibrated Holocene aqufer hydrauluc conductivities for modeled isalands.

Island	Climatic region	Calibrated K (m/day)	Observed lens volume (million m^3)	Simulated lens volume (million m^3)
N. Holhudhoo	5-10 N	15	0.203	0.202
N. Velidhoo	5-10 N	65	0.73	0.72
GDh. Thinadhoo	0-5 N	90	5.7	5.63
L. Gan	0-5 N	100	47.4	47.1

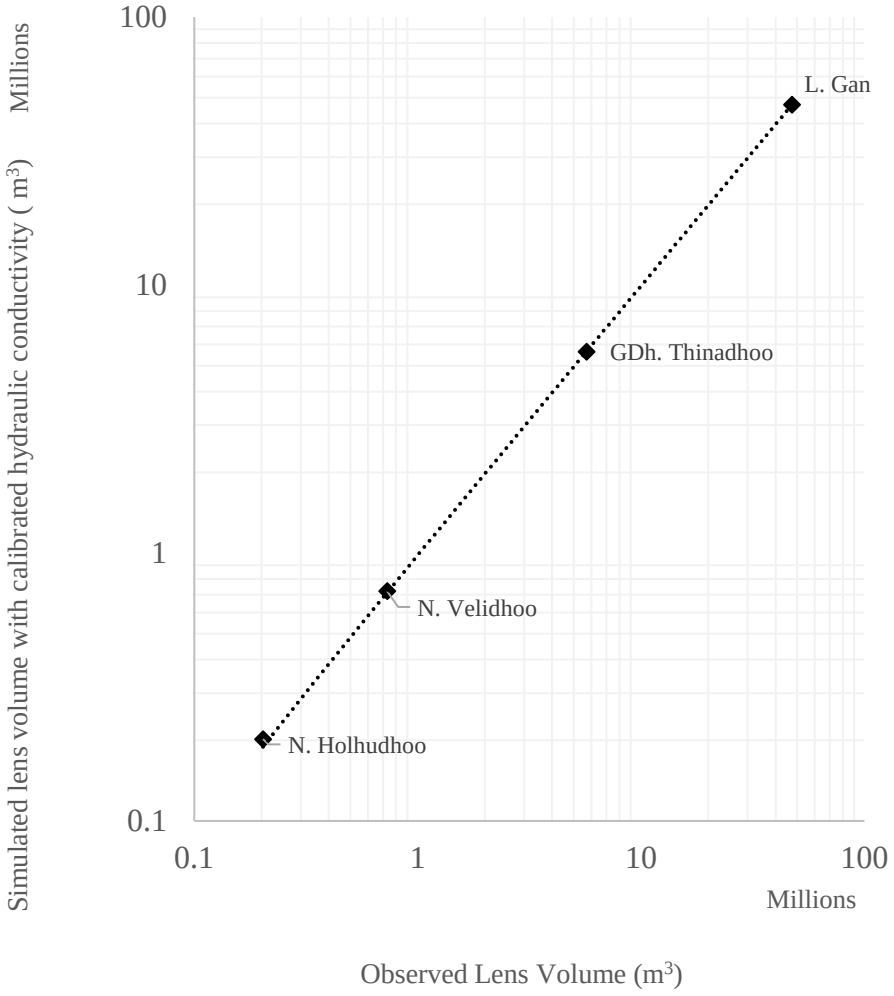

Figure 19 Simulated versus observed fresh ground lens volumes for different islands (for calibrated hydraulic conductivity values).

3.5 Discussion and Conclusion

Three dimensional models were developed using the USGS code SEAWAT to simulate the groundwater flow dynamics beneath Maldivian atoll islands. Islands selected for this research were: N. Holhudhoo on Noonu atoll, N. Velidhoo on Noonu atoll, GDh. Thinadhoo on Gaafu Dhaalu atoll, and L. Gan on Laamu atoll. Islands were selected in the Northern climatic region (5-10 N region), and the southern climatic region (0-5 N) of the Maldivian atolls to capture the effect of rainfall variability on the development of the fresh groundwater lens beneath the islands

and based on data availability for the fresh groundwater lens status. Calibration was performed for islands with observed values of lens volumes to ensure model output accurately reproducing historical values. Calibration procedure was based on minimizing groundwater lens volume discrepancy between observed and simulated values.

During calibration, it is concluded that a hydraulic conductivity value of 15 m/d was necessary for N. Holhudhoo Island to match groundwater lens volume. The calibrated hydraulic conductivity values for other islands are: 65 m/day for N. Velidhoo Island, 90 m/day for GDh. Thinadhoo Island, and 100 m/day for L. Gan Island. All calibrated hydraulic conductivity values seem reasonable and are of the same order of magnitude obtained from previous modeling studies and from boreholes data conducted by Falkland (Falkland, 2000; Falkland, 2001). A sensitivity analysis was conducted to investigate the influence of the upper Holocene aquifer horizontal hydraulic conductivity on the development and size of the freshwater lens. It is concluded that the hydraulic conductivity values have a significant impact on the development and size of the freshwater lens for all modeled islands.

CHAPTER 4. THE SUSTAINABILITY OF FRESH GROUNDWATER LENS UNDER NON-STATIONARY CLIMATIC CONDITIONS

In this chapter the fresh groundwater lens development is assessed under non-stationary climatic conditions. Rainfall rates from multiple Global Circulation Models (GCMs) are used to estimate recharge rates for the four study islands to quantify the future fresh ground availability under various precipitation patterns. The climate change induced sea level rise is discussed in Chapter 5.

4.1 Introduction

Effective water resources planning and management require a scientifically based knowledge of how water supply would fluctuate under future climatic conditions. In order to manage available water resources efficiently, future climate forecasts can be used to estimate future environmental forcing such as atmospheric carbon dioxide concentrations and resulting variable rainfall patterns. A set of coordinated climate model experiments under Model Intercomparison Project Phase 5 (CMIP5) were developed by the World Climate Research Program to facilitate future climate analysis and the expected Earth system variability and change. The overall objective of the research program is to develop models that are capable of predicting future climate as well as determining the effect of human activities on climate.

Many climate modeling groups are affiliated with the program, each of which employs General Circulation Models (GCMs) in their analysis. The climate models investigate the contribution of several factors when forecasting future climate such as: cloud cover circulation,

and ice meltdown. Statistical analysis is used to ensure that future climatic forecasts replicate historical climatic trends.

The amount of sun radiation is represented by CMIP5 global climatic models in various scenarios. Carbon dioxide concentration in the atmosphere, which may change because of greenhouse gases effects, affects energy balance in a global scale forcing the climate to change (Meehl et al., 1996). Greenhouse gases (GHGs) emission trajectory is modeled by different representative concentration pathways (RCPs). RCPs are labeled according to each scenario's target radiative forcing by 2100. The high emissions scenario is represented by RCP8.5, in which radiative forcing is expected to reach 8.5 W/m^2 by year 2100. RCP6.0 is an intermediate emissions scenario, where the radiative forcing in this scenario stabilizes at 6 W/m^2 after 2100. Another intermediate climate change scenario, where mitigation policies are imposed, is represented by RCP4.5, in which GHGs emissions are restrained and the radiative forcing stabilizes at 4.5 W/m^2 at year 2100. Extreme climate change mitigation, where effective policies are strictly enforced, and lifestyle change is accommodated to reduce greenhouse gases emissions, is represented by RCP2.6, in which radiative forcing peaks at 2.6 W/m^2 near 2100 (Taylor et al., 2012). A list of the various climate models (modified from Wallace et al., 2015) and their associated modeling centers is shown in Table 9. Climatic models that were developed by World Climate Research are employed in this research to estimate the future response of fresh groundwater lens dynamics in the Republic of Maldives under future climatic condition in the next few decades.

Table 9 CMIP5 climate modeling centers and associated climatic models (modified from Wallace et al. (2015)

Modeling Center (or Group)	Institute ID	Model Name	ID
Beijing Climate Center, China Meteorological Administration	BCC	BCC-CSM1.1	M1
National Center for Atmospheric Research	NCAR	CCSM4	M2
Community Earth System Model Contributors	NSF-DOE-NCAR	CESM1(CAM5)	M3
Commonwealth Scientific and Industrial Research Organization in collaboration with Queensland Climate Change Centre of Excellence	CSIRO-QCCCE	CSIRO-Mk3.6.0	M4
The First Institute of Oceanography, SOA, China	FIO	FIO-ESM	M5
NOAA Geophysical Fluid Dynamics Laboratory	NOAA GFDL	GFDL-CM3 GFDL-ESM2G GFDL-ESM2M	M6 M7 M8
NASA Goddard Institute for Space Studies	NASA GISS	GISS-E2-H-p1 GISS-E2-H-p2 GISS-E2-H-p3 GISS-E2-R-p1 GISS-E2-R-p2 GISS-E2-R-p3	M9 M10 M11 M12 M13 M14
National Institute of Meteorological Research/Korea Meteorological Administration	NIMR/KMA	HadGEM2-AO HadGEM2-ES	M15 M16
Institut Pierre-Simon Laplace	IPSL	IPSL-CM5A-LR	M17
	IPSL	IPSL-CM5A-MR	M18
Atmosphere and Ocean Research Institute (The University of Tokyo), National Institute for Environmental Studies, and Japan Agency for Marine-Earth Science and Technology	MIROC	MIROC5	M19
Japan Agency for Marine-Earth Science and Technology, Atmosphere and Ocean Research Institute (The University of Tokyo), and National Institute for Environmental Studies	MIROC	MIROC-ESM-CHEM MIROC-ESM	M20 M21
Meteorological Research Institute	MRI	MRI-CGCM3	M22
Nonhydrostatic Icosahedral Atmospheric Model Group	NCC	NorESM1-M	M23
Norwegian Climate Centre	NCC	NorESM1-ME	M24

4.2 GCMs Statistical Assessment

4.2.1 Methods

In this research, a multi-criteria score-based method is employed to assess the performance of the GCMs for the Northern and the Southern climatic regions in the Republic of Maldives. A statistical methodology developed by Fu et al.(2013) is used with modifications to assess GCMs based on multiple statistical criteria (Table 10). The modifications to Fu et al. (2013) include: using one method to assess the Trend analysis instead of two methods used in the paper, and ignoring the space-time variability variable in characterizing the similarity between observed data and GCMs outputs. Table 10 shows how the ability of GCMs to replicate historical monthly rainfall depths is assessed and ranked using statistical methods, formulations, and weights.

Table 10 GCMs statistical assessment variables, methods, and weights.

Statistics of climate variables	**Assessment Method**	**Weights**
Mean	Relative error (%)	1
Standard deviation	Relative error (%)	1
Temporal Variation	NRMSE	1
Monthly distribution	Correlation coefficient	1
Trend analysis	Mann-Kendall test	1
Probability density functions	BS	0.5
	S_{score}	0.5

In order to assess performance, the observed monthly rainfall data is compared to GCMs output from January 1998 through December 2011. GCMs outputs are compared to observed rainfall data based on assessment methods listed in Table 10. GCMs are ranked based on each assessment method shown in the table, and a weighted average ranking for each model is calculated according to Equation 4.1. The assessment criteria are used to characterize similarity

between observed data and GCMs outputs in terms of long term mean, standard deviation, temporal variation, seasonality, temporal variability, and probability distribution.

$$Total\ Score = \sum_{i=1}^{n} w_i R_i \qquad (4.1)$$

Where:

w_i is the weight for the i^{th} assessment method

R_i is the ranking for the i^{th} assessment method

To quantify similarity between observed data and climatic forecasts in long term mean and standard deviation, relative error formulation is used where:

$$RE = \frac{\frac{1}{n}\sum_{i=1}^{n} X_{mi} - \frac{1}{n}\sum_{i=1}^{n} X_{oi}}{\frac{1}{n}\sum_{i=1}^{n} X_{oi}} \qquad (4.2)$$

Where X_{mi}, and X_{oi} are the modeled and observed monthly rainfall, and n is the number of observations (168 months in this case).

The normalized root mean square error (NRMSE), that is defined as root mean square error divided by the corresponding standard deviation of the historical data (Randall, 2007), is used to compare the similarity of between observed and modeled rainfall data considering both mean and standard deviation.

$$NRMSE = \frac{\sqrt{\frac{1}{n}\sum_{i=1}^{n}(X_{mi} - X_{oi})^2}}{\sqrt{\frac{1}{n-1}\sum_{i=1}^{n}(X_{oi} - \bar{X}_o)^2}} \qquad (4.3)$$

The correlation coefficient is used to evaluate forecasts monthly distribution compared to observed rainfall data. Higher correlation coefficient indicates a strong statistical dependence between observed rainfall and modeled climatic forecasts. For the sake of evaluating GCMs performance in terms of replicating observed data long term trend, the Mann-Kendall test (Hirsch, 1982) is applied to characterize long-term monotonic trends and quantify their magnitudes. The comparison between observed rainfall data and modeled outputs is based on the Mann-Kendall slope. A positive slope for the data set indicates that there is an increasing trend for the data, while a negative slope indicates a decreasing trend.

The Brier verification score (BS) is a statistical measure of the accuracy of probabilistic predictions that was introduced by Glenn Brier (Brier, 1950) to compare the quality of weather forecasts. In its original formulation, it has a minimum value of zero for perfect forecasting and a maximum value of 2 for the worst possible forecasting. For the sake of evaluating Brier score (BS) in assessing similarity between probability density functions (PDFs) of observed and modeled climatic data, a modified formulation of the Brier score is used (Fu et al., 2013). The modified version of Brier score calculates the mean squared error between the predicted probability of GCMs climatic forecasts and the observed climatic rainfall data, reporting the accuracy of probabilistic predictions. In the modified formulation, a minimum value of zero indicates perfect forecasting and a maximum value of 1 indicates the worst possible forecasting. The modified version formulation is given by the following expression:

$$BS = \frac{1}{n}\sum_{i=1}^{n}(P_{mi} - P_{oi})^2 \qquad (4.4)$$

Where P_{mi} is the modeled i^{th} probability value of each bin and P_{oi} is the observed i^{th} probability value of each bin, and n is the number of bins. For this analysis, the number of bins was fixed at 10. Probability density functions are used to assess the likelihood of the GCMs output to adequately replicate historical data. The number of bins has an effect on the quality of the Brier score analysis. Using high number of bins, lower values of BS score are expected even if there is no significant PDFs similarity between observed and modeled rainfall data.

The last criterion that is used in GCMs statistical assessment is the Significance score (S_{score}). The S_{score} calculates the cumulative minimum value of observed and modeled distributions for each bin, quantifying the similarity between two observed and modeled PDFs (Perkins et al., 2007; Watterson, 2008). Therefore, an S_{score} value of one indicates a perfect match between observed and modeled PDFs, while an S_{score} value of zero is the worst achievable score. It is much more difficult for a model to match observed data PDF, which represents of overall climate patterns, than it is to match the mean and standard deviation of historical data. Mean analysis cannot reveal biases or seasonal errors. GCMs with an $S_{score} \geq 0.80$ are considered to accurately represent the regional climate system (Perkins et al., 2007). Significant overlap between the observed rainfall data and the modeled rainfall outputs from GCMs data indicates higher capability in matching climate patterns. S_{score} is calculated by the following expression:

$$S_{score} = \sum_{i=1}^{n} Minimum\ (P_{mi}, P_{oi}) \qquad (4.5)$$

Where, P_{mi} is the modeled i^{th} probability value of each bin and P_{oi} is the observed i^{th} probability value of each bin, and n is the number of bins (10 bins were used in this analysis).

CMIP5 GCMs are assessed for their capability of accurately reproducing historical trends for both the Northern climatic region and the Southern climatic region. Separate analysis is performed for both regions of the Republic of Maldives due to difference in rainfall patterns. Results for Northern and Southern regions are analyzed and discussed separately, with internal discussion on the different RCP scenarios considered. Each of the four forcing scenarios (i.e. RCP2.6, RCP4.5, RCP6.0, and RCP8.5) are analyzed for both regions to determine which models performed best.

4.2.2 Results

4.2.2.1 Top Performing GCMs for Northern Climatic Region

The CMIP5 GCMs output for Northern climatic Region State is first analyzed. Table 11 shows the monthly mean, monthly standard deviation, NRMSE, relative error, BS, and S_{score} for each of the GCMs analyzed for Northern climatic Region State under the RCP 2.6 forcing scenario.

Table 11 GCMs statistical assessment for the Northern climatic region under RCP2.6 scenario.

Model ID	Correlation	Rank	Mean RE	Rank	St Dev RE	Rank	SSE	NRMSE	Rank
M1	0.320	23	0.249	21	0.865	24	5801.19	1.832	24
M2	0.528	9	0.238	20	0.100	8	1989.04	1.073	10
M3	0.560	6	0.255	22	0.009	2	1746.01	1.005	7
M4	0.610	4	0.125	14	0.073	6	1291.27	0.864	2
M5	0.401	21	0.072	8	0.037	3	2129.94	1.110	11
M6	0.555	7	0.093	11	0.173	10	1853.34	1.035	8
M7	0.442	18	0.217	18	0.268	15	1681.33	0.986	5
M8	0.514	10	0.030	3	0.052	5	1743.92	1.004	6
M9	0.450	16	0.093	10	0.383	20	2860.86	1.286	20

M10	0.466	15	0.062	6	0.461	23	3021.91	1.322	21
M11	0.475	13	0.047	5	0.334	18	2574.36	1.220	15
M12	0.420	20	0.090	9	0.320	17	2802.72	1.273	19
M13	0.487	11	0.113	13	0.286	16	2425.19	1.184	13
M14	0.448	17	0.094	12	0.233	13	2435.23	1.187	14
M15	0.352	22	0.229	19	0.113	9	2661.27	1.241	16
M16	0.474	14	0.187	16	0.004	1	1920.23	1.054	9
M17	0.538	8	0.161	15	0.439	21	1301.33	0.868	3
M18	0.562	5	0.006	1	0.088	7	1367.36	0.889	4
M19	0.658	1	0.066	7	0.048	4	1235.09	0.845	1
M20	0.621	3	0.537	23	0.447	22	3264.64	1.374	23
M21	0.634	2	0.583	24	0.351	19	3138.85	1.347	22
M22	0.430	19	0.213	17	0.265	14	2731.24	1.257	17
M23	0.483	12	0.032	4	0.184	12	2137.77	1.112	12
M24	0.318	24	0.009	2	0.183	11	2794.77	1.271	18

Model ID	**Mann-Kendall Slope**	**Mann Kendall RE**	**Rank**	**BS (%)**	**Rank**	**S score**	**Rank**	**Total score**	**Final Rank**
M1	0.0091	7.273	24	0.0552	22	0.696	23	126.5	24
M2	0.0044	3.000	15	0.0229	14	0.720	20	71.5	12
M3	0.0019	0.727	4	0.0121	7	0.845	4	44.5	5
M4	0.0011	0.000	1	0.0105	5	0.839	5	31.5	3
M5	0.0024	1.182	5	0.0122	8	0.821	9	54	7
M6	0.003	1.727	8	0.0267	15	0.720	21	58	9
M7	0.0041	2.727	13	0.0100	4	0.857	2	65.5	11
M8	0.009	7.182	23	0.0092	2	0.851	3	38	4
M9	-0.0033	4.000	20	0.0803	24	0.649	24	100	23
M10	0.0046	3.182	16	0.0574	23	0.702	22	95.5	22
M11	0.0054	3.909	19	0.0421	18	0.744	15	77	15
M12	-0.0036	4.273	21	0.0459	19	0.726	18	94	21
M13	-0.0019	2.727	13	0.0535	21	0.726	18	79	17
M14	-0.0003	1.273	6	0.0352	16	0.744	16	75	14
M15	0.0067	5.091	22	0.0368	17	0.756	14	92.5	20
M16	0.0026	1.364	7	0.0223	13	0.768	13	56.5	8
M17	0.0037	2.364	12	0.0176	11	0.804	12	64.5	10
M18	0.003	1.727	8	0.0097	3	0.827	6	25.5	1
M19	0.0032	1.909	10	0.0146	10	0.821	8	27	2
M20	0.0034	2.091	11	0.0049	1	0.899	1	77.5	16
M21	0.0047	3.273	17	0.0106	6	0.827	7	82	18
M22	0.0005	0.545	3	0.0474	20	0.738	17	87	19
M23	0.0013	0.182	2	0.0218	12	0.810	10	52	6
M24	0.005	3.545	18	0.0146	9	0.810	10	73.5	13

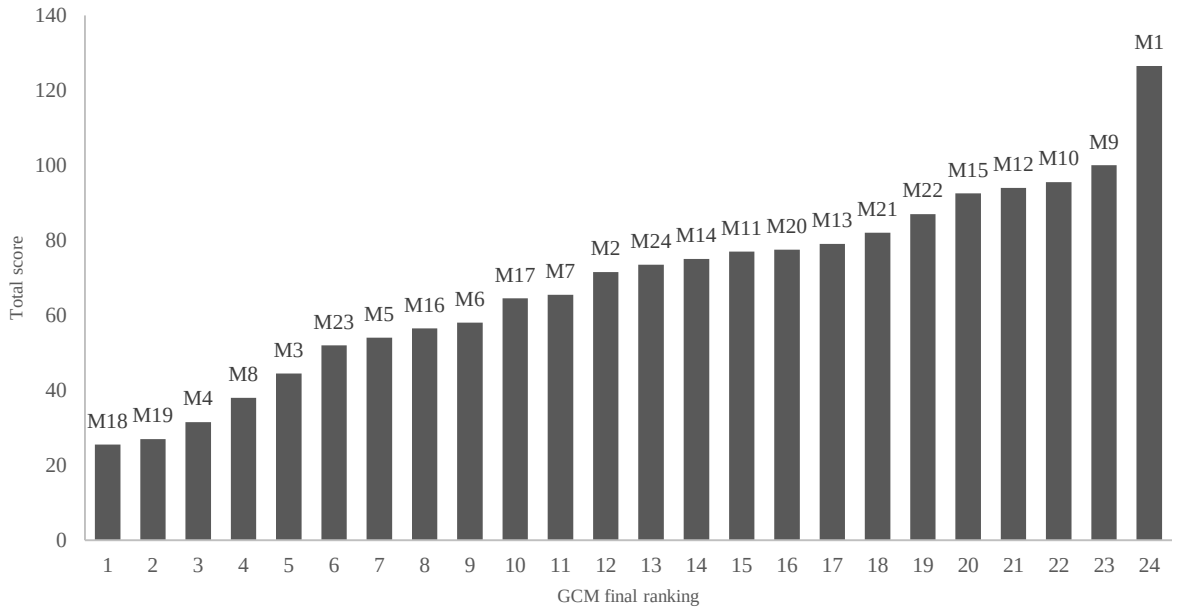

Figure 20 GCMs ranking results for the Northern climatic region under RCP2.6 climate change scenario.

Considering the results of the BS and S_{score} analyses (Table 11), M20 is the best performing model for the Northern climatic region under RCP 2.6 forcing scenario, while M9 is the worst performing. BS values ranged from 0.0049 to 0.0803, where a smaller value indicates a better replication of observed data. S_{score} values ranged from 64.9% to 89.9%, where models with a higher score show more overlap with the historical climate patterns. The S_{score} quantifies the overlap between the GCMs PDFs and the PDF produced by observed values of rainfall. The top three datasets selected for modeling under the RCP2.6 scenario for Northern climatic region are M18, M19, and M4. These models produced BS values of 0.0097, 0.0146, and 0.0105, respectively. Their S_{score} values were 82.7%, 82.1%, and 83.9 %, respectively, and they are considered to accurately represent the regional climate system (Perkins et al.,2007). These results emphasize the need for comprehensives GCMs analysis using probability density functions. Model M19 out of the top three performing GCMs according to the BS and S_{score} analyses was

determined to have high mean relative error. On the other hand, some other models had good performance in term of replicating observed data mean, correlation, and NRMSE, but they failed to characterize the probabilistic patterns of the historical data. Figure 21 shows the cumulative probability distribution for the best and worst GCMs compared to the observed rainfall data. Statistical analysis results for other RCP scenarios in the Northern climatic region are shown the Appendix. Table 12 summarizes the selected GCMs models for the sake of climate change analysis in the Northern climatic region.

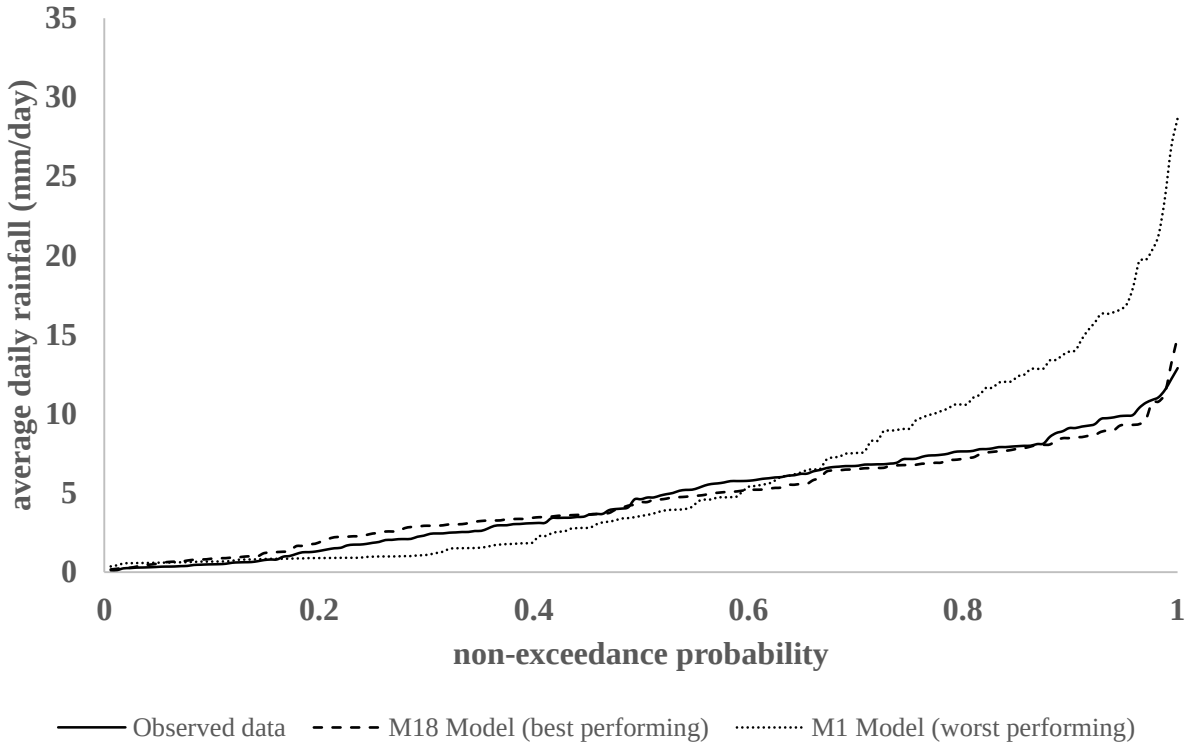

Figure 21 Cumulative probability distributions for the best and the worst performing GCMs under RCP2.6 forcing scenario for the Northern climatic region compared to the observed data.

Table 12 Accepted GCMs for the Northern climatic region.

RCP forcing scenario	Accepted GCMs ID
RCP2.6	M18, M19, M4
RCP4.5	M19, M8, M18
RCP6.0	M19, M18, M4
RCP8.5	M19, M8, M4

4.2.2.2 Top Performing GCMs for Southern Climatic Region

The CMIP5 GCMs output for Southern climatic Region results are presented in this section. Table 13 shows the monthly mean, monthly standard deviation, NRMSE, relative error, BS, and S_{score} for each of the GCMs analyzed for Southern climatic Region State under the RCP2.6 forcing scenario.

Table 13 GCMs statistical assessment for the Southern climatic region under RCP2.6 scenario.

Model ID	Correlation	Rank	Mean RE		St Dev RE		SSE	NRMSE	Rank
1	0.154	23	0.106	6	0.693	21	4239.18	1.814	22
2	0.462	4	0.136	11	0.019	1	1461.23	1.065	3
3	0.333	10	0.095	5	0.258	9	2229.70	1.316	4
4	0.457	5	0.585	24	0.492	15	3948.07	1.751	19
5	0.186	21	0.031	2	0.304	10	2778.35	1.469	12
6	0.454	6	0.136	10	0.570	19	2641.86	1.432	9
7	0.239	16	0.008	1	0.170	5	2267.86	1.327	5
8	0.418	9	0.263	17	0.863	23	3975.90	1.757	20
9	0.217	18	0.162	12	0.548	18	3536.31	1.657	17
10	0.251	14	0.267	18	0.486	14	3420.19	1.629	16
11	0.210	19	0.308	19	0.680	20	4349.78	1.838	23
12	0.314	11	0.068	4	0.422	11	2689.70	1.445	10
13	0.087	24	0.533	23	0.450	13	4842.46	1.939	24
14	0.268	13	0.122	9	0.544	17	3272.48	1.594	15
15	0.422	8	0.315	20	0.850	22	4052.56	1.774	21
16	0.526	1	0.251	16	0.516	16	2432.74	1.374	7
17	0.434	7	0.194	13	0.207	6	1355.25	1.026	2
18	0.293	12	0.248	15	0.160	4	2376.26	1.358	6
19	0.465	3	0.120	8	0.217	7	1175.86	0.955	1
20	0.197	20	0.427	21	0.043	2	2784.73	1.470	13

21	0.170	22	0.433	22	0.143	3	2690.44	1.445	11
22	0.486	2	0.228	14	0.898	24	3699.06	1.695	18
23	0.220	17	0.057	3	0.445	12	3086.98	1.548	14
24	0.242	15	0.120	7	0.248	8	2515.65	1.397	8

Model ID	**Mann-Kendall Slope**	**Mann Kendall RE**	**Rank**	**BS (%)**	**Rank**	**S score**	**Rank**	**Total score**	**Final Rank**
M1	-0.0083	6.545	20	0.1291	24	0.554	24	106	24
M2	0.0046	5.182	16	0.0198	13	0.780	11	39	4
M3	-0.002	0.818	3	0.0141	5	0.821	5	34.5	3
M4	0.0051	5.636	17	0.0397	21	0.631	21	92.5	19
M5	0.0062	6.636	21	0.0110	3	0.827	4	59	8
M6	0.0029	3.636	12	0.0195	12	0.821	5	58.5	7
M7	0.0022	3.000	9	0.0187	11	0.768	14	44	6
M8	0.0105	10.545	22	0.0808	23	0.577	23	103	23
M9	0.0018	2.636	8	0.0156	7	0.798	8	76.5	16
M10	0.0056	6.091	19	0.0110	4	0.815	7	77	17
M11	0.0121	12.000	24	0.0098	2	0.827	3	95.5	20
M12	-0.0033	2.000	7	0.0150	6	0.833	2	43.5	5
M13	0.004	4.636	15	0.0181	10	0.792	9	101	21
M14	-0.0011	0.000	1	0.0204	15	0.768	13	68.5	12
M15	0.0109	10.909	23	0.0288	18	0.702	19	101	21
M16	-0.0002	0.818	4	0.0363	20	0.696	20	62	10
M17	0.0007	1.636	6	0.0079	1	0.851	1	32	1
M18	0.0054	5.909	18	0.0767	22	0.625	22	68	11
M19	0.0023	3.091	10	0.0165	8	0.792	9	32.5	2
M20	-0.0025	1.273	5	0.0200	14	0.756	15	73	15
M21	-0.001	0.091	2	0.0181	9	0.750	17	72	14
M22	0.0031	3.818	13	0.0265	17	0.744	18	82	18
M23	0.0028	3.545	11	0.0317	19	0.756	15	68.5	12
M24	0.0034	4.091	14	0.0260	16	0.774	12	59	8

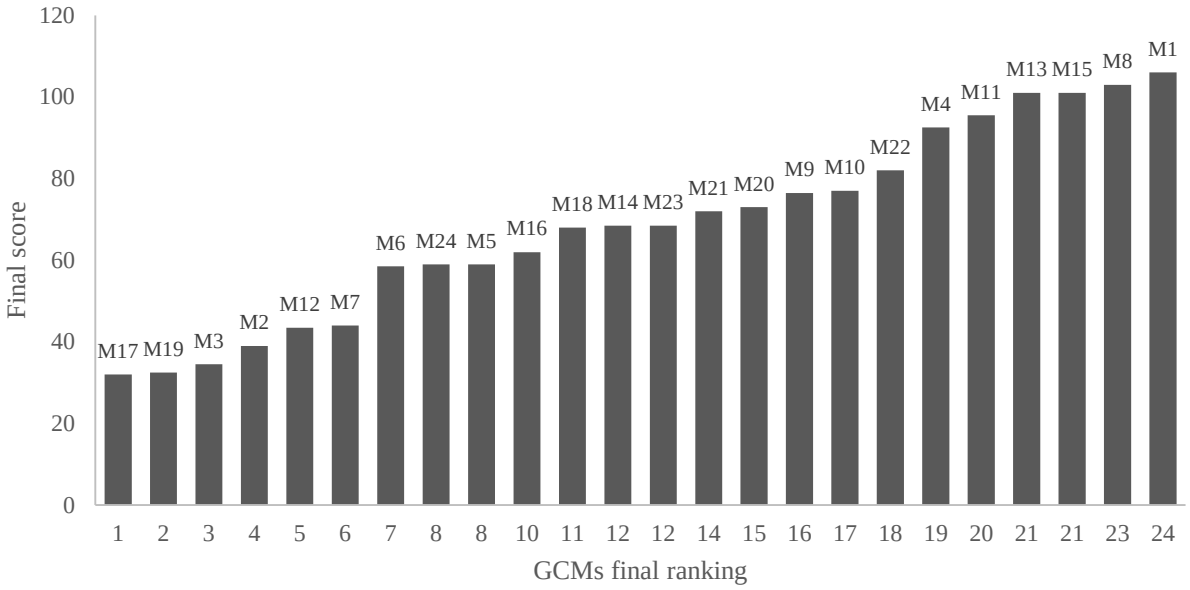

Figure 22 GCMs ranking results for the Southern climatic region under RCP2.6 climate change scenario.

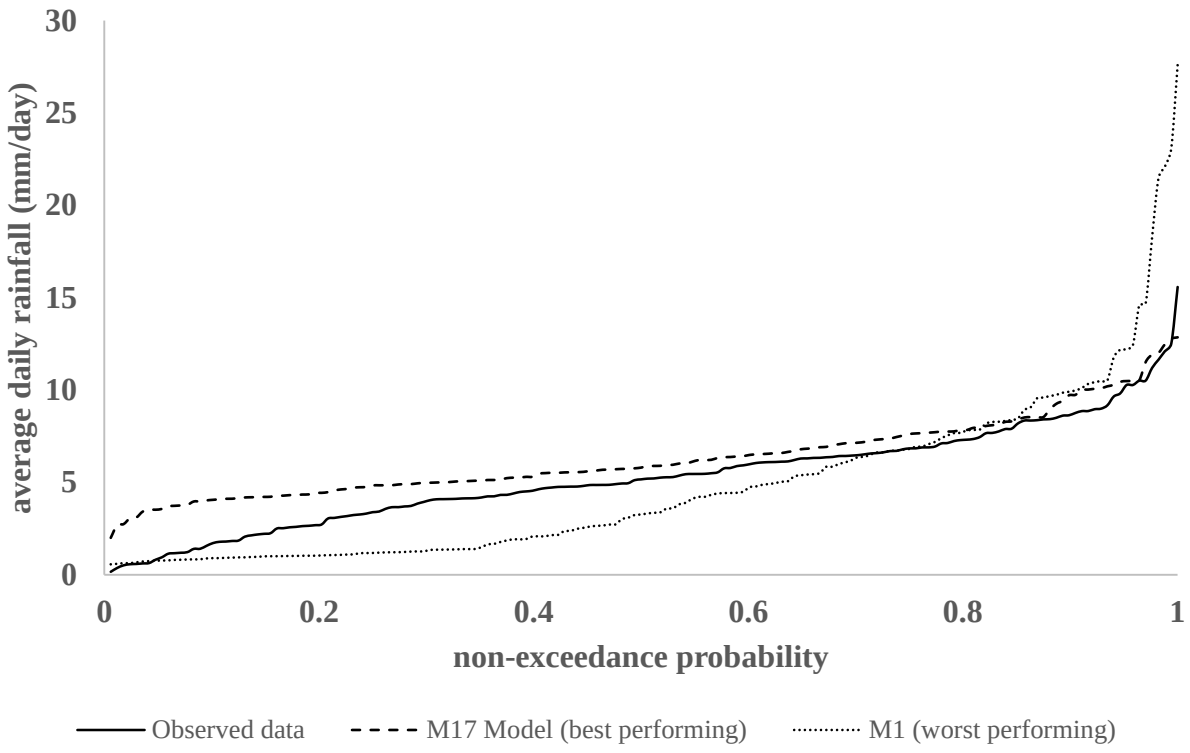

Figure 23 cumulative probability distributions for the best and the worst performing GCMs under RCP2.6 forcing scenario for the Southern climatic region compared to the observed data.

Considering the results of the BS and S_{score} analyses, M17 is the best performing model for the Southern climatic region under RCP 2.6 forcing scenario, while M1 is the worst performing. BS values ranged from 0.0079 to 0.1291, where a smaller value indicates a better replication of observed data. S_{score} values ranged from 55.35% to 85.12%, where models with a higher score show more overlap with the historical climate patterns. The top three datasets selected for modeling under the RCP2.6 scenario for Southern climatic region are M17, M19, and M3. These models produced BS values of 0.0097, 0.0146, and 0.0105, respectively. Their S_{score} values were 85.1%, 79.2%, and 82.1 %, respectively. Though the S_{score} for model M19 is slightly below 80%, we can still accept it due to its overall performance in other statistical measures. Statistical analysis results for other RCP scenarios in the Southern climatic region are shown the Appendix.

Table 14 Accepted GCMs for the Southern climatic region.

RCP forcing scenario	Accepted GCMs ID
RCP2.6	M17, M19, M3
RCP4.5	M3, M12, M7
RCP6.0	M3, M19, M2
RCP8.5	M3, M7, M2

4.3 2017-2050 Simulations to assess influence of Future Rainfall Patterns on Groundwater Dynamics

4.3.1 Methods

Future simulated climate data was extracted from the CMIP5 database and statistically assessed and ranked for four representative concentration pathway (RCP) forcing scenarios. The top three CMIP5 GCMs were chosen for each RCP forcing scenario for use in the future

SEAWAT model simulations, extending from 2017 to 2050. The top three models chosen have the ability to accurately replicate historical climate patterns, and hence, they are reliable in forecasting future conditions.

The depth of recharge to the freshwater lens was calculated for each month of the study period using constant percentages for each region following the same methodology described in Chapter 3. Future recharges for each forcing RCP scenario were assigned to the calibrated models for each island. The baseline salt concentrations for each grid-cells were assigned for each simulation as the initial condition. The future climatic models were run for four years (2013-2017) to allow salt concentration and groundwater heads to spin-up. The results of the future models runs are presented in the following sub-sections to give a detailed overview of how variable climate conditions may affect the fresh groundwater availability in both the Northern and the Southern climatic regions of the Republic of Maldives atoll islands in next few decades.

4.3.2 Results

4.3.2.1 Simulated Lens Volume for the RCP2.6 Forcing Scenario

Simulation results for available fresh groundwater volume for all islands in both climatic region are presented in this section for the period of 2017-2050 under the RCP2.6 forcing scenario. The best three climatic models resulted from the statistical assessment in a previous section are employed to calculate recharge forcing for the models. Figures 24-25 show the time series fluctuation for the fresh groundwater volumes in all islands as well as the frequency distribution plots. Table 15 shows the fresh groundwater lens statistics for the each island.

Table 15 Summary statistics of freshwater lens volume (in million cubic meters) during the 2017-2050 period for the selected islands under RCP2.6 climate change scenario.

Island	GCM ID	Min	Max	Mean	Median
N. Holhudhoo	M18	0.184	0.474	0.310	0.301
	M19	0.123	0.281	0.210	0.212
	M4	0.096	0.261	0.194	0.198
N. Velidhoo	M18	0.674	1.434	1.020	1.017
	M19	0.600	1.056	0.822	0.826
	M4	0.636	0.962	0.796	0.794
GDh. Thinadhoo	M17	5.43	7.58	6.55	6.57
	M19	4.88	7.10	5.92	5.94
	M3	5.07	7.26	6.00	6.00
L. Gan	M17	48.94	63.04	56.19	56.06
	M19	44.94	58.75	51.82	51.65
	M3	45.09	61.18	51.83	51.84

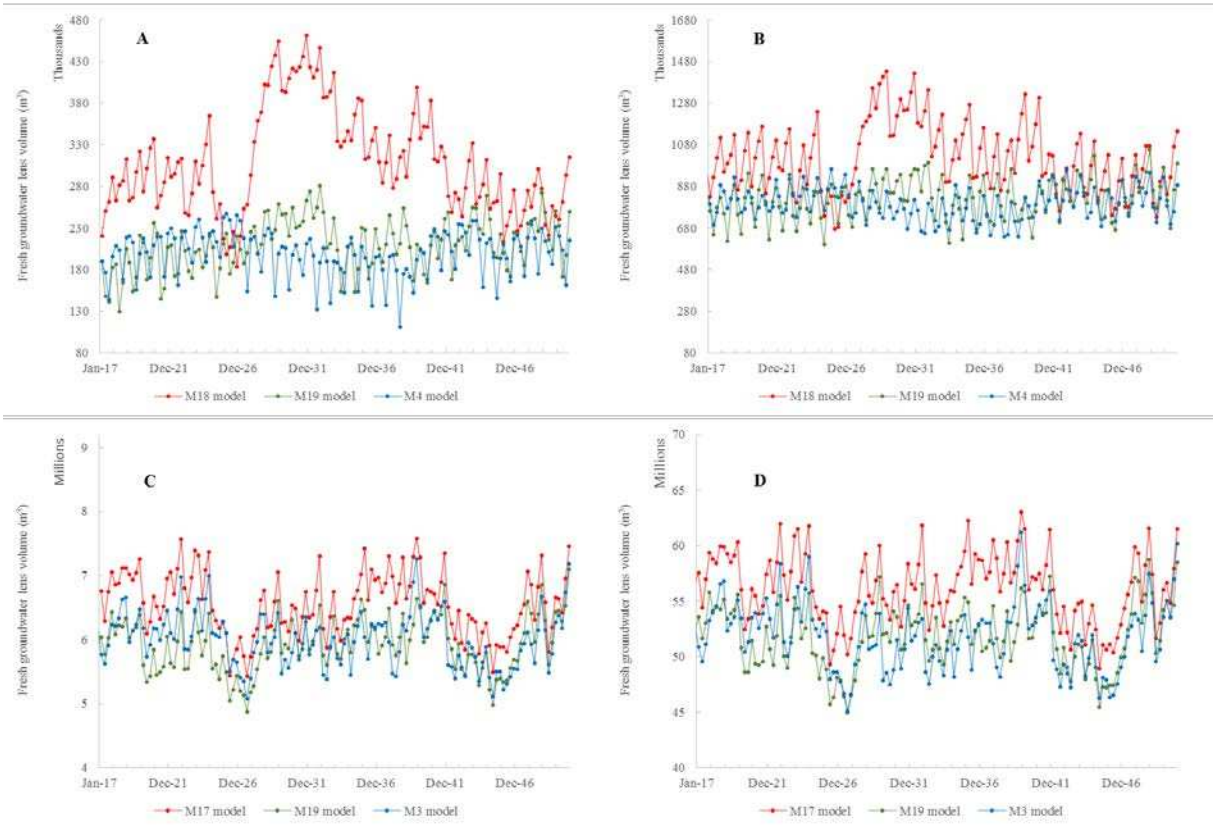

Figure 24 Time series of the fluctuation in freshwater lens volume in: **A**. N. Holhudhoo, **B**. N. Velidhoo. **C**. GDh. Thinadhoo, and **D**. L. Gan for the period between 2010-2050 under RCP2.6 climate change scanario.

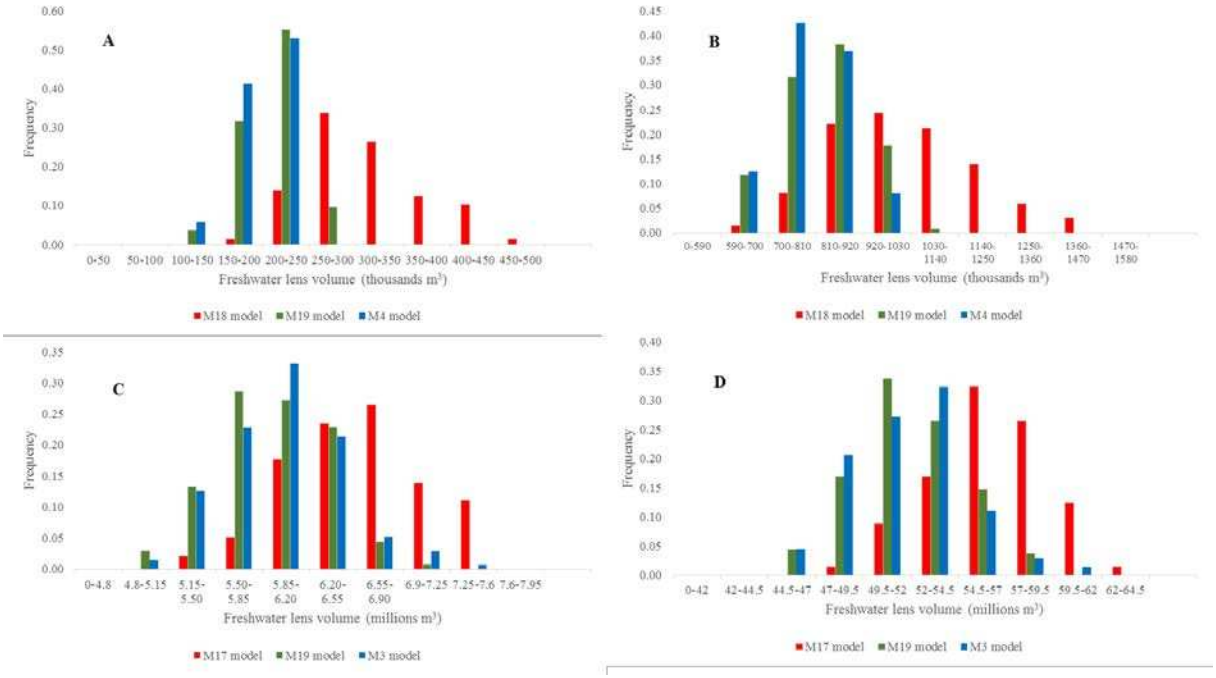

Figure 25 Frequency distribution fot the freshwater lens volume in: **A**. N. Holhudhoo, **B**. N. Velidhoo. **C**. GDh. Thinadhoo, and **D**. L. Gan for the period between 2010-2050 under RCP2.6 climate change scanario.

Figure 24A shows the time series fluctuation for fresh groundwater lens volume for N. Holhudhoo Island under different GCMs forcing in the RCP2.6 scenario. It is noted that there is a strong variability in the simulated lens volumes from different models for that small island in particular due to its small area and this makes it more vulnerable to climate change as it is strongly affected by changing rainfall patterns. Figure 25A shows the frequency distribution for the fresh groundwater volume in N. Holhudhoo Island. Mainly, the predicted fresh groundwater volumes in N. Holhudhoo Island are in the 150-250 thousand cubic meters range based on M19, and M4 models. Model M18 predicts freshwater volumes could reach up to 450 thousand cubic meters which is relatively a high forecast. Generally, fresh groundwater lens volume values are mostly clustered towards the center of the range of values and they can be classified as normally distributed.

Figure 24B corresponds to the time series fluctuation for fresh groundwater lens volume for N. Velidhoo Island under different GCMs forcing in the RCP2.6 scenario. It noted that the variability in the simulated lens volumes from different models is less than what is observed in N. Holhudhoo Island as N. Velidhoo Island is bigger in area. These results indicate that N. Velidhoo Island vulnerability to changing rainfall patterns less than N. Holhudhoo Island. Figure 25B shows the frequency distribution for the fresh groundwater volume for N. Velidhoo Island. Mainly, the predicted fresh groundwater volumes in N. Velidhoo Island are in the 700-1000 thousand cubic meters range based on M19, and M4 models. Model M18 is also predicting higher freshwater volumes could reach up to 1400 thousand cubic meters which is relatively a high forecast. The statistical analysis for different models outcomes shows that the median available fresh groundwater volume will not be deplete below 794 thousand cubic meters in worst cases. Figure 24C shows the time series fluctuation for fresh groundwater lens volume for GDh. Thinadhoo Island under different GCMs forcing in the RCP2.6 scenario. Unlike the northern region islands, it is observed that there is no strong variability in the simulated fresh lens volumes from different GCMs as GDh. Thinadhoo Island is a fairly big in area and this makes it less vulnerable to climate change as it slightly affected by changing rainfall patterns. Figure 25C shows the frequency distribution for the fresh groundwater volume for GDh. Thinadhoo Island. Mainly, the predicted fresh groundwater volumes are normally distributed and are in the 5-6 million cubic meters. Model M17 predicts that within more than 50% of the study period, the freshwater lens volume would be above the 6.5 million cubic meters mark.

Figure 24D corresponds to the time series fluctuation for fresh groundwater lens volume for L. Gan Island, the biggest modeled island, under different GCMs forcing in the RCP2.6 scenario. It noted that the variability in the simulated lens volumes from different models is less

than what is observed in the Northern climatic region islands. These results indicate L. Gan is less vulnerable to changing rainfall patterns as it has relatively a big area. Figure 25D shows the frequency distribution for the fresh groundwater volume in L. Gan Island. Generally, the predicted fresh groundwater volumes in L. Gan Island are in the 47-57 million cubic meters range as predicted by M19, and M3 models. Model M17 is predicting higher freshwater volumes could reach up to 64 million cubic meters threshold which is relatively a high forecast. The statistical analysis for different models outcomes shows that the median available fresh groundwater volume will not deplete below 44 million cubic meters in worst cases. Average volumes for L. Gan Island from different GCMs are between 51 and 56 million cubic meters.

4.3.2.2 Simulated Lens Volume for the RCP4.5 Forcing Scenario

Simulation results for available fresh groundwater volume for all islands in both climatic region are presented in this section for the period of 2017-2050 under the RCP4.5 forcing scenario. The best three climatic models resulted from the statistical assessment in a previous section are employed to calculate recharge forcing for the models. Figures 26-27 show the time series fluctuation for the fresh groundwater volumes in all islands as well as the frequency distribution plots. Table 16 shows the fresh groundwater lens statistics for the each island.

Results from the RCP4.5 forcing scenario presented in this section, which is an intermediate climate change scenario, where mitigation policies are imposed, in which Green House Gases emissions are restrained and the radiative forcing stabilizes at 4.5 W/m^2 at year 2100.

Table 16 Summary statistics of freshwater lens volume (in million cubic meters) during the 2017-2050 period for the selected islands under RCP4.5 climate change scenario.

Island	GCM ID	Min	Max	Mean	Median
N. Holhudhoo	M18	0.143	0.411	0.273	0.275
	M19	0.211	0.394	0.309	0.308
	M8	0.061	0.277	0.180	0.184
N. Velidhoo	M18	0.652	1.042	0.840	0.831
	M19	0.895	1.563	1.180	1.187
	M8	0.414	1.071	0.724	0.732
GDh. Thinadhoo	M12	4.82	6.92	5.93	5.96
	M7	4.46	6.85	5.69	5.68
	M3	5.04	7.31	6.12	6.13
L. Gan	M12	48.81	62.26	55.66	55.68
	M7	40.71	58.01	50.10	50.06
	M3	45.56	62.71	53.45	53.53

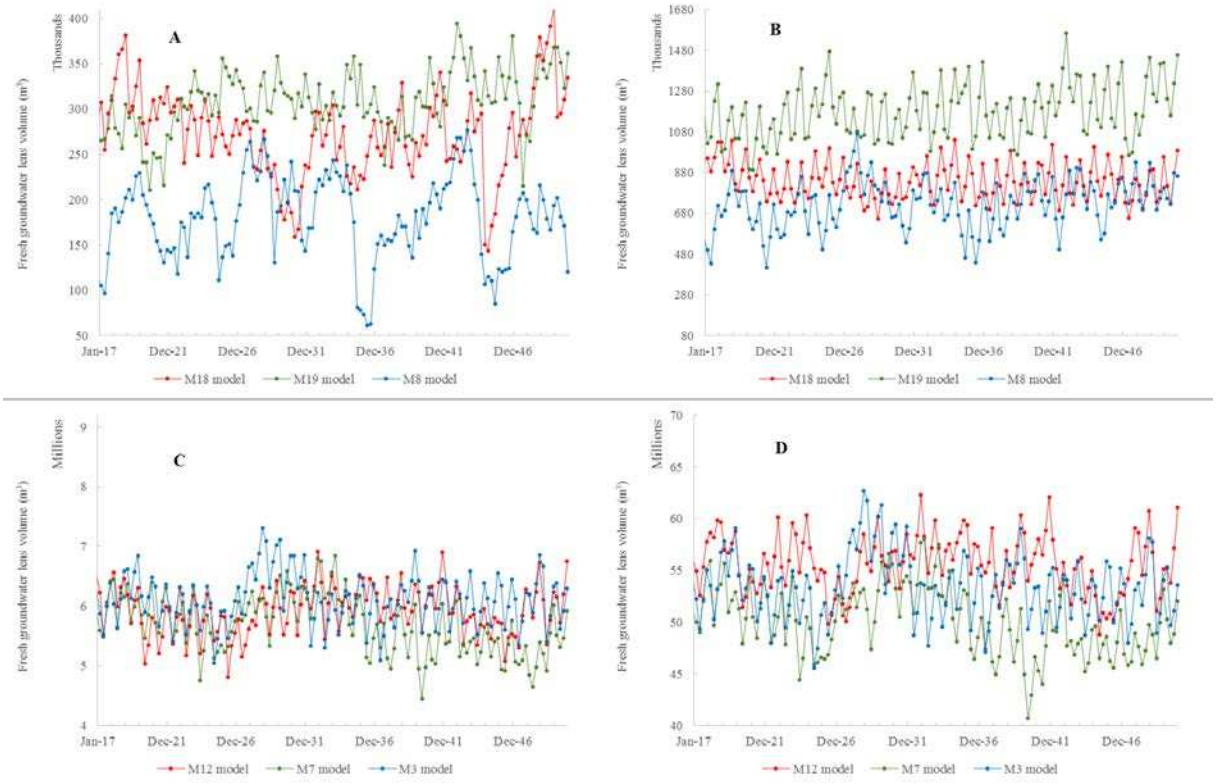

Figure 26 Time series of the fluctuation in freshwater lens volume in: **A**. N. Holhudhoo, **B**. N. Velidhoo. **C**. GDh. Thinadhoo, and **D**. L. Gan for the period between 2010-2050 under RCP4.5 climate change scanario.

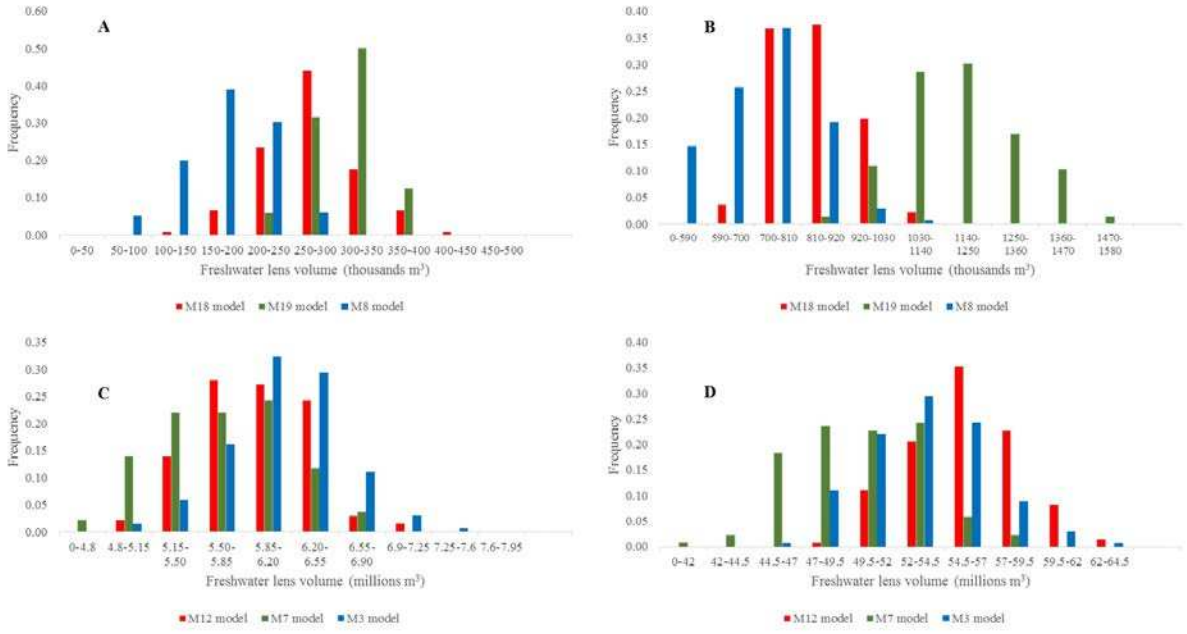

Figure 27 Frequency distribution fot the freshwater lens volume in: **A**. N. Holhudhoo, **B**. N. Velidhoo. **C**. GDh. Thinadhoo, and **D**. L. Gan for the period between 2010-2050 under RCP4.5 climate change scanario.

Figure 26A shows the time series fluctuation for fresh groundwater lens volume for N. Holhudhoo Island under different GCMs forcing in the RCP4.5 scenario. It is observed in this forcing scenario that there is a strong variability in the simulated lens volumes from different models for that small island in particular due to its small area which emphasizes the observed response for the fresh groundwater lens found in RCP2.6 forcing scenario and this makes this small island more prone to climate change effects as it strongly affected by changing rainfall patterns. Model M8 predicts heavy drought periods where freshwater lens could drop below 80 thousand cubic meters, which puts the availability of freshwater in this island under a serious threat. Figure 27A shows the frequency distribution for the fresh groundwater volume for N. Holhudhoo Island under RCP4.5 forcing scenario. Mainly, the predicted fresh groundwater volumes in N. Holhudhoo Island are in the 150-250 thousand cubic meters range, however, the

worst long term freshwater lens average predicted by RCP4.5 models is 180 thousand cubic meters which is the worst long term average predicted by all RCP scenarios.

Figure 26B shows to the time series fluctuation for fresh groundwater lens volume for N. Velidhoo Island under different GCMs forcing in the RCP4.5 scenario. It noted that the model M19 is constantly overestimate available freshwater other than the other two models (M18 and M8). Figure 27B shows the frequency distribution for the fresh groundwater volume for N. Velidhoo Island. Mainly, the predicted fresh groundwater volumes in N. Velidhoo Island are in the 600-1000 thousand cubic meters range from M18, and M8 models. Model M18 is predicting higher freshwater volumes with median volume exceeds 1150 thousand cubic meters which is relatively a high forecast. The statistical analysis for different models outcomes shows that the median available fresh groundwater volume will not be deplete below approximately 414 thousand cubic meters in worst cases which is less than what is predicted by RCP2.6.
Figure 26C shows the time series fluctuation for fresh groundwater lens volume for GDh. Thinadhoo Island under different GCMs forcing in the RCP4.5 scenario. There is no strong variability in the simulated lens volumes from different as GDh. Thinadhoo Island and the volume of the freshwater lens is fairly big in approximately all simulation period in under all models forcing, except a notable lens depletion forecasted by M7 models where lens volume could deplete slightly below 4.5 million cubic meters. Figure 27C shows the frequency distribution for the fresh groundwater volume for GDh. Thinadhoo Island. Mainly, the predicted fresh groundwater volumes are normally distributed and are clustered in the 5-7 million cubic meters bins. Model M3 predicts that freshwater volumes in the study period would be higher than other two models forecasts, hence the frequency distribution for M3 is skewed to the right. The freshwater lens volume would be above the 5.6 million cubic meters mark more than half of

the study period. Figure 27D shows to the time series fluctuation for fresh groundwater lens volume for L. Gan Island, the biggest modeled island, under different GCMs forcing in the RCP4.5 scenario. Different GCMs forecasts are bracketing future predicted freshwater volume between 40 and 63 million cubic meters. Model M7 forecasts that L. Gan Island may undergo a severe drought condition where freshwater lens may drop as low as 40 million cubic meters. Figure 28D shows the frequency distribution for the fresh groundwater volume in L. Gan Island. Generally, the predicted fresh groundwater volumes in L. Gan Island are above 50 million cubic meters mark most of the study period. Models M12, and M3 forecasts that the freshwater lens could exceed the 62 million cubic meters.

4.3.2.3 Simulated Lens Volume for the RCP6.0 Forcing Scenario

Simulation results for available fresh groundwater volume for all islands in both climatic region are presented in this section for the period of 2017-2050 under the RCP6.0 forcing scenario. The best three climatic models resulted from the statistical assessment in a previous section are employed to calculate recharge forcing for the models. Figures 28-29 show the time series fluctuation for the fresh groundwater volumes in all islands as well as the frequency distribution plots. Table 17 shows the fresh groundwater lens statistics for the each island. Results from the RCP6.0 forcing scenario presented in this section, which is another intermediate climate change scenario, where mitigation policies are imposed, in which Green House Gases emissions are restrained and the radiative forcing stabilizes at 6.0 W/m^2 after 2100.

Table 17 Summary statistics of freshwater lens volume (in million cubic meters) during the 2017-2050 period for the selected islands under RCP6.0 climate change scenario.

Island	GCM ID	Min	Max	Mean	Median
N. Holhudhoo	M18	0.162	0.422	0.300	0.304
	M19	0.210	0.416	0.315	0.313
	M4	0.132	0.239	0.195	0.202
N. Velidhoo	M18	0.631	1.393	1.008	1.013
	M19	0.884	1.585	1.187	1.187
	M4	0.657	0.938	0.785	0.781
GDh. Thinadhoo	M2	4.11	6.11	5.00	4.98
	M19	4.69	6.55	5.62	5.61
	M3	4.79	7.42	6.08	6.12
L. Gan	M2	38.93	53.28	44.99	44.92
	M19	41.35	55.26	48.14	48.17
	M3	43.57	61.77	52.58	52.73

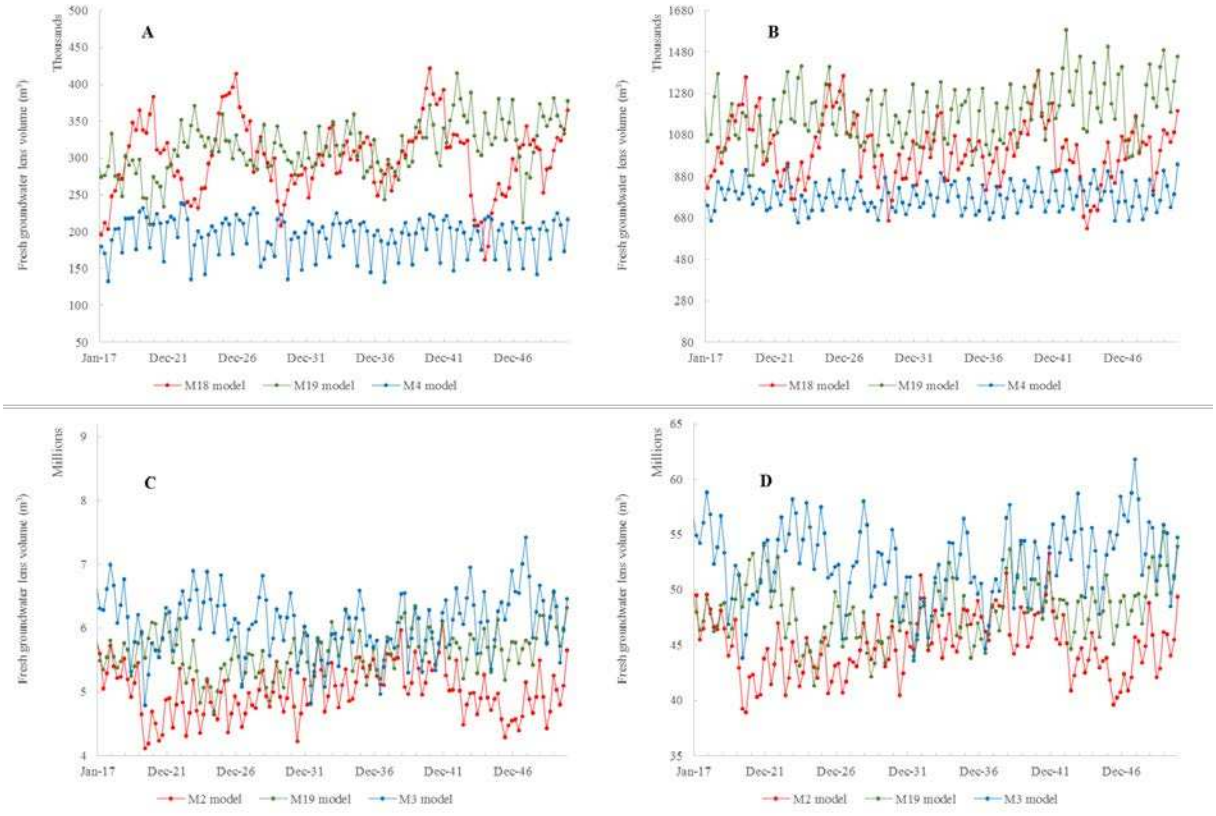

Figure 28 Time series of the fluctuation in freshwater lens volume in: **A**. N. Holhudhoo, **B**. N. Velidhoo. **C**. GDh. Thinadhoo, and **D**. L. Gan for the period between 2010-2050 under RCP6.0 climate change scanario.

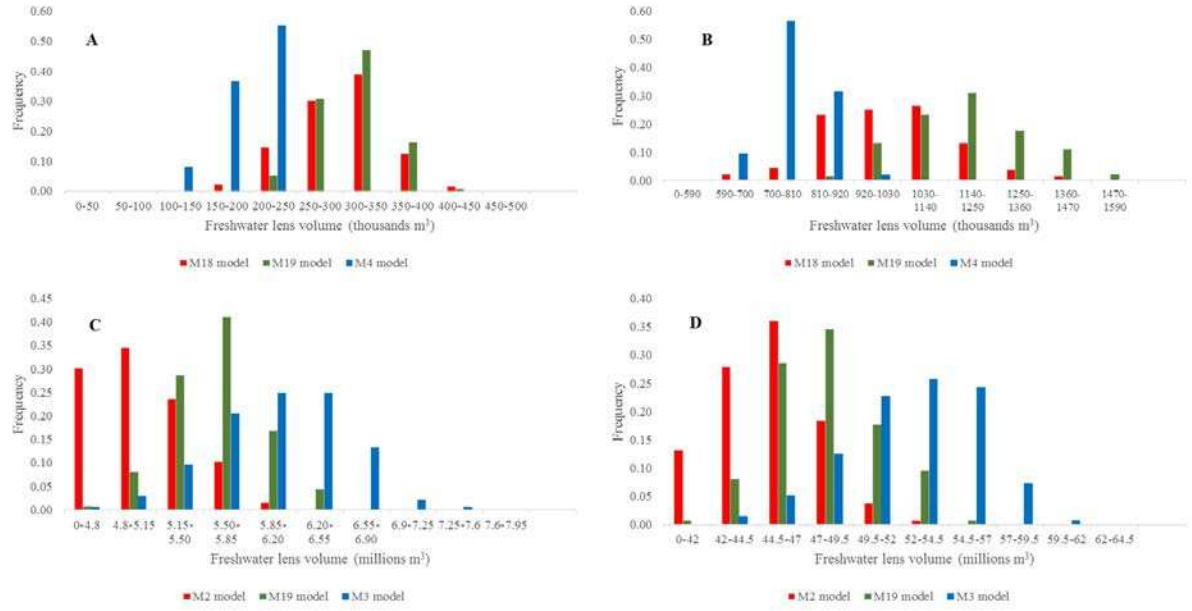

Figure 29 Frequency distribution fot the freshwater lens volume in: **A**. N. Holhudhoo, **B**. N. Velidhoo. **C**. GDh. Thinadhoo, and **D**. L. Gan for the period between 2010-2050 under RCP6.0 climate change scanario.

Figure 28A shows the time series fluctuation for fresh groundwater lens volume for N. Holhudhoo Island under different GCMs forcing in the RCP6.0 scenario. It is observed that in this forcing scenario, there is also a strong variability in the simulated lens volumes from different models for that small island in particular due to its small area which emphasizes the observed response of the fresh groundwater lens found in in RCP2.6 forcing scenario, and RCP4.5 forcing scenario and this makes this small island more prone to climate change effects as it strongly affected by changing rainfall patterns. Model M18 predicts intermittent relative drought periods, however freshwater lens volume in these drought periods is approximately 200 thousand cubic meters which is comparable to what other models predict for the same island in wet seasons. This observation reflects the high variability in forecasts associated with N. Holhudhoo Island due to its small land area. Figure 29A shows the frequency distribution for the fresh groundwater volume for N. Holhudhoo Island under RCP6.0 forcing scenario. Mainly, the predicted fresh groundwater volumes in N. Holhudhoo Island are in the 200-300 thousand cubic

meters range, however, the worst long term freshwater lens average predicted by RCP6.0 models is 195 thousand cubic meters which is slightly below than the worst long term average predicted by RCP2.6 models.

Figure 28B shows to the time series fluctuation for fresh groundwater lens volume for N. Velidhoo Island under different GCMs forcing in the RCP6.0 scenario. It noted that the model M4 is generally underestimating available freshwater other than the other two models (M18 and M19). Figure 29B shows the frequency distribution for the fresh groundwater volume for N. Velidhoo Island. Mainly, the predicted fresh groundwater volumes in N. Velidhoo Island are in the 800-1250 thousand cubic meters. Model M19 is predicting higher freshwater volumes with median volume exceeds 1180 thousand cubic meters which is relatively high forecast. The statistical analysis for different models outcomes shows that the median available fresh groundwater volume will not be deplete below approximately 631 thousand cubic meters in worst cases which is better than the minimum value predicted from RCP2.6.

Figure 28C shows the time series fluctuation for fresh groundwater lens volume for GDh. Thinadhoo Island under different GCMs forcing in the RCP6.0 scenario. Unlike the northern region islands, GDh. Thinadhoo Island has a fairly large volume of freshwater in approximately all simulation period in under all models forcing, except a notable lens depletion forecasted by M2 models where lens volume could be as low as 4.0 million cubic meters. Figure 29C shows the frequency distribution for the fresh groundwater volume for GDh. Thinadhoo Island. Mainly, the predicted fresh groundwater volumes are normally distributed and are clustered in the 5-6 million cubic meters bins. Model M3 forecasts freshwater volumes in the study period would be higher than other two models forecasts, hence the frequency distribution for M3 is skewed to the

right. The freshwater lens volume would be above the 4.98 million cubic meters mark more than half of the study period.

Figure 28D shows to the time series fluctuation for fresh groundwater lens volume for L. Gan Island under different GCMs forcing in the RCP6.0 scenario. Different GCMs forecasts are bracketing future predicted freshwater volume between 38.9 and 61.7 million cubic meters. Model M2 forecasts that L. Gan Island may undergo severe drought conditions where freshwater lens may drop below 39 million cubic meters. Figure 29D shows the frequency distribution for the fresh groundwater volume in L. Gan Island. Generally, the predicted fresh groundwater volumes in L. Gan Island are above 45 million cubic meters mark most of the study period. Model M3 forecasts that the freshwater lens could exceed the 61 million cubic meters.

4.3.2.4 Simulated Lens Volume for the RCP8.5 Forcing Scenario

Simulation results for available fresh groundwater volume for all islands in both climatic region are presented in this section for the period of 2017-2050 under the RCP8.5 forcing scenario. The best three climatic models resulted from the statistical assessment in a previous section are employed to calculate recharge forcing for the models. Figures 30-31 show the time series fluctuation for the fresh groundwater volumes in all islands as well as the frequency distribution plots. Table 18 shows the fresh groundwater lens statistics for the each island. Results from the RCP8.5 forcing scenario presented in this section, which is the high emission climate change scenario, where radiative forcing is expected to reach 8.5 W/m^2 by year 2100.

Table 18 Summary statistics freshwater lens volume (in million cubic meters) during the 2017-2050 period for the selected islands under RCP8.5 climate change scenario.

Island	GCM ID	Min	Max	Mean	Median
N. Holhudhoo	M8	0.068	0.292	0.181	0.184
	M19	0.226	0.398	0.314	0.312
	M4	0.113	0.245	0.199	0.205
N. Velidhoo	M8	0.402	1.089	0.738	0.734
	M19	0.901	1.497	1.174	1.172
	M4	0.636	0.972	0.799	0.800
GDh. Thinadhoo	M2	3.96	5.95	4.99	4.98
	M7	5.13	7.39	6.15	6.10
	M3	5.07	7.26	6.00	6.00
L. Gan	M2	37.47	51.95	44.72	44.71
	M7	45.75	61.80	52.86	52.95
	M3	45.09	61.18	51.83	51.84

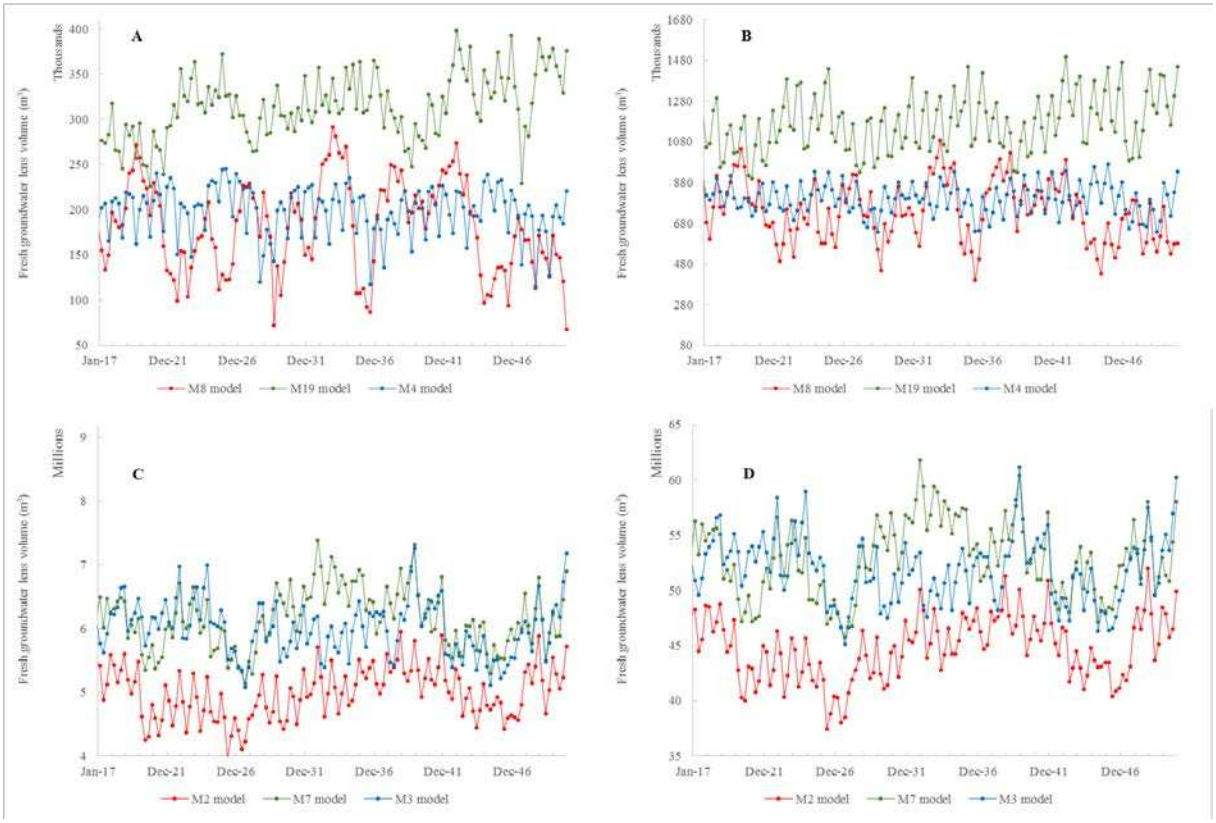

Figure 30 Time series of the fluctuation in freshwater lens volume in: **A**. N. Holhudhoo, **B**. N. Velidhoo. **C**. GDh. Thinadhoo, and **D**. L. Gan for the period between 2010-2050 under RCP8.5 climate change scanario.

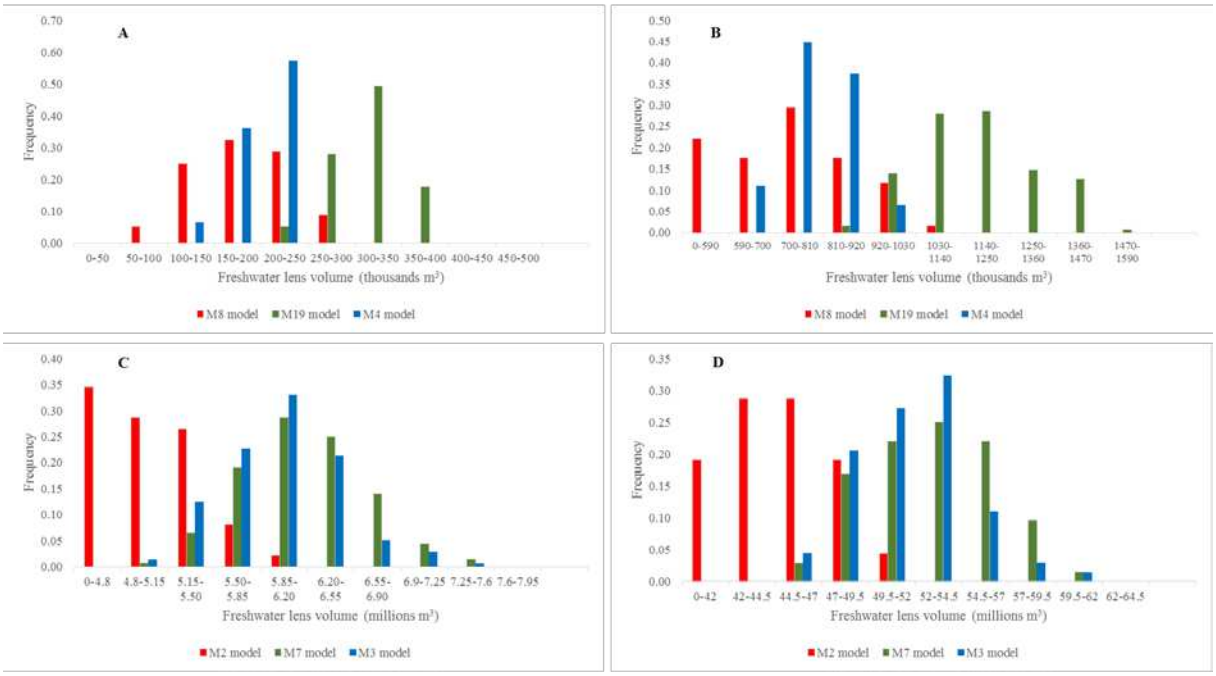

Figure 31 Frequency distribution fot the freshwater lens volume in: **A**. N. Holhudhoo, **B**. N. Velidhoo. **C**. GDh. Thinadhoo, and **D**. L. Gan for the period between 2010-2050 under RCP8.5 climate change scanario.

Figure 30A shows the time series fluctuation for fresh groundwater lens volume for N. Holhudhoo Island under different GCMs forcing in the RCP8.5 scenario. There are big differences in forecasts produced by different GCMs forcing which emphasizes what was observed for the same island in other RCP scenarios simulated. This strong variability makes this small island more prone to climate change effects as it strongly affected by changing rainfall patterns. Model M8 predicts intermittent relatively severe drought periods where fresh lens volume may drop to 50 thousand cubic meters, on the other hand, M8 model predicts freshwater volume to be more than 250 thousand cubic meters in the wet seasons. This strong seasonality trend in the available freshwater lens volume urges the need of implementing water management practices to secure adequate freshwater reserves in severe drought conditions. Figure 31A shows the frequency distribution for the fresh groundwater volume for N. Holhudhoo Island under RCP8.5 forcing scenario. Mainly, the predicted fresh groundwater volumes in N. Holhudhoo

Island are in the 200-300 thousand cubic meters range, however, the worst long term freshwater lens average predicted by RCP8.5 models is 181 thousand cubic meters which is slightly below than the worst long term average predicted by RCP2.6 models.

Figure 30B shows the time series fluctuation for fresh groundwater lens volume for N. Velidhoo Island under different GCMs forcing in the RCP8.5 scenario. It noted that the model M19 is generally overestimating available freshwater other than the other two models (M8 and M4). Model M8 predicts that the freshwater lens volume would have a strong seasonality trend. Figure 31B shows the frequency distribution for the fresh groundwater volume for N. Velidhoo Island. Mainly, the predicted fresh groundwater volumes in N. Velidhoo Island are in the 700-1000 thousand cubic meters. The statistical analysis for different models outcomes shows that the minimum available fresh groundwater volume will not be deplete below approximately 400 thousand cubic meters in worst cases which is 30% less than the minimum value predicted from RCP2.6 forcing scenario. The difference in minimum values shows the urgent need of imposing climate change mitigation, and emission control policies in the study area.

Figure 30C shows the time series fluctuation for fresh groundwater lens volume for GDh. Thinadhoo Island under different GCMs forcing in the RCP8.5 scenario. It is observed that there uncertainties in predicting freshwater lens volumes. While model M2 forecast that freshwater lens volume could drop to the 4 million cubic meters mark, models M7 and M3 forecast the freshwater lens will not drop below the 5 million cubic meters threshold. These uncertainties in models forecasts come from uncertainties in expected rainfall (freshwater forcing) that the island would receive if no climate change mitigation policies were imposed. Figure 31C shows the frequency distribution for the fresh groundwater volume for GDh. Thinadhoo Island. Mainly, the predicted fresh groundwater volumes are normally distributed and are clustered in the 4-6

million cubic meters bins and are normally distributed. The statistical analysis for different models outcomes shows that the median freshwater lens volume would not be less than 4.978 million cubic meters.

Figure 30D shows to the time series fluctuation for fresh groundwater lens volume for L. Gan Island under different GCMs forcing in the RCP8.5 scenario. Different GCMs forecasts are showing that future predicted freshwater volume could drop to 37.4 million cubic meters and this value the minimum value in all forecasts under all forcing scenarios and is 17% less than the minimum freshwater lens value forecasted by RCP2.6 scenario. Figure 31D shows the frequency distribution for the fresh groundwater volume L. Gan. Generally, in this high emission scenario, the distribution of the freshwater volume is clustered in the minimum range and lens volumes below 45 million cubic meters would become more frequent.

4.3.2.5 Results Uncertainty

As shown in the previous sections, simulations results for the future status of the freshwater volume showed considerable ranges of variability. Results for smaller islands showed stronger trends of variability which emerges the issue of forecasts reliability. In this section, results statistics for each modeled are grouped and shown in Tables 19-22 to get a better interception. This is important because the scenario that will actually happen is not known, and hence the 12 model simulations (4 RCPs, with 3 GCMs each) span the probable range of future lens volume possibilities. This may also quantify the wide uncertainty in future groundwater supply.

Table 19 Simulated freshwater lens volume (in million cubic meters) statistics for N. Holhudhoo Island under all RCPs scenarios.

RCP	GCM ID	Min	Max	Mean	Median	Std. Dev.
2.6	M18	0.184	0.461	0.310	0.301	0.062
	M19	0.130	0.281	0.210	0.210	0.031
	M4	0.111	0.247	0.199	0.203	0.027
4.5	M18	0.143	0.411	0.273	0.275	0.049
	M19	0.211	0.394	0.309	0.308	0.035
	M8	0.061	0.277	0.180	0.184	0.046
6.0	M18	0.162	0.422	0.300	0.304	0.050
	M19	0.210	0.416	0.315	0.313	0.036
	M4	0.132	0.239	0.195	0.202	0.025
8.5	M18	0.068	0.292	0.181	0.184	0.050
	M19	0.226	0.398	0.314	0.312	0.036
	M4	0.113	0.245	0.199	0.205	0.028

Table 20 Simulated freshwater lens volume (in million cubic meters) statistics for N. Velidhoo Island under all RCPs scenarios.

RCP	GCM ID	Min	Max	Mean	Median	Std. Dev
2.6	M18	0.674	1.434	1.020	1.017	0.168
	M19	0.600	1.056	0.822	0.826	0.098
	M4	0.636	0.962	0.796	0.794	0.077
4.5	M18	0.652	1.042	0.840	0.831	0.091
	M19	0.895	1.563	1.180	1.187	0.137
	M8	0.414	1.071	0.724	0.732	0.120
6.0	M18	0.631	1.393	1.008	1.013	0.150
	M19	0.884	1.585	1.187	1.187	0.141
	M4	0.657	0.938	0.785	0.781	0.067

	M18	0.402	1.089	0.738	0.734	0.147
8.5	M19	0.901	1.497	1.174	1.172	0.141
	M4	0.636	0.972	0.799	0.800	0.076

Table 21 Simulated freshwater lens statistics volume (in million cubic meters) for GDh. Thinadhoo Island under all RCPs scenarios.

RCP	**GCM ID**	**Min**	**Max**	**Mean**	**Median**	**Std. Dev**
	M17	5.43	7.58	6.55	6.57	0.48
2.6	M19	4.88	7.10	5.92	5.94	0.42
	M3	5.07	7.26	6.00	6.00	0.43
	M12	4.82	6.92	5.93	5.96	0.40
4.5	M7	4.46	6.85	5.69	5.68	0.49
	M3	5.04	7.31	6.12	6.13	0.43
	M2	4.11	6.11	5.00	4.98	0.40
6.0	M19	4.69	6.55	5.62	5.61	0.34
	M3	4.79	7.42	6.08	6.12	0.48
	M2	3.96	5.95	4.99	4.98	0.40
8.5	M7	5.13	7.39	6.15	6.11	0.47
	M3	5.07	7.26	6.00	6.00	0.43

Table 22 Simulated freshwater lens statistics volume (in million cubic meters) for L. Gan Island under all RCPs scenarios.

RCP	**GCM ID**	**Min**	**Max**	**Mean**	**Median**	**Std. Dev**
	M17	48.94	63.04	56.19	56.06	3.12
2.6	M19	44.94	58.75	51.82	51.65	2.86
	M3	45.09	61.18	51.83	51.84	3.05

	M12	48.81	62.26	55.66	55.68	2.80
4.5	M7	40.71	58.01	50.10	50.06	3.32
	M3	45.56	62.71	53.45	53.53	3.25
	M2	38.93	53.28	44.99	44.92	2.75
6.0	M19	41.35	55.26	48.14	48.17	2.75
	M3	43.57	61.77	52.58	52.73	3.49
	M2	37.47	51.95	44.72	44.71	2.87
8.5	M7	45.75	61.80	52.86	52.95	3.40
	M3	45.09	61.18	51.83	51.84	3.05

4.4 Discussion and Conclusion

The future volume of the freshwater lens provides water managers and policy makers on atoll islands nations with substantial information about water resources sustainability and sufficient living conditions. Annual recharge rates have significant effect in developing adequate freshwater volumes. If these rates drop below long term averages, the freshwater lens may become consistently too thin to support groundwater extraction as recharge rates may become insufficient to compensate extracted water volumes.

In this chapter, Global Circulation Models (GCMs) datasets were employed to investigate the potential effect of variable rainfall patterns, and consequently freshwater recharge rates, on the future status of freshwater lens in the atoll islands of the Republic of Maldives. To capture all possible scenarios of anticipated climate change, different expectations of Greenhouse gases (GHGs) are modeled by different representative concentration pathways (RCPs). RCPs are labeled according to each scenario's target radiative forcing by 2100. The high emissions scenario is represented by RCP8.5, in which radiative forcing is expected to reach 8.5 W/m^2 by

year 2100. RCP6.0 is an intermediate emissions scenario, where the radiative forcing in this scenario stabilizes at 6 W/m^2 after 2100. Another intermediate climate change scenario, where mitigation policies are imposed, is represented by RCP4.5, in which GHGs emissions are restrained and the radiative forcing stabilizes at 4.5 W/m^2 at year 2100. Extreme climate change mitigation, where effective policies are strictly enforced, and lifestyle change is accommodated to reduce greenhouse gases emissions, is represented by RCP2.6, in which radiative forcing peaks at 2.6 W/m^2 near 2100 (Taylor et al., 2012).

GCMs forecasts associated with different RCPs were statistically analyzed to determine the best models which could reproduce historical rainfall rates on two climatic regions in the study area. The statistical analysis technique adopted was based on the similarity between GCMs and historical rainfall data in various statistical measures and weights as listed in Table 10. Figures 20 and 22 show the statistical analysis results for both climatic regions considered. Tables 12 and 14 summarize the selected GCMs for climate change analysis in the Northern and the Southern climatic regions. GCMs rainfall datasets were utilized to calculate future recharge rates for the selected islands for the period of 2017-2050.

Future recharge rates were used as inputs to the calibrated islands models developed in Chapter 3 to simulate future freshwater lens volumes in the selected islands. Based on the outputs of these simulations, islands communities can prepare themselves to accommodate possible freshwater depletion, and to adapt the best management plans to secure sufficient freshwater supply as climate conditions change. It is concluded that small islands communities are more vulnerable to climate change conditions. The predicted freshwater volumes for these islands have strong variability in small islands (N. Holhudhoo and N. Velidhoo). These small islands in term of their land area are substantially affected as they respond quickly to any change

in precipitation (consequently recharge) quickly. The amount of freshwater which recharges the freshwater lens in the sub-surface is dependent on the amount of rainfall and land surface area. Due to the small land surface area, any change in rainfall pattern contributes significantly in freshwater lens depletion. On the other hand, larger islands are less affected by changing rainfall pattern, as their large surface areas relatively dominate over changing rainfall rates.

The frequency distribution analysis showed that there are no big differences in forecasts associated with different RCPs, however, in the high emission scenario, the distribution of the freshwater volume is clustered in the minimum ranges and minimum freshwater lens values would be more frequent, and higher seasonality is expected as values strongly deviate from long term averages. Results from the 2017-2050 simulations show that the pattern and the expected ranges for the freshwater volume will not significantly changed, as monthly rainfall rates patterns are similar to historical rates both geographic region of the Republic of Maldives. However, the selected GCMs used in this study predict a wide range of monthly rainfall. Hence, Fresh groundwater volumes may have strong variability during the coming decades. This expected strong variability may put available freshwater resources under serious threats if it combined with other climatic or anthropogenic stresses.

CHAPTER 5. ESTIMATION OF FUTURE FRESHWATER LENS VOLUME UNDER THE EFFECT OF SEA LEVEL RISE CONDITION

In this chapter the fresh groundwater lens fluctuation is assessed under the effect of possible sea level rise scenarios. Calibrated models for the islands N Holhudhoo, N. Velidhoo, GDh. Thinadhoo, and L. Gan (see Chapter 3) and future recharge rates estimated using GCMs (see Chapter 4) are used to determine the effect of shoreline recession and beach inundation due to sea level rise on the freshwater lens for the four study islands to quantify future fresh groundwater availability under various sea level rise scenarios.

5.1 Introduction

Sea level rise (SLR) is considered as a serious climate change induced threat on coastal and island aquifers. Seawater moves landward on the beachfronts, leading to a decrease in total land surface and cross-section widths of islands and promoting saltwater intrusion in the underlying aquifer system. Researchers typically investigate the interaction between SLR and seawater intrusion either by studying the problem on a generalized scheme (e.g. Werner and Simmons, 2009), or on site specific approach (e.g. Sherif and Singh, 1999).

The main task of research in this chapter is to run numerical simulations to quantify the amount of freshwater that will be lost due to the SLR-induced decrease in islands widths. Different rates of sea level rise will be considered and, since beach slope determines the extent of shoreline inundation, several beach slopes also will be considered. It is expected that the amount of freshwater will decrease drastically if significant reductions in island width occur. The SLR

simulations will be coupled with the climatic conditions forecasts (see Chapter 4) for the period of 2017-2050.

5.2 Sea Level Rise: Causes, Rates, and Consequences

Sea level rise is the increase of the mean high tide level over years, which could be a result of glacier melt due to increased temperatures over years, or water expansion due to increasing seawater temperature (Inman and Nordstrom, 1971; Church et al.,1991). Sea levels around the world are rising; current sea level rise potential may affect people living in coastal communities, and ecosystems. A study conducted by Church and White (2006) showed that sea level rose 195 mm on average globally between 1870 and 2004, and a study conducted by Nicholls and Cazenave (2010) showed that the average annual increase in the sea level was measured to be 1.7 ± 0.3 mm/year using tide gauge measurements while recent satellite images data showing a rise rate of 3.26 mm/year. In addition to that, the study points out that atoll islands in the Indian Ocean, for example the islands of the Maldives, are among communities most vulnerable to coastal flooding by future relative, or climate induced SLR.

Sea level rise estimates for the Republic of Maldives are highly variable. Conservative forecasts expect sea level to rise at a rate of 1.0 mm/yr (Church et al., 2006). On the other hand, aggressive forecasts expect sea level to rise at a rate of 6.5 mm/yr (Woodworth et al., 2002). Other researchers (Khan et al., 2002) reported a rate of 4 mm/yr for the islands of Male and Gan in Kaafu and Addu atolls respectively (Parry et al., 2007). Another study conducted by Woodworth (2005) states that a 50 cm sea level rise during the 21st century is a reasonable scenario. Figure 32 shows a schematic illustration for the sea level rise evolution in the past, and how scientists predict future levels of sea levels

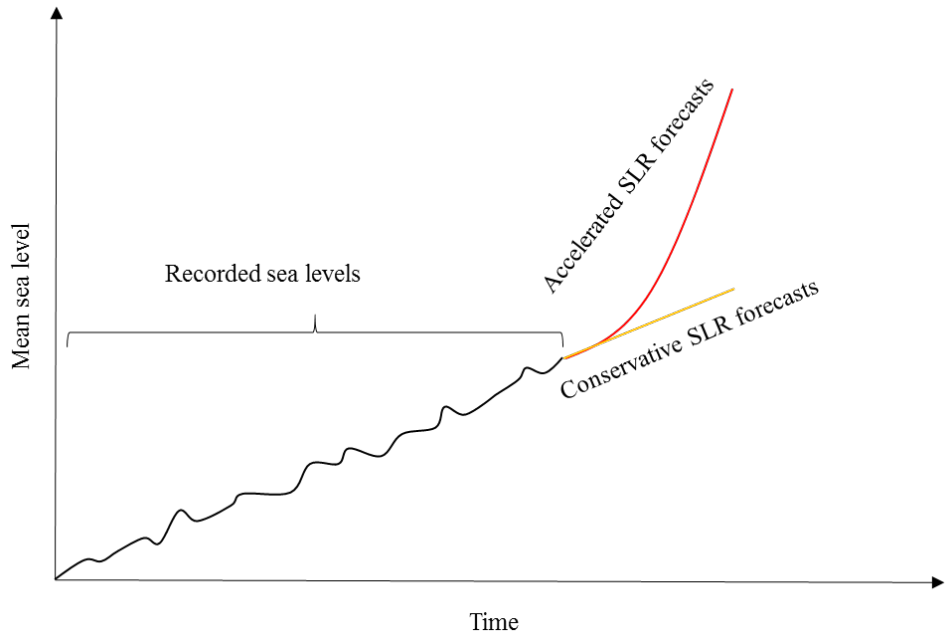

Figure 32 Schematic illustration for global mean sea level evolution over time and how scientist predictions for the future trends of sea level rise vary. The black curve represents recorded sea levels, the red curve reflects accelerated sea level rise rates, and the yellow curve represents conservative sea level rise forecasts

As sea level rises, and depending on beach slope, seawater may inundate coastal areas leading to beachlines recession. The movement of the beachline in the landward direction will lead to a reduction in island surface area. Consequently, and as island's surface area decreases, the total amount of freshwater received as a recharge will eventually decrease. Also, the smaller land surface area lowers the water table in the middle of the island, and hence the resulting thickness of the lens. With the boundary conditions for head set to sea level at the shoreline, the water table is not able to mound as much.This reduction in the freshwater source which feeds the freshwater lens will put it under a serious threat depending on the percentage of the island area that may be inundated. A study conducted by Bailey et al. (2015) used a simplistic algebraic model to simulate the future status of freshwater lens under the effect of sea level rise in the Republic of Maldives concluded that the average percent decrease in freshwater lens thickness,

lens volume, and safe yield is approximately 10, 11, and 34%, respectively. The paper employed a variety of reported beach slopes to estimate the percent of island area that might be inundated.

5.3 Previous Efforts in Modelling Sea Level Rise Impact on Fresh Groundwater Resources on Small Islands

There have been numerous studies relating sea level rise phenomena and the consequent hydrological impact due to seawater intrusion problem in coastal aquifers in general, and in small island aquifers in particular. The seawater intrusion problem caused by sea level rise has multiple contributing factors influencing its extent. These factors include the topographic slope of the beach, variable sea level rise rate, future recharge pattern, and the existence of extensive pumping stress near the beach areas. In particular, small islands are under serious threat of sea level rise effect because of their flat topography where significant land-surface inundation can occur (Falkland, 1991; Bricker, 2007). A study published by Ataie-Ashtiani et al. (2013) points out that most of the work done on unconfined aquifers, to quantify sea level impact, ignored beachline recession and the consequent land surface inundation and most of that previous work focused on pressure changes in the coastlines. The authors showed that the land surface inundation promotes more extensive seawater intrusion than atmospheric pressure changes. The authors emphasized the need to research the combined effect of sea level rise and climate change.

Sherif and Singh (1999) were one of the first researchers to provide predictive case studies of sea level rise impact on seawater intrusion in coastal areas by applying a two dimensional (2D) model to coastal aquifers, in Egypt and in India. They applied 2D-FED model on large scale areas (Nile Delta area is about 22,000 km^2). They included several factors that

account for climate change including variations in atmospheric pressures and melting ice sheets to investigate these factors effects on sea level rise. Their paper concluded that the Nile Delta is more vulnerable to sea level rise inundation. Another group of scholars coupled analytical models and numerical experiments to examine groundwater-seawater intrusion induced by sea level rise (Kooi et al, 2000) by applying 2D-METROPOL3 model on hypothetical aquifer systems. Another study conducted by Feseker (2007) investigated the effect of climate change, sea level rise, and changes in land use on salinity profile in field site on the North Sea Coast at Germany by using a steady state, two dimensional, density dependent solute model to simulate salt concentration profile. The author showed that rapid sea level rise is causing a rapid increase in groundwater salinity near the shoreline. Watson et al. (2010) studied the transience of sea level rise and the consequent seawater intrusion affecting a hypothetical unconfined, homogenous coastal aquifer using two dimensional variable density flow model FEFLOW. The researchers concluded that the seawater-freshwater sharp interface may take decades to respond to 1 meter of sea level rise. Bailey et al. (2014) employed a two dimensional empirical model to estimate future water resource of the Republic of Maldives. The model was applied to 52 small islands which spans all islands sizes in the Maldivian atoll. The paper concluded that mid-size islands (300-800 meters in width) are the most vulnerable to freshwater lenses reduction due future sea level rise and beachline encroachment, the freshwater lens could be reduced as much as 16% in accelerated SLR rates (Bailey et al. 2014).

Three dimensional modeling for sea level rise impact on groundwater systems has been conducted in several studies (e.g. Masterson and Garabedian, 2007; Oude Essink et al., 2010; Sulzbacher et al., 2012). Masterson and Garabedian (2007) applied the 3D-SEAWAT model on hypothetical, and single layer semi-confined aquifer with a constant SLR rate of 2.65 mm/yr.

The researchers concluded that the freshwater lens thickness may be reduced by 22%-31% due to SLR effect. Also, the SEAWAT model was utilized to study the effects of sea-level rise on the depth to the fresh water/saltwater interface. Other researchers examined the effect of combined climate change and anthropogenic stresses groundwater quality in the low-lying Dutch delta in Netherlands by implementing three dimensional density dependent groundwater flow model (MOCDENS3D model) by including land subsidence factor into consideration (Essink et al., 2010). The climate change effect was included in a numerical modeling study to examine the impacts of sea level rise on freshwater lenses on the North Sea Island of Borkum in the coming decades. Researchers concluded that groundwater reserves should be managed effectively to secure current future demands of domestic groundwater supply in the study area (Sulzbacher et al., 2012). Table 23 shows some of the research done to model sea level rise impact on the groundwater system.

Numerical modeling studies simulating the transient processes accompanying sea level rise were conducted by several researchers (see Table 23). Even though some of the previous work included the land inundation induced by sea level rise as an influential factor promoting seawater intrusion in the coastal groundwater systems (e.g. Kooi et al., 2000; Loaiciga et al., 2012; Ferguson and Gleeson, 2012), however, researchers did not quantify the effect of that important factor. Specifically, conducted studies did not address the movement of the beachline landward and the consequent coastal area inundation in a comprehensive manner which might be of a special concern in small atoll islands.

In this research, several land inundation percentages are simulated in islands. These different land inundation percentages should represent all potential scenarios that may occur in the coming decades to bracket all possible reductions in freshwater reserves in the study area.

Addressing the landing inundation problem using the transient, multi-layer, three dimensional saltwater intrusion modeling based on transition zone approach, rather than sharp interface approach will provide fundamental contribution the area of atoll islands hydrology and would form a future foundation for the research of sea level rise effect on small atoll islands groundwater resources system.

Table 23 Summary of some studies relating the impact of sea level rise on fresh groundwater resources depletion, CON, Confined; UCON, Unconfined; NU, Numerical, SLR, sea level rise

Reference	Aquifer type	Simulation method	Application/notes
Sherif and Singh (1999)	UCON-leaky	2D-FED model-NU	coastal aquifers in Egypt and India
Kooi et al. (2000)	UCON	2D-METROPOL3-NU and analytical	hypothetical
Feseker (2007)	UCON	2D- SWIMMOC-NU	hypothetical aquifer with real data
Masterson and Garabedian (2007)	Semi-CON	3D-SEAWAT-NU	hypothetical/constant SLR rate- single layer
Watson et al. (2010)	UCON	2D-FEFLOW-NU	hypothetical-sharp interface model
Oude Essink et al. (2010)	UCON	3D-MOCDENS3D-NU	Low lying delta in Netherlands – coarse cell resolution 250x250 m^2
Sulzbacher et al. (2012)	UCON-CON	3D-FEFLOW-NU	North Sea island of borkum
Chui and Terry (2013)	UCON	2D-SUTRA	Hypothetical islands

Ketabchi et al. (2014)	UCON	2D-Analytical-NU (SUTRA)	hypothetical small island-steady state and two layers
Bailey et al. (2015)	UCON	2D-algebraic models	52 small islands with real data

5.4 Methods

5.4.1 Future Shoreline Recession Estimation

As sea level rises, the seawater advances gradually beyond usual beachfront of the island, hence, shoreline recession is produced and island land surface area is decreased. The volume of the freshwater lens is strongly dependent on island land surface area, as the smaller island width yields a smaller rise in the water table above mean sea level, which in turn yields a proportionate decrease in the thickness of the lens below sea level. In addition, beach slope has a significant contribution to the extent to which sea level may encroach.

Shoreline recession induced by sea level rise can have a significant impact on atoll islands' groundwater resources, particularly for islands with gentle beach slopes (about 0.5%). On the other hand, islands with steeper beach slope (1% or 2%) are less vulnerable to the risk of shoreline recession induced by sea level rise, as rising sea level will encroach less on the coastline. As presented in a previous section, the minimum reported rate (1.0 mm/yr) and the maximum reported rate (6.5 mm/yr) of sea level rise are possible. To provide a plausible range of how far island beachfronts may retreat, different annual sea level rise rates are combined with different beach slopes (0.5%-2%) (Tsyban et al., 1990) to provide:

$$\text{Shoreline Recession} = \frac{n * SLR}{S} \qquad (5.1)$$

where:

n is the number of years [T]

SLR is the annual sea level rise rate [L/T]

S is the average beach slope [L/L]

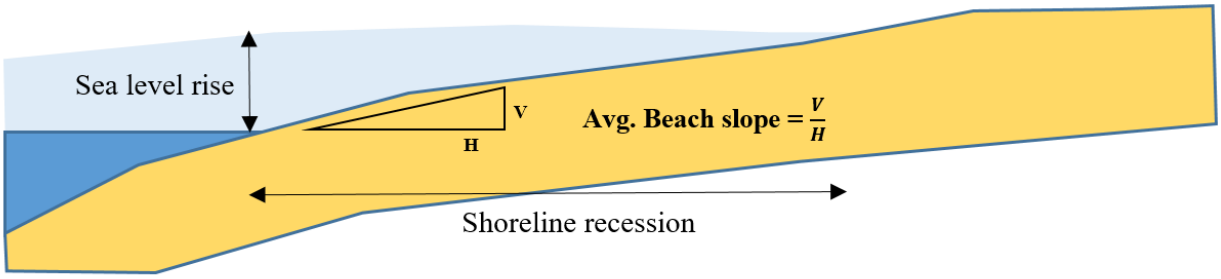

Figure 33 schematic diagram illustrating shoreline recession extent based on sea level rise and beach slope.

Figure 33 shows a schematic illustration of coastal areas inundation caused by the increase of the mean sea level. Table 24 shows possible ranges of shoreline recession according to different combinations of sea level rates, and beach slopes for 40 years period.

Table 24 Possible shoreline recession within 40 years period in meters according to different sea level rise rates, and different beach slopes.

SLR (mm/year)	**Gentle slope of 0.5%**	**Steep slope of 2%**
	shoreline recession (m)	**shoreline recession (m)**
1	8	2
3.5	28	7
6.5	52	13

As shown in Table 24, the islands in the study area may anticipate shorelines recession ranging between 2 and 52 meters. For the purpose of this research, and to capture all possible scenarios for sea level rise, several shoreline recession scenarios are simulated. Scenarios include conservative conditions, where sea level rise rates are at their minimum value of 1 mm/yr. On the other hand, aggressive scenarios of sea level rise are simulated also assuming that sea level will be rising at the high rate of 6.5 mm/yr. Table 25 shows the anticipated shoreline recession included in each scenario for each island.

Table 25 Simulated sea level rise induced shoreline recession.

Island	Conservative SLR shoreline recession	Aggressive SLR shoreline recession
N. Holhudhoo	10 m	20 m
N. Velidhoo	10 m	20 m
GDh. Thinadhoo	20 m	40 m
L. Gan	40 m	-

5.4.2 Modified Specified head Boundary Condition

The models for all islands which were developed in Chapter 3 contained specified head cells that simulate the presence of coastal line bounding each island with values of zero head and solute concentration of 1 (which means 100% seawater). As we are interested in estimating the effect of shoreline recession on available freshwater volume, the specified head boundary condition is modified to account for the anticipated shoreline recession. A buffer of new added specified head cells are added to each island SEAWAT calibrated models. The buffer width is set according to the shoreline scenarios presented in Table 25. Figure 34 illustrates the modification of specified head boundary condition to account for anticipated shoreline recession for N. Velidhoo Island.

Figure 34 Illustration for specified head (S.H.) boundary condition modification for N. Velidhoo to simulate shoreline recession. **A.** pre-SLR specified head boundary condition. **B.** modified boundary condition after shoreline recession.

5.4.3 2040-2050 Sea Level Rise Impact Simulations

Sea level rise, and consequently beach line recession, is a slow (i.e. decadal) process. Based on rates of sea level rise, it might take few decades for rising sea level to have a significant impact on groundwater resources of a small coral island. The climate change scenarios developed in Chapter 4 are used to assess the impact of beach line recession after 2040. Specified head boundary conditions were adjusted to account for the new location of the beachline (see Figure 34 for an example) based on conservative and aggressive sea level rise scenarios. Calibrated hydraulic conductivities (see Chapter 3), and other aquifer parameters derived from atoll island modeling literature as presented in Chapter 3 are used to characterize each island's sub-surface geology. The models were run from 2035 till 2040 for a spin-up simulation before simulating post-2040 sea level rise impact. The baseline simulations conducted earlier were used as initial conditions for the sea level rise models to establish the baseline conditions for salt concentrations in the islands and to assure models convergence.

Sea level rise simulations results are compared to the climate change simulations results through 2040-2050 with no anticipated sea level rise simulations, as presented in Chapter 4. Results are presented for each island with and without sea level rise under each climate change scenario to provide a quantitative estimate of freshwater lens depletion due to shoreline recession. Moreover, applying multiple sea level rise scenarios for each island is meant to provide an estimation of possible ranges of freshwater lens fluctuation and to overcome the uncertainty associated with sea level rise estimates. In the following sections the results of the 2040-2050 simulations are presented for each island under the conservative and the aggressive (see Table 25) scenarios for the four RCPs (2.6, 4.5, 6.0, 8.5) climate change scenarios.

5.5 Results

5.5.1 Sea Level Rise Impact under RCP2.6 Climate Change Scenario

In this section, the sea level rise simulations results are presented for each island under the mitigated RCP2.6 climate change scenario. Shoreline recession values are assigned for each island in the study area according to Table 25 to simulate conservative and aggressive sea level rise scenarios.

Figures 35 and 36 show the sea level rise impact simulations results for each island. The best (i.e. most accurate compared to historical regional climate) GCM in each region under the RCP2.6 forcing scenario is used to estimate monthly freshwater recharge during 2040-2050. Table 26 shows the percentages of average freshwater lens volume in each island and associated volume reduction. Complete simulations results for all climatic models in RCP2.6 are shown in the Appendix of the dissertation.

Table 26 Average freshwater lens volume during 2040-2050 under no SLR, conservative SLR, and aggressive SLR scenarios with associated percentages of freshwater volume reduction.

Island	Average freshwater lens volume w/o SLR (Mm^3)	Average freshwater lens volume w/ conservative SLR (Mm^3)	Average freshwater lens volume w/ aggressive SLR (Mm^3)	% change Conserve.	% change Agg.
N. Holhudhoo	0.28	0.22	0.19	20.9%	32.7%
N. Velidhoo	0.95	0.84	0.73	11.8%	23.2%
GDh. Thinadhoo	6.40	5.54	4.73	13.8%	26.3%
L. Gan	55.13	49.50	-	10.2%	-

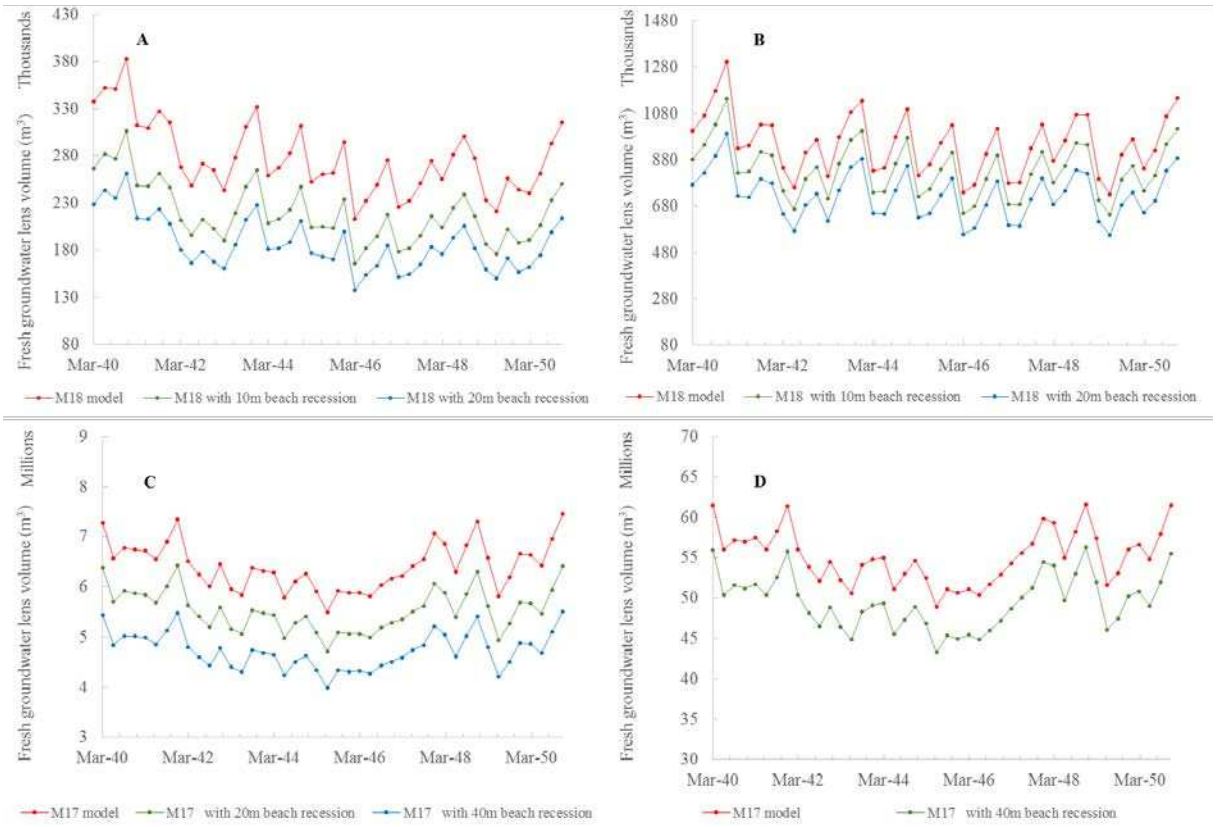

Figure 35 Simulated freshwater volume in the four islands in the study area under different sea level rise scenarios coupled with the 1st ranked climatic model under RCP2.6 scenario; **A**. N. Holhudhoo; **B**. N. Velidhoo; **C**. GDh. Thinadhoo; **D**. L. Gan.

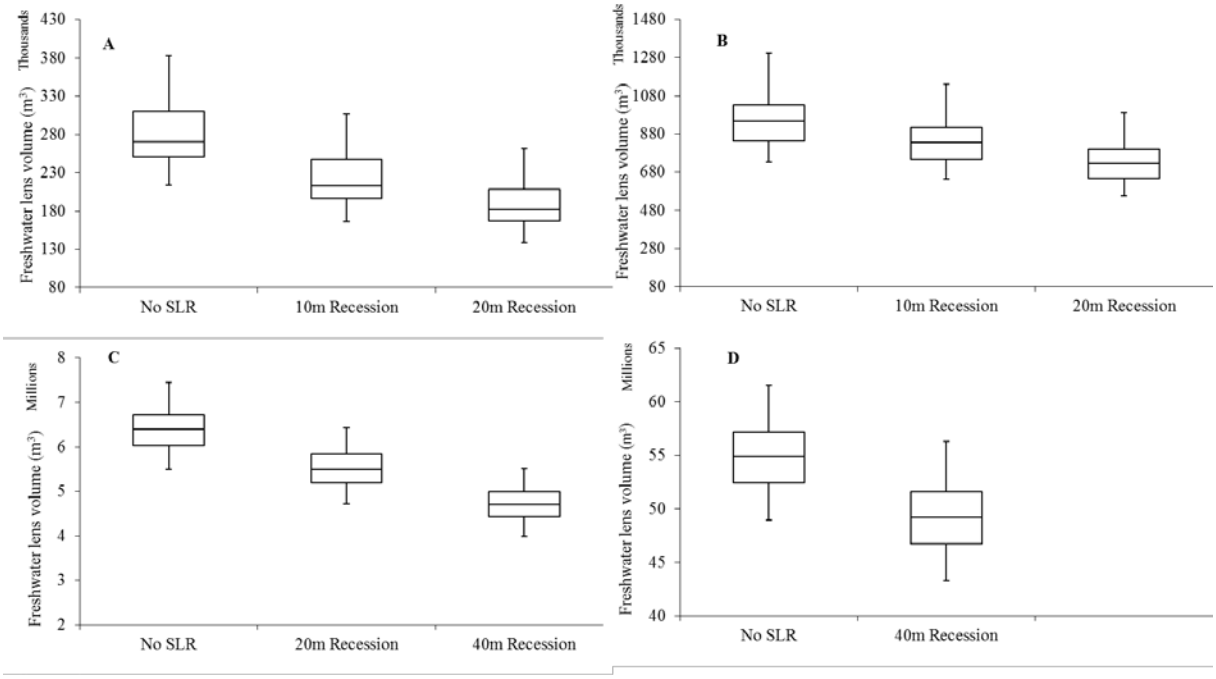

Figure 36 Boxplots for freshwater volume in the four islands in the study area under different sea level rise scenarios coupled with the 1st ranked climatic model under RCP2.6 scenario; **A**. N. Holhudhoo; **B**. N. Velidhoo; **C**. GDh. Thinadhoo; **D**. L. Gan.

Figures 35A and 36A show the sea level impact simulations result for N. Holhudhoo Island which is the smallest modeled island in this study (19.9 ha) . With a small surface area, the freshwater lens volume in this tiny island could be reduced 21% even with the conservative sea level rise rates. The freshwater lens volume could be reduced by 32% if sea level rises at the accelerated rates. The main reason for this drastic reduction in freshwater lens volume stems from the small island width. Even a small beachline recession would eventually lead to a significant decrease in island width. The decrease in island width will reduce the surface area where fresh precipitation recharges the sub-surface freshwater lens. Hence, the available freshwater lens volume will be decreased. Moreover, the boxplot for N. Holhudhoo (Figure 36A) shows a strong variability in freshwater lens volume, which emphasizes the conclusion made in Chapter 3 that small islands exhibit strong variability trends. The sea level rise effect increases the variability of the freshwater lens as it introduces new margins at which the available freshwater lens volume fluctuates. The island is around 350-400 meters wide which means that it could lose about 40 meters (around 10%) of its current width under the extreme sea level rise scenario.

Figures 35B and 36B show the sea level impact simulations result for N. Velidhoo Island that is the second modeled island located in the northern climatic region. The reduction in the island's freshwater lens volume ranged between 12% and 23% in the conservative and aggressive scenarios respectively. The decrease in lens volume in this island is still significant especially if we consider the conservative sea level rise case. However, this island is less vulnerable to freshwater resources depletion due to the sea level rise phenomenon than N. Holhudhoo Island as it is has a wider width and larger area. N. Velidhoo island and as shown in Figure 35B has less variability than N. Holhudhoo Island. The island is around 650-700 meters

wide which means that it could lose about 40 meters (around 6%) of its current width under extreme sea level rise scenario which this island freshwater resources less vulnerable to sea level rise impact than N. Holhudhoo.

Figures 35C and 36C show the sea level impact simulations result for GDh. Thinadhoo Island that is located in the southern climatic region. It is concluded that the freshwater lens volume in this island could be reduced substantially even with aggressive sea level rise rates. As shown in Table 25, the shoreline recession conditions simulated for this islands are 20 meters and 40 meters. The reduction in the average freshwater lens volume ranges between 13.75% and 26.33%. The reduction percentages in GDh. Thinadhoo are fairly comparable to those values in N. Velidhoo under mitigated sea level rise scenarios. This matter of fact tells that larger islands are more sustainable in terms of relatively preserving its freshwater resources even with aggressive sea level rates. GDh. Thinadhoo Island is about 850-900 meters wide and according to the simulated shoreline recession values. The reductions in island width are approximately 2.5%, and 5% for conservative and aggressive scenarios respectively.

Figures 35D and 36D show the sea level impact simulations result for L. Gan Island that is the biggest modeled island in this study. Only one scenario of sea level is simulated where shoreline encroaches 40 meters landward. Even with this aggressive condition of shoreline recession, the freshwater lens is reduced by less than 10% through the simulation period. The width of the island is more than 1 kilometers in most locations and it has a fairly big area. This geometrical aspects of L. Gan Island provide adequate space for receiving freshwater recharge through precipitation and consequently compensate any reduction in islands width due to sea level rise induced shoreline recession as only less than 4% of island width is lost shoreline encroachment.

5.5.2 Sea Level Rise Impact under RCP4.5 Climate Change Scenario

In this section, the sea level rise simulations results are presented for each island under the intermediate emission RCP4.5 climate change scenario. Shoreline recession values are assigned for islands in the study area according to Table 25 to simulate conservative and aggressive sea level rise scenarios. Figures 37 and 38 show the sea level rise impact simulations results for each island. The best climate change forecast models in each region under the RCP4.5 forcing scenario are used to estimate freshwater recharge during 2040-2050. Table 27 shows the percentages of average freshwater lens volume in each island and associated volume reduction. Complete simulations results for all climatic models in RCP4.5 are shown in the appendix.

Table 27 Average freshwater lens volume during 2040-2050 under no SLR, conservative SLR, and aggressive SLR scenarios with associated percentages of freshwater volume reduction.

Island	Average freshwater lens volume w/o SLR (Mm^3)	Average freshwater lens volume w/ conservative SLR (Mm^3)	Average freshwater lens volume w/ aggressive SLR (Mm^3)	% change Conserve.	% change Agg.
N. Holhudhoo	0.33	0.27	0.23	18.4%	29.4%
N. Velidhoo	1.24	1.09	0.94	12.2%	24.4%
GDh. Thinadhoo	6.08	5.18	4.53	14.8%	25.4%
L. Gan	52.64	47.44	-	9.9%	-

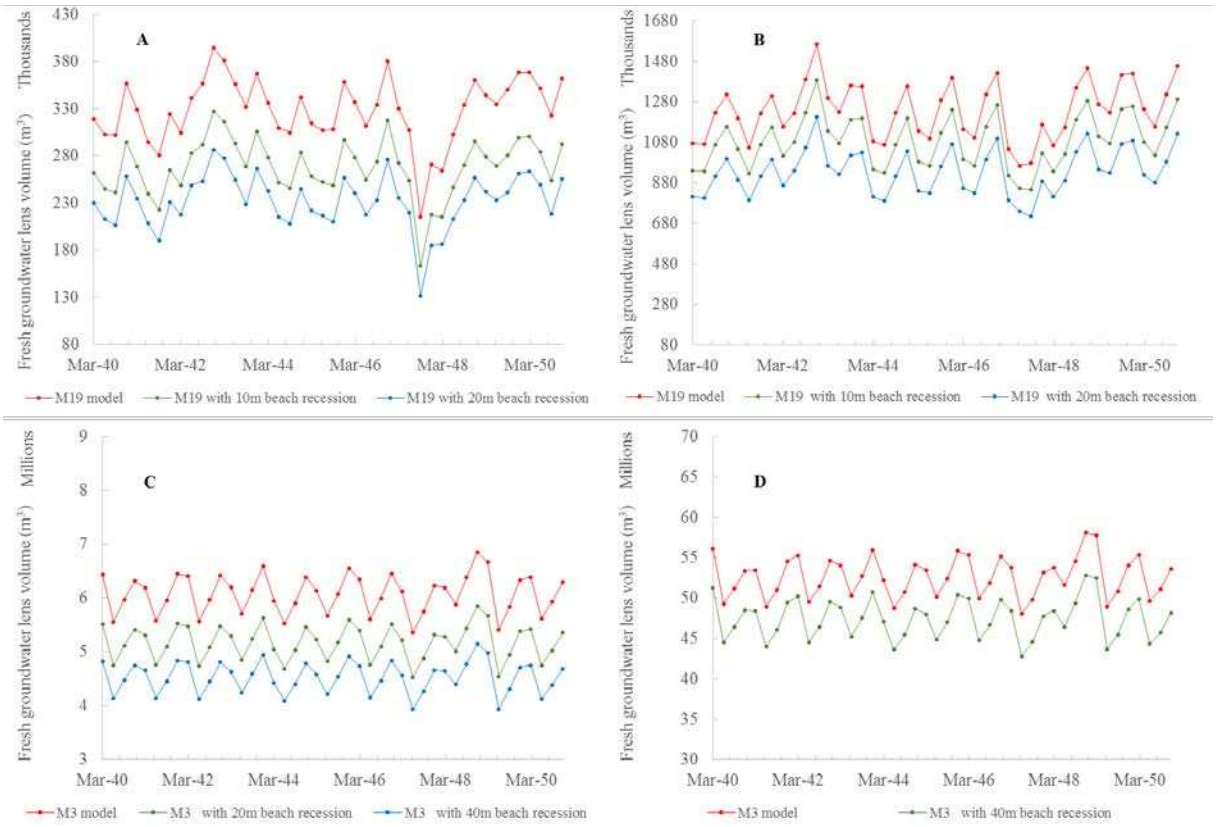

Figure 37 Simulated freshwater volume in the four islands in the study area under different sea level rise scenarios coupled with the 1st ranked climatic model under RCP4.5 scenario; **A**. N. Holhudhoo; **B**. N. Velidhoo; **C**. GDh. Thinadhoo; **D**. L. Gan.

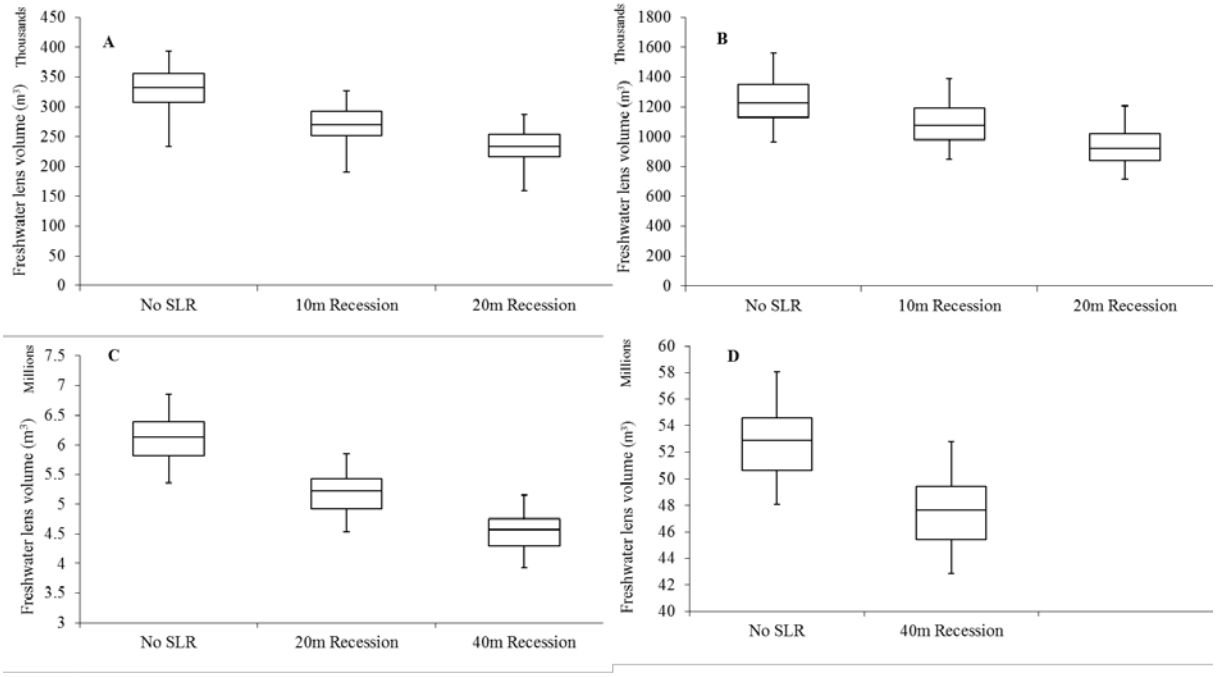

Figure 38 Boxplots for freshwater volume in the four islands in the study area under different sea level rise scenarios coupled with the 1st ranked climatic model under RCP4.5 scenario; **A**. N. Holhudhoo; **B**. N. Velidhoo; **C**. GDh. Thinadhoo; **D**. L. Gan.

Figures 37A and 38A show the sea level impact simulations result for N. Holhudhoo Island. The results for this intermediate emission scenario emphasizes the observed pattern in the mitigated emission scenario where the freshwater lens is substantially reduced even under conservative rates of anticipated sea level rise rates. Table 27 shows that N. Holhudhoo may undergo an approximately 18% freshwater lens volume reduction under conservative sea level rise rates. The limited island width and small land area are making the freshwater resources in this island under severe threats. Figures 37B and 38B show the sea level impact simulations result for N. Velidhoo Island that is the second modeled island located in the northern climatic region. The reduction in the island's freshwater lens volume ranges between 12.15% and 24.38% in the conservative and aggressive scenarios respectively. These percentages are a bit higher than percentages forecasted under RCP2.6 scenario which reflects the role of changing rainfall pattern on the future status of the freshwater lens. The reduction in the island's freshwater lens volume is also substantial for N. Velidhoo for its small area.

Figures 37C and 38C show the sea level impact simulations result for GDh. Thinadhoo Island. Also, the freshwater lens volume. In this mitigated climate change scenario, sea level rise may reduce the freshwater lens volume at significant rates between 14% and 25%. However, the fairly large island are a makes this island less vulnerable to freshwater lens depletion than other smaller islands. Figures 37D and 38D show the sea level impact simulations results for L. Gan Island that is the biggest modeled island in this study. As a big island, L. Gan might be slightly affected sea level rise effect, even with accelerated sea level rise rates. Table 27 shows the freshwater lens average is reduced by 9.88% under the RCP4.5 scenario which comparable the results obtained in the under RCP2.6 scenario.

5.5.3 Sea Level Rise Impact under RCP6.0 Climate Change Scenario

In this section, the sea level rise simulations results are presented for each island under the intermediate emission RCP6.0 climate change scenario. Shoreline recession values are assigned for each island in the study area according to Table 25 to simulate conservative and aggressive sea level rise scenarios. Figures 39 and 40 show the sea level rise impact simulations results for each island. The best climate change forecast models in each region under the RCP6.0 forcing scenario are used to estimate freshwater recharge during 2040-2050. Table 28 summarizes the percentages of average freshwater lens volume in each island and associated volume reduction. Complete simulations results for climate change scenario shown in the appendix.

Table 28 Average freshwater lens volume during 2040-2050 under no SLR, conservative SLR, and aggressive SLR scenarios with associated percentages of freshwater volume reduction.

Island	Average freshwater lens volume w/o SLR (Mm^3)	Average freshwater lens volume w/ conservative SLR (Mm^3)	Average freshwater lens volume w/ aggressive SLR (Mm^3)	% change Conserve.	% change Agg.
N. Holhudhoo	0.34	0.28	0.24	17.7%	29.4%
N. Velidhoo	1.27	1.12	0.96	11.9%	23.9%
GDh. Thinadhoo	6.22	5.18	4.67	16.8%	25.0%
L. Gan	53.83	48.93	-	9.1%	-

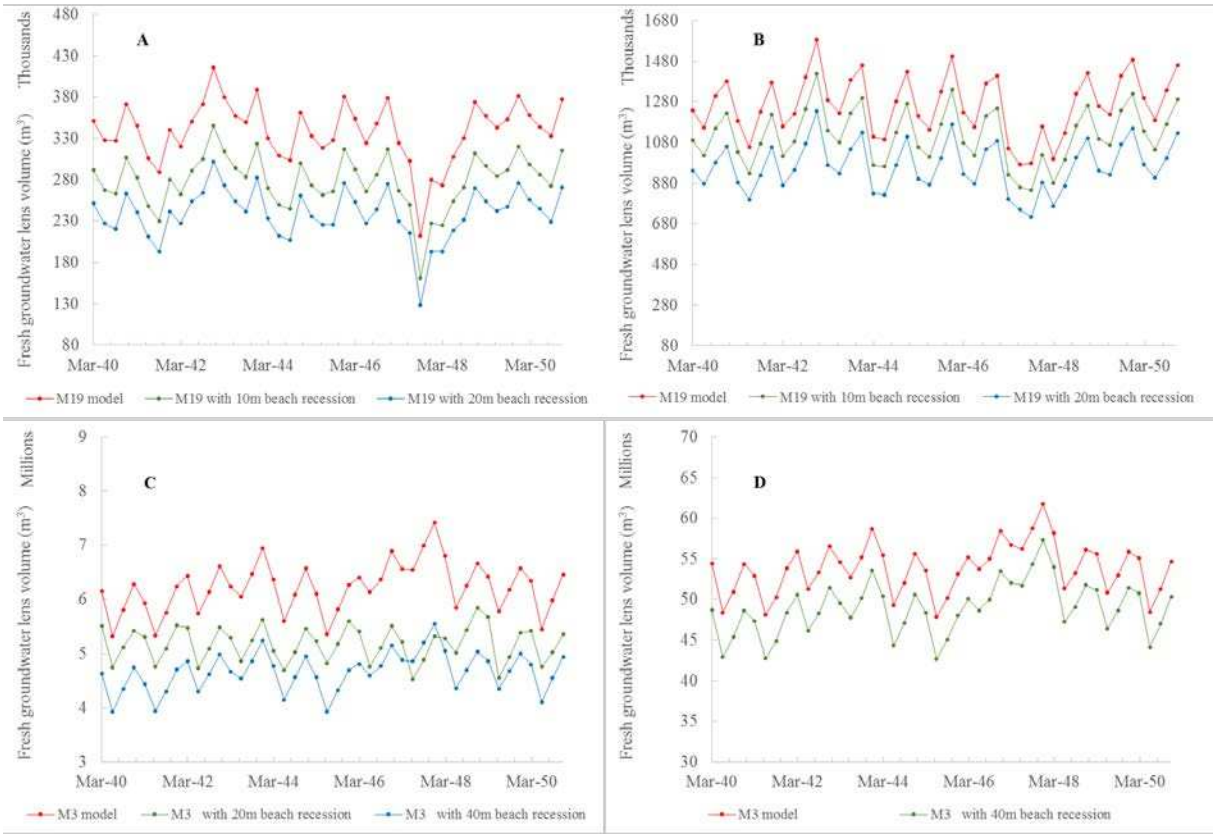

Figure 39 Simulated freshwater volume in the four islands in the study area under different sea level rise scenarios coupled with the 1st ranked climatic model under RCP6.0 scenario; **A**. N. Holhudhoo; **B**. N. Velidhoo; **C**. GDh. Thinadhoo; **D**. L. Gan.

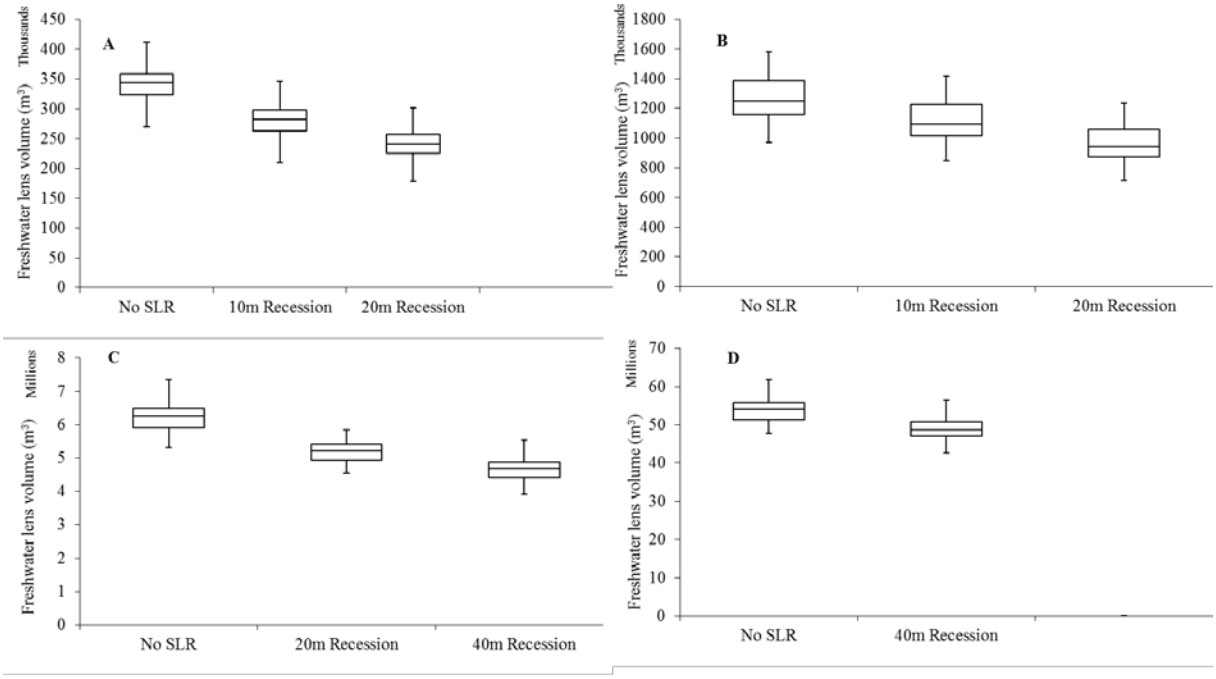

Figure 40 Boxplots for freshwater volume in the four islands in the study area under different sea level rise scenarios coupled with the 1st ranked climatic model under RCP6.0 scenario; **A**. N. Holhudhoo; **B**. N. Velidhoo; **C**. GDh. Thinadhoo; **D**. L. Gan.

Figures 39A and 40A show the sea level impact simulations result for N. Holhudhoo Island. The observed pattern in N. Holhudhoo still prevails. The freshwater lens had a similar response of drastic reduction of the freshwater lens in the RCP6.0 scenario. As shown in Table 28, the reductions in the freshwater lens are approximately 17% to 29%, which are comparable to the percentages obtained in the other intermediate emission scenario. Figures 39B and 40B show the sea level impact simulations result for N. Velidhoo Island. The reduction in the island's freshwater lens volume ranged between 11.85% and 23.90% in the conservative and aggressive scenarios respectively. These percentages are lower than percentages forecasted under RCP4.5 scenario which reflects the role of climate change forecasts uncertainty on the future status of the freshwater lens.

Figures 39C and 40C show the sea level impact simulations result for GDh. Thinadhoo Island that is located in the southern climatic region. The simulation result show that the freshwater lens volume in this island could be reduced significantly even with conservative sea level rise rates, where freshwater lens volume might be reduced by more than 16%. Despite the fact that the freshwater lens in GDh. Thinadhoo might be significantly reduced, freshwater resources in the island are more sustainable as the island has adequate land area and could receive large amount of annual freshwater recharge. Figures 39D and 40D show the sea level impact simulations result for L. Gan Island. Even with this aggressive condition of shoreline recession, the freshwater lens is reduced by 9.11% through the simulation period. The size of that big island preserves it from the severe consequences of sea level rise impact. Island width is more than 1 kilometers in most locations, and hence, shoreline recession would be less than 5% in worst cases if sea water intrudes 50 meters in the accelerated sea level rates by the year 2050.

5.5.4 Sea Level Rise Impact under RCP8.5 Climate Change Scenario

In this section, the sea level rise simulations results are presented for each island under the high emission RCP8.5 climate change scenario. Shoreline recession values are assigned for islands in the study area according to Table 25 to simulate conservative and aggressive sea level rise scenarios. Figures 41 and 42 show the sea level rise impact simulations results for each island. The best climate change forecast models in each region under the RCP8.5 forcing scenario are used to estimate freshwater recharge during 2040-2050. Table 29 shows results summary for this scenario. Complete simulations results for all climatic models in RCP8.5 are shown in the appendix.

Table 29 Average freshwater lens volume during 2040-2050 under no SLR, conservative SLR, and aggressive SLR scenarios with associated percentages of freshwater volume reduction.

Island	Average freshwater lens volume w/o SLR (Mm^3)	Average freshwater lens volume w/ conservative SLR (Mm^3)	Average freshwater lens volume w/ aggressive SLR (Mm^3)	% change Conserve.	% change Agg.
N. Holhudhoo	0.33	0.27	0.24	19.1%	29.4%
N. Velidhoo	1.24	1.09	0.94	12.1%	24.1%
GDh. Thinadhoo	5.90	5.17	4.37	12.3%	26.0%
L. Gan	51.57	47.48	-	8.0%	-

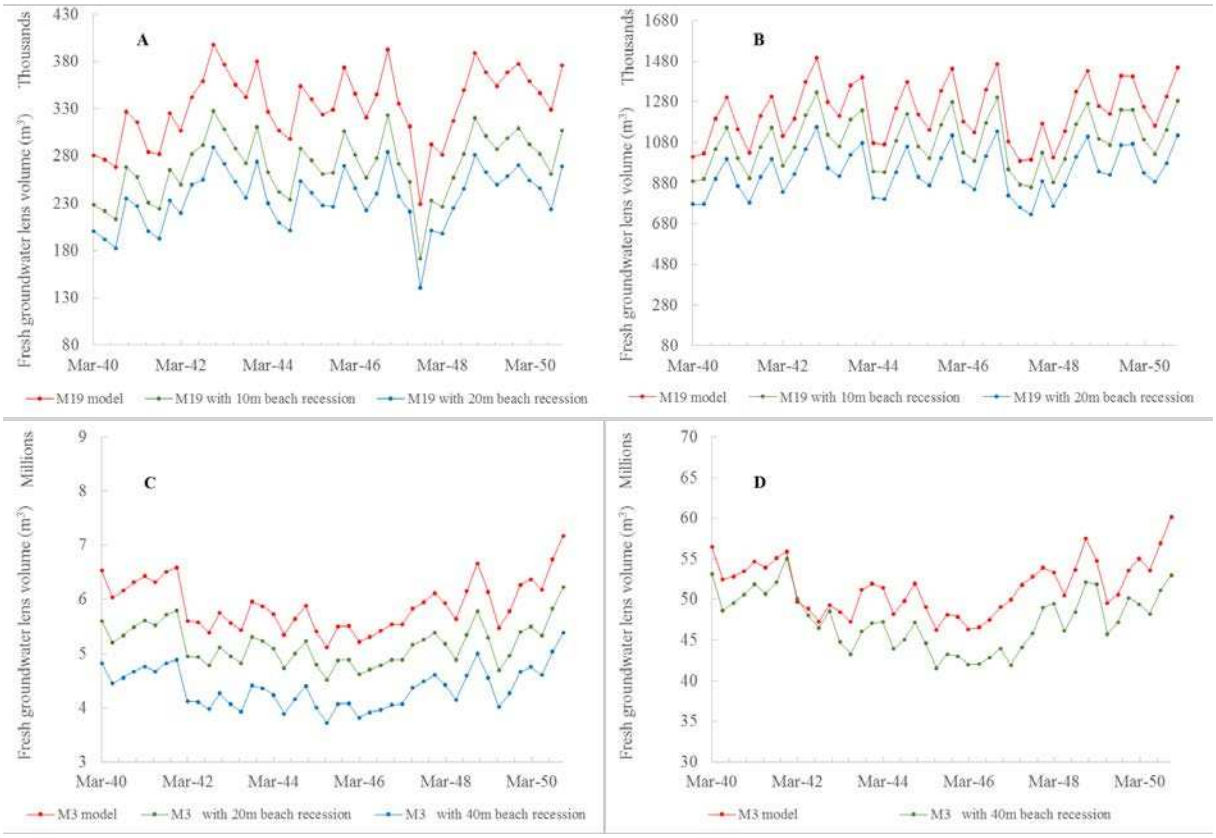

Figure 41 Simulated freshwater volume in the four islands in the study area under different sea level rise scenarios coupled with the 1st ranked climatic model under RCP8.5 scenario; **A**. N. Holhudhoo; **B**. N. Velidhoo; **C**. GDh. Thinadhoo; **D**. L. Gan.

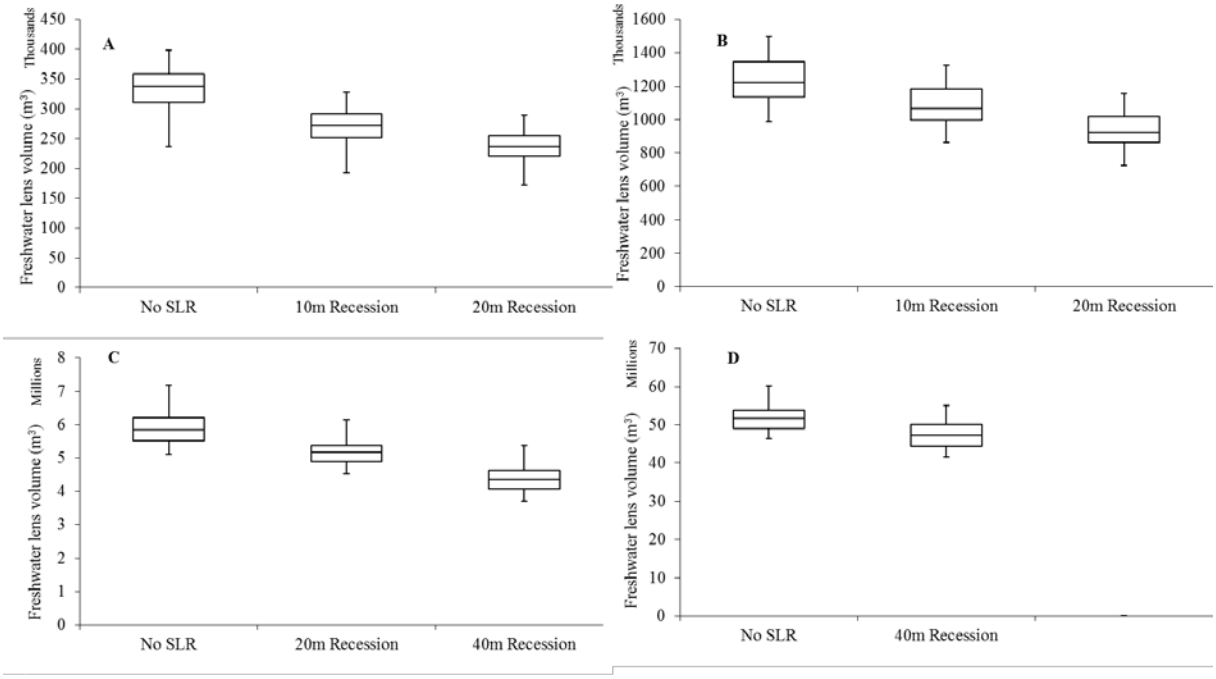

Figure 42 Boxplots for freshwater volume in the four islands in the study area under different sea level rise scenarios coupled with the 1st ranked climatic model under RCP8.5 scenario; **A**. N. Holhudhoo; **B**. N. Velidhoo; **C**. GDh. Thinadhoo; **D**. L. Gan.

Figures 41A and 42A show the sea level impact simulations result for N. Holhudhoo Island. For this extreme-high emission scenario, results for N. Holhudhoo Island does not differ from those results in the mitigated and intermediate emission scenarios. It seems that shoreline recession effect dominates the rainfall variability effect. In this scenario, the freshwater lens volume for N. Holhudhoo is expected to drop by 19.09% and 29.42% in the conservative and aggressive scenarios respectively. Having different Green House Gases emissions scenarios did not show a significant deviations in results and the observed pattern still prevails. Figures 41B and 42B show the sea level impact simulations result for N. Velidhoo Island. The reduction in the island's freshwater lens volume ranges between 12.14% and 24.12% in the conservative and aggressive scenarios respectively. These percentages are comparable to other percentages forecasted by other RCP scenarios, however, there are slight differences caused by climate change forecasts uncertainty.

Figures 41C and 42C show the sea level impact simulations results for GDh. Thinadhoo Island that is located in the southern climatic region. The simulations results show that the hydrologic response for sea level rise condition in this extreme emission scenario does not differ from the mitigated and intermediate emission scenarios where the predicted percentages of freshwater volume are between 12% and 26%. Figures 41D and 42D show the sea level impact simulations results for L. Gan Island. Even with this aggressive condition of shoreline recession, the freshwater lens is reduced by 8.03% through the simulation period. The results for L. Gan Island assures that its groundwater system is sustainable and slightly affected by sea level rise and variable rainfall patterns.

5.5.5 Results Uncertainty

Results were presented in the previous sections for different islands under different representative concentration pathways (RCPs). The simulations results for each island showed that predicted future freshwater lens volumes span over a probable range possibilities. Results variability implies a wide uncertainty in future groundwater supply, which is an important matter to consider. In this section, the results from the previous section are grouped for each island to show forecasts uncertainty for each island and to provide a comprehensive overview for the future groundwater status in each island in the study area.

5.5.5.1 N. Holhudhoo Island

N. Holhudhoo is the smallest modeled island and it showed a strong variability trend in future groundwater reserves as it has a limited land area. Moreover, the highest percentages of freshwater lens volume reductions is for N. Holhudhoo. Table 30 shows the predicted percentages of freshwater lens reductions with comparison to the no sea level rise scenario. According to the conservative sea level rise scenario, the freshwater lens is expected to be reduced between 17.74% and 23.37%. On the other hand, according to the aggressive sea level rise scenario, the freshwater lens is expected to be reduced between 29.40% and 36.28%. The variability in the results comes from different forecasts of rainfall patterns depending on different greenhouse emission concentrations in the coming decades. Extreme emission scenarios, predict the highest reduction in average freshwater lens volume (model M8). On the other hand, the extreme emission scenario forecasts, predict that the freshwater lens may be reduced less than the mitigated emission scenarios (model M19 forecast). The outcomes of the forecasts emphasize that results have a considerable range of uncertainty.

Table 30 Predicted averages freshwater lens (Mm^3) (2040-2050) for sea level rise impact on N. Holhudhoo Island according to different possible sea level rise rates coupled with different possible RCPs forcing scenarios.

RCP	GCM ID	GCM ranking	No SLR (Mm^3)	Conserv. SLR (Mm^3)	Aggres. SLR (Mm^3)	% reduction Conserve.	% reduction Aggres.
2.6	M18	1st	0.28	0.22	0.19	20.9%	32.7%
2.6	M19	2nd	0.22	0.17	0.15	21.0%	33.0%
2.6	M4	3rd	0.21	0.16	0.14	20.9%	33.0%
4.5	M19	1st	0.33	0.27	0.23	18.4%	29.4%
4.5	M8	2nd	0.18	0.14	0.12	23.4%	34.8%
4.5	M18	3rd	0.28	0.22	0.19	20.6%	32.3%
6.0	M19	1st	0.34	0.28	0.24	17.7%	29.4%
6.0	M18	2nd	0.30	0.24	0.21	21.1%	31.4%
6.0	M4	3rd	0.20	0.15	0.13	21.4%	34.2%
8.5	M19	1st	0.33	0.27	0.24	19.1%	29.4%
8.5	M8	2nd	0.17	0.13	0.11	22.8%	36.3%
8.5	M4	3rd	0.20	0.16	0.13	21.3%	32.5%

5.5.5.2 N. Velidhoo Island

N. Velidhoo also showed a strong variability in future groundwater reserves as it has a limited land area. Moreover. Table 31 shows the predicted percentages of how much freshwater lens may drop compared to the no sea level rise scenario through the simulation period. According to the conservative sea level rise scenario, the freshwater lens is expected to be reduced between 11.49% and 12.15%. On the other hand, according to the aggressive sea level rise scenario, the freshwater lens is expected to be reduced between 22.98% and 24.78%. It noticed that the margin at which reduction percentages fluctuate is narrowed for N. Velidhoo. N.

Velidhoo has bigger area and island width than N. Holhudhoo which reduced the range of forecasts uncertainty. It is noted also that the percentages are almost the same for each sea level rise scenario with 1-2% fluctuation. This narrow range of freshwater lens forecasts reduces sea level rise impact modeling uncertainty, and increases results reliability.

Table 31 Predicted averages freshwater lens (Mm^3) (2040-2050) for sea level rise impact on N. Velidhoo Island according to different possible sea level rise rates coupled with different possible RCPs forcing scenarios.

RCP	GCM ID	GCM ranking	No SLR	Conserv. SLR	Agg. SLR	% reduction Conserv.	% reduction Agg.
2.6	M18	1st	0.95	0.84	0.73	11.8%	23.2%
2.6	M19	2nd	0.85	0.75	0.65	11.7%	23.2%
2.6	M4	3rd	0.82	0.72	0.63	11.5%	23.0%
4.5	M19	1st	1.24	1.09	0.94	12.1%	24.4%
4.5	M8	2nd	0.77	0.68	0.59	11.8%	23.7%
4.5	M18	3rd	0.83	0.74	0.64	11.5%	23.2%
6.0	M19	1st	1.27	1.12	0.96	11.9%	24.0%
6.0	M18	2nd	1.00	0.89	0.77	11.7%	23.0%
6.0	M4	3rd	0.80	0.70	0.61	11.8%	23.4%
8.5	M19	1st	1.24	1.09	0.94	12.2%	24.1%
8.5	M8	2nd	0.69	0.61	0.52	12.4%	24.8%
8.5	M4	3rd	0.80	0.71	0.62	11.6%	23.2%

5.5.5.3 GDh. Thinadhoo Island

Results for sea level rise impact for GDh. Thinadhoo are shown in Table 32. According to the conservative sea level rise scenario, the freshwater lens is expected to be reduced between 10.49% and 16.81%. On the other hand, according to the aggressive sea level rise scenario, the

freshwater lens is expected to be reduced between 25.04% and 26.73%. There is no evidence that the variable rainfall patterns are affecting freshwater lens volume hydrological response, and that is concluded from comparing low emission versus high emission climate change scenarios. The predicted average freshwater volumes are almost the same under all RCPs scenarios for the same sea level rise condition.

Table 32 Predicted averages freshwater lens (Mm^3) (2040-2050) for sea level rise impact on GDh. Thinadhoo Island according to different possible sea level rise rates coupled with different possible RCPs forcing scenarios.

RCP	GCM ID	GCM ranking	No SLR	Conserv. SLR	Aggressive SLR	% reduction Conserv.	% reduction Agg.
2.6	M17	1st	6.42	5.54	4.73	13.8%	26.3%
2.6	M19	2nd	5.97	5.14	4.41	13.9%	26.1%
2.6	M3	3rd	5.90	5.17	4.37	12.3%	26.0%
4.5	M3	1st	6.08	5.18	4.53	14.8%	25.4%
4.5	M12	2nd	5.93	5.16	4.43	13.0%	25.2%
4.5	M7	3rd	5.32	4.60	3.90	13.5%	26.7%
6.0	M3	1st	6.22	5.18	4.67	16.8%	25.0%
6.0	M19	2nd	5.76	5.16	4.30	10.5%	25.4%
6.0	M2	3rd	4.99	4.28	3.71	14.2%	25.5%
8.5	M3	1st	5.90	5.17	4.37	12.3%	26.0%
8.5	M7	2nd	6.00	5.09	4.34	15.1%	27.7%
8.5	M2	3rd	5.06	4.34	3.77	14.1%	25.5%

5.5.5.4 L. Gan Island

L. Gan Island is the largest modeled island. Only one sea level rise situation is simulated. Table 33 shows the sea level rise impact on freshwater lens volume in L. Gan Island under different RCPs scenarios. The percentages at which fresh groundwater reserve may deplete are between 8.03% and 11.01%. The island has a fairly big area to sustain beachline recession. By comparing freshwater lens responses to variable rainfall patterns under the same sea level rise situation, we cannot notice any effect that climate change may contribute to, as extreme emission models versus mitigated emission models have the same range of predicted freshwater lens volume reduction.

Table 33 predicted averages freshwater lens (Mm^3) (2040-2050) for sea level rise impact on L. Gan Island according to different possible sea level rise rates coupled with different possible RCPs forcing scenarios.

RCP	**GCM ID**	**GCM ranking**	**No SLR**	**Conserv. SLR**	**Agg. SLR**	**% reduction Conserv.**	**% reduction Agg.**
2.6	M17	1st	55.13	49.50	-	10.2%	-
2.6	M19	2nd	51.93	47.08	-	9.3%	-
2.6	M3	3rd	51.57	46.61	-	9.6%	-
4.5	M3	1st	52.64	47.44	-	9.9%	-
4.5	M12	2nd	54.98	49.21	-	10.5%	-
4.5	M7	3rd	47.93	43.58	-	9.1%	-
6.0	M3	1st	53.83	48.93	-	9.1%	-
6.0	M19	2nd	49.19	44.96	-	8.6%	-
6.0	M2	3rd	44.87	39.93	-	11.0%	-

8.5	M3	1st	51.57	47.43	-	8.0%	-
8.5	M7	2nd	51.96	46.59	-	10.3%	-
8.5	M2	3rd	45.17	40.67	-	10.0%	-

5.5.5.5 The Effect of Island Size on Freshwater Lens Reduction Induced by SLR

The results section showed the hydrologic response of freshwater lens in modeled islands due to beach line recession induced by SLR. Bigger islands showed more sustainable response as their freshwater lens reduction percentages were lower than smaller islands. In this section, the results of Islands: N. Holhudhoo, N. Velidhoo, and GDh. Thinadhoo are compared with the 20m beachline recession scenario (Figure 43). The vertical axis represents the average freshwater lens reduction due to SLR coupled with all recharge patterns in 2040-2050 compared with no SLR case. Figure 43 shows that there is an inversely proportional relation between average freshwater lens reduction and the natural logarithm of the island surface area. This finding can be used to extrapolate for the effect of SLR on other atoll islands in the Indian and the Pacific Oceans.

5.6 Discussion and Conclusion

Sea level rise is an observed phenomena that is mainly induced by climate change and earth global warming. As the planet warms, the ice sheets melts down and sea level rises. In addition, atmospheric pressure change on oceans contributes to the sea level rise phenomenon. As sea level rises, and depending on topographic features of coastlines, significant portions of coastal areas are under inundation threats. Atoll islands with their low elevations, flat coastal topography, and small islands area, are subject to severe threats of coastal inundation and beachline recession. These threats can substantially affect islands fresh groundwater lenses as

seawater intrusion problem is promoted. Seawater inundating coastal areas will percolate through the soil and damage the fresh groundwater lens which will eventually lead to freshwater reserve depletion in atoll island aquifers.

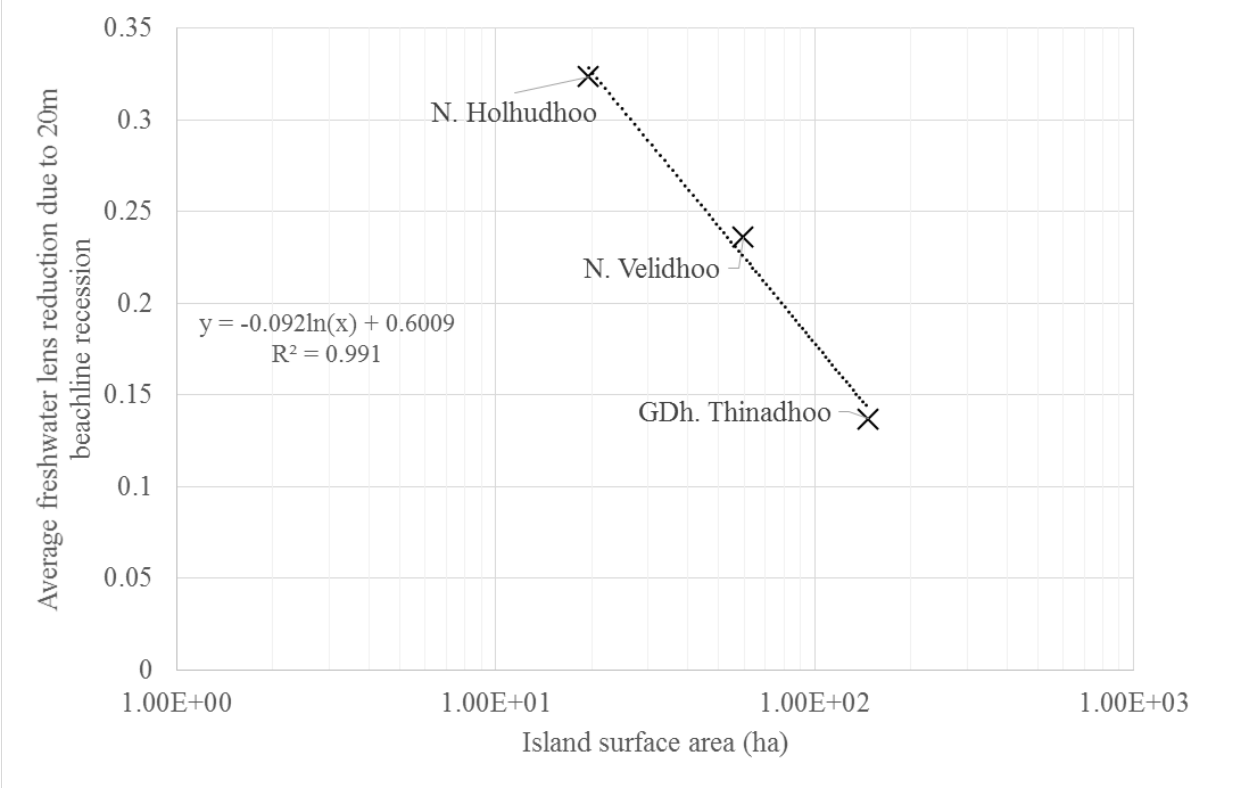

Figure 43 Relation between average freshwater lens reduction (20m beachline recession) and island surface area (semi-log scale).

In this chapter, the problem of sea level rise effect on freshwater resources in small atoll islands sub-surface hydrological system is addressed. A survey of global and study area annual rates of observed sea level rise rates recorded from tidal gauges was introduced as published in sea level rise modelling literature. Previous observations revealed that average annual increase in the sea level was measured to be 1.7 ± 0.3 mm/year using tide gauge measurement while recent satellite images data showing a rise rate of 3.26 mm/year. Similarly, sea level rise predictions for the study area in the Republic Maldives are highly variable. Conservative forecasts are expecting

sea level to rise at a rate of 1.0 mm/yr. (Church et al., 2006). On the other hand, aggressive forecasts expect that sea level is rising at accelerated rates up to 6.5 mm/yr. (Woodworth et al., 2002).

Several authors conducted research studies (see Table 23) to assess the impact of seawater intrusion induced by sea level rise on coastal groundwater systems. Most of the early efforts that were done neglected coastal areas inundation and beachline recession and focused on atmospheric pressure changes. However, other authors included the coastal area inundation in their modeling studies. This research was meant to quantify the sea level rise impact on small atoll islands groundwater systems by considering the coastal lands inundation as the most influential factors. The conducted sea level rise analysis was coupled with climate change forecast to include the possible variable rainfall rates signature.

Simulations were conducted to estimate the future status of available fresh groundwater lens in four selected islands in the Republic of Maldives atolls. Three dimensional, density dependent, transient, and solute transport models were built up and calibrated in Chapter 3 for the four selected islands in the study area. The calibrated models boundary conditions were adjusted to accommodate the new location of beachline after the predicted sea level rise by the year 2040. The best climate forecasts associated with different greenhouse gases emission scenarios that were introduced in Chapter 4 were used to estimate future recharge rates in two climatic region in the study area. Recharge rates were used as inputs to the calibrated and adjusted islands models to simulate future freshwater lens volumes in the selected islands. The conducted simulations included all possible scenarios of conservative sea level rise rates where sea level rises at minimal rates (the mitigated scenario), and the aggressive sea level rise where sea level would rise at the maximum observed rates. Also, all possible future greenhouse gases

emission scenario were included and coupled with both conservative and aggressive sea level rise rates to bracket all possible values at which the freshwater reserve in the modeled islands may reduce.

The responses of the studied islands fresh groundwater lenses varied in magnitude. While small islands were substantially affected and their fresh sub-surface water reserve depleted by approximately 11-36 %, bigger islands had a mitigated situation where the freshwater reserve depleted by 8-26% (Tables 30-33) although more aggressive sea level rise conditions were imposed on bigger islands. The variation in responses is due to different island sizes, and a linear relation is found between island size and freshwater lens reduction due to SLR (Figure 43). It is concluded that bigger islands are less vulnerable to the combined sea level rise and climate change effect. Specifically, island width dimension is a key factor in quantifying island risk due to coastal inundation and the consequent sub-surface groundwater reserve damage. Wider islands (width > 600 meters) would lose less than 7% of their widths if sea level encroaches 20 meters landward. On the other hand, this same amount of beachline recession would cause 20% reduction in small islands widths (islands width < 200m). The reduction in island width and as sea level encroaches landward, will eventually intrude the fresh groundwater lens that floats above seawater beneath islands surface. The predicted reduction percentages as modeled in this chapter are higher than those predicted by Bailey et al. (2015) who modeled the effect of beachline recession and SLR on 52 atoll islands in the Republic of Maldives using a two dimensional, and empirical model. The higher reduction percentages predicted in this chapter are due to modeling the groundwater system with a physically based, and 3D models rather than an empirical, and 2D approach. In addition, the findings of this chapter are comparable to the findings of Masterson and Garabedian (2007) who predicted a reduction in the freshwater lens

thickness by 22-31%. Comparisons between islands responses to variable rainfall patterns under the same sea level rise situation showed that there is no added threat to freshwater reserve depletion, as extreme emission models versus mitigated emission models share the same range of predicted freshwater lens volume reduction margins. The findings outlined in this chapter emphasize that small islands are more vulnerable to environmental threats. Small islands communities should appraise water management plans to secure freshwater access for islands inhabitants during extreme environmental conditions.

CHAPTER 6. THREE DIMENSIONAL MODELING FOR FRESHWATER LENS RECOVERY AFTER OVER-WASH EVENTS

In this chapter, the time required for the freshwater lens to recover its pre-overwash status after marine overwash events is assessed. Different land inundation percentages based on potential storm categories are imposed to Islands' calibrated models presented in Chapter 3.

6.1 Introduction

Among the many threats to freshwater reserves of atoll islands, such as, groundwater mining from the subsurface freshwater lens, variable rainfall patterns, and shoreline recession induced by sea level rise, seawater inundation induced by marine overwash events represents a serious threat to the freshwater reserves in small atoll islands aquifers. Marine overwash events can emerge critical freshwater shortage emergency in islands communities as they occur suddenly. Unlike drought events, which slowly deplete water reserves, marine overwash events can cause, with only a short notice, significant damages to groundwater supply and impose a great challenge for island community in managing their freshwater reserves. Marine overwash events occur due to several factors including: tsunamis, storm surge, rogue waves, strong wave set-up accompanied with enhanced winds activity, extreme high tide, or high regional sea level rise level (Bricker and Hughes, 2007; White et al., 2007; Yamano et al., 2007; Terry and Falkland, 2010).

Atoll islands have small surface area, relatively flat beach slope, with maximum elevation of few meters above mean sea level (Wheatcraft and Buddemeier, 1981). Due to that topographic nature, complete or partial island inundation due to overwash events can occur. Seawater flooding coastal area will percolate through the high-hydraulic conductivity soil profile causing

salinization to the shallow groundwater. After overwash events, freshwater recharge will recover the damaged freshwater lens and rebuild the freshwater lens again. Depending on overwash events intensity, rainfall patterns, and other geologic characteristics, the time required for the freshwater lens to restore its pre-overwash status is determined (Chui and Terry, 2012; Bailey and Jenson, 2013). In this chapter, storms of different intensities as well as different recharge patterns based on both historical and climatic forecasts for future recharge patterns according to different Representative Concentration Pathways of greenhouse gases emission RCPs forecasts are used as inputs for the calibrated models presented in Chapter 3 to quantify the time required for the freshwater lens to recover after over wash events. In addition, the effect of groundwater pumping in extending recovery time is also examined.

6.2 Previous Efforts in Modeling Post Overwash Fresh Groundwater Lens Recovery

Several published studies have quantified the response of a coral island freshwater lens to over-wash events. The previous efforts included both field studies (Oberdorfer and Buddemeier, 1984; Richards, 1991; Yamano et al., 2007; Terry and Falkland, 2010) which provided site specific information, and numerical modeling efforts which studied the response of generic and specific islands to various overwash scenarios (Chui and Terry, 2012; Terry and Chui, 2012; Bailey and Jenson, 2013; Chui and Terry, 2013; Bailey, 2015).

Terry and Falkland (2010) conducted on-site work to study the overwash events induced by tropical cyclone that struck Pukapuka atoll in the Northern Cook Islands in 2005. They monitored freshwater lens salinity shortly after the cyclone struck the atoll, and tracked freshwater lens recovery for 11 months following the overwash. They observed that seawater that percolated through the unsaturated zone formed a plume of seawater floating atop the

freshwater lens. Consequently, the freshwater lens is relocated between that plume and the underlying seawater. This plume was observed to disperse gradually through time. Their concluded that the lens needs at least 11 months to recover for each of the three studied islands in Pukapuka atoll. Terry and Falkland (2010) work is the most in-depth field study that was conducted to characterize freshwater lens recovery after being suddenly inundated with seawater.

As for the numerical modeling approach, several scholars employed simulation codes to quantify freshwater lens recovery after overwash events. Bailey et al. (2008) employed the density-dependent groundwater flow and solute transport SUTRA model (Voss and Provost, 2010) to simulate groundwater salinization and quantify recovery time for generic atoll islands by applying a 1 ft. storm surge on modeled islands and applying normal rainfall conditions after that. Also, Chui and Terry (2012) and Terry and Chui (2012) worked on numerical simulations to investigate the effect of overwash events on generic islands by employing SUTRA model also, however, scholars applied constant recharge rates to recover the damaged lens which may not account for the variability and seasonality of rainfall. Later on, Chui and Terry (2013) extended their work by modeling fresh groundwater in only the top 1-2 meters of a 600 meters generic aquifer by running transient simulations for 1 years after the overwash event. Bailey and Jenson (2013) worked on modeling post overwash events recovery in the Federated States of Micronesia. They used daily recharge rate and hourly tidal data to simulate the freshwater lens recovery in the subsequent 3 years after imposing overwash events. Bailey and Jenson (2013) concluded that it takes up to 20 months on average to achieve 80% of pre-overwash freshwater lens status. Recently, Bailey (2015) developed and applied two dimensional SUTRA model to investigate freshwater lens recovery dynamics across ranges of island sizes, rainfall patterns, and aquifer conductivity in the Federated States of Micronesia following hypothetical overwash

events. The study concluded that there is a high variability in the time required for modeled islands to restore their pre overwash event freshwater lens depending on the size of the island and the hydraulic conductivity of the aquifers.

The published literature in modeling post overwash events freshwater lens recovery lacks a comprehensive and three dimensional study that characterizes the post overwash lens dynamics. Moreover, researchers did not address the future possibility of climate change and how that could affect freshwater lens recovery time. In addition, this research quantifies the effect of groundwater pumping from atoll island aquifers on the recovery of the freshwater lens. In this chapter, the research gaps in the hydrological modeling of the atoll islands aquifer over-wash event recovery is addressed by applying 3D calibrated variable density groundwater flow and transport model to selected islands in the Republic of Maldives. This research provides a novel contribution by forcing the calibrated 3D models with the best climatic models extracted from CMIP5 datasets (see Chapter 4) and historical monthly recharge to include climate variability. Also, groundwater pumping in the over-washed islands is included to examine its effect in delaying recovery time. This work is important as it helps in establishing further understanding of post marine overwash events dynamics to help atoll islands communities in managing and planning for their freshwater resources efficiently in catastrophic cases.

6.3 Methods

6.3.1 Screening of Variables Controlling Overwash Events Damage

The damage which can occur to the fresh groundwater due to an overwash event is controlled by multiple factors that contribute to its severity. These factors include:

- The extent of seawater inundation of island surface area (either partial or complete inundation)
- Overwash event duration (the time at which seawater floods the island)
- Seawater ponding depth (i.e. the height of the waves)

These factors seem to be influential in controlling overwash events severity. Several test storms with different combinations of the above listed factors were run on the smallest modeled island under steady recharge to examine the effect of each factor in determining the extent of freshwater lens damage. These initial simulations serve as a guide in applying over-wash events to the other islands during future climate change scenarios. Hypothetical storms were simulated with different seawater ponding depths, storm durations, and inundation percentages. Table 34 shows the post overwash simulated freshwater lens volume. The pre-overwash volume was 293,270 m^3, which is the baseline volume for N. Holhudhoo. The results show that the percentage of inundated island surface controls the overwash event severity. The storm duration and seawater ponding depth effects seem to have minimal impacts. Hence, the percent of land inundation factor would be used as the only factor that determines overwash event severity, and other factors will be neglected.

Table 34 Different hypothetical storms post overwash freshwater lens volume in m^3 (pre-overwash volume is 293,270 m^3).

Seawater ponding		**1m**		**2m**	
Storm duration		**4 hrs.**	**8 hrs.**	**4 hrs.**	**8 hrs.**
Post overwash freshwater lens (m^3)	**25% inundation**	212,500	210,000	212,400	207,700
	50% inundation	132,000	130,000	131,500	127,300

6.3.2 The Extent of Seawater Inundation in Islands

Overwash event is a term used to describe the landward movement of seawater induced by a sudden sea level rise due to the occurrence of tsunami events, or tropical cyclone. This landward movement of seawater would eventually cause partial or complete inundation of islands with seawater. The extent at which seawater will move landward is controlled by the wave height and the beach topographic slope (Figure 44).

The extent of overwash is calculated by dividing average wave height by the average beach slope. Thus, higher waves with flatter beach slope will cause the worst inundation scenario. As for wave heights expected during tsunamis events in the study area, recorded observations for sea levels following a 9.3 Richter scale earthquake in 2004 (earthquake epicenter is 2500 km east of the Republic of Maldives) the study area was reported by Kench et al. (2006). Observations ranged between 1.1-1.8 meters. Table 35 shows different combinations of the resulted landward inundation in meters based on variety of plausible beach slopes and average wave heights.

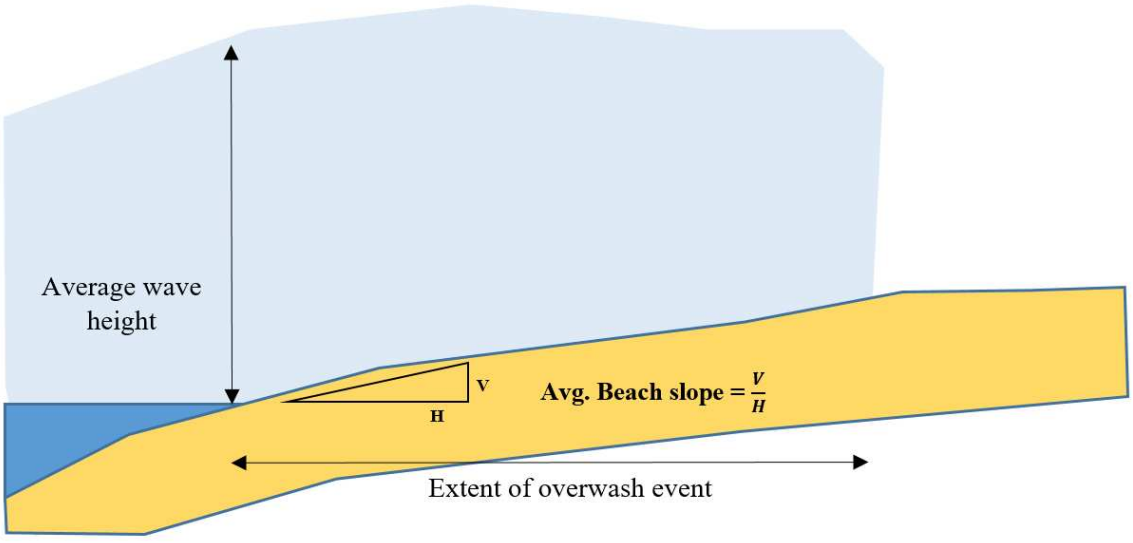

Figure 44 Schematic illustration to the extent of overwash events based on average wave height and average beach slope.

Table 35 Different possible landward inundation extent (meters) based on different wave heights and different beach slopes.

	Average beach slope		
Avg. wave height (m)	**0.50%**	**1.00%**	**2.00%**
1.1	220	110	55
1.3	260	130	65
1.6	320	160	80
1.8	360	180	90

6.3.3 Overwash Event Simulations

Calibrated SEAWAT models that were developed in Chapter 3 were used with modified specified head boundary condition to simulate the event of sweater flooding and inundating coastal areas based on the extents of landward seawater movement as shown above in Table 35. Two categories of overwash events are simulated to assess the damage of freshwater lens under intermediate and extreme overwash events. Category 1 is an overwash event where seawater moves 120-160 meters landward (intermediate overwash event), while Category 2 is a more severe situation where seawater moves 220-260 meters landward. These categories were selected to span possible ranges of overwash events extent. The specified head boundary condition that represents static sea level was adjusted and moved landward to simulate the movement of seawater landward. The baseline freshwater lens volumes were used as pre-overwash lens volumes. A storm duration of 8 hours and seawater ponding depth of 1 meter were selected. Figure 45 shows how the specified head boundary condition is adjusted for the coastal grid cells to simulate seawater movement during overwash events.

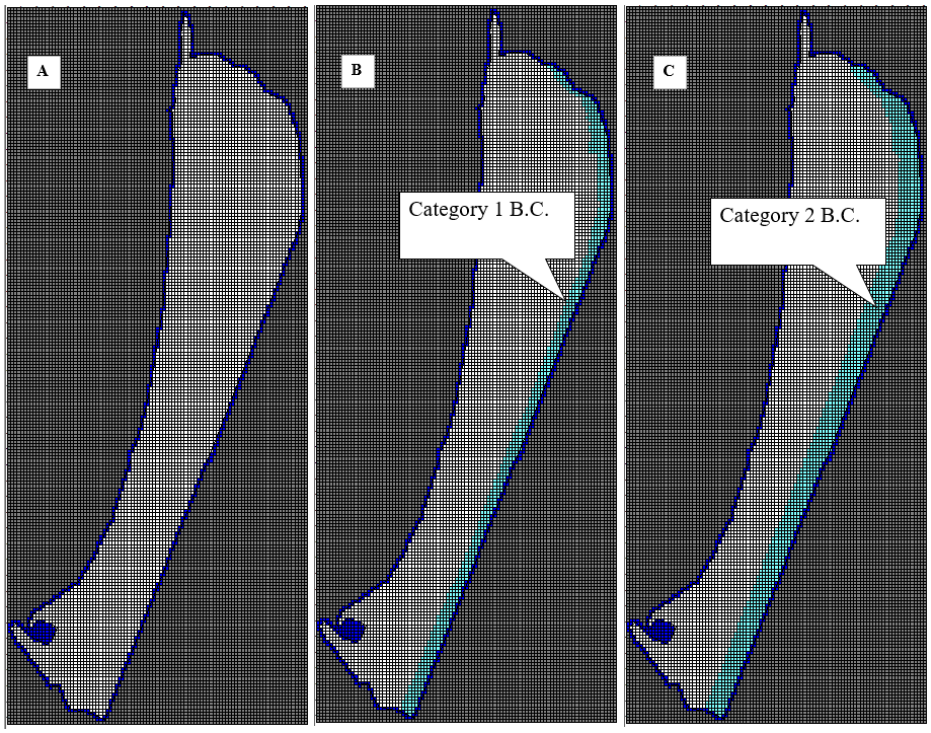

Figure 45 Specified head seawater boundary condition (B.C.) for L. Gan Island in: **A.** No overwash case; **B.** Category 1 overwash event; **C.** Category 2 overwash event. Dark blue cells denote static sea level.

6.3.4 Post Overwash Events Freshwater Lens Recovery Simulations

After overwash simulations were created, post storms concentrations were used as initial concentrations for the recovery simulations. Recovery simulations were run for 5 years and the freshwater lens volume is estimated at different time steps to simulate freshwater lens recovery. Monthly recharge averages from historical rainfall data as well as the best climatic model 2010-2050 monthly averages in each RCP scenario are used to force to the models to examine recovery patterns based on rainfall variability in terms of anticipated climate change. The monthly average was applied to each month during the 5-year recovery period Also, sustainable pumping rates as reported by Bangladesh Consultants groundwater investigation reports (2010a; b; c; d) for the four studied islands were coupled with historical precipitation averages to quantify the effect of groundwater pumping in delaying freshwater lens recovery.

6.4 Results and Discussions

In this section, the results of post overwash events recovery simulations are presented. For each island, two overwash categories were simulated to examine the recovery pattern under intermediate and severe flooding events. In analyzing results, the upper limit of salt concentration for freshwater (i.e., water suitable for drinking) is defined as 2.5% seawater which corresponds to 875 mg/L for total dissolved solids (seawater is assumed to have a total dissolved solids concentration of 35,000 mg/L). Despite the fact that health agencies define the acceptable threshold for the drinking water to be 500 mg/L, 875 mg/L is still acceptable concentration as long as it is below 1,000 mg/L benchmark and it can be considered as a sub-optimal target for freshwater. Defining the acceptable freshwater threshold is important to track freshwater lens recovery and estimate the time needed for islands communities to reuse their water reserves.

6.4.1 N. Holhudhoo Island Results

Figures 46-47 show the freshwater lens recovery after intermediate and severe overwash events. Figure 48 shows two dimensional cross sections for freshwater recovery lens with historical monthly average recharge rates.

Table 36 Freshwater lens recovery percentages 2 years after overwash events under different recharge rates in N. Holhudhoo Island.

Recharge input	GCM ID	% of pre overwash volume after 2 years intermed. storm	% of pre overwash volume after 2 years - severe storm
Historical averages	-	79.2%	55.5%
Historical averages with pumping	-	63.5%	43.0%
RCP2.6 averages	M18	88.1%	60.2%

RCP4.5 averages	M19	67.6%	47.0%
RCP6.0 averages	M19	69.8%	48.7%
RCP8.5 averages	M19	67.9%	47.2%

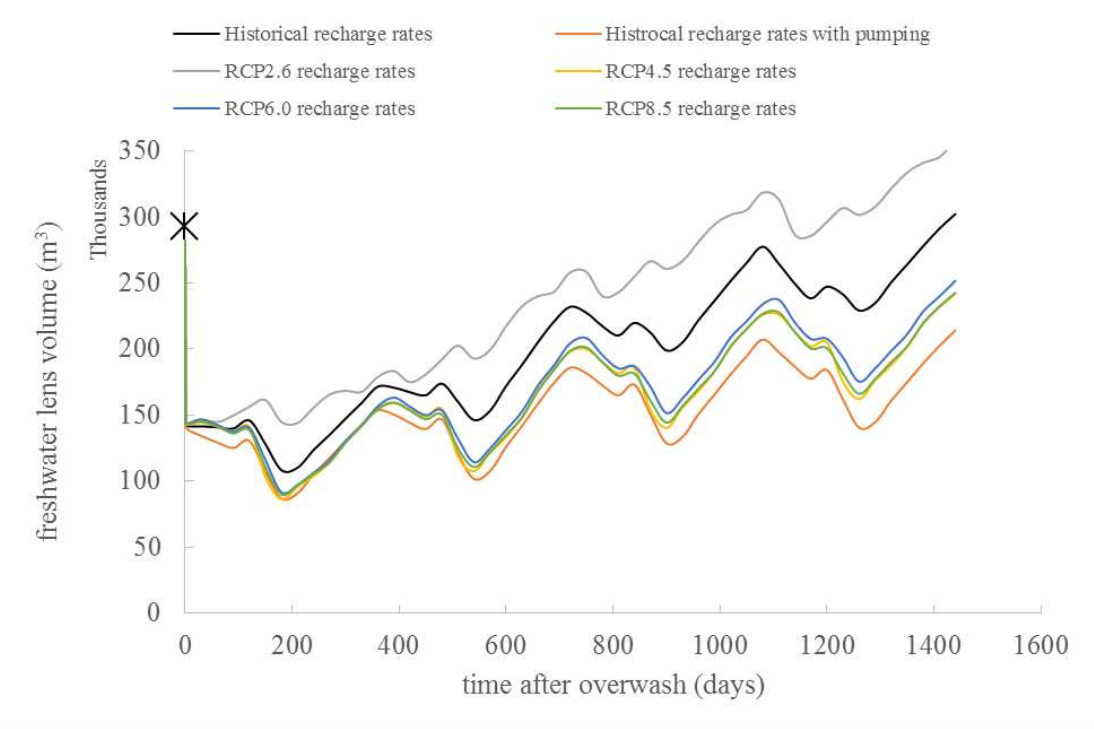

Figure 46 Freshwater lens recovery after intermediate overwash event with different recharge rates inputs (**X** denotes pre-overwash volume).

As shown in Figures 46-48 and in Table 36, N. Holhudhoo Island is seriously (reduced by approximately 60%) affected by simulated overwash events. In the intermediate storm scenario, seawater encroached 120-160 meters landward, and that represents about 35% of Islands width. The small land area of N. Holhudhoo led to a severe freshwater lens salinization. Furthermore, the high hydraulic conductivity of the aquifer promotes rapid transition of the ponding seawater to the shallow groundwater table. The Island showed a more drastic freshwater

lens damage in the severe overwash event scenario, where the post overwash volume dropped by more than 60% which can classified as a catastrophic situation.

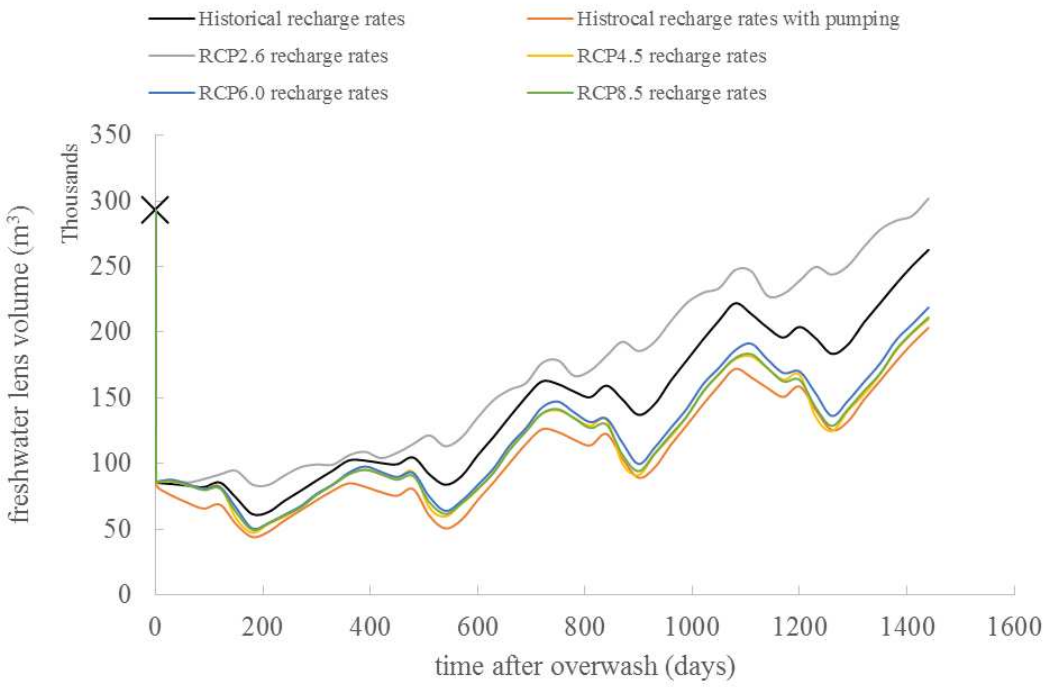

Figure 47 freshwater lens recovery after severe overwash event with different recharge rates inputs (**X** denotes pre-overwash volume).

As for recovery patterns, we note that all recharge rates used are comparable except for RCP2.6 scenario where higher recharge rates are expected by model M18 in the 2010-2050 period. The freshwater lens is expected to restore 65-70% of its pre overwash volume after 2 years following an intermediate overwash event, while under severe overwash events, the freshwater lens will restore 45-55% of its pre overwash volume after 2 year after the overwash event. Figure 48 shows cross sections of freshwater lens at different time steps after overwash events. The shallow freshwater lens is instantly damaged after the overwash and a plume of

seawater is observed. The extent of the seawater water plume remains the same even after 180 days.

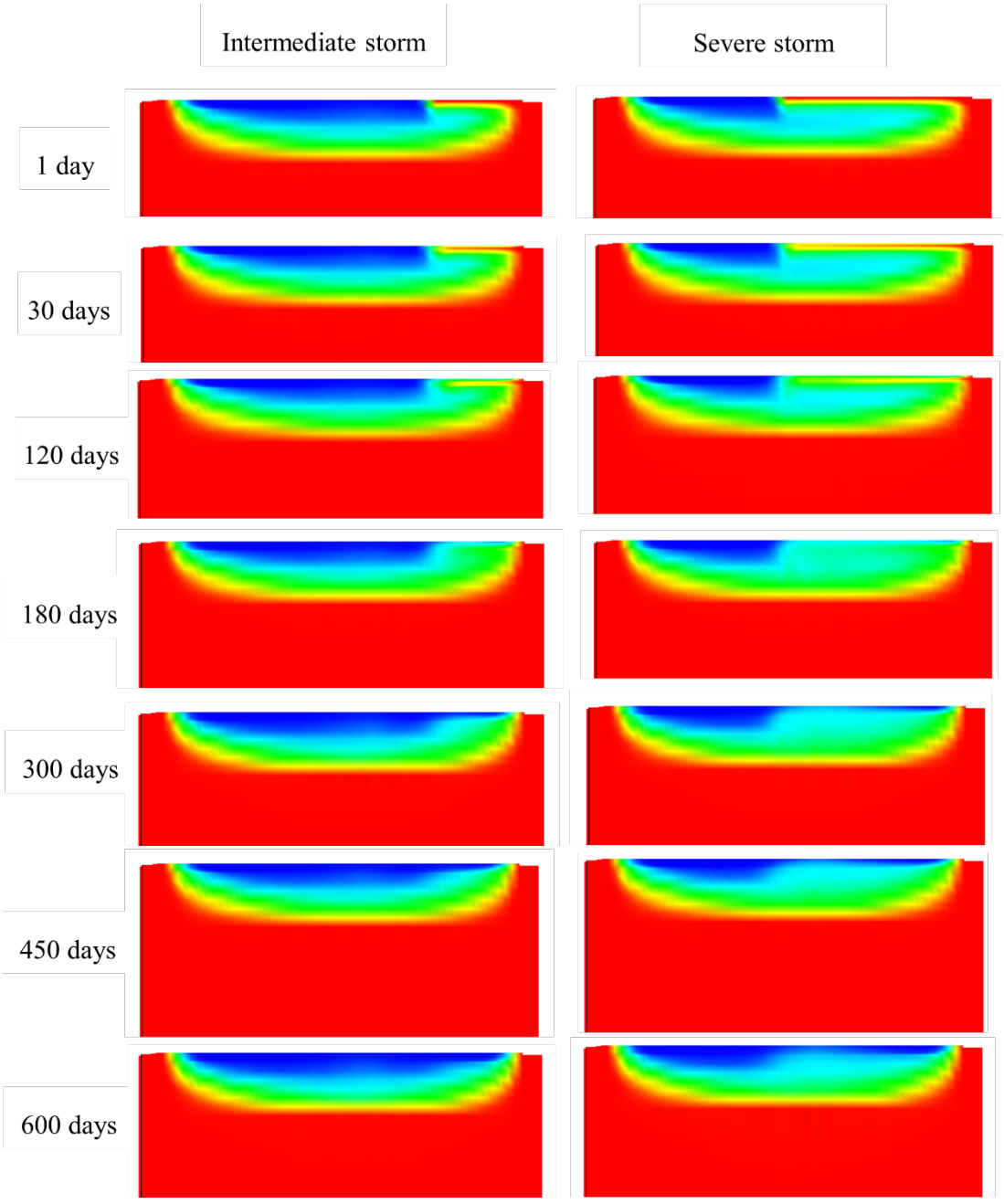

Figure 48 Two dimensional cross section for freshwater lens recovery progression after intermediate and severe storms for N. Holhudhoo Island under historical monthly average recharge rates.

A thin layer of freshwater is formed atop the seawater plume after 300 days. The newly formed freshwater begins to expand after 450 days of the overwash. After 600 days, the freshwater lens seem to have its pre overwash shape in the intermediate overwash scenario, however, in the severe overwash scenario, the seawater plume can be noticed even after that long time. Groundwater pumping lens is found to have a substantial effect on freshwater lens recovery. It is concluded that the freshwater lens will restore 63.47%, and 43.02% with pumping, in intermediate storm and severe storm scenarios respectively, of its pre overwash volume after 2 years of freshwater recharge in comparison to 79.23%, and 55.47% without pumping. Pumping lags the time required for freshwater lens recovery as it sinks freshwater water that would dilute the shallow salinized water table. Limited island width and limited land area are the main reasons for the drastic freshwater lens depletion and slow recovery. As the width of the island is about 350-400 meters which makes it vulnerable to 50% or more inundation during severe overwash events and consequently, serious damage to the freshwater lens can occur. The limited island area is also contributing to the slow freshwater lens recovery, small land area captures less amount of freshwater which dilutes the newly formed shallow seawater plume. The results for overwash events recovery for N. Holhudhoo Island emphasizes the conclusions made in Chapters 4 and 5 that smaller islands' freshwater resources are more vulnerable to depletion due to environmental and anthropogenic stresses.

6.4.2 N. Velidhoo Island Results

The results of N. Velidhoo are presented in this section and are shown in Figures 49-51, and in Table 37

Table 37 Freshwater lens recovery percentages 2 years after overwash events under different recharge rates in N. Velidhoo Island.

Recharge input	GCM ID	% of pre overwash volume after 2 years intermed. storm	% of pre overwash volume after 2 years severe storm
Historical average	-	62.9%	56.3%
Historical average with pumping	-	59.1%	52.1%
RCP2.6 averages	M18	67.7%	59.9%
RCP4.5 averages	M19	55.4%	49.1%
RCP6.0 averages	M19	56.9%	50.6%
RCP8.5 averages	M19	55.8%	49.5%

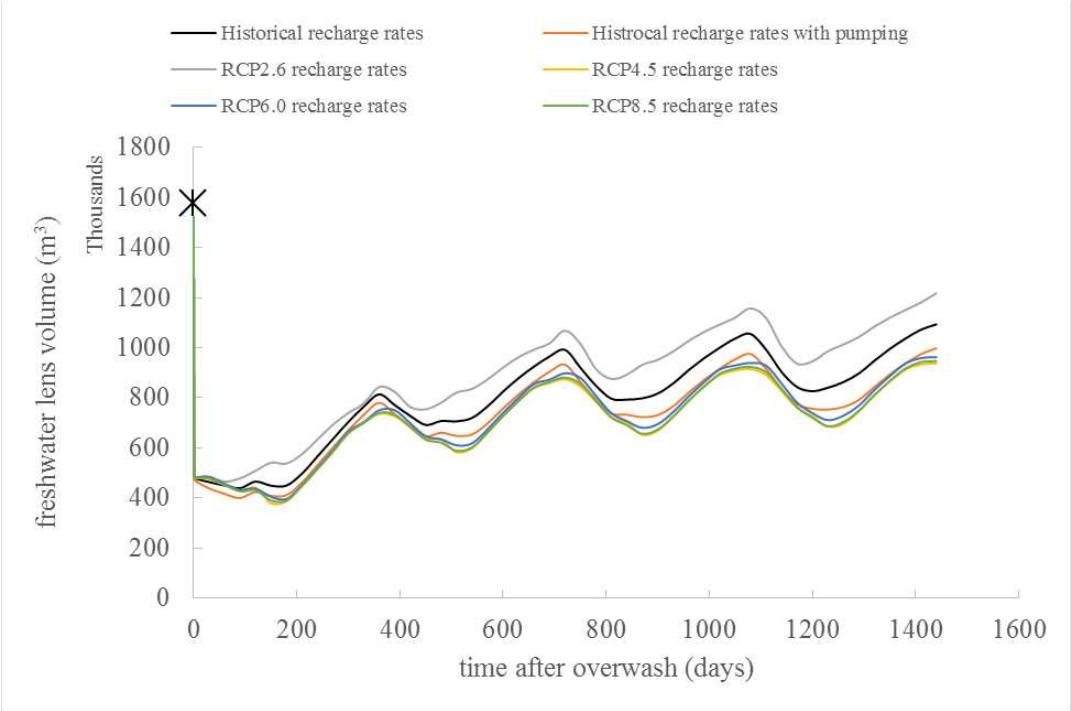

Figure 49 Freshwater lens recovery after intermediate overwash event with different recharge rates inputs for N. Velidhoo Island (**X** denotes pre-overwash volume).

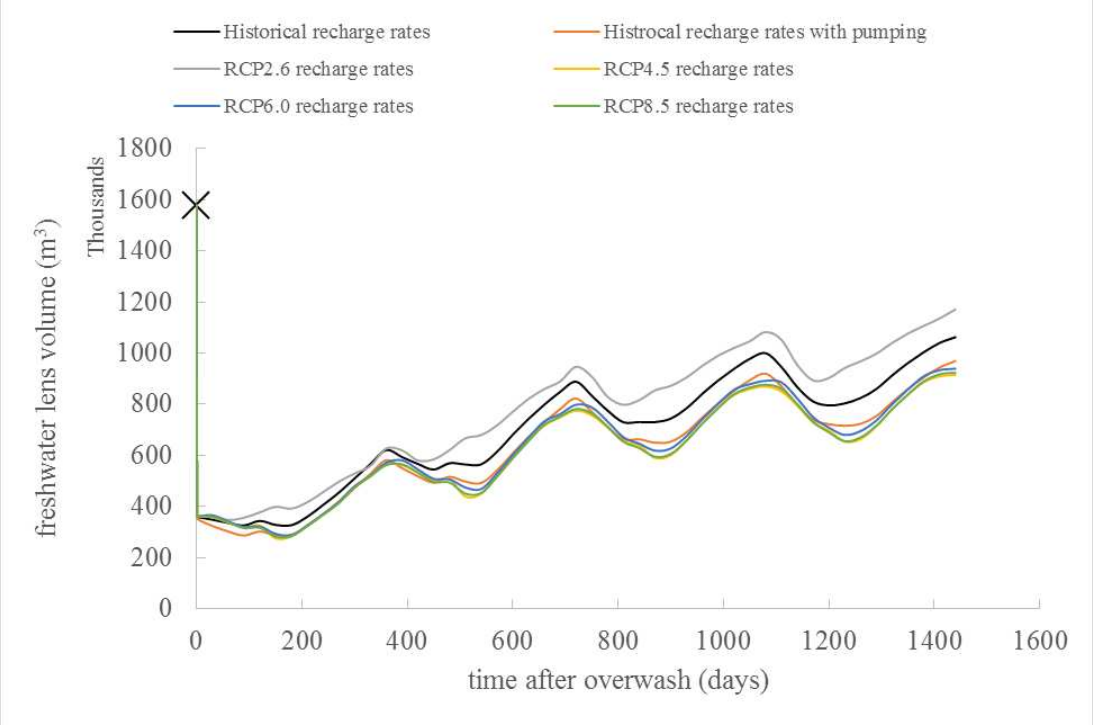

Figure 50 Freshwater lens recovery after severe overwash event with different recharge rates inputs for N. Velidhoo Island (**X** denotes pre-overwash volume).

As shown in Figures 49-50 and in Table 37, N. Velidhoo Island is substantially affected by simulated overwash events. In the intermediate storm scenario, seawater encroached 120-160 meters landward, and that represents about 25% of Islands width. The Island showed a drastic freshwater lens damage in the severe overwash event scenario, where the post overwash volume reduction ranged between approximately 49-56% which is considered a serious condition, however, it is a better result if compared to N. Holhudhoo Island.

As for recovery patterns, we note that all recharge rates used are comparable with RCP2.6 which is scenario forecasting quicker recovery. The freshwater lens is expected to restore 55-67% of its pre overwash volume after 2 years following an intermediate overwash event, while under severe overwash events, the freshwater lens will restore 49-56% of its pre overwash volume after 2 year after the overwash event

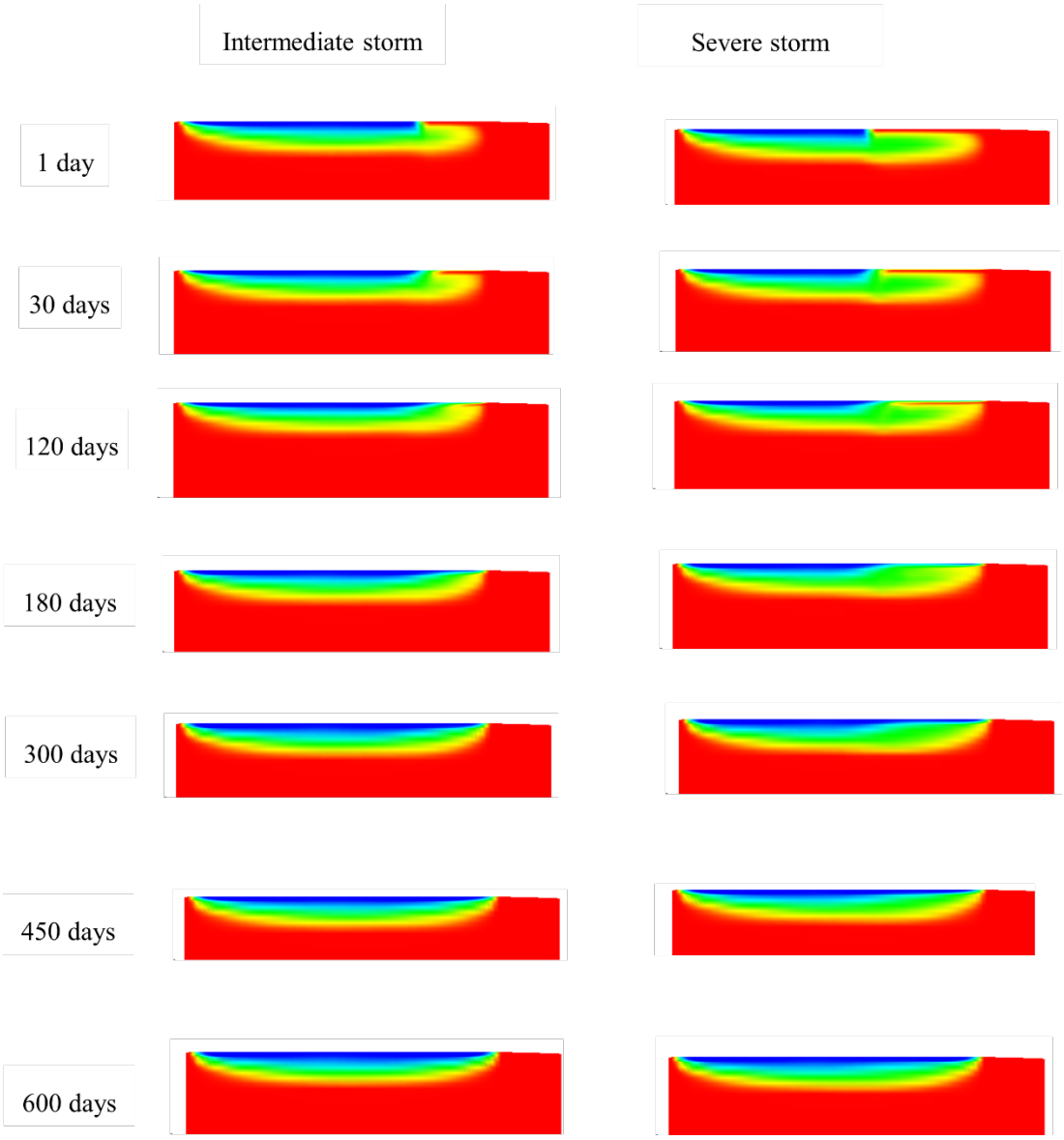

Figure 51 Two dimensional cross section for freshwater lens recovery progression after intermediate and severe storms for N. Velidhoo Island under historical monthly average recharge rates.

The shallow freshwater lens is instantly damaged after the overwash and a plume of seawater is observed. The extent of the seawater water plume remains the same even after 120 days in both storm scenarios. A thin layer of freshwater is formed atop the seawater plume after 180 days in the intermediate storm scenario, while it takes about 300 days to form that thin layer in the severe storm scenario. After 600 days, the freshwater lens begins to restore pre overwash

shape in the both overwash scenarios (Figure 51). Groundwater pumping lens is found to have a minimal impact on freshwater lens recovery in the intermediate storm scenario, while in severe storms scenario the effect of pumping is found to be significant.

6.4.3 GDh. Thinadhoo Island Results

Figures 52-53 show the freshwater lens recovery after intermediate and severe overwash events. Figure 54 shows two dimensional cross sections for the freshwater lens recovery with historical monthly average recharge rates.

Table 38 Freshwater lens recovery percentages 2 years after overwash events under different recharge rates in Gdh. Thinadhoo Island.

Recharge input	GCM ID	% of pre overwash volume after 2 years intermed. Storm	% of pre overwash volume after 2 years severe storm
Historical average	-	49.1%	45.7%
Historical average with pumping	-	43.7%	39.9%
RCP2.6 averages	M17	55.0%	51.5%
RCP4.5 averages	M3	49.0%	45.5%
RCP6.0 averages	M3	49.0%	45.5%
RCP8.5 averages	M3	49.6%	46.1%

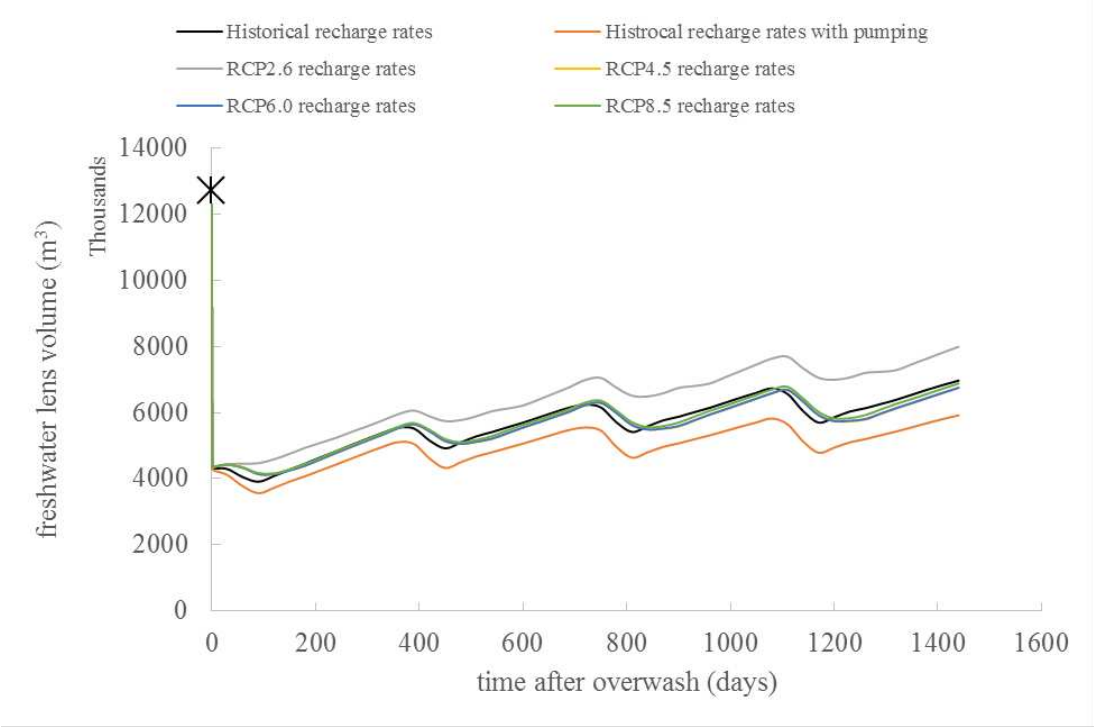

Figure 52 Freshwater lens recovery after intermediate overwash event with different recharge rates inputs for GDh. Thinadhoo Island (**X** denotes pre-overwash volume).

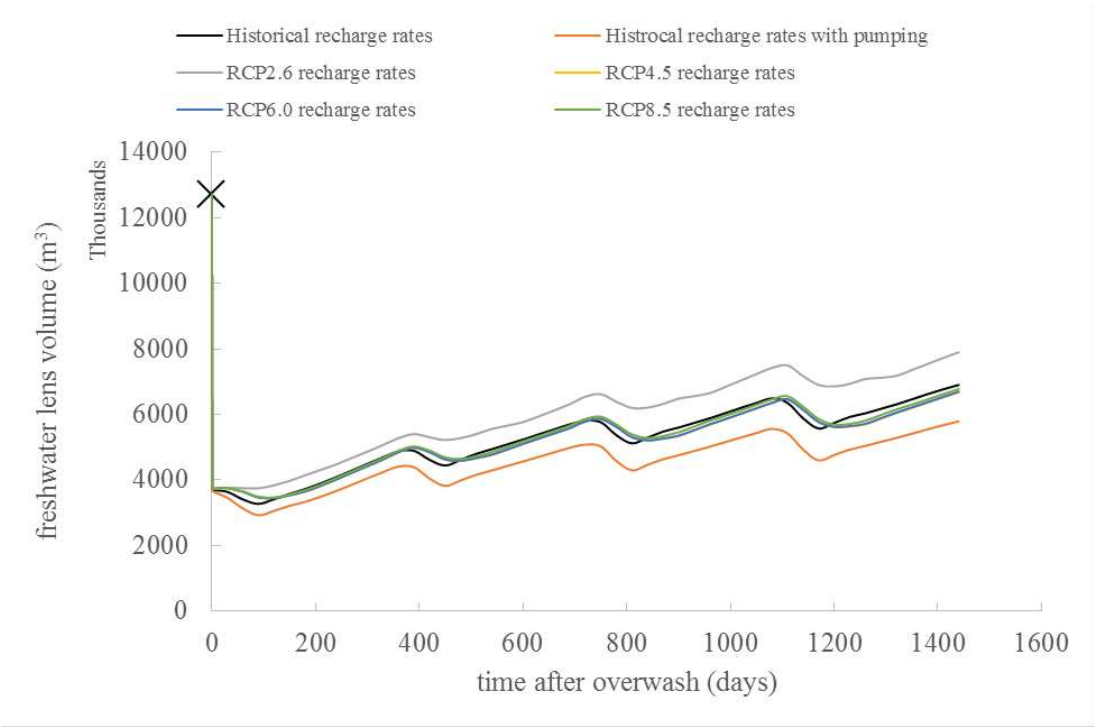

Figure 53 Freshwater lens recovery after severe overwash event with different recharge rates inputs for GDh. Thinadhoo Island (X denotes pre-overwash volume).

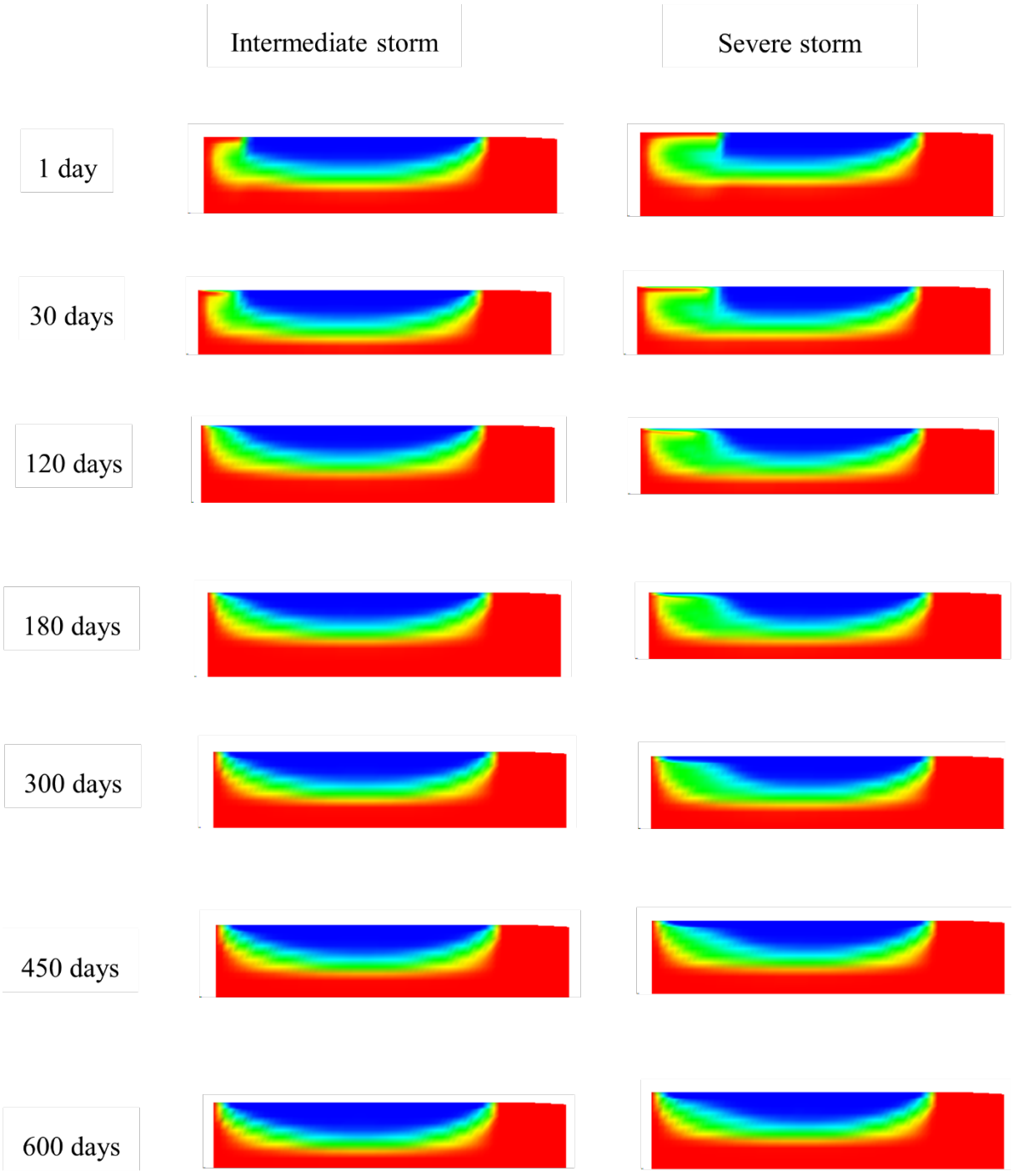

Figure 54 Two dimensional cross sections for freshwater lens recovery progression after intermediate and severe storms for GDh. Thinadhoo Island under historical monthly average recharge rates.

As shown in Figures 52-53 and in Table 38, the freshwater lens in GDh. Thinadhoo Island is abruptly reduced after seawater overwash. The freshwater volume reduction percentages in the intermediate and the severe overwash scenarios are comparable. The adequate island width minimizes the contribution of storm severity in damaging the freshwater lens. As for recovery patterns, we note that all recharge rates recover the freshwater lens at the same pattern with no variability trend noticed. However, in the mitigated emission scenario, RCP2.6, a quicker freshwater lens recovery is predicted. The freshwater lens is expected to restore 43-55% of its pre overwash volume after 2 years following an intermediate overwash event, while under severe overwash events, the freshwater lens will restore 40-52% of its pre overwash volume after 2 year after the overwash event. Generally, slower recovery trends are noticed in this island especially in low rainfall seasons as bigger lens needs longer time to rebuild its pre overwash status. As for pumping effect, results show that groundwater extraction reduced the freshwater lens recovery after 2 years by 5-6% in the intermediate and severe overwash scenarios which is considered a minimal impact. The shallow freshwater lens is instantly damaged after the overwash and as shown in Figure 54. The extent of the seawater water plume remains the same even after 120 days in the severe storm scenario, while a thin layer of freshwater is formed atop the seawater plume after 120 days in the intermediate storm scenario. It takes about 180 days to that thin freshwater layer to form in the severe storm scenario. After 600 days, the freshwater lens begins to restore its pre overwash shape in the both overwash scenarios.

6.4.4 L. Gan Island Results

Figures 55-56 show the freshwater lens recovery after intermediate and severe overwash events. Figure 57 shows two dimensional cross sections for the progress of freshwater lens recover with historical monthly average recharge rates.

Table 39 Freshwater lens recovery percentages 2 years after overwash events under different recharge rates in L. Gan Island.

Recharge input	GCM ID	% of pre overwash volume after 2 years - intermed. Storm	% of pre overwash volume after 2 years - severe storm
Historical average	-	41.2%	38.6%
Historical average with pumping	-	36.1%	33.5%
RCP2.6 averages	M17	48.4%	45.4%
RCP4.5 averages	M3	41.5%	38.8%
RCP6.0 averages	M3	41.4%	38.7%
RCP8.5 averages	M3	42.1%	39.4%

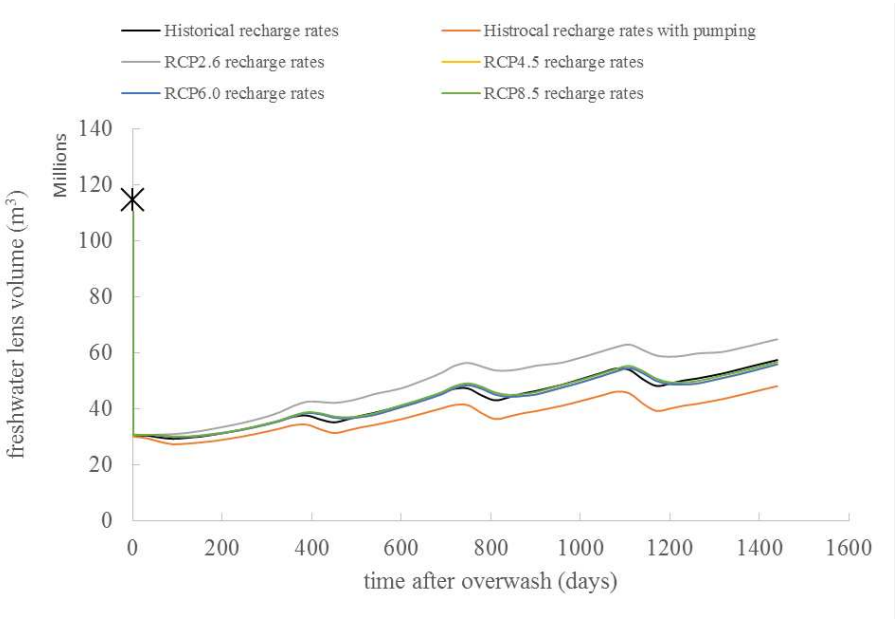

Figure 55 Freshwater lens recovery after severe overwash event with different recharge rates inputs for L. Gan Island (**X** denotes pre-overwash volume).

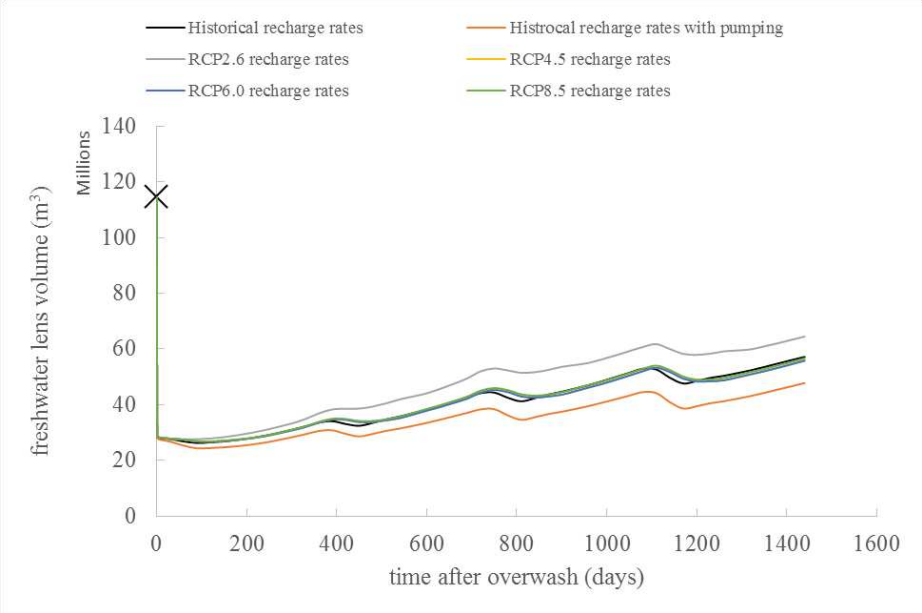

Figure 56 Freshwater lens recovery after severe overwash event with different recharge rates inputs for L. Gan Island (**X** denotes pre-overwash volume).

As shown in Figures 55-56 and in Table 39, the freshwater lens in L. Gan Island is abruptly reduced after seawater overwash. The freshwater volume reduction percentages in the intermediate and the severe overwash scenarios are nearly the same. This confirms that the response that GDh. Thinadhoo Island had, that larger islands are less affected by the extent of the overwash event flooding. Figures 55-56 show recovery patterns in L. Gan Island under different recharge rates. Generally, it is observed that there is no strong variability between patterns. However, the results show that a quicker freshwater lens recovery is anticipated under mitigated emission scenario.

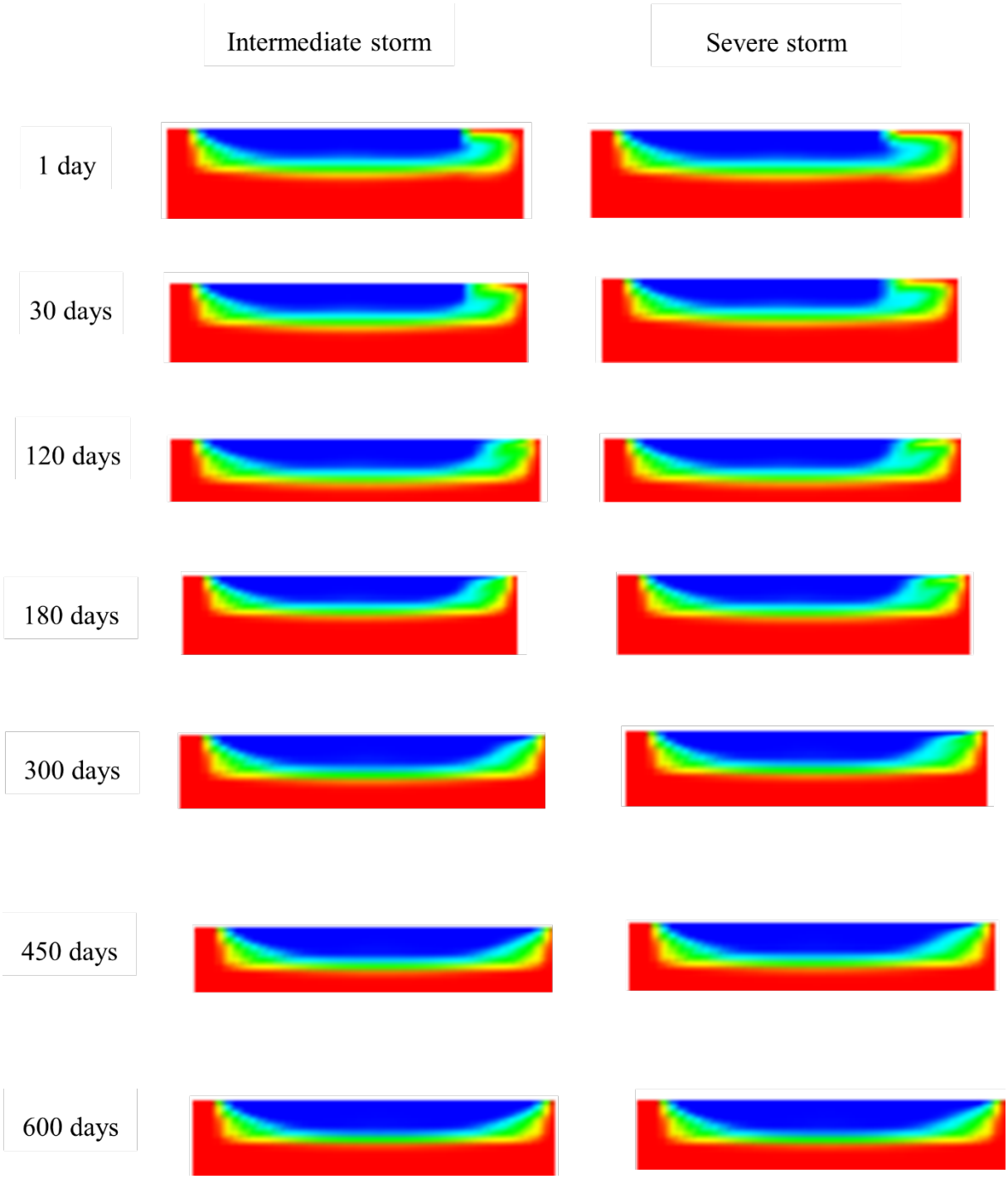

Figure 57 Two dimensional cross sections for freshwater lens recovery progression after intermediate and severe storms for L. Gan Island under historical monthly average recharge rates.

The freshwater lens is expected to restore 43-55% of its pre overwash volume after 2 years following an intermediate overwash event, while under severe overwash events, the freshwater lens will restore 34-45% of its pre overwash volume after 2 year after the overwash event. Moreover, recovery curves seem to be flatter for L. Gan Island if compared to smaller islands such as N. Holhudhoo. As for pumping effect, results show that groundwater extraction reduced the freshwater lens recovery after 2 years by 5-6% in the intermediate and severe overwash scenarios which is considered a minimal impact. The shallow freshwater lens is instantly damaged. After the overwash, a plume of seawater is observed. The extent of the seawater water plume remains the same even after 120 days in the severe storm scenario, while a thin layer of freshwater is formed atop the seawater plume after 120 days in the intermediate storm scenario. It takes about 180 days to form that thin freshwater layer in the severe storm scenario. After 450 days, the freshwater lens begins to restore pre overwash shape in the both overwash scenarios (Figure 57).

6.4.5 Island Size Effect on Recovery Time

As shown above in the previous sections, larger showed relatively less recovery percentages even after two years. The bigger volume of the freshwater lens needs longer time to have that lens recovered after being salinized by seawater. Figure 58 shows the relation between the pre overwash lens volume, and the average lens recovery percentages (from Category 1, and Category 2 storms) with the historical recharge forcing. The relation is linear, hence, the average recovery percentages of other islands can be easily determined.

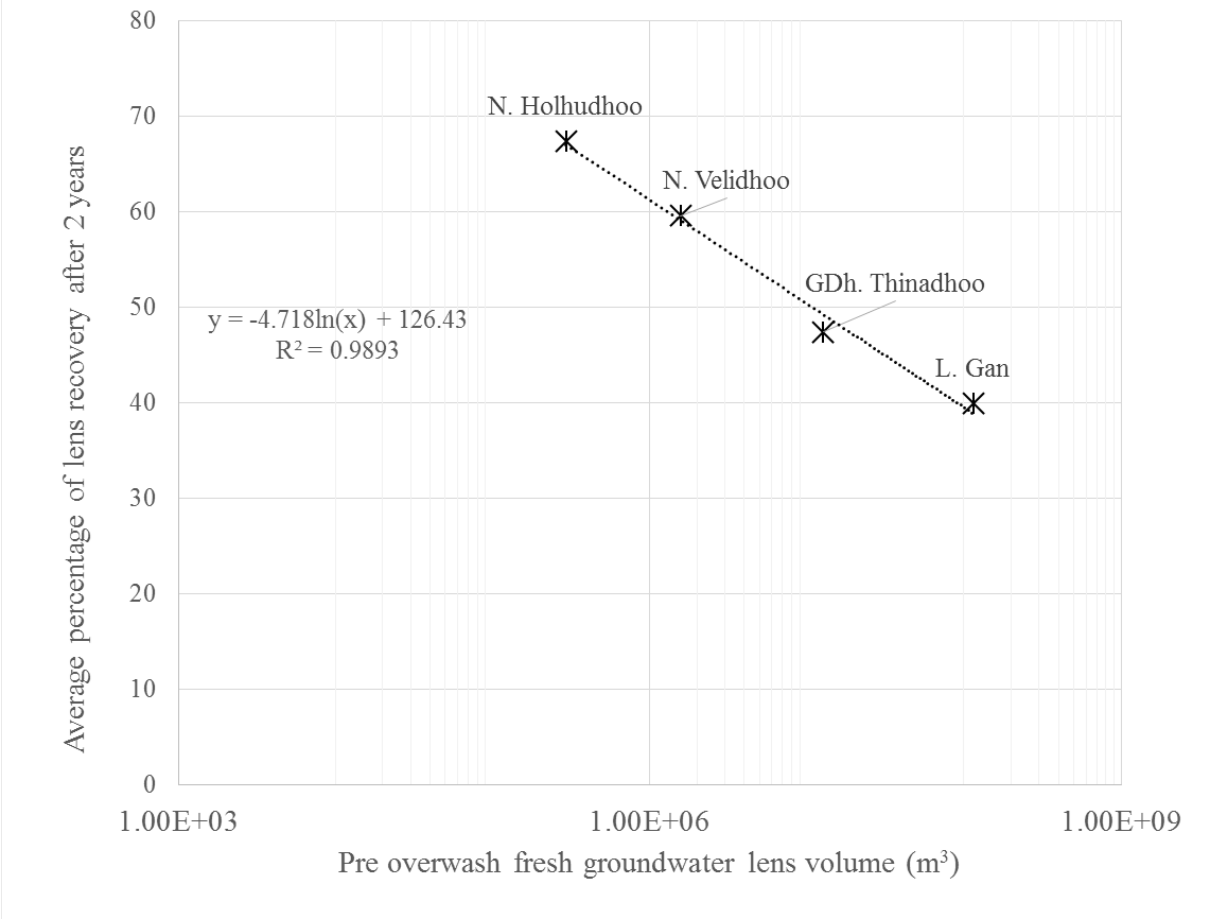

Figure 58 Relation between pre overwash lens volume and average lens recovery after 2 years (semi-log scale).

6.5 Conclusion

Marine overwash event is the process of sudden increase of sea level induced by the occurrence of tsunamis, storm surge, rogue waves, strong wave set-up accompanied with enhanced winds activity. Such kind of environmental conditions represent serious threat to the freshwater resources in small and low lying atoll islands. Seawater may partially or completely inundate islands and seawater ponds are formed. Ponding seawater infiltrates through the unsaturated zone and salinizes the shallow water table. Advanced understanding of the transient aquifer recovery and freshwater lens development following an overwash induced aquifer

salinization is essential. While most published research in this field did not model the problem in three dimensions, neither included variable rainfall patterns induced by climate change into account. This research developed and applied numerical models to atoll islands within the study area to quantify freshwater lens recovery dynamics.

Calibrated SEAWAT models which were developed in Chapter 3 were employed to investigate the recovery patterns for the studied islands in the Republic of Maldives following two categories of hypothetical intermediate and severe overwash events. Variations in overwash extents (seawater ponding depth, and storm duration) did not show significant additional damages to the freshwater lens. The controlling factor into classifying the severity of overwash events is the percentage of land area inundated. Selected islands represent various island widths, two climatic regions and associated rainfall pattern (Northern and Southern regions), and geologic characteristics (hydraulic conductivity) to provide a comprehensive assessment of freshwater lens post overwash events recovery in atoll islands aquifers.

Results showed instant damage of freshwater lens in all islands. Freshwater reserves depleted to critical levels in small islands especially in severe overwash events simulations as seawater inundated as high as one third of islands land area. Larger islands showed relatively slower recovery patterns, where percentages for the recovered freshwater lenses after two years following the storms were a bit lower than percentages in smaller islands. Mitigated emission climate change models showed that freshwater lenses may recover quicker in both climatic regions studied, while other RCPs scenarios did not show any variability in freshwater lens recovery in comparison to historical averages. The effect of pumping caused a lag in freshwater lens recovery especially in smaller islands under severe overwash events scenarios. Generally, freshwater lenses in modeled islands restored 35-65% of their pre overwash status within 2 years

flowing overwash events. The results of the expected recovery times in this research seem higher than the recovery times predicted by other studies (e.g. Bailey and Jenson, 2013; and Bailey, 2015). Using monthly variable recharges, which account for dry seasons, rather than just applying steady recharge rates caused that prolonged recovery times. Understanding the recovery patterns of post overwash freshwater lens and quantifying the time required to restore the pre overwash status is an important aspect of effective water resources management for individual atoll island communities and for governments of atoll nations. Although this study was applied to a specific region, the applied methodology can be generalized to similar atoll island aquifers of comparable sizes and aquifer characteristics to provide an indication of freshwater lens recovery after overwash events for islands in other atoll islands nations.

CHAPTER 7. FRESHWATER SUPPLY VULNERABILITY ANALYSIS IN ATOLL ISLANDS UNDER ANTHROPOGENIC AND ENVIRONMENTAL STRESSES

In this chapter, the fresh groundwater supply fluctuation in atoll islands' communities due various stresses such as: rainfall variability, coastal areas inundation, and pumping is addressed to provide an overall evaluation of water security in atoll islands based on the previous chapters findings.

7.1 Introduction

Groundwater represents a crucial and valuable water resource in small atoll islands. Usually, people in atoll islands communities extract groundwater manually using hand dug wells which penetrate few meters through the unsaturated zone. Electric pumps also exist in these developing nations where larger amounts of water can be extracted. The groundwater is extracted from the lens shaped, and shallow water that floats over more saline seawater. Due to the extreme fragility of the fresh groundwater lens, extracted groundwater is subject to seasonal and occasional depletion due to various reasons such as drought periods, or catastrophic fresh groundwater lens damage due to overwash events. On the other hand, extreme pumping rates in wet seasons could cause seawater upconing and temporary salinization of the aquifer as higher pumping rates promotes seawater mixing with freshwater.

To optimize water supply, efficient water management practices should be enforced and appropriate groundwater extraction rates should be taken into future water shortage plans. In this chapter the findings of the previous work done regarding threats that could deplete freshwater reserves are employed to conduct a vulnerability analysis of the future status of fresh

groundwater supply for domestic purposes under variety of stresses (variable rainfall patterns, sea level rise, overwash events, and population growth) that could deplete freshwater reserves in atoll islands communities.

7.2 Methods

7.2.1 Population Growth Estimation

The number of island inhabitants is a key factor in determining water needs in atoll islands communities. Hence, a future projection of islands population is needed to estimate water demands. Population growth rates as reported by islands offices as reported in Bangladesh Ltd. groundwater investigation reports (2010a, b, c, d) are used as well as total population in 2009 to forecast population in the upcoming decades. Table 40 shows islands population in 2009 and associated growth rates.

Table 40 Islands population and associated population growth rates (Islands office data as reported by Bangladesh Consultant Ltd. field reports 2010 a; b; c; d).

Island	Population in 2009	Growth rate
N. Holhudhoo	2,063	0.34%
N. Velidhoo	2,256	1.15%
GDh. Thinadhoo	6,745	1.25%
L. Gan	4,208	13.5%

The population growth rates listed in Table 40 are based on 2006 till 2009 population increase, we note that L. Gan island population increased by 13.5% annually, which is a huge increase, so,

a more realistic growth rate of 4% will be used. To estimate future growth, an exponential growth equation is used. Equation (7.1) forecasts future population after *n* years for developing regions with population more than 2000 (SANAA, 1991) as follows:

$$P_f = P_c(1+G)^n \qquad (7.1)$$

where

P_f is the future population after *n* years

P_c is the current population

G is the annual population growth rate

n is the number of years

7.2.2 Fresh groundwater supply estimation and reliability curves

Available fresh groundwater lens volumes until 2050 were modeled in the study area under variety of environmental conditions that may affect the freshwater quantity. The porosity of the upper Holocene aquifer is multiplied by the saturated freshwater lens volume to provide an estimate of the amount freshwater volume residing in the pore spaces which is considered. However, the maximum quantity of water that can be pumped out of the unconfined aquifer is defined by the specific yield (S_y) as not all water can be pumped out due to retention. However, the amount that is usually pumped is very less than the saturated volume multiplied by the specific yield (which equals the porosity if the specific retention is neglected) as pumping is constrained to the sustainability constraint where pumped water should not exceed the amount of annual recharge in addition to the pumping technologies limitations in such a developing nation.

Falkland (2010 a,b,c,d) estimated that only 30% of recharge volume can be extracted to retain freshwater lens sustainability in the Northern atoll islands of the Maldives and 35% in the Southern atoll islands of the Maldives in the study area. Other investigations on other small islands recommend that 25%-50% of the annual recharge to the groundwater lens can be pumped without causing lens depletion (Falkland, 1991). The estimation of Falkland (2010) examined and selected in the context of analyzing future groundwater trends in the Maldivian atolls by running simulations to assess such pumping rates long term impact on the depletion of the freshwater lens.

The recharge volume is calculated by multiplying the depth of recharge by the island surface area. The depth of recharge is subject to variability according to the climatic forecasts which were presented and analyzed in Chapter 4. Moreover, the island area can change if shoreline recession occurs or over-wash events salinize portions of islands area making pumping in the over washed parts inappropriate. To provide a normalized approach to compare all possible threats that may affect the freshwater lens, cumulative probability distributions for each of the scenarios modeled in Chapters 4, 5, and 6 are created to assess the probability of attaining the minimum accepted threshold for securing daily domestic demands of freshwater supply.

7.2.3 Groundwater Pumping Rates Evaluation

Pumping rates impact assessment is conducted by running simulations with the suggested pumping rates to the calibrated models for 10 years and adding the pumping stress through a number of wells (5 wells in N. Holhudhoo, and N. Velidhoo; 10 wells in GDh. Thinadhoo; 20 wells in L. Gan) spread across each island. The pumping rates are assigned to be 30% and 35% of recharge in the Northern and in the Southern Islands respectively. According to Falkland

(2010) these percentages are converted based on the annual recharge average to 6.3 KL/ha/day, and 10 KL/ha/day in the Northern and Southern climatic regions respectively. The observed lens volumes in December, 2009 were taken as initial conditions for the models. The freshwater lens volume during the 10-year period with and without pumping is shown in Figure 57 for the four islands. It is concluded that the suggested pumping rates do not cause long term depletion from initial condition to the freshwater lens for all islands except L. Gan where higher pumping rates can be applied. By estimating the groundwater volume that can be extracted from the groundwater lens, available freshwater to island communities under each scenario is known. And so, the vulnerability of groundwater supply according to each potential threat is quantified. Hence, a rank of the most severe situations of water shortage can be found, and the most critical threat to the water lens can be identified. This information can promote more efficient water resources management practices by giving island communities what environmental or anthropogenic threats that are most severe so future water security plans are made accordingly.

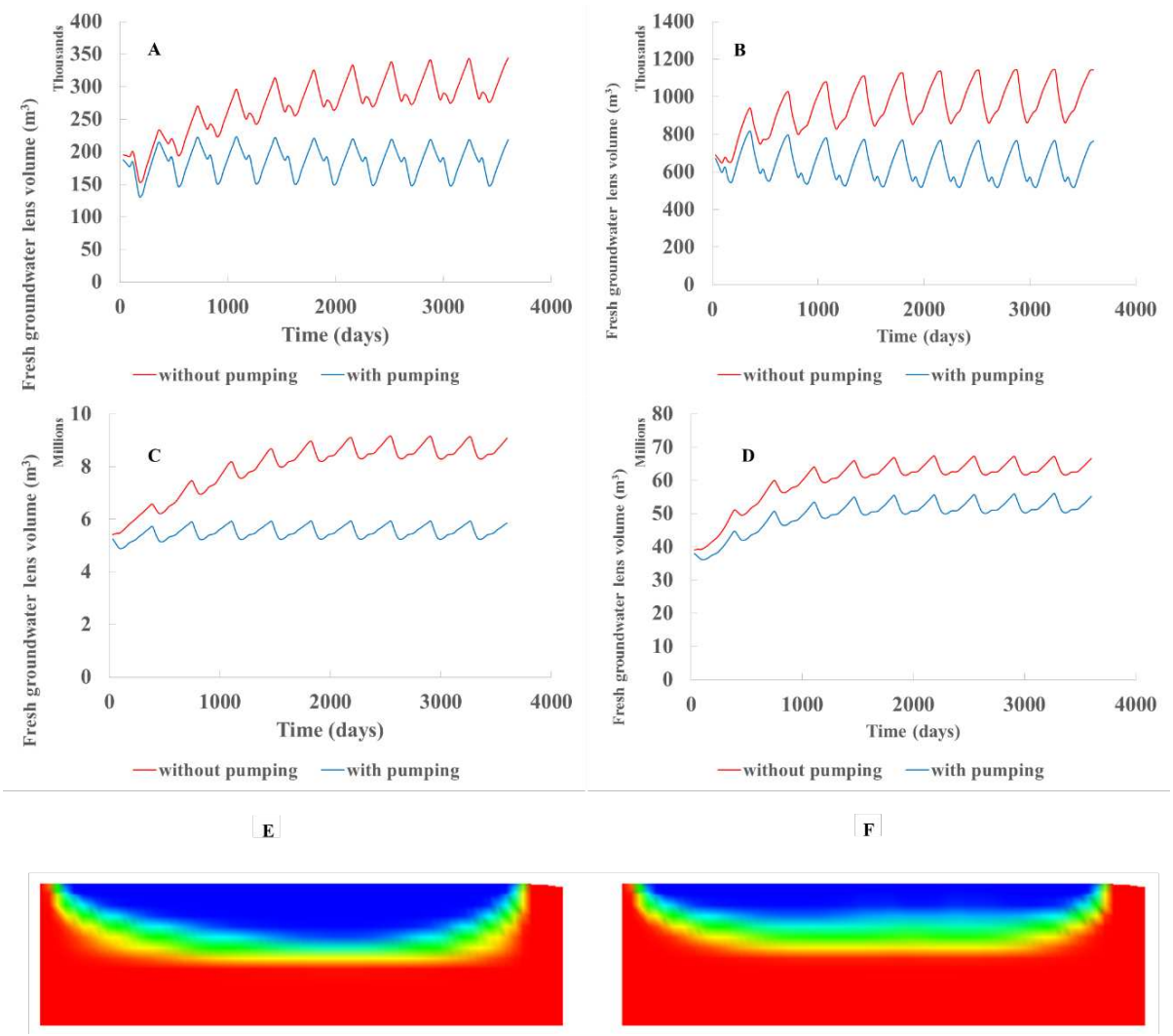

Figure 59 Pumping rates suggested by Falkland (2010) evaluation for **A.** N. Holhudhoo Island; **B.** N. Velidhoo Island; **C.** GDh. Thinadhoo; **D.** L. Gan; **E.** Mid-Island cross section for GDh. Thinadhoo after 10 years without pumping; **F.** Mid-Island cross section for GDh. Thinadhoo after 10 years with pumping. Red color denotes seawater, and blue denotes freshwater with transitional zone in between.

7.2.4 Domestic Water Demand Estimation

Estimates of water demand are necessary to plan for water supply. In atoll islands communities, residential sector is the main water consuming sector especially in small islands with no industrial demand. The domestic (residential) freshwater demand includes consumptive (drinking, and cooking) and non-consumptive uses (clothes washing, sanitary cleaning and toilet flushing). Through the field work that was done by Falkland (2001) on the islands in the

Republic of Maldives, estimations were made for islands inhabitants' water uses and demands. The domestic freshwater supply is dependent on the used sewage water discharge system according to the following:

- 50 Liters/capita/day if no toilet flush is used
- 70 Liters/capita/day if pour flush is used
- 100 Liters/capita/day if cistern flush is used

Based on different classes of sanitation systems, the water demand is calculated and multiplied by island total population.

7.3 Results

7.3.1 N. Holhudhoo Island

The groundwater supply from the freshwater lens in N. Holhudhoo Island analysis results under the base scenario (only climate change through 2050), sea level rise scenarios, and two categories of overwash events are presented in this section. Category 1 storm refers to the intermediate storm scenario, while Category 2 refers to the severe storm scenario. Figures 61 shows exceedance probability distributions for monthly average groundwater supply under each scenario. Figure 62 shows the annual averages and time series fluctuation for the groundwater supply under each scenario. Population growth for N. Holhudhoo Island is calculated using the exponential growth equation (7.1) and is shown in Figure 60. The best climatic model in each RCP scenario is used in Figure 60. The results of other climatic models are shown in the Appendix.

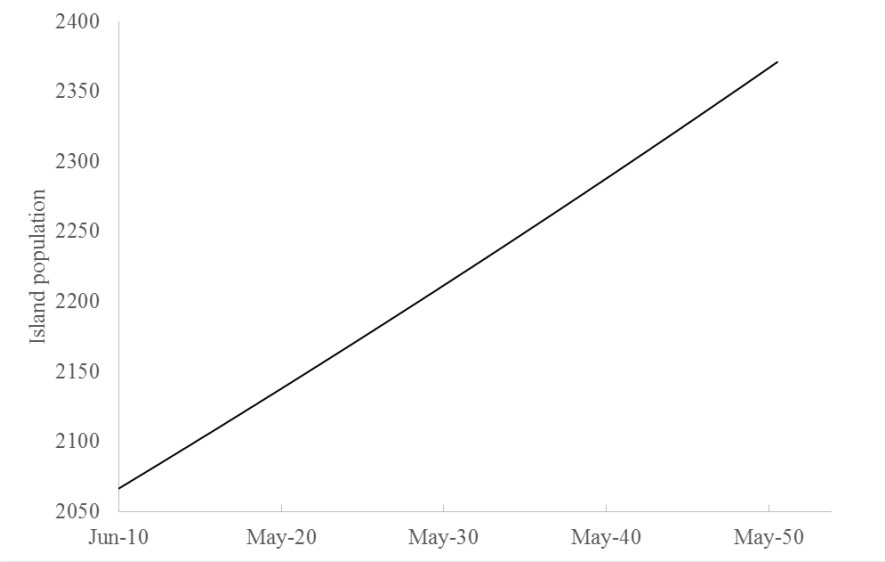

Figure 60 Population growth in N. Holhudhoo Island from 2010-2050.

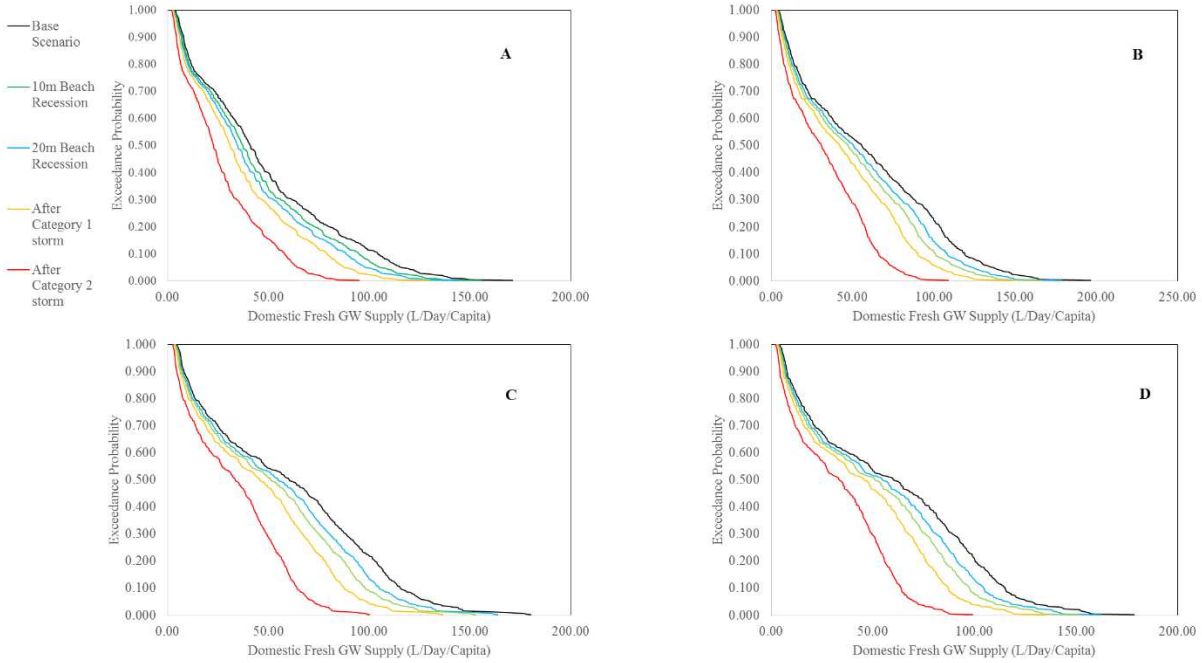

Figure 61 Exceedance probability distribution for monthly groundwater supply average (based on pumping rate = 30% of the monthly recharge) in N. Holhudhoo Island under different climatic RCPs forecasts; **A.** RCP2.6 using model M18; **B.** RCP4.5 using model M19; **C.** RCP6.0 using model M19; **D.** RCP8.5 using model M19.

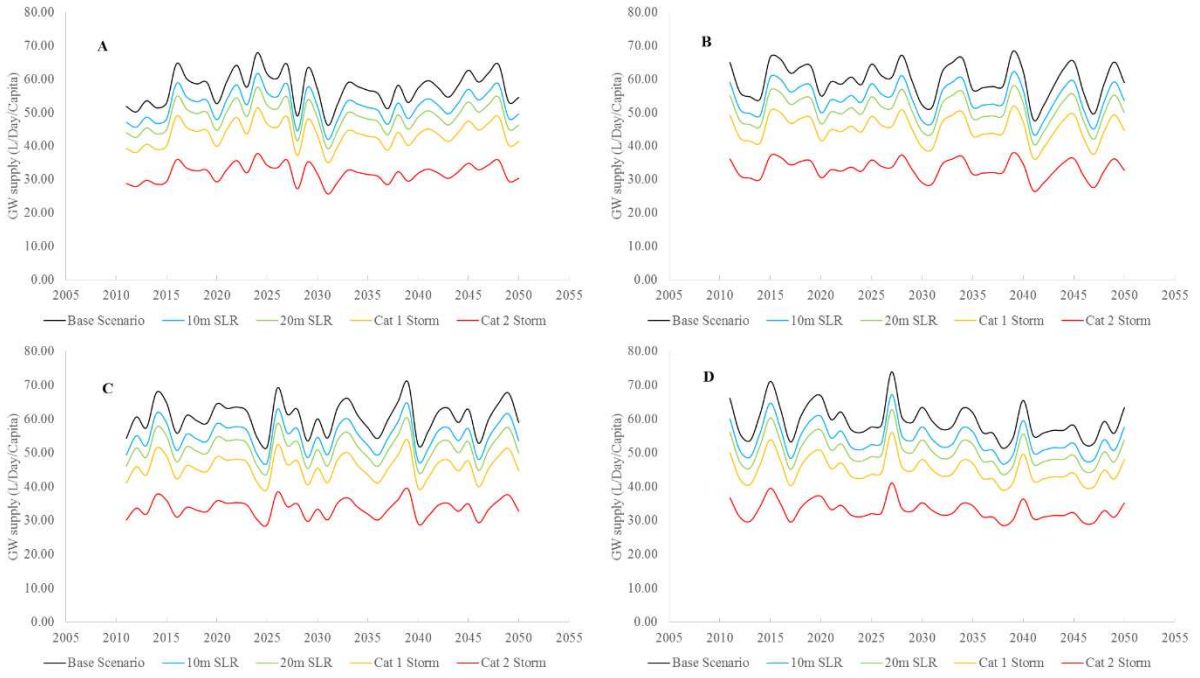

Figure 62 Average annual groundwater supply average (based on pumping rate = 30% of the monthly recharge) in N. Holhudhoo Island under different climatic RCPs forecasts; **A.** RCP2.6 using model M18; **B.** RCP4.5 using model M19; **C.** RCP6.0 using model M19; **D.** RCP8.5 using model M19.

The results for N. Holhudhoo show that domestic groundwater supply is subject to a substantial depletion during overwash events where per capita share of groundwater supply drops below the 40 liters/capita/day in Category 2 overwash events. Sea level rise and consequent beachline recession is ranked second in terms of depleting groundwater supply. If sea level rose, the groundwater supply would range between 40 and 50 liters/capita/day. The expected increase in population in the island is small and this reduces the threat to the freshwater lens due increasing demand. The results show a seasonality trend in fresh groundwater supply where per capita groundwater supply share fluctuate between 60s and 70s liters/capita/day. Island inhabitants should follow the most conservative water sanitation system by using the most water efficient system to preserve their fragile and vulnerable groundwater lens. Future water plans

should be established on frequent water shortages and should include other water resources to secure water demands.

7.3.2 N. Velidhoo Island

The groundwater supply from freshwater lens analysis results in N. Velidhoo Island under the base scenario (only climate change through 2050), sea level rise scenarios, and two categories of overwash events are presented in this section. Category 1 storm refers to the intermediate storm scenario, while Category 2 refers to the severe storm scenario. Figures 64 shows exceedance probability distributions for monthly average groundwater supply under each scenario. Figure 65 shows the annual averages and time series fluctuation for the groundwater supply under each scenario. Population growth for N. Velidhoo Island is calculated using the exponential growth equation (7.1) and is shown in Figure 63. The best climatic model in each RCP scenario is used in the shown Figures. The results of other climatic models are shown in the Appendix. As shown in Figures 64-65, the predicted fresh groundwater supply has a seasonality trend and the reliable supply in extreme overwash scenarios can barely secure the demand with no freshwater surplus which can be used for other consumptions. It also noted the freshwater subsurface reserve is vulnerable to the anthropogenic stress induced by population growth. Despite the relatively low population growth rate, the average annual fresh groundwater supply curves have long terms declining trends unlike N. Holhudhoo Island where the projected annual fresh groundwater supply curves have a near zero long term slope. The type of water sanitation used in this island would significantly affect whether or not water shortages can occur, so more efficient water sanitation usage is critical in this island.

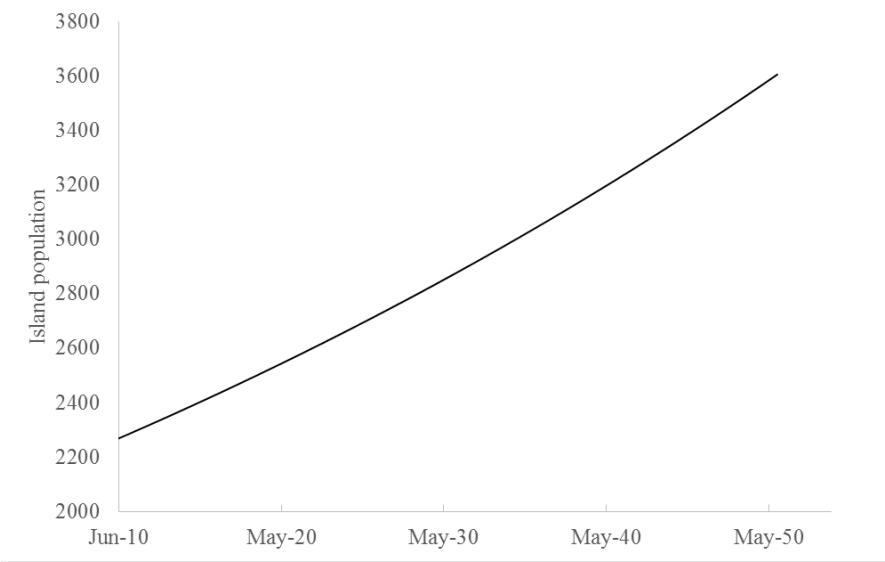

Figure 63 Population growth in N. Velidhoo Island from 2010-2050.

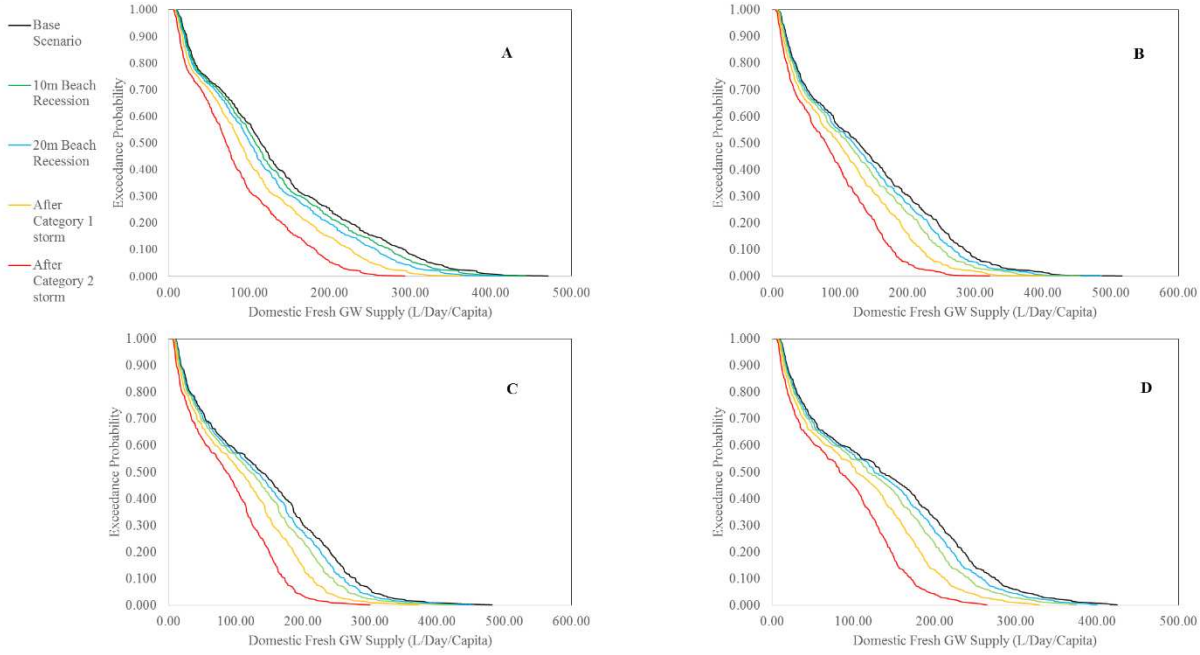

Figure 64 Exceedance probability distribution for monthly groundwater supply average (based on pumping rate = 30% of the monthly recharge) in N. Velidhoo Island under different climatic RCPs forecasts; A. RCP2.6 using model M18; B. RCP4.5 using model M19; C. RCP6.0 using model M19; D. RCP8.5 using model M19.

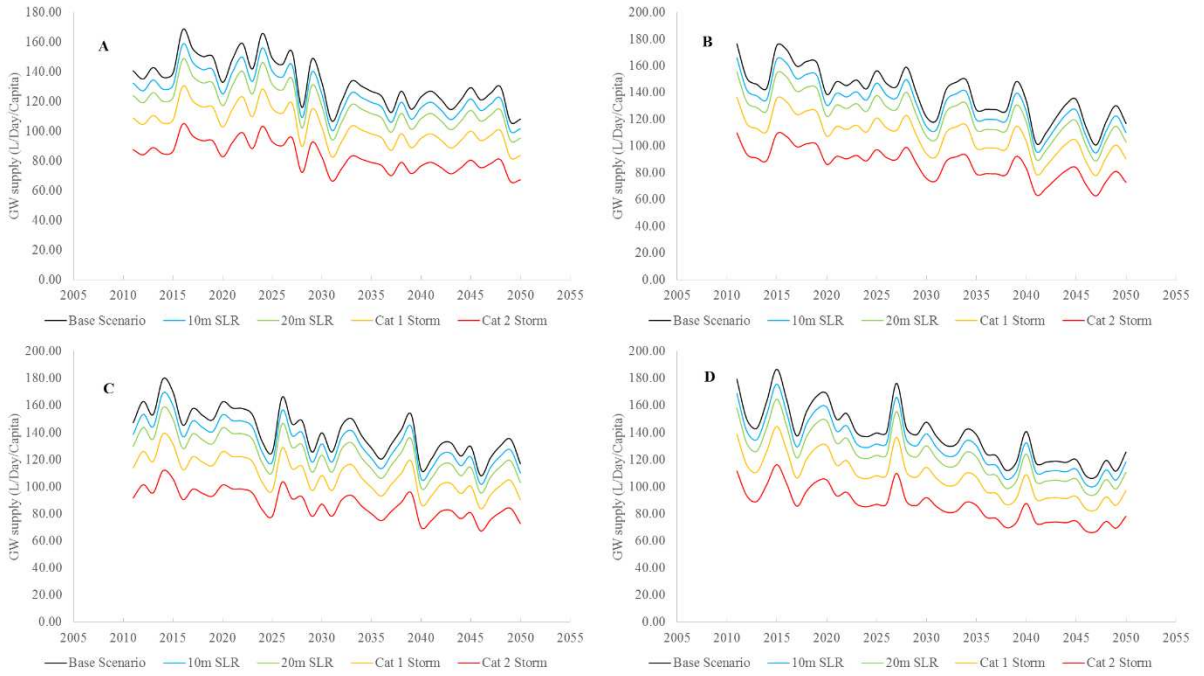

Figure 65 Average annual groundwater supply average (based on pumping rate = 30% of the monthly recharge) in N. Velidhoo Island under different climatic RCPs forecasts; **A.** RCP2.6 using model M18; **B.** RCP4.5 using model M19; **C.** RCP6.0 using model M19; **D.** RCP8.5 using model M19.

7.3.3 GDh. Thinadhoo Island

The groundwater supply from freshwater lens in GDh. Thinadhoo Island analysis results under the base scenario (only climate change through 2050), sea level rise scenarios, and two categories of overwash events are presented here. Category 1 storm refers to the intermediate storm scenario, while Category 2 refers to the severe storm scenario. Figures 67 shows exceedance probability distributions for monthly average groundwater supply under each scenario. Figure 68 shows the annual averages and time series fluctuation for the groundwater supply under each scenario. Population growth for N. Holhudhoo Island is calculated using the exponential growth equation (7.1) and is shown in Figure 66. The best climatic model in each RCP scenario is used in the shown Figures. The results of other climatic models are shown in the Appendix.

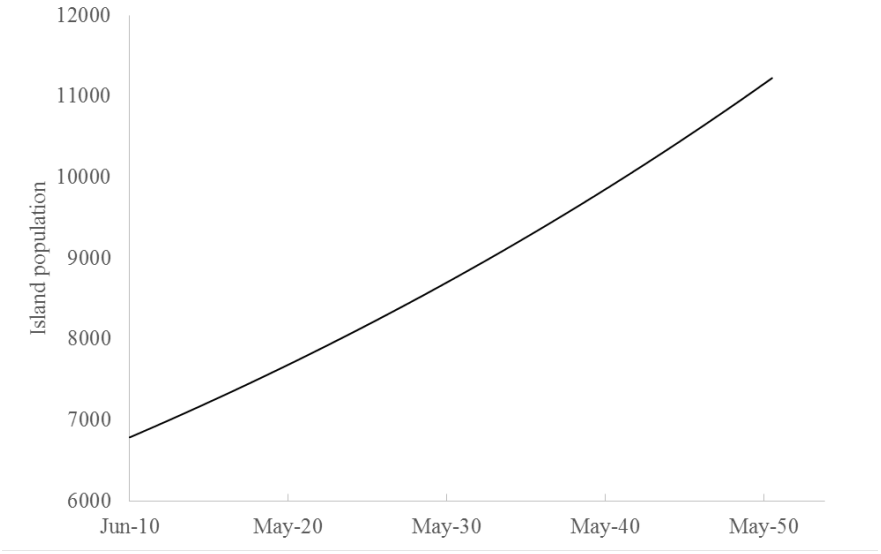

Figure 66 Population growth in GDh. Thinadhoo Island from 2010-2050.

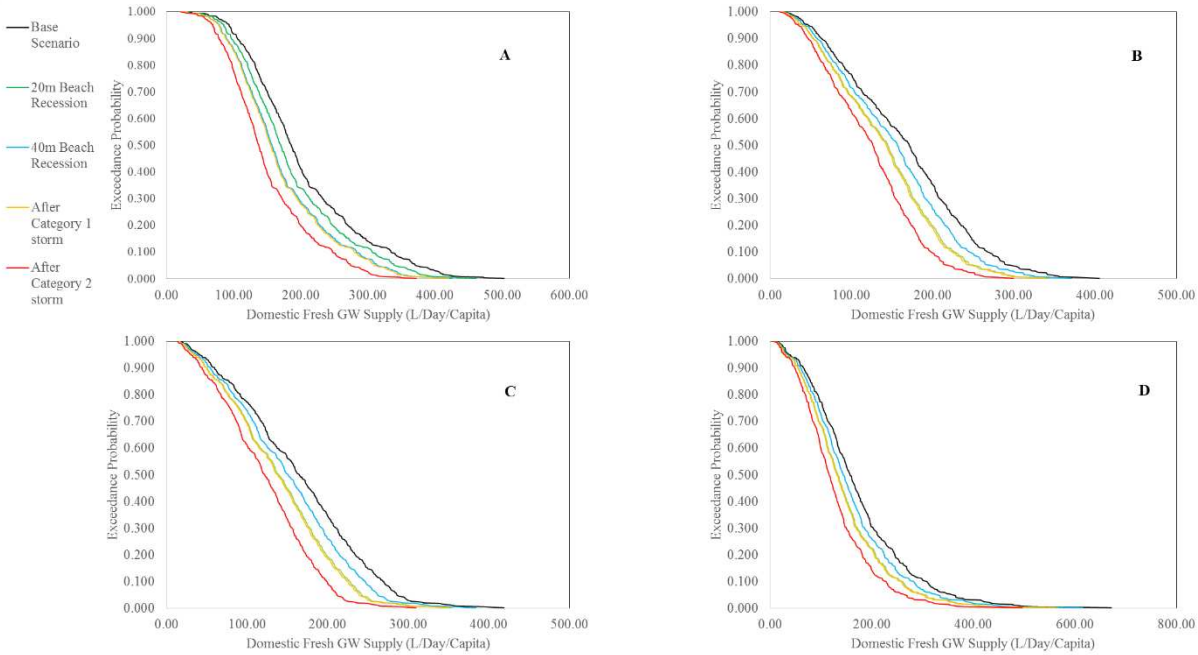

Figure 67 Exceedance probability distribution for monthly groundwater supply average (based on pumping rate = 35% of the monthly recharge) in GDh. Thinadhoo Island under different climatic RCPs forecasts; A. RCP2.6 using model M17; B. RCP4.5 using model M3; C. RCP6.0 using model M3; D. RCP8.5 using model M3.

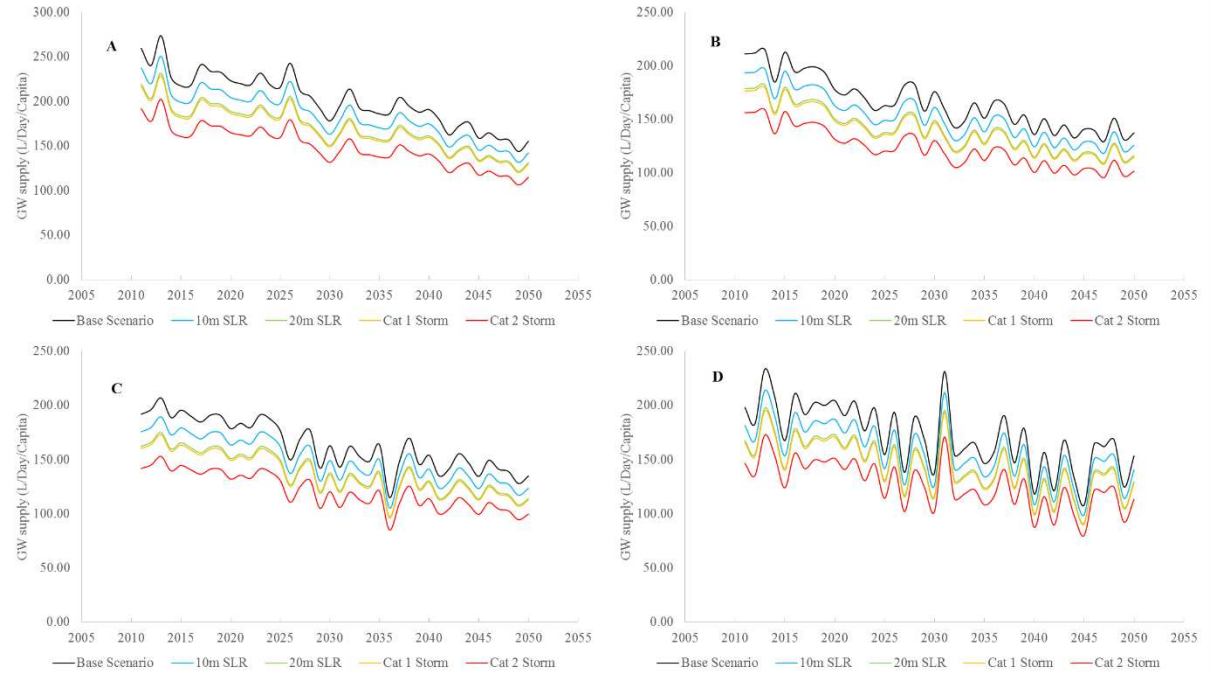

Figure 68 Average annual groundwater supply average (based on pumping rate = 35% of the monthly recharge) in GDh. Thinadhoo Island under different climatic RCPs forecasts; **A.** RCP2.6 using model M17; **B.** RCP4.5 using model M3; **C.** RCP6.0 using model 3 **D.** RCP8.5 using model M3.

As shown in Figures 67-68, the results of GDh. Thinadhoo are less variable and groundwater reserves are more sustainable in terms of securing domestic supply in cases of extreme environmental conditions such as severe droughts and overwash events. The overwash events are the most dangerous threat that endanger the water supply in this island, however, accelerated sea level rise rates may have as severe as intermediate overwash events impact on the depletion of the fresh lens. Moreover, the population growth in this big island seems to have a clearer impact on the freshwater depletion. The selection of appropriate water sanitation system is important in determining the status of the fresh groundwater supply status especially in overwash events and accelerated sea level rise. Alternative freshwater resources should be considered to secure demands for accelerated population growth.

7.3.4 L. Gan Island

The groundwater supply from freshwater lens in L. Gan Island analysis results under the base scenario (only climate change through 2050), one sea level rise scenario (accelerated scenario), and two categories of overwash events are presented in this section. Category 1 storm refers to the intermediate storm scenario, while Category 2 refers to the severe storm scenario. Figures 70 shows exceedance probability distributions for monthly average groundwater supply under each scenario. Figure 71 shows the annual averages and time series fluctuation for the groundwater supply under each scenario. Population growth for L. Gan Island is calculated using the exponential growth equation (7.1) and is shown in Figure 69. The best climatic model in each RCP scenario is used in the shown Figures. The results of other climatic models are shown in the Appendix.

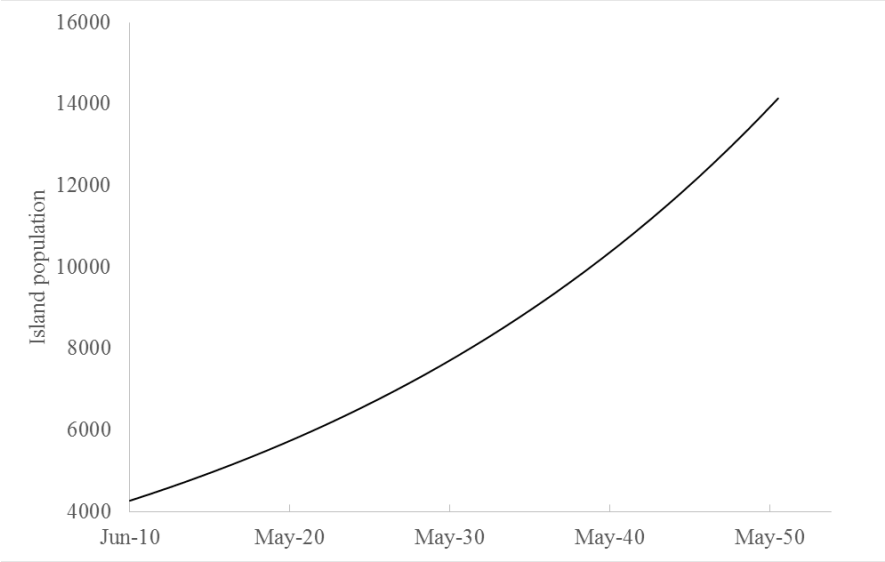

Figure 69 Population growth in L. Gan Island from 2010-2050.

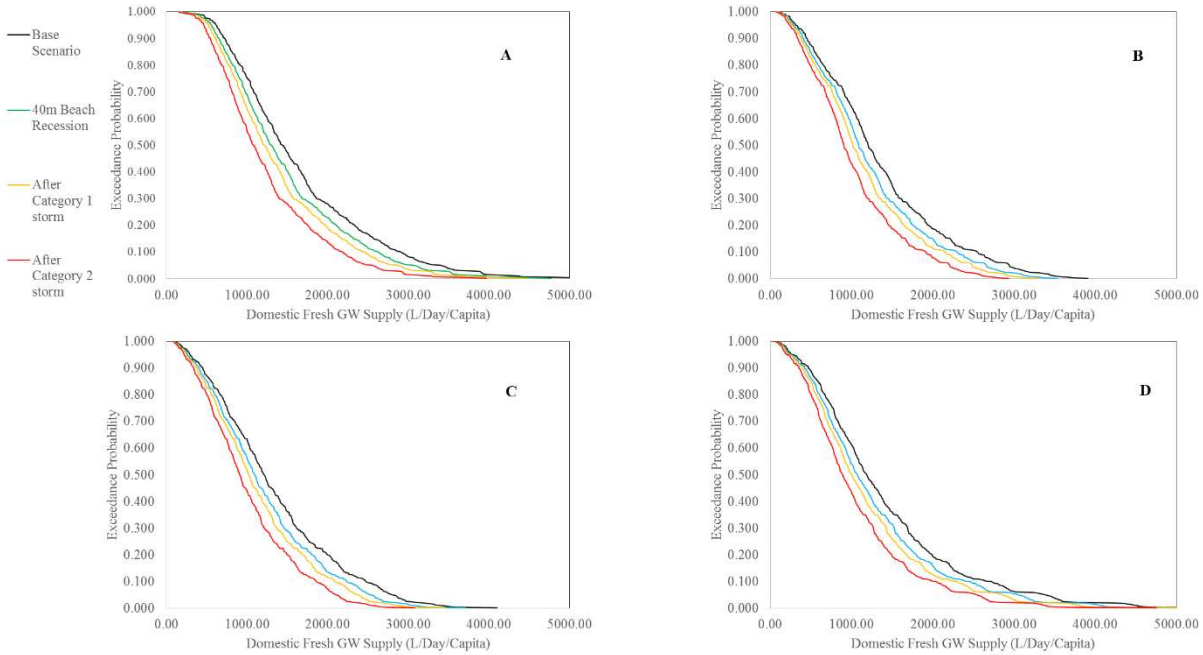

Figure 70 Exceedance probability distribution for monthly groundwater supply average (based on pumping rate = 35% of the monthly recharge) in L. Gan Island under different climatic RCPs forecasts; A. RCP2.6 using model M17; B. RCP4.5 using model M3; C. RCP6.0 using model M3; D. RCP8.5 using model M3.

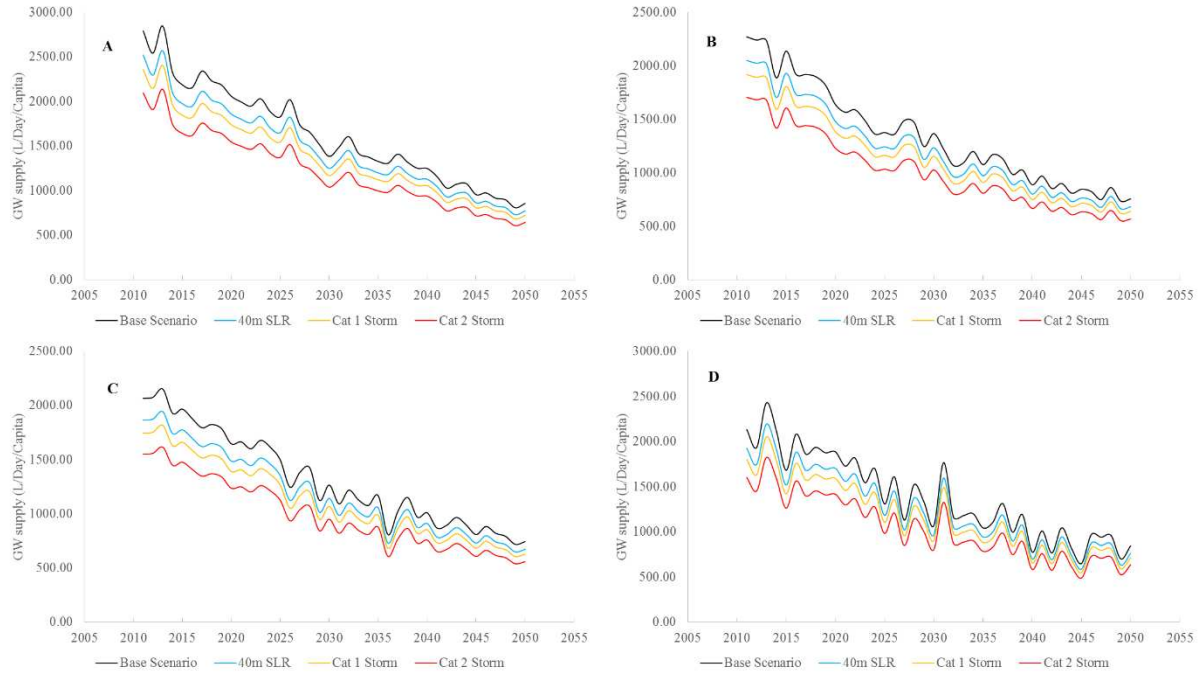

Figure 71 Average annual groundwater supply average (based on pumping rate = 35% of the monthly recharge) in L. Gan Island under different climatic RCPs forecasts; **A.** RCP2.6 using model M17; **B.** RCP4.5 using model M3; **C.** RCP6.0 using model 3 **D.** RCP8.5 using model M3.

As shown in Figures 69-70, the fresh groundwater reserve in L. Gan Island is fairly sufficient for domestic water supply even in extreme environmental conditions. The domestic supply will be above the 1000 Liter/capita/day more than 50% of the study period. The plenty of available fresh groundwater reserve promote the usage of water in other sectors such as agriculture. However, the rapid population growth will certainly deplete the fresh lens if growth rate increased than the expected percentage described in the Methods section. The variability in fresh groundwater quantity due to climate change, accelerated sea level rise, and overwash events does not contribute to water shortage situations as the groundwater lens can sustain against these stresses. In general, the groundwater in the island is plenty and the vulnerability of freshwater lens to depletion is minimal due to environmental conditions.

7.3.5 Results Summary

In this section, the results of groundwater supply analysis are summarized. Tables 41-44 show the average annual yield from groundwater lens in the modeled islands in each decade until 2050.

Table 41 Average groundwater yield from freshwater lens in each decade until 2050 under variety of environmental stresses in N.Holhudhoo Island (L/Capita/Day).

Year	RCP	climate change only	climate change with conservative SLR	climate change with aggressive SLR	climate change with Category 1 overwash event	climate change with Category 2 overwash event
2020		53	48	45	40	29
2030		57	52	48	43	32
2040	**2.6**	57	52	49	43	32
2050		55	50	46	41	30
2020		55	50	47	42	31
2030		52	48	44	40	29

2040	**4.5**	62	57	53	47	35
2050		59	54	50	45	33
2020		64	59	55	49	36
2030		60	55	51	45	33
2040	**6.0**	52	48	44	40	29
2050		59	54	50	45	33
2020		67	61	57	51	37
2030		63	58	54	48	35
2040	**8.5**	65	60	56	50	36
2050		63	58	54	48	35

Table 42 Average groundwater yield from freshwater lens in each decade until 2050 under variety of environmental stresses in N.Velidhoo Island (L/Capita/Day).

Year	**RCP**	**climate change only**	**climate change with conservative SLR**	**climate change with aggressive SLR**	**climate change with Category 1 overwash event**	**climate change with Category 2 overwash event**
2020		133	125	117	103	83
2030	**2.6**	133	125	117	103	83
2040		123	116	109	95	77
2050		108	102	95	84	67
2020		139	131	122	107	86
2030	**4.5**	122	115	107	94	76
2040		134	126	118	104	83
2050		117	110	103	90	73
2020		163	153	143	126	101
2030	**6.0**	140	132	123	108	87
2040		112	106	99	87	70
2050		117	110	103	90	73
2020		169	159	149	130	105
2030	**8.5**	148	139	130	114	92
2040		141	132	124	109	88
2050		126	118	111	97	78

Table 43 Average groundwater yield from freshwater lens in each decade until 2050 under variety of environmental stresses in GDh. Thinadhoo Island (L/Capita/Day).

Year	RCP	climate change only	climate change with conservative SLR	climate change with aggressive SLR	climate change with Category 1 overwash event	climate change with Category 2 overwash event
2020	**2.6**	223	204	189	187	165
2030		178	163	151	149	132
2040		191	175	161	159	141
2050		155	142	131	130	115
2020	**4.5**	178	163	150	149	131
2030		176	161	149	147	130
2040		136	124	115	113	100
2050		137	126	116	115	101
2020	**6.0**	179	164	151	149	132
2030		163	149	138	136	120
2040		154	141	130	129	114
2050		135	123	114	113	100
2020	**8.5**	205	187	173	171	151
2030		138	126	116	115	102
2040		118	108	100	99	88
2050		153	140	130	128	113

Table 44 Average groundwater yield from freshwater lens in each decade until 2050 under variety of environmental stresses in L. Gan Island (L/Capita/Day).

Year	RCP	climate change only	climate change with conservative SLR	climate change with aggressive SLR	climate change with Category 1 overwash event	climate change with Category 2 overwash event
2020	**2.6**	2058	1859	-	1738	1546
2030		1384	1250	-	1169	1039
2040		1248	1127	-	1054	937
2050		856	773	-	723	643
2020	**4.5**	1639	1480	-	1384	1230
2030		1366	1234	-	1154	1026
2040		888	802	-	750	666
2050		756	683	-	639	568

2020	**6.0**	1646	1486	-	1390	1236
2030		1265	1142	-	1068	950
2040		1008	910	-	851	757
2050		743	671	-	627	558
2020	**8.5**	1887	1704	-	1594	1417
2030		1068	965	-	902	802
2040		775	700	-	655	582
2050		845	763	-	714	635

7.4 Discussion and Conclusion

Freshwater supply is an essential need for human being existence. In atoll islands communities, groundwater reserves existing in the form of a thin lens floating atop seawater are one of the most important freshwater supply for islands inhabitant. This fresh groundwater lens is subject to damage due environmental stresses which have been discussed in details Chapters 4, 5, and 6. In order to assess the vulnerability of this fragile and thin freshwater lens, the ability of four selected islands to secure freshwater needs for islands' inhabitant in different climatic and environmental situations is analyzed. In order to successfully maintain adequate freshwater supply, reliability curves were developed to quantify the expected probability for the yield of per capita demand from the freshwater lens under potential scenarios of sea level rise and overwash events coupled with variable rainfall patterns due to anticipated climate through the study period.

Recommended pumping rates by Falkland (2010) were examined to determine the appropriate pumping rates that do not cause long term fresh groundwater lens depletion. It is concluded that pumping 30%, and 35% of the monthly recharge volume in the Northern, and Southern islands are appropriate to sustainably preserve the fresh groundwater lens. The analysis of the vulnerability of fresh groundwater lenses in the study area islands showed that overwash events are the most severe environmental threat that can significantly reduce fresh groundwater supply. The anthropogenic population growth stress contributed to significant per capita daily

supply reduction in bigger islands which expect rapid population growth, while the population growth effect in smaller islands is minimal where lower rates of population growth are expected. The use of appropriate water sanitation system is critical in smaller islands in determining the frequency of water shortages events, while this factor impact in larger islands can be neglected due larger amounts of available fresh groundwater.

CHAPTER 8. SUMMARY, CONCLUSIONS, AND RECOMMENDATIONS

In this chapter, the main conclusions of this dissertation are summarized, and future recommendations regarding atoll islands freshwater resources management and future research challenges in the field of atoll islands groundwater hydrology are presented.

8.1 Atoll Islands Fresh Groundwater Lens Sustainability

The fresh groundwater supply on atoll islands is very fragile and is under continual threat due to the general small geographic size of the islands and from climatic and anthropogenic stresses such as changing rainfall patterns, sea level rise, wave over-wash events, and population growth. The dissertation presented methods for quantifying the extent of these stresses and the consequent effects on islands inhabitants' per capita freshwater share. It is concluded that the main attribute that controls the sustainability of the fresh groundwater lens is the area of the island. Bigger islands possess adequate space for fresh groundwater lens development. Hence, bigger islands tend to have sufficient fresh groundwater reserves that sustain against environmental and anthropogenic stresses. On the contrary, smaller islands have thinner fresh groundwater lenses which are extremely vulnerable to any environmental or anthropogenic stresses.

Groundwater lens in atoll islands aquifers is recharged from rainfall that percolates through the coarse unsaturated zone and is considered the only forcing for developing that sub-surface lens. Recharge rates in the upcoming decades are subject to variability due to climate change. Variable rainfall patterns forcing was found to have a significant impact on smaller islands rather than bigger ones. Smaller islands showed strong variability trends due to

uncertainty associated with climatic forecasts for the upcoming decades. On the other side, variable rainfall patterns did not contribute to a similar seasonality trends in the bigger islands.

The sea level rise threat impact on reducing fresh groundwater lens volume was also investigated. Smaller islands would substantially be affected by beachline recession induced by sea level rise even with slower rates of sea level rise. Results showed that smaller islands may loss significant portions of their fresh groundwater lens volume due to the effect of landward coastal line movement, while bigger (wider) islands exhibited minor damages for the freshwater lens even with accelerated sea level rise rates. Moreover, the dissertation contributed to field of atoll islands hydrology by modelling in three dimensional approach the fresh groundwater lens recovery following marine overwash events. The recovery patterns were modeled using different recharge patterns and including the top performing GCMs that predict the future rainfall in the study area. Overwash freshwater lens recovery modelling presents a novel and in depth understanding for the recovery patterns to help water managers in atoll islands in appraising alternatives for freshwater supply in such catastrophic events. Fresh groundwater supply reliability curves were developed to predict fresh groundwater yield from atoll islands aquifer under different situation of variable rainfall patterns, sea level rise scenarios, and overwash events.

8.1.1 Rainfall Variability

Tables 45-48 summarize the results of predicted freshwater lens volumes for the four study islands from 2017-2050 under variable rainfall rates to account for anticipated climate change. The best GCMs in different RCPs scenarios in terms of matching historical rainfall data

were employed to calculate transient recharge for two climatic regions in the Republic of Maldives (see Chapter 4).

Table 45 Predicted averages freshwater lens (Mm^3) (2040-2050) for sea level rise impact on N. Holhudhoo Island according to different possible sea level rise rates coupled with different possible RCPs forcing scenarios.

RCP	GCM ID	GCM ranking	No SLR (Mm^3)	Conserv. SLR (Mm^3)	Aggres. SLR (Mm^3)	% reduction Conserve.	% reduction Aggres.
2.6	M18	1st	0.28	0.22	0.19	20.9%	32.7%
2.6	M19	2nd	0.22	0.17	0.15	21.0%	33.0%
2.6	M4	3rd	0.21	0.16	0.14	20.9%	33.0%
4.5	M19	1st	0.33	0.27	0.23	18.4%	29.4%
4.5	M8	2nd	0.18	0.14	0.12	23.4%	34.8%
4.5	M18	3rd	0.28	0.22	0.19	20.6%	32.3%
6.0	M19	1st	0.34	0.28	0.24	17.7%	29.4%
6.0	M18	2nd	0.30	0.24	0.21	21.1%	31.4%
6.0	M4	3rd	0.20	0.15	0.13	21.4%	34.2%
8.5	M19	1st	0.33	0.27	0.24	19.1%	29.4%
8.5	M8	2nd	0.17	0.13	0.11	22.8%	36.3%
8.5	M4	3rd	0.20	0.16	0.13	21.3%	32.5%

Table 46 Predicted averages freshwater lens (Mm^3) (2040-2050) for sea level rise impact on N. Velidhoo Island according to different possible sea level rise rates coupled with different possible RCPs forcing scenarios.

RCP	GCM ID	GCM ranking	No SLR	Conserv. SLR	Agg. SLR	% reduction Conserv.	% reduction Agg.
2.6	M18	1st	0.95	0.84	0.73	11.8%	23.2%

2.6	M19	2nd	0.85	0.75	0.65	11.7%	23.2%
2.6	M4	3rd	0.82	0.72	0.63	11.5%	23.0%
4.5	M19	1st	1.24	1.09	0.94	12.1%	24.4%
4.5	M8	2nd	0.77	0.68	0.59	11.8%	23.7%
4.5	M18	3rd	0.83	0.74	0.64	11.5%	23.2%
6.0	M19	1st	1.27	1.12	0.96	11.9%	24.0%
6.0	M18	2nd	1.00	0.89	0.77	11.7%	23.0%
6.0	M4	3rd	0.80	0.70	0.61	11.8%	23.4%
8.5	M19	1st	1.24	1.09	0.94	12.2%	24.1%
8.5	M8	2nd	0.69	0.61	0.52	12.4%	24.8%
8.5	M4	3rd	0.80	0.71	0.62	11.6%	23.2%

Table 47 Predicted averages freshwater lens (Mm^3) (2040-2050) for sea level rise impact on GDh. Thinadhoo Island according to different possible sea level rise rates coupled with different possible RCPs forcing scenarios.

RCP	**GCM ID**	**GCM ranking**	**No SLR**	**Conserv. SLR**	**Aggressive SLR**	**% reduction Conserv.**	**% reduction Agg.**
2.6	M17	1st	6.42	5.54	4.73	13.8%	26.3%
2.6	M19	2nd	5.97	5.14	4.41	13.9%	26.1%
2.6	M3	3rd	5.90	5.17	4.37	12.3%	26.0%
4.5	M3	1st	6.08	5.18	4.53	14.8%	25.4%
4.5	M12	2nd	5.93	5.16	4.43	13.0%	25.2%
4.5	M7	3rd	5.32	4.60	3.90	13.5%	26.7%
6.0	M3	1st	6.22	5.18	4.67	16.8%	25.0%
6.0	M19	2nd	5.76	5.16	4.30	10.5%	25.4%
6.0	M2	3rd	4.99	4.28	3.71	14.2%	25.5%

8.5	M3	1st	5.90	5.17	4.37	12.3%	26.0%
8.5	M7	2nd	6.00	5.09	4.34	15.1%	27.7%
8.5	M2	3rd	5.06	4.34	3.77	14.1%	25.5%

Table 48 predicted averages freshwater lens (Mm^3) (2040-2050) for sea level rise impact on L. Gan Island according to different possible sea level rise rates coupled with different possible RCPs forcing scenarios.

RCP	**GCM ID**	**GCM ranking**	**No SLR**	**Conserv. SLR**	**Agg. SLR**	**% reduction Conserv.**	**% reduction Agg.**
2.6	M17	1st	55.13	49.50	-	10.2%	-
2.6	M19	2nd	51.93	47.08	-	9.3%	-
2.6	M3	3rd	51.57	46.61	-	9.6%	-
4.5	M3	1st	52.64	47.44	-	9.9%	-
4.5	M12	2nd	54.98	49.21	-	10.5%	-
4.5	M7	3rd	47.93	43.58	-	9.1%	-
6.0	M3	1st	53.83	48.93	-	9.1%	-
6.0	M19	2nd	49.19	44.96	-	8.6%	-
6.0	M2	3rd	44.87	39.93	-	11.0%	-
8.5	M3	1st	51.57	47.43	-	8.0%	-
8.5	M7	2nd	51.96	46.59	-	10.3%	-
8.5	M2	3rd	45.17	40.67	-	10.0%	-

8.1.2 Sea Level Rise

Tables 49-52 summarize the results of predicted freshwater lens volumes for the four study under the influence of potential SLR scenarios coupled with GCMs forecasts for the period of 2040-2050. Two SLR scenarios were simulated (except for one SLR scenario for L. Gan Island) to examine the effect of beachline recession due to SLR (see chapter 5).

Table 49 Predicted averages freshwater lens (Mm^3) (2040-2050) for sea level rise impact on N. Holhudhoo Island according to different possible sea level rise rates coupled with different possible RCPs forcing scenarios.

RCP	**GCM ID**	**GCM ranking**	**No SLR (Mm^3)**	**Conserv. SLR (Mm^3)**	**Aggres. SLR (Mm^3)**	**% reduction Conserve.**	**% reduction Aggres.**
2.6	M18	1st	0.28	0.22	0.19	20.9%	32.7%
2.6	M19	2nd	0.22	0.17	0.15	21.0%	33.0%
2.6	M4	3rd	0.21	0.16	0.14	20.9%	33.0%
4.5	M19	1st	0.33	0.27	0.23	18.4%	29.4%
4.5	M8	2nd	0.18	0.14	0.12	23.4%	34.8%
4.5	M18	3rd	0.28	0.22	0.19	20.6%	32.3%
6.0	M19	1st	0.34	0.28	0.24	17.7%	29.4%
6.0	M18	2nd	0.30	0.24	0.21	21.1%	31.4%
6.0	M4	3rd	0.20	0.15	0.13	21.4%	34.2%
8.5	M19	1st	0.33	0.27	0.24	19.1%	29.4%
8.5	M8	2nd	0.17	0.13	0.11	22.8%	36.3%
8.5	M4	3rd	0.20	0.16	0.13	21.3%	32.5%

Table 50 Predicted averages freshwater lens (Mm^3) (2040-2050) for sea level rise impact on N. Velidhoo Island according to different possible sea level rise rates coupled with different possible RCPs forcing scenarios.

RCP	GCM ID	GCM ranking	No SLR	Conserv. SLR	Agg. SLR	% reduction Conserv.	% reduction Agg.
2.6	M18	1st	0.95	0.84	0.73	11.8%	23.2%
2.6	M19	2nd	0.85	0.75	0.65	11.7%	23.2%
2.6	M4	3rd	0.82	0.72	0.63	11.5%	23.0%
4.5	M19	1st	1.24	1.09	0.94	12.1%	24.4%
4.5	M8	2nd	0.77	0.68	0.59	11.8%	23.7%
4.5	M18	3rd	0.83	0.74	0.64	11.5%	23.2%
6.0	M19	1st	1.27	1.12	0.96	11.9%	24.0%
6.0	M18	2nd	1.00	0.89	0.77	11.7%	23.0%
6.0	M4	3rd	0.80	0.70	0.61	11.8%	23.4%
8.5	M19	1st	1.24	1.09	0.94	12.2%	24.1%
8.5	M8	2nd	0.69	0.61	0.52	12.4%	24.8%
8.5	M4	3rd	0.80	0.71	0.62	11.6%	23.2%

Table 51 Predicted averages freshwater lens (Mm^3) (2040-2050) for sea level rise impact on GDh. Thinadhoo Island according to different possible sea level rise rates coupled with different possible RCPs forcing scenarios.

RCP	GCM ID	GCM ranking	No SLR	Conserv. SLR	Aggressive SLR	% reduction Conserv.	% reduction Agg.
2.6	M17	1st	6.42	5.54	4.73	13.8%	26.3%
2.6	M19	2nd	5.97	5.14	4.41	13.9%	26.1%
2.6	M3	3rd	5.90	5.17	4.37	12.3%	26.0%
4.5	M3	1st	6.08	5.18	4.53	14.8%	25.4%
4.5	M12	2nd	5.93	5.16	4.43	13.0%	25.2%

4.5	M7	3rd	5.32	4.60	3.90	13.5%	26.7%
6.0	M3	1st	6.22	5.18	4.67	16.8%	25.0%
6.0	M19	2nd	5.76	5.16	4.30	10.5%	25.4%
6.0	M2	3rd	4.99	4.28	3.71	14.2%	25.5%
8.5	M3	1st	5.90	5.17	4.37	12.3%	26.0%
8.5	M7	2nd	6.00	5.09	4.34	15.1%	27.7%
8.5	M2	3rd	5.06	4.34	3.77	14.1%	25.5%

Table 52 predicted averages freshwater lens (Mm^3) (2040-2050) for sea level rise impact on L. Gan Island according to different possible sea level rise rates coupled with different possible RCPs forcing scenarios.

RCP	**GCM ID**	**GCM ranking**	**No SLR**	**Conserv. SLR**	**Agg. SLR**	**% reduction Conserv.**	**% reduction Agg.**
2.6	M17	1st	55.13	49.50	-	10.2%	-
2.6	M19	2nd	51.93	47.08	-	9.3%	-
2.6	M3	3rd	51.57	46.61	-	9.6%	-
4.5	M3	1st	52.64	47.44	-	9.9%	-
4.5	M12	2nd	54.98	49.21	-	10.5%	-
4.5	M7	3rd	47.93	43.58	-	9.1%	-
6.0	M3	1st	53.83	48.93	-	9.1%	-
6.0	M19	2nd	49.19	44.96	-	8.6%	-
6.0	M2	3rd	44.87	39.93	-	11.0%	-
8.5	M3	1st	51.57	47.43	-	8.0%	-
8.5	M7	2nd	51.96	46.59	-	10.3%	-

8.5	M2	3rd	45.17	40.67	-	10.0%	-

8.1.3 Overwash Events

Tables 53-56 summarize the results of freshwater lens recovery in the study area after overwash events. Two categories of overwash events were simulated to account for different storms. The overwash islands were allowed to recover using both historical and best performing GCMs. Moreover, the effect of pumping was included to examine its effect in delaying freshwater lens recovery (see Chapter 6).

Table 53 Freshwater lens recovery percentages 2 years after overwash events under different recharge rates in N. Holhudhoo Island.

Recharge input	GCM ID	% of pre overwash volume after 2 years intermed. Storm	% of pre overwash volume after 2 years - severe storm
Historical averages	-	79.2%	55.5%
Historical averages with pumping	-	63.5%	43.0%
RCP2.6 averages	M18	88.1%	60.2%
RCP4.5 averages	M19	67.6%	47.0%
RCP6.0 averages	M19	69.8%	48.7%
RCP8.5 averages	M19	67.9%	47.2%

Table 54 Freshwater lens recovery percentages 2 years after overwash events under different recharge rates in N. Velidhoo Island.

Recharge input	GCM ID	% of pre overwash volume after 2 years intermed. storm	% of pre overwash volume after 2 years severe storm
Historical average	-	62.9%	56.3%
Historical average with pumping	-	59.1%	52.1%
RCP2.6 averages	M18	67.7%	59.9%
RCP4.5 averages	M19	55.4%	49.1%
RCP6.0 averages	M19	56.9%	50.6%
RCP8.5 averages	M19	55.8%	49.5%

Table 55 Freshwater lens recovery percentages 2 years after overwash events under different recharge rates in Gdh. Thinadhoo Island.

Recharge input	GCM ID	% of pre overwash volume after 2 years intermed. Storm	% of pre overwash volume after 2 years severe storm
Historical average	-	49.1%	45.7%
Historical average with pumping	-	43.7%	39.9%
RCP2.6 averages	M17	55.0%	51.5%
RCP4.5 averages	M3	49.0%	45.5%
RCP6.0 averages	M3	49.0%	45.5%

Table 56 Freshwater lens recovery percentages 2 years after overwash events under different recharge rates in L. Gan Island.

Recharge input	GCM ID	% of pre overwash volume after 2 years - intermed. Storm	% of pre overwash volume after 2 years - severe storm
Historical average	-	41.2%	38.6%
Historical average with pumping	-	36.1%	33.5%
RCP2.6 averages	M17	48.4%	45.4%
RCP4.5 averages	M3	41.5%	38.8%
RCP6.0 averages	M3	41.4%	38.7%
RCP8.5 averages	M3	42.1%	39.4%

8.2 Methods Applicability for Similar Atoll Islands Systems

Although the methods in this dissertation were applied specifically to selected islands in the Republic of Maldives, they can be extrapolated for other islands as atoll islands have similar aquifer hydrogeological settings. The methods in this dissertation were applied to islands with different sizes and different climatic regions, and hence the results presented for estimating freshwater resources can be easily extrapolated. Figure 72 shows that there is a linear relation between average lens volumes predicted by different RCP models and island area. A preliminary prediction of the average freshwater lens volume can be made by using results in shown in Figure 72. Figure 73 shows the concluded linear relation (on a semi-log scale) between island surface are and average reduction in the freshwater lens due to 20 meters of beachline recession (average is calculated from 2040-2050 using variable rainfall patterns). It is concluded that larger islands in term of surface area are less affected by shoreline recession. The relation between the percent of volume reduction percentage and island surface area is inversely proportional on a semi-log scale. Figure 74 shows the concluded relation between the pre-overwash freshwater

lens volume and the average percentage of lens recovery after 2 years (average is based on different recharge rates). It is concluded that larger volumes of freshwater lens need longer time to recover. The relation between the pre overwash lens volume and the percentage at which the lens is recovered after 2 years is inversely proportional on a semi-log scale. The results of this research can be used to estimate the sustainability of the freshwater lens in other atoll islands aquifers as atoll islands aquifers share the same hydrogeological settings.

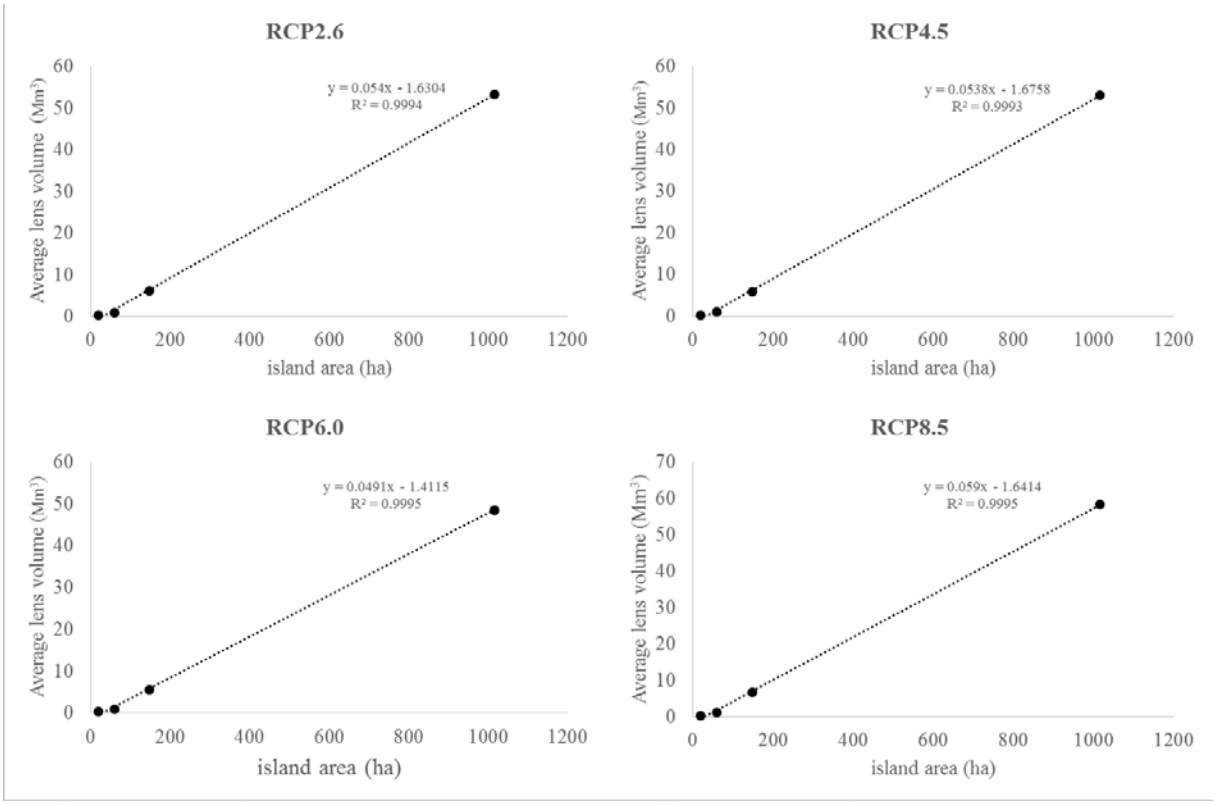

Figure 72 Average lens volumes predicted by different RCPs models versus island area.

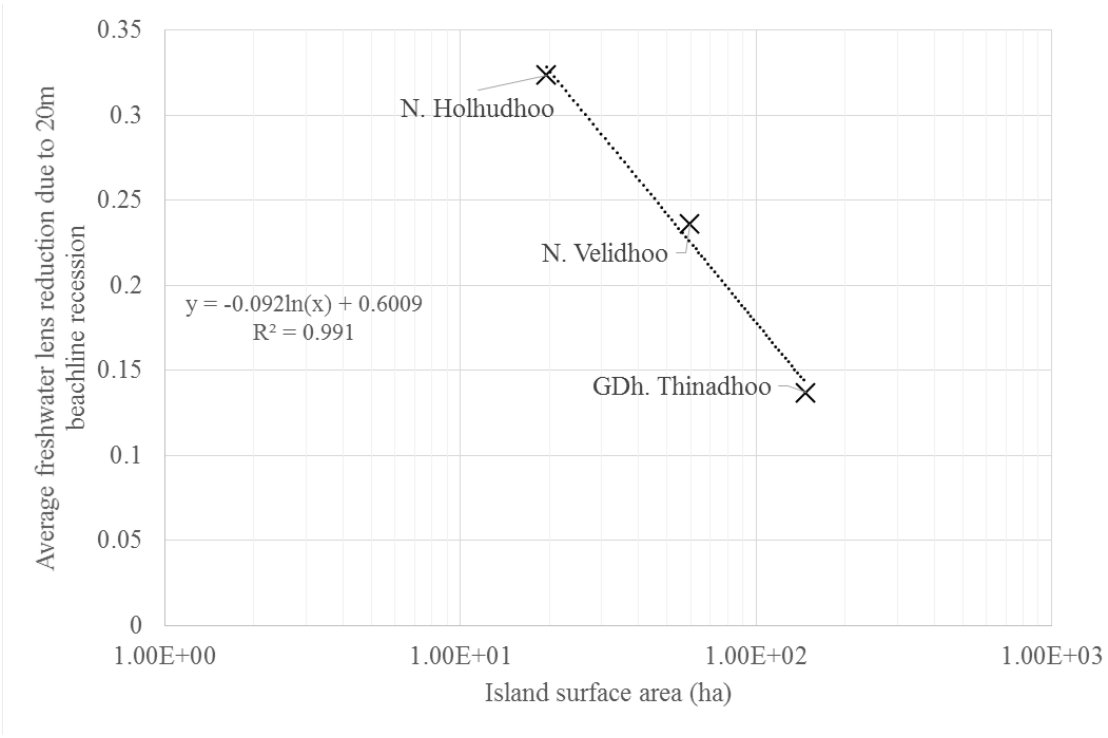

Figure 73 Relation between average freshwater lens reduction (20m beachline recession) and island surface area (semi-log scale).

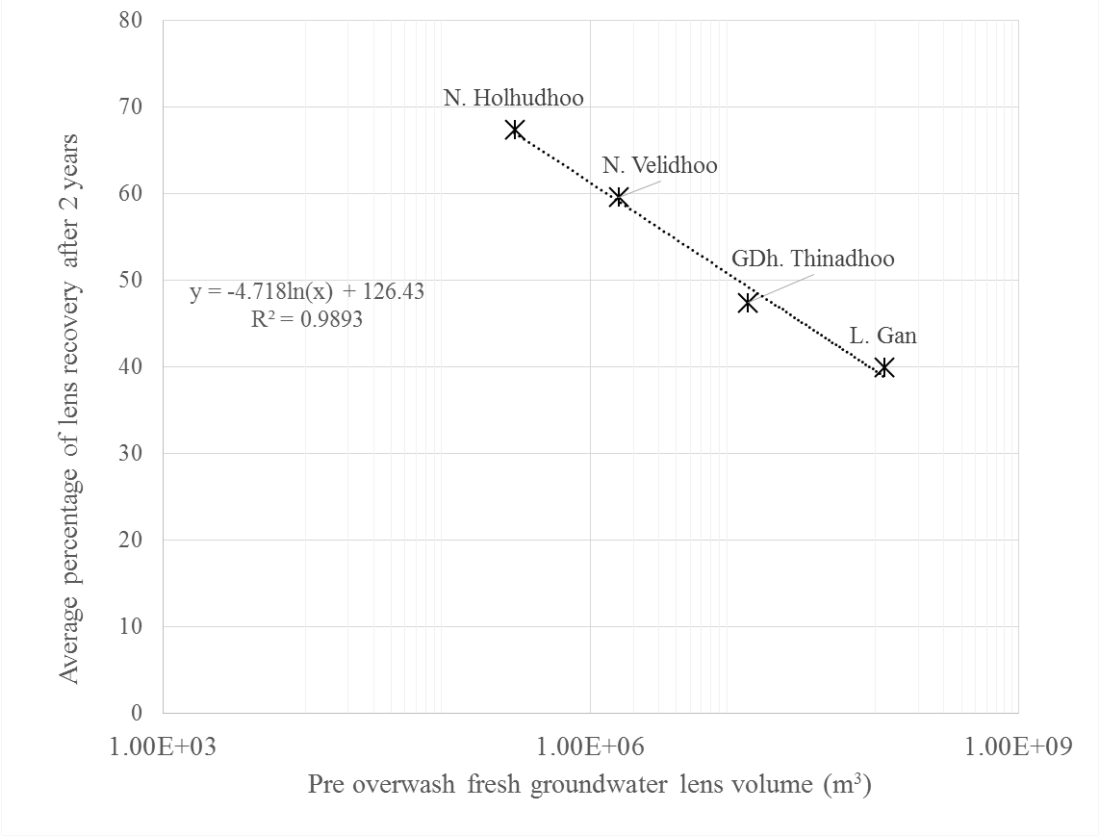

Figure 74 Relation between pre overwash lens volume and average lens recovery after 2 years (semi-log scale).

8.3 Future Research Recommendations

This dissertation presented methods to model the hydrological groundwater system in atoll islands aquifers. Further research in the hydrology of the unsaturated zone and vegetation contribution to the quantity groundwater recharge is needed. Also, the effect of land use on the volume of freshwater recharge is considered one of potential research opportunities in the field of atoll islands groundwater hydrology. However, the future research cannot be conducted without more detailed data that describe the atoll islands land uses in atoll islands. More data collection efforts are needed to make further contributions to the field of atoll islands hydrology. Required data sets include islands land use, more detailed subsurface lithology data, water demands estimates, sea level tidal gauges measurements, and field observations of groundwater salinity following overwash events. Developing our understanding for the water resources in atoll islands aquifers would help atoll islands nations to manage their water resources efficiently.

REFERENCES

(NASA), N. A. (2014, Febraury 4). *The Tropical Rainfall Measuring Mission (TRMM).* Retrieved from The Tropical Rainfall Measuring Mission (TRMM) Web site: ftp://trmmopen.gsfc.nasa.gov/pub/merged/

Anthony, S. (2004). Hydrogeology of selected islands of the Federated States of Micronesia. *Developments in Sedimentology, 54,* 693-706. doi:http://dx.doi.org/10.1016/S0070-4571(04)80045-1

Anthony, S. S. (1987). Master Thesis: Hydrogeochemistry of a small limestone-island: Laura, Majuro Atoll, Marshall Islands. *M. S. thesis, Department of Geology and Geophysics, University of Hawaii at Manoa*.

Anthony, S. S. (1996). *Hydrogeology and ground-water resources of Pingelap Island, Pingelap Atoll, State of Pohnpei, Federated States of Micronesia (No. 92-4005).* US Geological Survey; Branch of Information Services [distributor].

Ataie-Ashtiani, B., Werner, A., Simmons, C., Morgan, L., & Lu, C. (2013). How important is the impact of land-surface inundation on seawater intrusion caused by sea-level rise? *Hydrogeology Journal, 21*(7), 1673-1677. doi:10.1007/s10040-013-1021-0

Ayers, J. F., & Vacher, H. L. (1986). Hydrogeology of an atoll island: A conceptual model from detailed study of a Micronesian example. *Groundwater, 24*(2), 2-15. doi:10.1111/j.1745-6584.1986.tb00994.x

Bailey, R. T. (2015). Quantifying transient post-overwash aquifer recovery for atoll islands in the Western Pacific. *Hydrological Processes, 29*(20), 4470-4482. doi:10.1002/hyp.10512

Bailey, R. T., & Jenson, J. W. (2013). Effects of Marine Overwash for Atoll Aquifers: Environmental and Human Factors. *Groundwater, 52*(5), 694-704. doi:10.1111/jawr.12236

Bailey, R. T., Jenson, J. W., & Olsen, A. E. (2009). Numerical Modeling of Atoll Island Hydrogeology. *Groundwater, 47*(2), 184-196. doi:10.1111/j.1745-6584.2008.00520.x

Bailey, R. T., Jenson, J. W., & Olsen, A. E. (2010). Estimating the Groundwater Resources of Atoll Islands. *Water, 2*(1), 1-27. doi:10.3390/w2010001

Bailey, R. T., Jenson, J. W., Rubinstein, D., & Olsen, A. E. (2008). *Groundwater resources of atoll islands: observations, modeling, and management, Technical Report: 119.* University of Guam. Retrieved from http://www.weriguam.org/docs/reports/119.pdf

Bailey, R., Khalil, A., & Chatikavanij, V. (2014). Estimating transient freshwater lens dynamics for atoll islands. *Journal of Hydrology, 515*, 247-256. doi:http://dx.doi.org/10.1016/j.jhydrol.2014.04.060

Bailey, R., Khalil, A., & Chatikavanij, V. (2015). Estimating Current and Future Groundwater Resources of The Maldives. *JAWRA Journal of the American Water Resources Association, 51*(1), 112-122. doi:10.1111/jawr.12236

Barnett, J., & Adger, W. N. (2003). Climate dangers and atoll countries." Climatic change. *Climatic change, 61*(3), 321-327. doi:10.1023/B:CLIM.0000004559.08755.88

Barthiban, S., Lloyd, B., & Maier, M. (2012). Sanitary Hazards and Microbial Quality of Open Dug Wells in the Maldives Islands. *Journal of Water Resource and Protection, 4*(07), 474-486. doi:http://dx.doi.org/10.4236/jwarp.2012.47055

Batu, V. (1998). *Aquifer Hydraulics: A Comprehensive Guide to Hydrogeologic Data Analysis (Vol. 1).* New York: John Wiley & Sons.

Bear, J., & Dagan, G. (1964). Some exact solutions of interface problems by means of the hodograph method. *Journal of Geophysical Research, 69*(8), 1563-1572. doi:10.1029/JZ069i008p01563

Beckley, B. D., Lemoine, F. G., Luthcke, S. B., Ray, R. D., & Zelensky, N. P. (2007). A reassessment of global and regional mean sea level trends from TOPEX and Jason-1 altimetry based on revised reference frame and orbits. *Geophysical Research Letters, 34*(14). doi:10.1029/2007GL030002

Bricker, S., & Hughes, A. (2007). *Impacts of climate change on small island hydrogeology—a literature review*. British Geological Survey, Groundwater Science Programme Open Report OR/09/025.

Brier, G. W. (1950). Verification of forecasts expressed in terms of probability. *Monthly weather review, 78*(1), 1-3.

Buddemeier, R. W., & Holladay, G. (1977). Atoll hydrology: Island groundwater characteristics and their relationship to diagenesis. *Third International Coral Reef Symposium, 2*, 167-174.

Burns, W. C. (2000). The impact of climate change on Pacific island developing countries in the 21st century. In W. C. Burns, *Climate change in the South Pacific: Impacts and responses in Australia, New Zealand, and small island states* (pp. 233-250). Springer Netherlands.

Chapman, T. G. (1985). The use of water balances for water resources estimation with special reference to small islands. *Australian Development Assistance Bureau Bulletin No. 4.*

Chui, T. F., & Terry, J. P. (2013). Influence of sea-level rise on freshwater lenses of different atoll island sizes and lens resilience to storm-induced salinization. *Journal of Hydrology, 502*, 18-26. doi:http://dx.doi.org/10.1016/j.jhydrol.2013.08.013

Chui, T., & Terry, J. (2012). Modeling fresh water lens damage and recovery on atolls after storm-wave washover. *Groundwater, 50*(3), 412-420. doi:10.1111/j.1745-6584.2011.00860.x

Church, J. A., Godfrey, J. S., Jackett, D. R., & McDougall, T. J. (1991). A model of sea level rise caused by ocean thermal expansion. Journal of Climate. *Journal of Climate, 4*(4), 438-465. doi:http://dx.doi.org/10.1175/1520-0442(1991)004<0438:AMOSLR>2.0.CO;2

Church, J. A., White, N., & Hunter, J. (2006). Sea Level Rise at Tropical Pacific and Indian Ocean Islands. *Global and Planetary Change, 53*(3), 155-168. doi:http://dx.doi.org/10.1016/j.gloplacha.2006.04.001

Church, J., & White, N. (2006). A 20th century acceleration in global sea-level rise. *Geophysical Research Letters, 33*(1). doi:10.1029/2005GL024826

Church, J., Clark, P., Cazenave, A., Gregory, J., Jevrejeva, S., Levermann, A., . . . Unnikrishnan, A. (2013). *Climate Change 2013: The Physical Science Basis. Contribution of Working Group I to the Fifth Assessment Report of the Intergovernmental Panel on Climate Change.* Cambridge, UK: Cambridge University Press. Retrieved from http://drs.nio.org/drs/handle/2264/4605

Collins, M. A., & Gelbar, L. W. (1971). Seawater intrusion in layered aquifers. *Water Resources Research, 7*(4), 971-979. doi:10.1029/WR007i004p00971

Comte, J.-C., Join, J.-L., Banton, O., & Nicolini, E. (2014). Modelling the response of fresh groundwater to climate and vegetation changes in coral islands. *Hydrogeology Journal, 22*(8), 1905-1920. doi:10.1007/s10040-014-1160-y

Crennan, & Berry. (2002). *Review of community-based issues and activities in waste management, pollution prevention and improved sanitation in the Pacific Islands region.* Samoa: International Waters Programme, South Pacific Regional Environmental Programme.

Darwin, C. (1842). *The Structure and Distribution of Coral Reefs.* London: Smith, Elder and Co.

De Freitas, C. R., & McLean, J. D. (2013). Update of the chronology of natural signals in the near-surface mean global temperature record and the Southern Oscillation Index. *International Journal of Geosciences, 4*(1A-2013). doi:DOI:10.4236/ijg.2013.41A020

Dickinson, W. R. (2004). Impacts of eustasy and hydro-isostasy on the evolution and landforms of Pacific atolls. *Palaeogeography, Palaeoclimatology, Palaeoecology, 213*(3), 251-269. Retrieved from http://dx.doi.org/10.1016/j.palaeo.2004.07.012

Dickinson, W. R. (2009). Pacific Atoll Living: How Long Already and Until When? *GSA Today, 19*(3), 4-10. Retrieved from http://www.geosociety.org/gsatoday/archive/19/3/pdf/i1052-5173-19-3-4.pdf

Doll, P. (2009). Vulnerability to the impact of climate change on renewable groundwater resources: a global-scale assessment. *Environmental Research Letter, 4*. doi:10.1088/1748-9326/4/3/035006

Douglas, B. C. (1997). Global sea level rise: a redetermination. *Surveys in Geophysics, 18*(2-3), 279-292. doi:10.1023/A:1006544227856

Falkland, A. (1991). *Hydrology and water resources of small islands: a practical guide. A contribution to the International Hydrological Programme.* Paris, France: UNESCO.

Falkland, A. (2000). Addu Atoll, Maldives. *Report on Groundwater Investigations, Regional Development Project, First Phase*.

Falkland, A. (2002). Proceedings of the Pacific Regional Consultation. *Theme 1. Water resource management.* Suva, Fiji: Asian Development Bank and South.

Falkland, A. C. (1983). *Christmas Island (Kiritimati) Water Resources Study Vol. 1.* Victoria: Australian Department of Housing and Construction.

Falkland, A. C. (1994). Climate, Hydrology and Water Resources of the Cocos (Keeling) Islands. *National Museum of Natural History Atoll Research Bulletin No. 400*.

Falkland, T. (2000). *Report On Groundwater Investigations Addu Atoll, Southern Development Region.* Republic of Maldives: Ministry of Planning and National Development.

Falkland, T. (2001). *REPORT ON GROUNDWATER INVESTIGATIONS, NORTHERN DEVELOPMENT REGION.* Republic of Maldives: Ministry of Planning and National Development.

Falkland, T. (2010). *Groundwater Investigations Report A, for N.Holhudhoo.* Republic of Maldives: Bangladesh Consultants Ltd.

Falkland, T. (2010). *Groundwater Investigations Report B, for N.Velidhoo.* Rebuplic of Maldives: Bangladesh Consultants Ltd.

Falkland, T. (2010). *Groundwater Investigations Report C, for GDh.Thinadhoo.* Republic of Maldives: Bangladesh Consultants Ltd.

Falkland, T. (2010). *Groundwater Investigations Report D, for L. Gan.* Republic of Maldives: Tony Falkland Bangladesh Consultants Ltd.

Ferguson, G., & Gleeson, T. (2012). Vulnerability of coastal aquifers to groundwater use and climate change. *Nature Climate Change, 2*(5), 342-345. doi:10.1038/nclimate1413

Feseker, T. (2007). Numerical studies on saltwater intrusion in a coastal aquifer in northwestern Germany. *Hydrogeology Journal, 15*(2), 267-279. doi:10.1007/s10040-006-0151-z

Fetter, C. W. (1972). Position of the saline water interface beneath oceanic islands. *Water Resources Research, 8*(5), 1307-1314.

Fu, G., Liu, Z., Charles, S. P., Xu, Z., & Yao, Z. (2013). A score-based method for assessing the performance of GCMs: A case study of southeastern Australia. *Journal of Geophysical Research: Atmospheres, 118*(10), 4154-4167. doi:10.1002/jgrd.50269

Ghassemi, F., Molson, J. W., Falkland, A., & Alam, K. (1998). Three-dimensional simulation of the Home Island freshwater lens: preliminary results. *Environmental Modelling & Software, 14*(2), 181-190. Retrieved from http://dx.doi.org/10.1016/S1364-8152(98)00069-3

Glover, R. E. (1964). The pattern of fresh water flow in coastal aquifer. In: Cooper H.H. Jr., Kohout F.A., Henry H.R. and Glover R.E. , Sea water in coastal aquifers. *Sea Water in Coastal Aquifers, USGS Water Supply Paper 1613-C*, C32-C35.

Griffiths, G. M., & et al. (2005). Change in mean temperature as a predictor of extreme temperature change in the Asia-Pacific region. *International Journal of Climatology, 25*(10), 1301-1330. doi:10.1002/joc.1194

Griggs, J. E., & Peterson, F. L. (1993). Ground-Water Flow Dynamics and Development Strategies at the Atoll Scale. *Groundwater, 31*(2), 209-220. doi:10.1111/j.1745-6584.1993.tb01813.x

Hamlin, S. N., & Anthony, S. S. (1987). *Ground-water resources of the Laura area, Majuro Atoll, Marshall Islands (No. 87-4047).* US Geological Survey.

Helen J., P. (1991). *Recent advances in atoll hydrogeology. In Ground Water in the Pacific Rim Countries: (pp. 2-8).* ASCE.

Henry, H. R. (1964). Interfaces between saltwater and fresh water in coastal aquifers. *Sea Water in Coastal Aquifers, US Geological Survey Water Supply Paper*, C35-70.

Herman, M. E., & Wheatcraft, S. W. (1984). Groundwater Dynamics investigation of Enjebi Island, Enewetak Atoll: An interpretive computer model simulation. In *Finite Elements in*

Water Resources (pp. 133-142). Springer Berlin Heidelberg. doi:10.1007/978-3-662-11744-6_12

Hirsch, R. M. (1982). Techniques of trend analysis for monthly water quality data. *Water Resources Research, 18*(1), 107-121. doi:10.1029/WR018i001p00107

Hogan, P. (1988). Modeling of freshwater-seawater interaction on Enjebi Island, Enewetak Atoll. *Master's thesis (Geology).*

Houghton, J. T. (1995). *Climate change 1995: The science of climate change: contribution of working group I to the second assessment report of the Intergovernmental Panel on Climate Change (Vol. 2).* Cambridge University Press.

Hubbert, M. K. (1940). The theory of groundwater motion. *Journal of Geology, 48*(8, part1), 785-944.

Hunt, J. C., & Peterson, F. L. (1980). *Groundwater resources of Kwajalein Island, Marshall Islands. Technical Report 126.* Water Resources Research Centre, Univ. of Hawaii .

Inman, D. L., & Nordstrom, C. E. (1971). On the tectonic and morphologic classification of coasts. *The Journal of geology, 79*(1), 1-21.

Kench, P., McLean, R., Brander, R., Nichol, S., Smithers, S., Ford, M., . . . Aslam, M. (2006). Geological effects of tsunami on mid-ocean atoll islands: the Maldives before and after the Sumatran tsunami. *Geology, 34*(3), 177-180.

Ketabchi, H., Mahmoodzadeh, D., Ataie-Ashtiani, B., Werner, A., & Simmons, C. (2014). Sea-level rise impact on fresh groundwater lenses in two-layer small islands. *Hydrological Processes, 28*(24), 5938-5953. doi:10.1002/hyp.10059

Khan, T., Quadir, D., Murty, T., Kabir, A., Aktar, F., & Sarker, M. (2002). Relative Sea Level Changes in Maldives and Vulnerability of Land Due to Abnormal Coastal Inundation. *Marine Geodesy, 25*(1-2), 133-143.

Kipp, K. (1987). *a computer code for simulation of heat and solute transport in three-dimensional ground-water flow systems.* United States Geological Survey.

Kooi, H., Groen, J., & Leijnse, J. (2000). Modes of seawater intrusion during transgressions. *Water Resources Research, 32*(12), 3581-3589.

Lam, R. K. (1974). Atoll permeability calculated from tidal diffusion. *Journal of Geophysical Research, 79*(21), 3073-3081.

Langevin, C., Thorne, D., Dausman, A., Sukop, M., & Guo, W. (2007). *SEAWAT Version 4: A Computer Program for Simulation of Multi-Species Solute and Heat Transport.* U.S. Geological Survey.

Latheefa, A., Shafia, A., & Shafeega, F. (2011). *State of Environment: Maldives.* Republic of Maldives: Maldives Ministry of Environment and Energy.

Lee, A. G. (2003). 3-D Numerical Modeling of Freshwater Lens on Atoll Islands. *TOUGH Symposium*, (pp. 12-14). Berkeley.

Lloyd, J. W., Miles, J. C., Chessman, G. R., & Bugg, S. F. (1980). A groundwater resources study of a Pacific Ocean atoll - Tarawa, Gilbert Islands. *Water Resources Bulletin 16, No. 4*, 646-653.

Loaiciga, H., Pingel, T., & Garcia, E. (2011). Sea Water Intrusion by Sea-Level Rise: Scenarios for the 21st Century. *Groundwater, 50*(1), 37-47. doi:10.1111/j.1745-6584.2011.00800.x

Mahmoodzadeh, D., Ketabchi, H., Ataie-Ashtiani, B., & Simmons, C. T. (2014). Conceptualization of a fresh groundwater lens influenced by climate change: A modeling study of an arid-region island in the Persian Gulf, Iran. *Journal of Hydrology, 519*, 399-413.

Masterson, J., & Garabedian, S. (2007). Effects of Sea-Level Rise on Ground Water Flow in Coastal Aquifer System. *Groundwater, 45*(2), 209-207. doi:10.1111/j.1745-6584.2006.00279.x

McCarthy, J. J. (2001). *Climate change 2001: impacts, adaptation, and vulnerability: contribution of Working Group II to the third assessment report of the Intergovernmental Panel on Climate Change. .* Cambridge University Press.

Meehl, G. A., Washington, W. M., Erickson III, D. J., Briegleb, B. P., & Jaumann, P. J. (1996). Climate change from increased CO2 and direct and indirect effects of sulfate aerosols. *Geophysical Research Letters 23, 23*(25), 3755-3758. doi:10.1029/96GL03478

Meier, M. F., Dyurgerov, M. B., Rick, U. K., O'Neel, S., Pfeffer, W. T., Anderson, R. S., & Glazovsky, A. F. (2007). Glaciers dominate eustatic sea-level rise in the 21st century. *Science, 318*(5814), 1064-1067. doi:10.1126/science.1143906

Molson, J. W., & Frind, E. O. (1994). *User Guide for Density Dependent Flow and Mass Transport in Three Dimensions.* University of Waterloo.

Morgan, L. K., & Werner, A. D. (2014). Seawater intrusion vulnerability indicators for freshwater lenses in strip islands. *Journal of Hudrology, 508*, 322-327.

Morris, D. A., & Johnson, A. I. (1967). *Summary of hydrologic and physical properties of rock and soil materials, as analyzed by the hydrologic laboratory of the U.S. Geological Survey, 1948-60.* Washington: United States Government Printing Office.

Nicholls, R., & Cazenave, A. (2010). Sea-Level Rise and Its Impact on Coastal Zones. *Science, 328*(5985), 1517-1520. doi:10.1126/science.1185782

Oberdorfer, J. A., & Buddemeier, R. W. (9-11 Oct. 1984). Atoll island groundwater contamination: rapid recovery from saltwater intrusion. *Annual Meeting of the Association of Engineering Geologists.* Boston: USA.

Oberdorfer, J. A., Hogan, P. J., & Buddemeier, R. W. (1990). Atoll island hydrogeology: Flow and freshwater occurence in a tidally dominated system. *Journal of Hydrology, 120*(1-4), 327-340.

Oude Essink, G. H., van Bareen, E. S., & de Louw, P. G. (2010). Effects of climate change on coastal groundwater systems: A modeling study in the Netherlands. *WATER RESOURCES RESEARCH, 46*(10), W00F04. doi:10.1029/2009WR008719

Parry, M., Canziani, O. F., Palutikof, J. P., van der Linden, P. J., & Hanson, C. E. (2007). *Climate change 2007: impacts, adaptation and vulnerability (Vol. 4). Contribution of Working Group II to the Fourth Assessment Report of the Intergovernmental Panel on Climate Change.* (M. Parry, Ed.) Cambridge: Cambridge University Press.

Perkins, S. E., Pitman, A. J., Holbrook, N. J., & McAneney, J. (2007). Evaluation of the AR4 Climate Models' Simulated Daily Maximum Temperature, Minimum Temperature, and Precipitation over Australia Using Probability Density Functions. *Journal of Climate, 20*(17), 4356-4376.

Peterson, F. L. (1990). *Groundwater Recharge Storage and Development on Small Atoll Islands.* Honolulu: University of Hawaii at Manoa, Honolulu Water Resources Research Center.

Peterson, F., & Gingerich, S. (1995). Modeling atoll groundwater systems. *Groundwater Models for Resources and Management* , 275-292.

Peterson, T. C., & et al. (1998). Homogeneity adjustments of in-situ atmospheric data: A review. *International Journal of Climatology, 18*(13), 1493-1517.

Pfeffer, W. T., Harper, J. T., & O'Neel, S. (2008). Kinematic constraintes on glacier contributions to 21st century sea-level rise. *Science, 321*(5894), 1340-1343. doi:10.1126/science.1159099

Presley, T. K. (2005). *Effects of the 1998 drought on the freshwater lens in the Laura area, Majuro Atoll, Republic of the Marshall Islands.* Geological Survey (U.S.).

Ragoonaden, S., Agricole, W., Mohabeer, R., & Appadu, S. (2006). CLIMATE CHANGE IN THE INDIAN OCEAN SMALL ISLANDS STATES: CURRENT STATUS AND FUTURE INITIATIVES. Retrieved from http://www.hkccf.org/download/iccc2007/30May/S4A/Sachooda%20RAGOONADEN/Climate%20Change%20in%20the%20Indian%20Ocean%20Small%20Island%20States%20-%20Current%20Status%20and%20Future%20Initiatives.pdf

Rahmstorf, S. (2007). A semi-empirical approach to projecting future sea-level rise. *Science, 315*(5810), 368-370. doi:10.1126/science.1135456

Randall, D. A. (2007). Climate models and their evaluation. In *Climate Change 2007: The Physical Science Basis.* Cambridge: Cambridge University Press.

Raper, S. C., & Braithwaite, R. J. (2006). Low sea level rise projections from mountain glaciers and icecaps under global warming. *Nature, 439*(7074), 311-313. doi:10.1038/nature04448

Richards, R. (1991). Atoll vulnerability: the storm waves on Tokelau on February 1987. *South Pacific environments: interactions with weather and climate.*, (pp. 155-156). University of Auckland.

Rumbaugh, J., & Rumbaugh, D. (2011). *Guide to Using Groundwater Vistas.* Reinholds, PA: Environmental Simulations, Inc.

Rumer, Jr., R. R., & Shiau, J. C. (1968). Salt Water Interface in a Layered Coastal Aquifer. *Water Resources Research, 4*(6), 1235-1247. doi:10.1029/WR004i006p01235

Shamir, U., & Dagan, G. (1971). Motion of the seawater interface in coastal aquifer: A numerical solution. *Water Resources Research, 3*, 644-657. doi:10.1029/WR007i003p00644

Sherif, M., & Singh, V. P. (1999). Effect of climate change on sea water intrusion in coastal aquifers. *Hydrological Processes, 13*, 1277-1287.

Sobir, R., Shinna, F., Ibrahim, L., & Shafeeq, S. (2014). *Maldives Human Development Report.* Male, Republic of Maldives: The Ministry of Finance and Treasury and the United Nations Development Programme in the Maldives. Retrieved from http://www.mv.undp.org/content/dam/maldives/docs/Policy%20and%20Inclusive%20Growth/Maldives_HDR_2014/Maldives_HDR2014_Summary.pdf

Spennemann, D. H. (2006). Freshwater Lens, Settlement Patterns, Resources Use and Connectivity in the Marshall Islands. *Tranforming Cultures eJournal, 1*(2), 44-63.

Storlazzi, C. D., Elias, E. P., & Berkowitz, P. (2015). Many atolls may be uninhabitable within decades due to climate change. *Scientific Report, 5*. doi:10.1038/srep14546

Sulzbacher, H., Wiederhold, H., Siemon, B. G., Igel, J., Burschil, T. G., & Hinsby, K. (2012). Numerical modelling of climate change impacts on freshwater lenses on the North Sea Island of Borkum using hydrological and geophysical methods. *Hydrology and Earth System Sciences, 16*(10), 3621-3643.

Swartz, J. H. (1962). *Some physical constants for the Marshall Island area.* USGS.

Taboroši, D., & Martin, M. (2011). Pakein Atoll: freshwater resourcesand their usage, state, and infrastructure. *Island Research & Eduation Initiative*.

Taylor, K. E., Stouffer, R. J., & Meehl, G. A. (2012). An Overview of CMIP5 and the experiment design. *Bulletin of the American Meteorological Society 93, 93*(4), 485-498.

Terry, J. P., & Chui, T. F. (2012). Evaluating the fate of freshwater lenses on atoll islands after eustatic sea-level rise and cyclone-driven inundation; A modelling approach. *Global and Planetary Change, 88-89*, 76-84.

Terry, J., & Falkland, A. (2010). Responses of atoll freshwater lenses to storm-surge overwash in the Northern Cook Islands. *Hydrogeology Journal, 18*(3), 227-246.

Tsyban, A., Everett, J., & Titus, J. (1990). *World oceans and coastal zones.* Paris: UNESCO.

Underwood, M. R. (1990). Atoll island hydrogeology: Conceptual and numerical models. *Ph.D. Dissertation*. University of Hawaii at Manoa, Honolulu.

Underwood, M., Peterson, F., & Voss, C. (1992). Groundwater Lens Dynamics of Atoll Islands. *Water Resources Researck, 28*(11), 2889-2902. doi:10.1029/92WR01723

Urish, D. (1974, January-February). Fresh water on the Coral Atoll Island. *The Military Engineer, 429*, 25-27.

Voss, C., & Provost, A. (2010). A finite-element simulation model for saturated-unsaturated, fluid density-dependent ground-water flow with energy transport of chemically-reactive single-species solut transport. *USGS Water Resources Investigation Report 84-4369*.

Wallace, C. (2015). *Thesis: ATOLL ISLAND FRESHWATER RESOURCES: MODELING, ANALYSIS, AND OPTIMIZATION.* Fort Collins, CO: Colorado State University.

Wallace, C. D., Bailey, R. T., & Arabi, M. (2015). Rainwater catchment system design using simulated future climate data. *Journal of Hydrology, 529*, 1798-1809.

Watson, A., Werner, A. D., & Simmons, C. T. (2010). Transience of seawater intrusion in response to sea level rise. *Water Resources Research, 46*(12), W12533. doi:10.1029/2010WR009564

Watson, R. T., Zinyowera, M. C., & Moss, R. H. (1998). *The regional impacts of climate change: an assessment of vulnerability.* Cambridge University Press.

Watson, R., Zinyowera, M., Moss, R., & Dokken, D. (1997). *The Regional Impacts of Climate Change: An Assessment of Vulnerability.* INTERGOVERNMENTAL PANEL ON CLIMATE CHANGE.

Watterson, I. G. (2008). Calculation of probability density functions for temperature and precipitation change under global warming. *Journal of Geophysical Research: Atmospheres, 113*(D12). doi:10.1029/2007JD009254

Werner, A. D., & Simmons, C. T. (2009). Impact of Sea-Level Rise on Sea Water Intrusion in Coastal Aquifers. *Groundwater, 47*(2), 197-204. doi:10.1111/j.1745-6584.2008.00535.x

Wheatcraft, S. W., & Buddemeier, R. W. (1981). Atoll island hydrology. *Ground Water, 19*(3), 311-320. doi:10.1111/j.1745-6584.1981.tb03476.x

White, I., & Falkland, T. (2010). Management of freshwater lenses on small Pacific islands. *Hydrogeology Journal, 18*(1), 227-249. doi:10.1007/s10040-009-0525-0

White, I., Falkland, A., Crennan, L., Jones, P., Metutera, T., Etuati, B., & Metai, E. (1999). Groundwater recharge in low coral islands Bonriki, South Tarawa, Republic of Kiribati: isues, traditions and conflicts in groundwater use and management. *Technical documents in hydrology, 25*.

White, I., Falkland, T., & Scott, D. (1999). *Droughts in small coral islands: Case study, South Tarawa, Kiribati.* Paris: UNESCO.

White, I., Falkland, T., Perez, P., Dray, A., Metutera, T., Metai, E., & Overmars, M. (2007). Challenges in freshwater management in low coral atolls. *Journal of Cleaner Production, 15*(16), 1522-1528.

Woodroffe, C. (2007). Reef-island topography and the vulnerability of atolls to sea level rise. *Global and Planetry Change, 62*(1-2), 77-96.

Woodroffe, C. D., & Falkland, A. C. (1997). Geology and hydrogeology of the Cocos (Keeling) Islands. *Geology and Hydrogeology of Carbonate Islands. Developments in Sedimentology 54*, 885-908. doi:DOI: 10.1016/s0070-4571(04)80053-0

Woodworth, P. (2005). Have there been large recent sea level changes in the Maldive Islands? *Global Planetery Change, 49*(1-2), 1-18.

Woodworth, P., Le Provost, C., Richards, J., Mitchum, G. T., & Merrifield, M. (2002). A Review of Sea Level Research from Tide Gauges during the World Ocean Current Experiment. *Oceanography and Marine Biology, 40*, 1-35.

Yamano, H., Kayanne, H., Yamaguchi, T., Kuwahara, Y., Yokoki, H., Shimazaki, H., & Chikamori, M. (2007). Atoll island vulnerability to flooding and inundation revealed by historical reconstruction: Fongafale Islet, Funafuti Atoll, Tuvalu. *Global and Planetary Change, 57*(3), 407-416.

APPENDIX

Table A1 GCMs statistical assessment for the Northern climatic region under RCP4.5 scenario

Model ID	Correlation	Rank	Mean RE	Rank	St Dev RE	Rank	SSE	NRMSE	Rank
1	0.318	23	0.238	19	0.796	24	5439.77	1.774	24
2	0.524	10	0.240	20	0.079	7	1964.18	1.066	10
3	0.551	9	0.282	22	0.015	2	1839.93	1.032	8
4	0.610	4	0.164	15	0.115	8	1291.49	0.864	4
5	0.408	21	0.067	6	0.005	1	2034.13	1.085	12
6	0.569	7	0.133	13	0.183	14	1852.83	1.035	9
7	0.446	20	0.249	21	0.224	17	1773.53	1.013	6
8	0.557	8	0.108	9	0.036	4	1495.94	0.930	5
9	0.488	15	0.092	7	0.279	18	2381.92	1.174	18
10	0.513	11	0.061	5	0.287	20	2281.46	1.149	17
11	0.505	13	0.103	8	0.177	13	2069.26	1.094	13
12	0.472	17	0.125	12	0.193	15	2257.69	1.143	16
13	0.497	14	0.116	11	0.205	16	2177.64	1.122	14
14	0.506	12	0.114	10	0.056	6	1824.14	1.027	7
15	0.405	22	0.215	18	0.146	10	2521.53	1.208	19
16	0.474	16	0.196	16	0.021	3	1965.91	1.066	11
17	0.574	6	0.160	14	0.430	22	1231.57	0.844	2
18	0.574	5	0.044	3	0.142	9	1280.95	0.861	3
19	0.671	1	0.054	4	0.051	5	1187.56	0.829	1
20	0.629	2	0.553	23	0.456	23	3314.79	1.385	22
21	0.618	3	0.586	24	0.420	21	3405.09	1.403	23
22	0.469	18	0.202	17	0.279	19	2586.28	1.223	20
23	0.450	19	0.037	2	0.172	12	2240.88	1.139	15
24	0.290	24	0.001	1	0.163	11	2846.26	1.283	21

Model ID	Kendal Slope	KS RE	Rank	BS (%)	Rank	S score	Rank	Total score	Final Rank
1	0.0075	5.818	24	0.0487	23	0.714	18	122.5	24
2	0.0055	4.000	19	0.0195	11	0.762	15	69.5	13
3	0.0059	4.364	21	0.0130	6	0.827	5	57	6
4	-0.0026	3.364	16	0.0091	4	0.827	5	43.5	4
5	0.002	0.818	7	0.0058	1	0.869	2	45	5
6	0.0071	5.455	22	0.0239	14	0.744	16	69	11
7	0.0002	0.818	9	0.0135	7	0.839	4	74	14
8	-0.003	3.727	17	0.0116	5	0.815	8	41	3
9	0.0011	0.000	1	0.0406	20	0.720	17	77	17
10	0.0014	0.273	4	0.0348	19	0.685	23	76	15
11	0.0015	0.364	5	0.0318	18	0.702	21	69	11
12	0.002	0.818	7	0.0415	21	0.714	18	83	21
13	-0.0003	1.273	10	0.0440	22	0.690	22	82	20

14	-0.0013	2.182	13	0.0315	17	0.714	18	59	7
15	0.0073	5.636	23	0.0293	16	0.792	10	93.5	22
16	0.0013	0.182	3	0.0219	12	0.786	11	59	7
17	0.0033	2.000	12	0.0230	13	0.786	11	62	9
18	0.0003	0.727	6	0.0142	8	0.786	13	33.5	2
19	0.0047	3.273	15	0.0175	10	0.821	7	27	1
20	0.0053	3.818	18	0.0086	3	0.887	1	81	19
21	0.0041	2.727	14	0.0065	2	0.863	3	80.5	18
22	0.0011	0.000	1	0.0624	24	0.673	24	98.5	23
23	-0.0007	1.636	11	0.0262	15	0.774	14	68	10
24	0.0057	4.182	20	0.0157	9	0.810	9	76	15

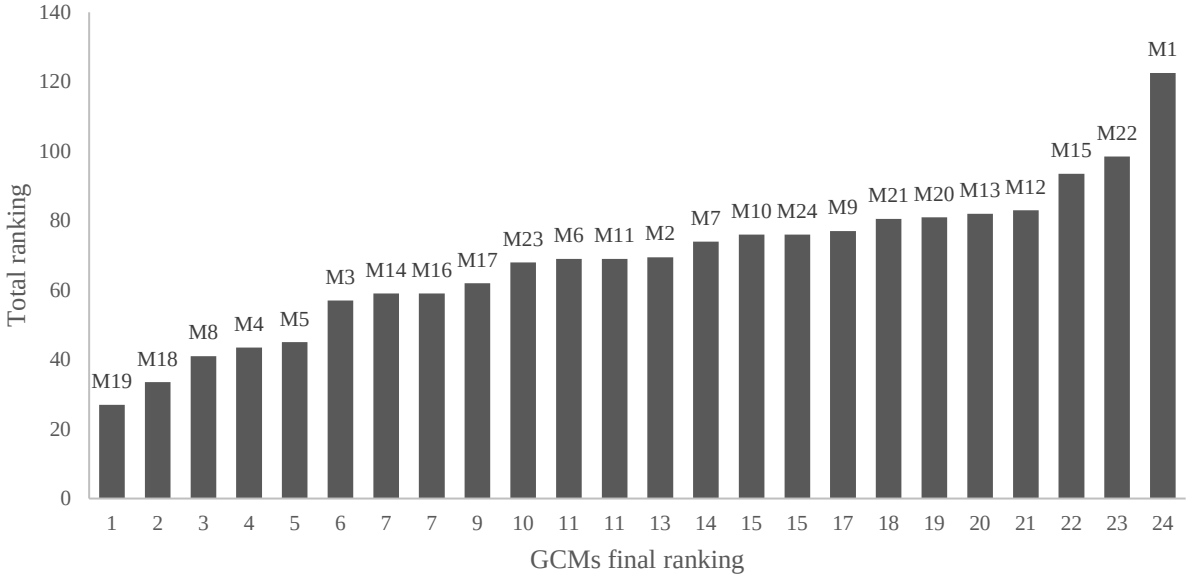

Figure A1 GCMs ranking results for the Northern climatic region under RCP4.5 climate change scenario

Table A2 GCMs statistical assessment for the Northern climatic region under RCP6.0 scenario

Model ID	Correlation	Rank	Mean RE	Rank	St Dev RE	Rank	SSE	NRMSE	Rank
1	0.376	22	0.213	18	0.736	24	4763.33	1.660	24
2	0.532	7	0.239	21	0.109	7	1993.21	1.074	9
3	0.559	6	0.242	22	0.011	2	1727.70	1.000	5
4	0.619	4	0.121	14	0.060	5	1275.21	0.859	2
5	0.394	21	0.069	7	0.011	1	2095.60	1.101	11
6	0.565	5	0.069	6	0.150	8	1754.30	1.007	7
7	0.452	17	0.194	17	0.162	9	1739.91	1.003	6
8	0.515	8	0.043	5	0.063	6	1761.96	1.010	8
9	0.464	12	0.041	4	0.466	23	3042.05	1.327	21
10	0.467	11	0.105	13	0.448	22	2999.96	1.317	20
11	0.490	10	0.073	8	0.251	16	2291.66	1.151	12
12	0.462	13	0.078	9	0.327	19	2626.24	1.233	16
13	0.459	14	0.088	10	0.296	18	2552.72	1.215	15
14	0.433	18	0.103	12	0.210	13	2444.12	1.189	13
15	0.373	23	0.232	20	0.165	11	2721.65	1.255	18
16	0.458	15	0.163	16	0.057	4	2047.93	1.088	10
17	0.421	19	0.127	15	0.225	15	1667.37	0.982	4
18	0.500	9	0.003	1	0.169	12	1459.09	0.919	3
19	0.655	1	0.090	11	0.042	3	1252.08	0.851	1
20	0.629	3	0.548	23	0.408	20	3158.46	1.352	22
21	0.647	2	0.576	24	0.437	21	3267.01	1.375	23
22	0.457	16	0.215	19	0.274	17	2646.30	1.237	17
23	0.418	20	0.008	2	0.217	14	2484.48	1.199	14
24	0.292	24	0.012	3	0.164	10	2841.86	1.282	19

Model ID	Kendal Slope	KS RE	Rank	BS (%)	Rank	S score	Rank	Total score	Final Rank
1	0.0055	4.000	21	0.0415	19	0.720	19	117.5	24
2	0.0045	3.091	18	0.0217	13	0.726	18	68.5	12
3	0.0005	0.545	4	0.0078	4	0.863	4	41	4
4	0.0026	1.364	9	0.0082	5	0.827	7	35.5	3
5	0.0028	1.545	12	0.0067	2	0.869	2	48	6
6	0.0026	1.364	9	0.0256	15	0.708	20	48	6
7	0.0046	3.182	19	0.0075	3	0.863	3	61.5	8
8	0.0052	3.727	20	0.0132	10	0.804	10	47	5
9	0.0021	0.909	6	0.0637	24	0.679	24	87	20
10	-0.0007	1.636	13	0.0621	23	0.685	23	95.5	22
11	0.0027	1.455	11	0.0291	16	0.798	13	66	10
12	-0.0009	1.818	14	0.0477	20	0.738	17	82.5	18
13	0.0009	0.182	2	0.0546	21	0.690	22	79.5	16
14	-0.0019	2.727	17	0.0358	17	0.756	16	81	17
15	0.0089	7.091	23	0.0388	18	0.756	15	100	23
16	0.0033	2.000	16	0.0189	11	0.804	11	64	9
17	0.0089	7.091	23	0.0119	8	0.815	8	72.5	14
18	0.0013	0.182	1	0.0116	7	0.804	12	35	2
19	0.0006	0.455	3	0.0210	12	0.815	9	28	1
20	0.0056	4.091	22	0.0121	9	0.845	6	86.5	19
21	0.0025	1.273	8	0.0022	1	0.929	1	75	15

22	0.0019	0.727	5	0.0599	22	0.702	21	93	21
23	0.0024	1.182	7	0.0221	14	0.792	14	67.5	11
24	0.0032	1.909	15	0.0087	6	0.857	5	69	13

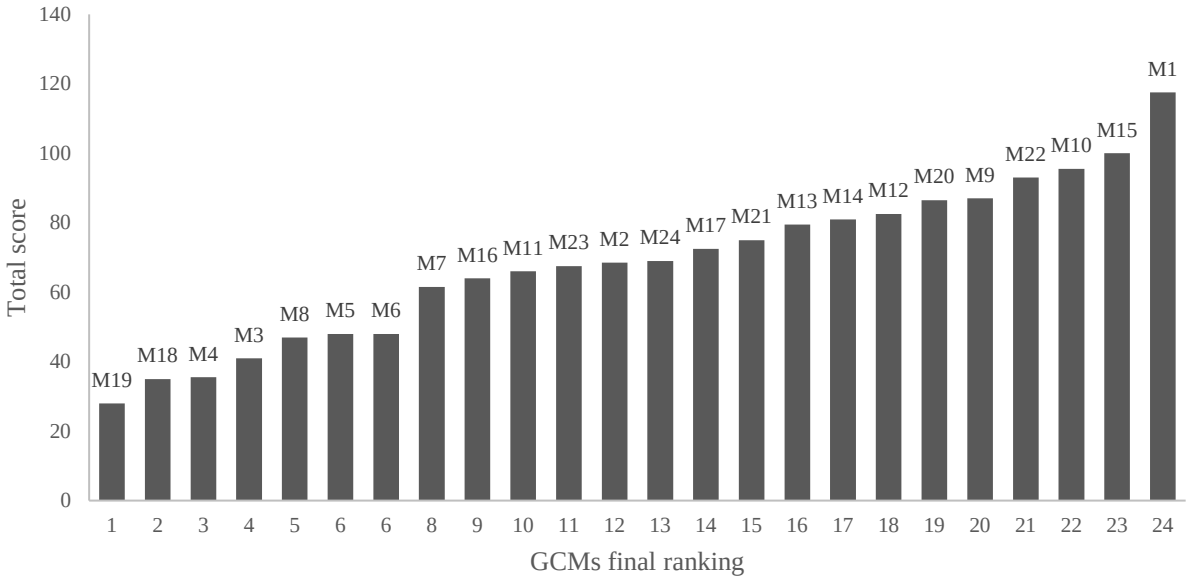

Figure A2 GCMs ranking results for the Northern climatic region under RCP6.0 climate change scenario

Table A3 GCMs statistical assessment for the Northern climatic region under RCP8.5 scenario

Model ID	Correlation	Rank	Mean RE	Rank	St Dev RE	Rank	SSE	NRMSE	Rank
1	0.307	23	0.122	14	0.662	24	4708.16	1.650	24
2	0.524	9	0.243	20	0.100	8	2012.04	1.079	11

3	0.580	5	0.264	21	0.038	4	1739.89	1.003	7
4	0.612	4	0.126	15	0.076	7	1285.32	0.862	3
5	0.424	18	0.045	6	0.005	1	1970.28	1.068	9
6	0.577	6	0.110	13	0.160	9	1751.19	1.006	8
7	0.473	12	0.215	19	0.234	13	1632.80	0.972	6
8	0.519	10	0.085	10	0.018	2	1629.53	0.971	5
9	0.470	14	0.044	5	0.441	23	2927.58	1.301	20
10	0.450	17	0.093	11	0.398	20	2910.14	1.297	19
11	0.470	15	0.047	7	0.295	15	2485.32	1.199	13
12	0.377	21	0.074	8	0.336	18	3034.24	1.325	22
13	0.476	11	0.074	9	0.327	17	2561.21	1.217	15
14	0.416	20	0.097	12	0.209	12	2504.43	1.204	14
15	0.367	22	0.278	22	0.069	6	2590.24	1.224	16
16	0.459	16	0.190	17	0.020	3	2006.65	1.077	10
17	0.544	7	0.142	16	0.417	21	1271.84	0.858	2
18	0.529	8	0.026	2	0.201	11	1347.54	0.883	4
19	0.666	1	0.044	4	0.059	5	1211.40	0.837	1
20	0.638	3	0.526	23	0.386	19	2972.37	1.311	21
21	0.651	2	0.552	24	0.419	22	3104.95	1.340	23
22	0.421	19	0.192	18	0.315	16	2889.07	1.293	18
23	0.473	13	0.034	3	0.263	14	2379.80	1.173	12
24	0.292	24	0.012	1	0.164	10	2841.86	1.282	17

Model ID	**Kendal Slope**	**KS RE**	**Rank**	**BS (%)**	**Rank**	**S score**	**Rank**	**Total score**	**Final Rank**
1	-0.0035	4.182	20	0.0502	20	0.690	22	116	24
2	0.0055	4.000	18	0.0228	13	0.732	18	72.5	13
3	0.0021	0.909	9	0.0128	8	0.851	5	48	6
4	0.0016	0.455	4	0.0092	5	0.815	8	37.5	3
5	0.0004	0.636	7	0.0078	2	0.869	2	39.5	5
6	0.0056	4.091	19	0.0266	15	0.714	20	63	9
7	0.0032	1.909	13	0.0080	3	0.869	2	59	7
8	0.0016	0.455	4	0.0106	7	0.833	6	35.5	2
9	0.0035	2.182	15	0.0736	24	0.661	24	93.5	22
10	0.002	0.818	8	0.0523	21	0.720	19	91	21
11	0.0074	5.727	23	0.0314	17	0.780	13	76.5	17
12	0.0016	0.455	4	0.0394	19	0.756	16	88.5	19
13	0.0015	0.364	2	0.0572	22	0.702	21	74.5	15
14	0.0012	0.091	1	0.0306	16	0.786	12	72.5	13
15	0.0023	1.091	11	0.0340	18	0.750	17	89	20
16	-0.0007	1.636	12	0.0253	14	0.774	14	66	12
17	0.0064	4.818	22	0.0150	9	0.821	7	65	10
18	0.0007	0.364	3	0.0181	10	0.774	14	38.5	4
19	0.0059	4.364	21	0.0204	11	0.792	11	32.5	1
20	0.0039	2.545	17	0.0037	1	0.917	1	75.5	16
21	0.0001	0.909	10	0.0102	6	0.815	9	83.5	18

22	0.0038	2.455	16	0.0588	23	0.673	23	102	23
23	0.0104	8.455	24	0.0208	12	0.804	10	65	10
24	0.0032	1.909	13	0.0087	4	0.857	4	62.5	8

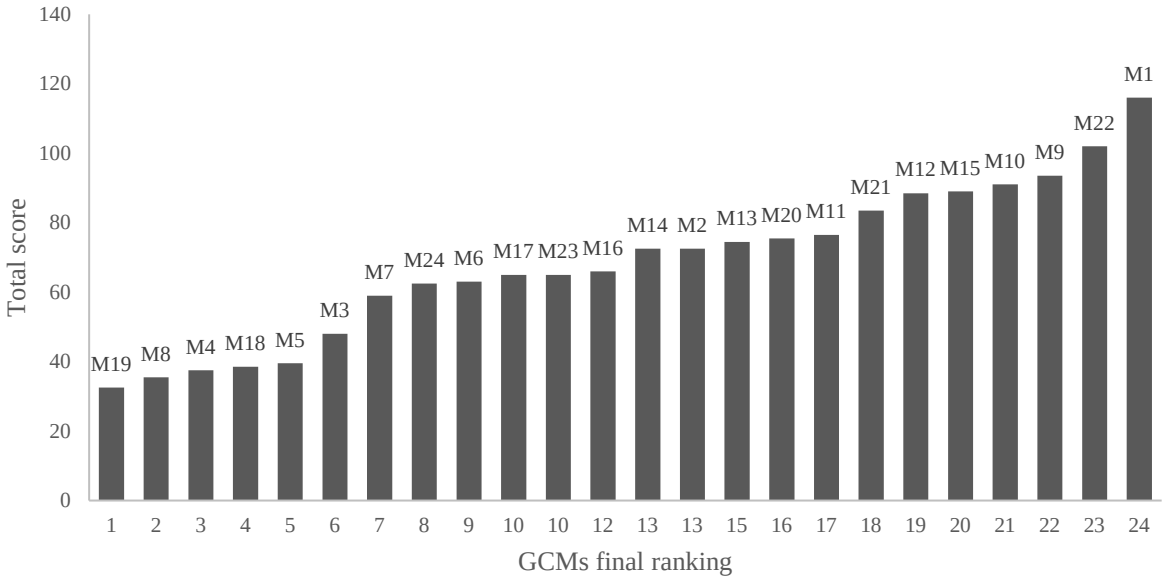

Figure A3 GCMs ranking results for the Northern climatic region under RCP8.5 climate change scenario

Table A4 GCMs statistical assessment for the Southern climatic region under RCP4.5 scenario

Model ID	Correlation	Rank	Mean RE	Rank	St Dev RE	Rank	SSE	NRMSE	Rank
1	0.163	23	0.086	7	0.690	21	4173.17	1.800	21
2	0.462	6	0.125	11	0.028	2	1459.83	1.065	4
3	0.525	1	0.001	1	0.113	5	1071.56	0.912	1
4	0.451	8	0.571	22	0.466	18	3822.37	1.723	19
5	0.173	22	0.018	3	0.217	11	2579.24	1.415	11
6	0.467	5	0.173	13	0.613	20	2765.38	1.465	14

7	0.275	16	0.014	2	0.102	4	2014.17	1.250	7
8	0.348	13	0.290	19	1.092	24	5306.99	2.030	24
9	0.388	12	0.155	12	0.247	13	2099.95	1.277	9
10	0.251	17	0.614	23	0.456	17	4768.57	1.924	22
11	0.197	21	0.657	24	0.444	16	5186.11	2.006	23
12	0.429	10	0.050	4	0.060	3	1533.28	1.091	5
13	0.403	11	0.073	5	0.119	6	1715.09	1.154	6
14	0.339	14	0.111	10	0.183	9	2058.40	1.264	8
15	0.456	7	0.280	18	0.886	22	3922.46	1.745	20
16	0.516	2	0.263	17	0.561	19	2610.91	1.424	12
17	0.451	9	0.188	14	0.177	8	1337.78	1.019	3
18	0.295	15	0.238	16	0.220	12	2482.81	1.388	10
19	0.474	4	0.106	9	0.190	10	1165.64	0.951	2
20	0.160	24	0.437	20	0.021	1	2962.20	1.516	17
21	0.202	20	0.463	21	0.147	7	2740.26	1.459	13
22	0.496	3	0.197	15	0.912	23	3637.00	1.680	18
23	0.217	19	0.077	6	0.356	14	2848.17	1.487	16
24	0.239	18	0.097	8	0.361	15	2802.49	1.475	15

Model ID	**Kendal Slope**	**KS RE**	**Rank**	**BS (%)**	**Rank**	**S score**	**Rank**	**Total score**	**Final Rank**
1	-0.0086	6.818	22	0.1195	24	0.554	23	106.5	23
2	0.0064	6.818	23	0.0141	5	0.792	6	40	6
3	0.0028	3.545	11	0.0097	3	0.851	3	16.5	1
4	0.0038	4.455	16	0.0440	21	0.631	22	96.5	20
5	0.0047	5.273	18	0.0119	4	0.821	4	60	10
6	0.005	5.545	20	0.0262	13	0.756	9	73	12
7	0.0022	3.000	10	0.0036	1	0.905	1	35	3
8	0.0173	16.727	24	0.0868	23	0.554	23	115	24
9	0.0005	1.455	5	0.0158	7	0.786	7	55.5	8
10	0.0034	4.091	14	0.0238	10	0.732	14	98	21
11	0.0012	2.091	9	0.0303	15	0.690	19	105.5	22
12	-0.0006	0.455	2	0.0223	9	0.750	10	32.5	2
13	0.0008	1.727	6	0.0275	14	0.732	14	45	7
14	0.0034	4.091	14	0.0178	8	0.774	8	56	9
15	0.0049	5.455	19	0.0345	19	0.696	18	95	19
16	0.001	1.909	7	0.0323	16	0.720	17	70	11
17	-0.0002	0.818	3	0.0063	2	0.863	2	37.5	4
18	0.0033	4.000	13	0.0742	22	0.655	21	81	16
19	0.0043	4.909	17	0.0143	6	0.810	5	39	5
20	0.0002	1.182	4	0.0330	17	0.673	20	82.5	18
21	0.001	1.909	7	0.0246	11	0.726	16	78	15
22	-0.0012	0.091	1	0.0411	20	0.750	11	75	14
23	0.0031	3.818	12	0.0256	12	0.744	12	73	12
24	0.0057	6.182	21	0.0337	18	0.738	13	82	17

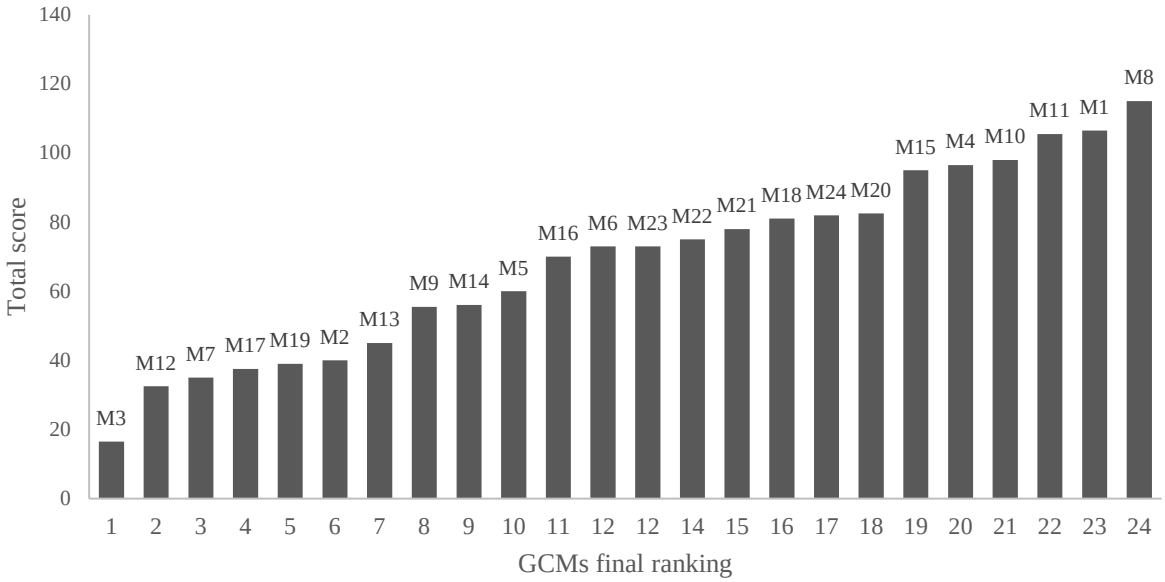

Figure A4 GCMs ranking results for the Southern climatic region under RCP4.5 climate change scenario

Table A5 GCMs statistical assessment for the Southern climatic region under RCP6.0 scenario

Model ID	Correlation	Rank	Mean RE	Rank	St Dev RE	Rank	SSE	NRMSE	Rank
1	0.212	21	0.064	3	1.003	24	5230.18	2.015	24
2	0.453	5	0.132	11	0.036	2	1501.79	1.080	3
3	0.515	1	0.008	1	0.121	4	1086.52	0.918	1
4	0.457	3	0.609	24	0.528	17	4171.69	1.800	23
5	0.140	23	0.027	2	0.300	9	2916.11	1.505	13
6	0.435	6	0.127	10	0.513	16	2545.28	1.406	6
7	0.254	16	0.067	5	0.261	8	2461.91	1.382	5
8	0.413	8	0.254	19	0.782	21	3689.31	1.692	18
9	0.150	22	0.200	16	0.560	18	3902.24	1.740	21

10	0.301	12	0.168	13	0.411	12	2813.53	1.478	10
11	0.287	13	0.206	17	0.635	20	3623.44	1.677	17
12	0.352	10	0.133	12	0.501	15	2834.07	1.483	11
13	0.276	14	0.067	4	0.413	13	2795.74	1.473	9
14	0.262	15	0.123	9	0.448	14	2998.72	1.526	16
15	0.393	9	0.186	15	0.832	22	3813.92	1.721	20
16	0.501	2	0.281	20	0.617	19	2871.54	1.493	12
17	0.313	11	0.214	18	0.165	5	2254.61	1.323	4
18	0.047	24	0.495	23	0.219	7	4125.75	1.790	22
19	0.420	7	0.122	8	0.182	6	1300.24	1.005	2
20	0.233	18	0.455	22	0.024	1	2942.74	1.511	14
21	0.242	17	0.442	21	0.076	3	2683.34	1.443	7
22	0.457	4	0.181	14	0.915	23	3807.50	1.719	19
23	0.215	20	0.073	6	0.395	11	2962.15	1.516	15
24	0.221	19	0.108	7	0.327	10	2777.63	1.468	8

Model ID	**Kendal Slope**	**KS RE**	**Rank**	**BS (%)**	**Rank**	**S score**	**Rank**	**Total score**	**Final Rank**
1	0.0057	6.182	16	0.0919	24	0.601	23	103.5	24
2	0.0053	5.818	15	0.0137	4	0.792	7	34	3
3	0.0033	4.000	13	0.0066	1	0.869	1	14.5	1
4	0.0087	8.909	23	0.0316	19	0.667	22	99	22
5	0.0057	6.182	16	0.0229	12	0.780	9	65.5	12
6	0.0013	2.182	7	0.0166	8	0.833	2	46.5	4
7	0.0074	7.727	21	0.0192	10	0.774	11	55	6
8	0.0086	8.818	22	0.0796	23	0.571	24	100.5	23
9	0.0089	9.091	24	0.0146	7	0.792	7	96	21
10	-0.0053	3.818	12	0.0112	2	0.810	6	57	7
11	0.001	1.909	6	0.0186	9	0.774	10	79.5	16
12	0.0066	7.000	19	0.0143	6	0.833	3	62	9
13	0.0036	4.273	14	0.0222	11	0.756	14	59.5	8
14	-0.0015	0.364	2	0.0235	13	0.750	15	69	13
15	-0.0023	1.091	4	0.0370	22	0.702	19	88.5	19
16	0.0068	7.182	20	0.0334	20	0.690	21	83.5	18
17	0.0061	6.545	18	0.0141	5	0.815	5	52	5
18	-0.0007	0.364	3	0.0316	18	0.750	15	94	20
19	0.0018	2.636	8	0.0123	3	0.821	4	30.5	2
20	0.0026	3.364	11	0.0246	14	0.762	12	73.5	15
21	-0.0011	0.000	1	0.0256	15	0.726	18	65	11
22	0.0001	1.091	5	0.0364	21	0.702	20	83	17
23	0.0023	3.091	9	0.0293	16	0.726	17	73	14
24	0.0025	3.273	10	0.0303	17	0.762	12	63.5	10

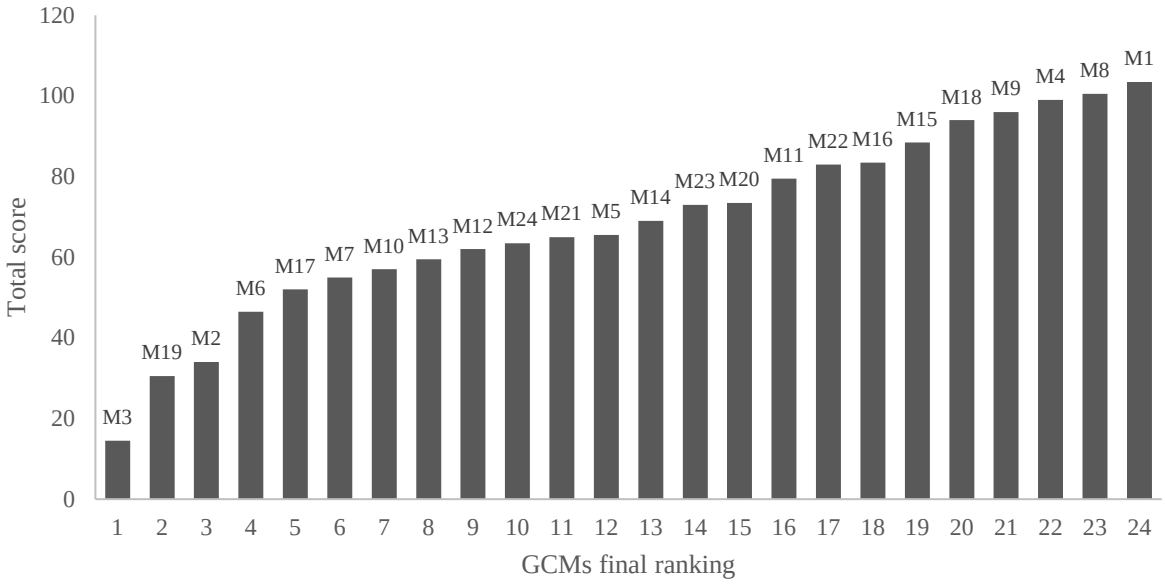

Figure A5 GCMs ranking results for the Southern climatic region under RCP6.0 climate change scenario

Table A6 GCMs statistical assessment for the Southern climatic region under RCP8.5 scenario

Model ID	Correlation	Rank	Mean RE	Rank	St Dev RE	Rank	SSE	NRMSE	Rank
1	0.419	8	0.086	6	0.469	16	2448.93	1.379	5
2	0.429	6	0.126	11	0.010	1	1518.26	1.086	2
3	0.473	3	0.025	3	0.099	3	1203.47	0.967	1
4	0.459	4	0.588	24	0.414	10	3757.34	1.708	23
5	0.172	24	0.009	1	0.210	6	2566.48	1.412	8
6	0.441	5	0.131	12	0.511	19	2526.06	1.400	6
7	0.227	20	0.021	2	0.091	2	2124.27	1.284	4
8	0.339	10	0.189	18	0.766	22	3830.22	1.724	24
9	0.210	23	0.140	13	0.508	18	3402.12	1.625	20
10	0.254	14	0.182	17	0.545	20	3415.88	1.628	21
11	0.292	13	0.206	19	0.484	17	3125.55	1.558	16

12	0.313	11	0.105	7	0.445	12	2784.88	1.470	9
13	0.222	21	0.107	9	0.413	8	3023.01	1.532	14
14	0.241	16	0.157	14	0.461	14	3163.12	1.567	17
15	0.313	11	0.105	7	0.445	12	2784.88	1.470	9
16	0.222	21	0.107	9	0.413	8	3023.01	1.532	14
17	0.241	16	0.157	14	0.461	14	3163.12	1.567	17
18	0.422	7	0.212	20	0.822	24	3697.71	1.694	22
19	0.521	1	0.263	22	0.650	21	2834.22	1.483	12
20	0.369	9	0.221	21	0.106	4	1657.49	1.134	3
21	0.232	19	0.433	23	0.140	5	2564.37	1.411	7
22	0.499	2	0.182	16	0.817	23	3271.86	1.594	19
23	0.237	18	0.034	4	0.442	11	3004.64	1.527	13
24	0.241	15	0.074	5	0.372	7	2804.76	1.476	11

Model ID	**Kendal Slope**	**KS RE**	**Rank**	**BS (%)**	**Rank**	**S score**	**Rank**	**Total score**	**Final Rank**
1	0.0104	10.455	24	0.0696	23	0.583	23	70	10
2	0.0062	6.636	18	0.0209	16	0.762	17	45.5	3
3	0.0064	6.818	19	0.0103	4	0.857	2	22.5	1
4	0.0047	5.273	17	0.0397	22	0.625	22	91.5	22
5	0.0041	4.727	14	0.0119	5	0.821	8	52.5	7
6	0.0016	2.455	11	0.0136	8	0.827	7	55	8
7	0.0041	4.727	14	0.0050	1	0.881	1	36	2
8	0.0022	3.000	12	0.1044	24	0.518	24	104	24
9	0.0009	1.818	6	0.0166	11	0.786	13	89	21
10	-0.002	0.818	1	0.0188	15	0.792	10	85	20
11	0.0002	1.182	3	0.0075	3	0.845	6	71	11
12	0.0015	2.364	9	0.0121	6	0.851	4	48.5	5
13	0.0084	8.636	22	0.0177	12	0.774	14	76	16
14	0.0013	2.182	7	0.0151	9	0.792	10	74	13
15	0.0015	2.364	9	0.0121	6	0.851	4	48.5	5
16	0.0084	8.636	22	0.0177	12	0.774	14	76	16
17	0.0013	2.182	7	0.0151	9	0.792	10	74	13
18	0.0008	1.727	5	0.0312	20	0.720	19	95	23
19	0.0038	4.455	13	0.0336	21	0.702	21	83.5	19
20	0.0045	5.091	16	0.0071	2	0.857	2	47	4
21	-0.0028	1.545	4	0.0181	14	0.768	16	71	11
22	0.0001	1.091	2	0.0258	17	0.738	18	78.5	18
23	0.0075	7.818	20	0.0280	18	0.720	20	75	15
24	0.0081	8.364	21	0.0297	19	0.792	9	62.5	9

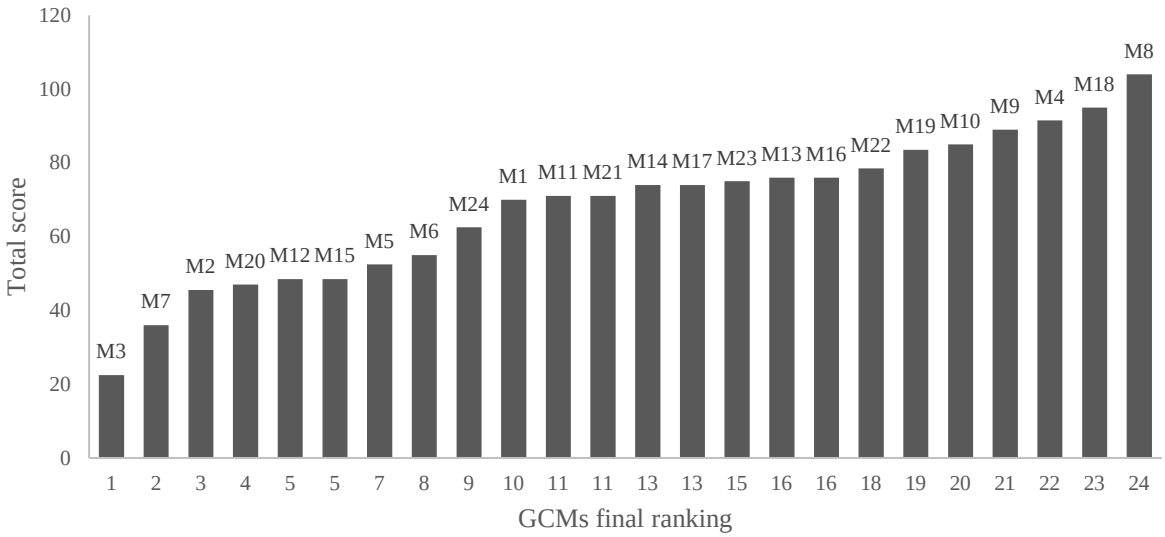

Figure A6 GCMs ranking results for the Southern climatic region under RCP8.5 climate change scenario

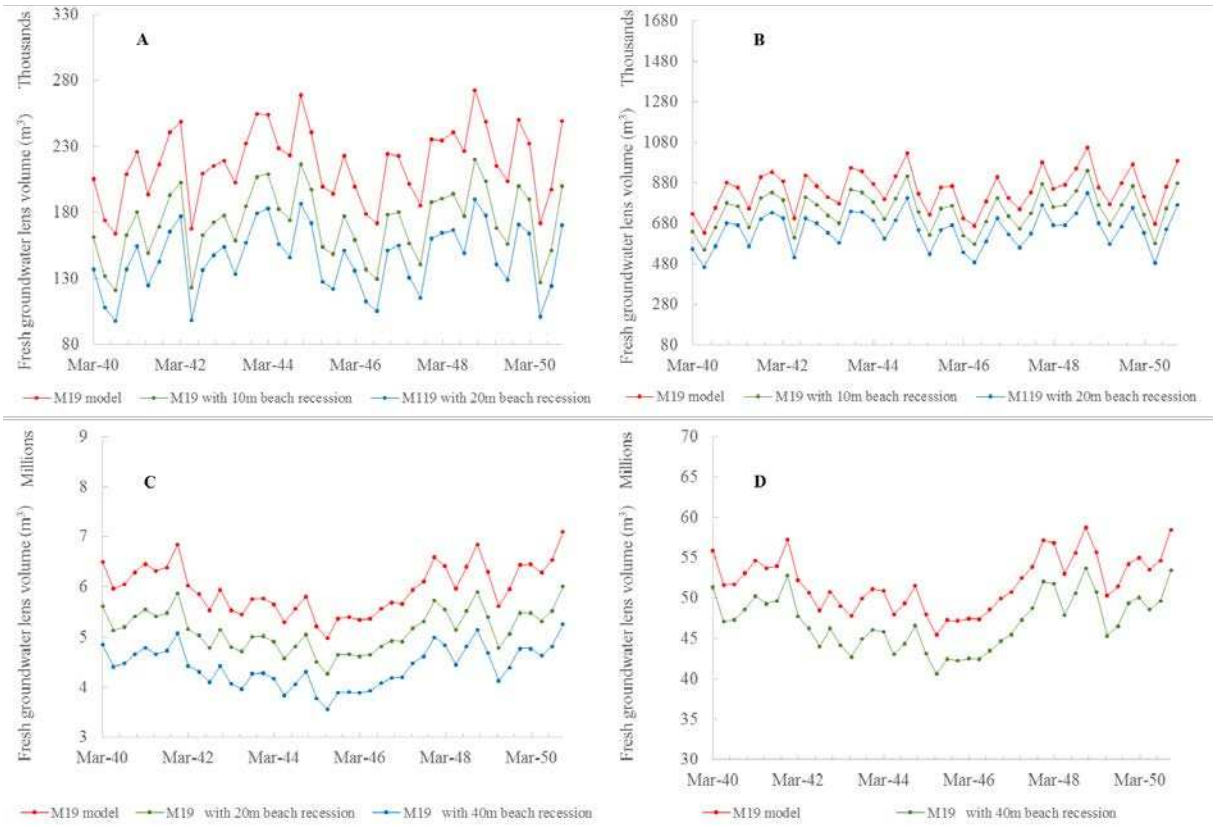

Figure A7 simulated freshwater volume in the four islands in the study area under different sea level rise scenarios coupled with the 2nd ranked climatic models under RCP2.6 scenario; **A**. N. Holhudhoo; **B**. N. Velidhoo; **C**. GDh. Thinadhoo; **D**. L. Gan

Table A7 statistical summary for simulated freshwater lens volume under different sea level rise scenario coupled with 2nd ranked climatic models under RCP2.6

Island	Average freshwater lens volume w/o SLR (Mm^3)	Average freshwater lens volume w/ conservative SLR (Mm^3)	Average freshwater lens volume w/ aggressive SLR (Mm^3)	% reduction conserv.	% reduction Aggres.
N. Holhudhoo	0.218	0.172	0.146	20.96%	33.01%
N. Velidhoo	0.846	0.747	0.650	11.65%	23.13%
GDh. Thinadhoo	5.965	5.136	4.408	13.91%	26.11%
L. Gan	51.927	47.081	-	9.33%	-

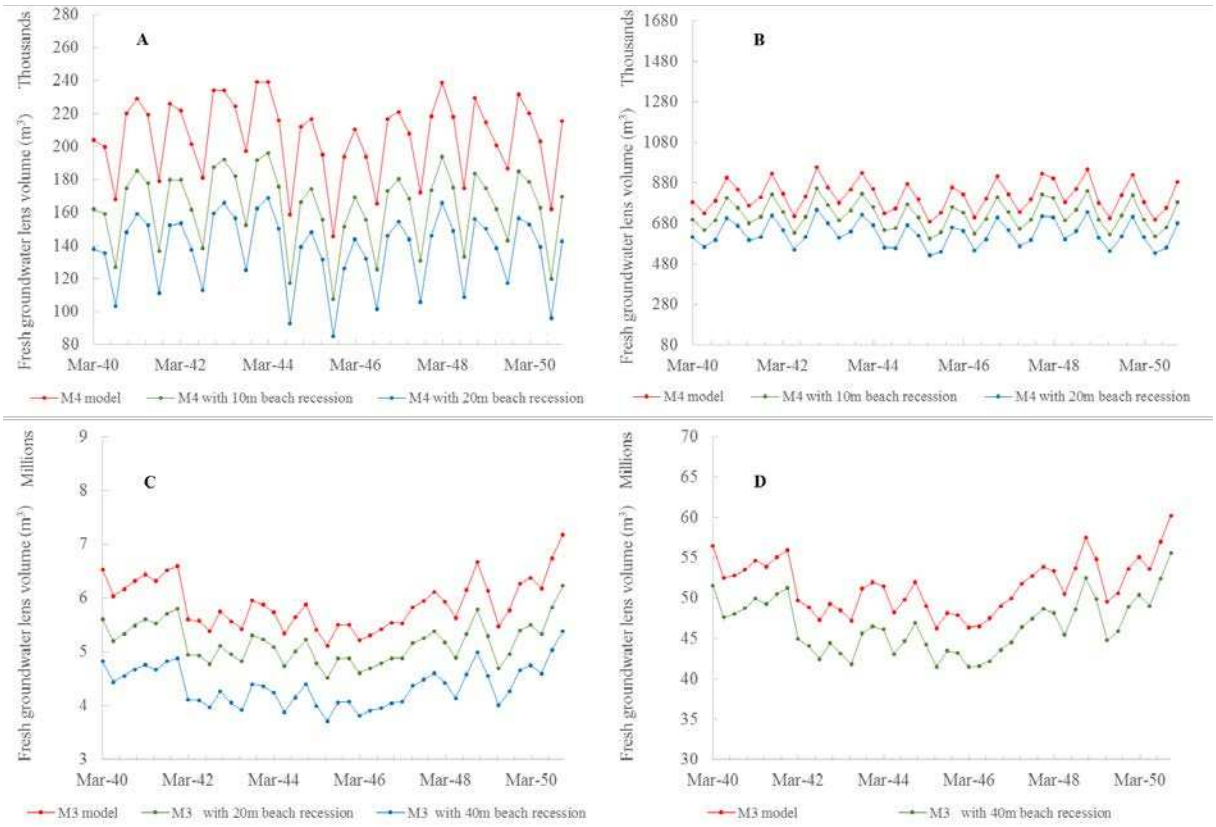

Figure A8 simulated freshwater volume in the four islands in the study area under different sea level rise scenarios coupled with the 3rd ranked climatic models under RCP2.6 scenario; **A**. N. Holhudhoo; **B**. N. Velidhoo; **C**. GDh. Thinadhoo; **D**. L. Gan

Table A8 statistical summary for simulated freshwater lens volume under different sea level rise scenario coupled with 3rd ranked climatic models under RCP2.6

Island	**Average freshwater lens volume w/o SLR (Mm^3)**	**Average freshwater lens volume w/ conservative SLR (Mm^3)**	**Average freshwater lens volume w/ aggressive SLR (Mm^3)**	**% reduction conserv.**	**% reduction Aggres.**
N. Holhudhoo	0.206	0.163	0.138	20.59%	33.06%
N. Velidhoo	0.818	0.724	0.630	11.43%	22.92%
GDh. Thinadhoo	5.901	5.173	4.366	12.34%	26.01%
L. Gan	51.570	46.614	-	9.61%	-

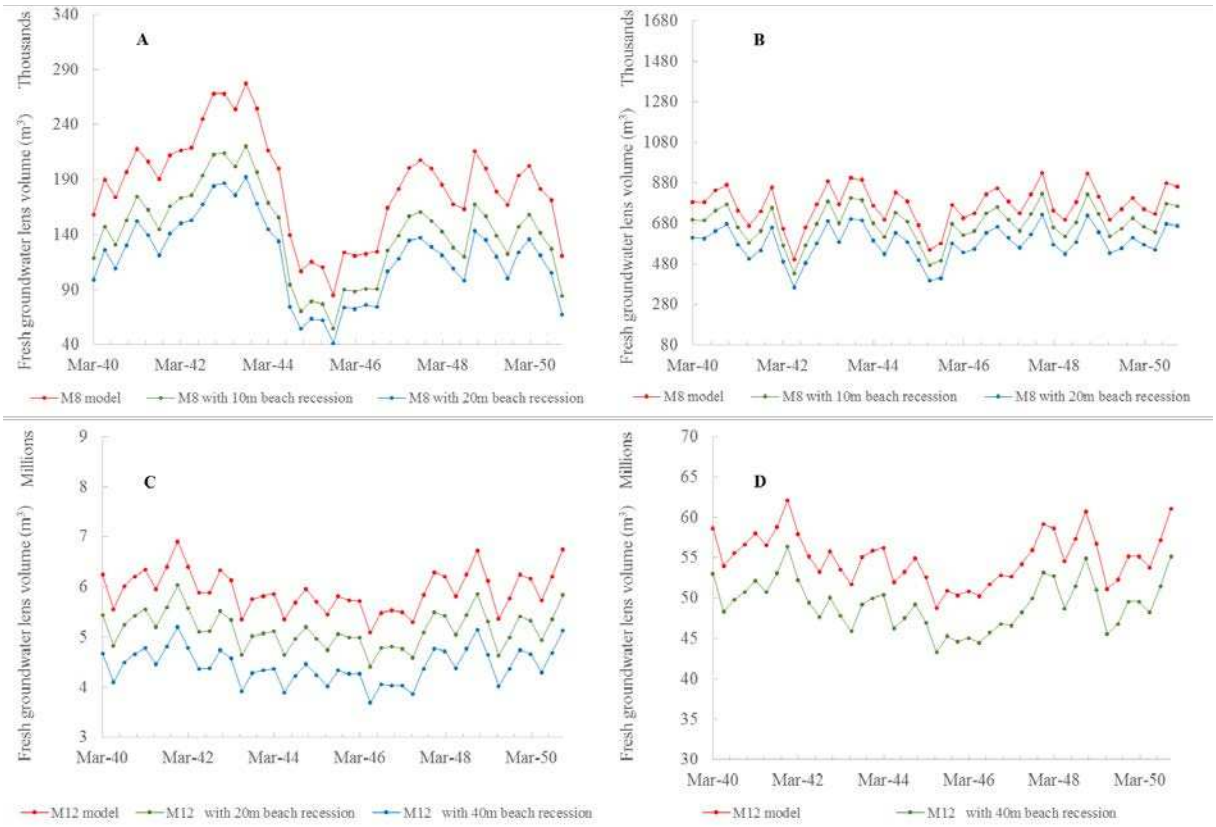

Figure A9 simulated freshwater volume in the four islands in the study area under different sea level rise scenarios coupled with the 2nd ranked climatic models under RCP4.5 scenario; **A**. N. Holhudhoo; **B**. N. Velidhoo; **C**. GDh. Thinadhoo; **D**. L. Gan

Table A9 statistical summary for simulated freshwater lens volume under different sea level rise scenario coupled with 2nd ranked climatic models under RCP4.5

Island	**Average freshwater lens volume w/o SLR (Mm^3)**	**Average freshwater lens volume w/ conservative SLR (Mm^3)**	**Average freshwater lens volume w/ aggressive SLR (Mm^3)**	**% reduction conserv.**	**% reduction Aggres.**
N. Holhudhoo	0.184	0.141	0.120	23.40%	35.04%
N. Velidhoo	0.769	0.678	0.587	11.83%	23.70%
GDh. Thinadhoo	5.927	5.156	4.431	13.02%	25.24%
L. Gan	54.977	49.209	-	10.49%	-

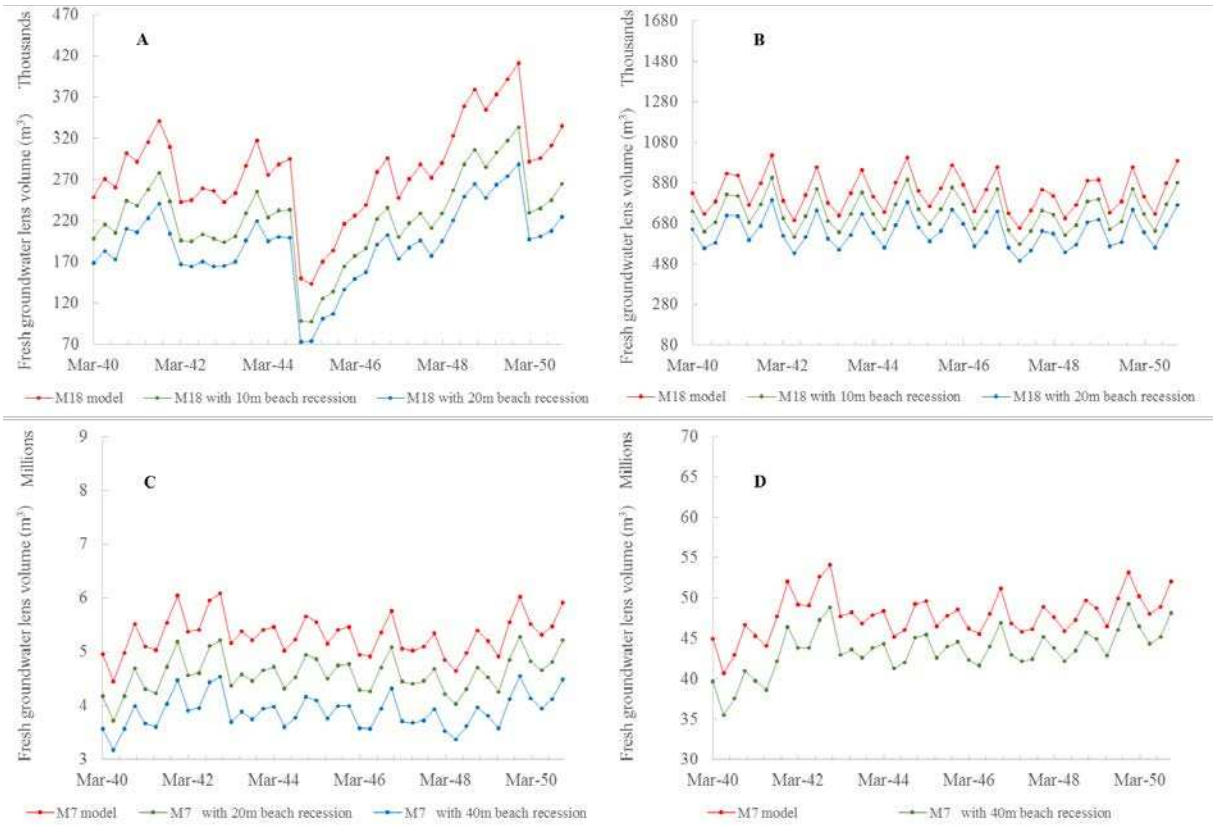

Figure A10 simulated freshwater volume in the four islands in the study area under different sea level rise scenarios coupled with the 3rd ranked climatic model under RCP4.5 scenario; **A**. N. Holhudhoo; **B**. N. Velidhoo; **C**. GDh. Thinadhoo; **D**. L. Gan

Table A10 statistical summary for simulated freshwater lens volume under different sea level rise scenario coupled with 3rd ranked climatic models under RCP4.

Island	**Average freshwater lens volume w/o SLR (Mm^3)**	**Average freshwater lens volume w/ conservative SLR (Mm^3)**	**Average freshwater lens volume w/ aggressive SLR (Mm^3)**	**% reduction conserv.**	**% reduction Aggres.**
N. Holhudhoo	0.282	0.224	0.191	20.64%	32.36%
N. Velidhoo	0.833	0.737	0.640	11.54%	23.11%
GDh. Thinadhoo	5.317	4.598	3.896	13.52%	26.72%
L. Gan	47.933	43.578	-	9.08%	-

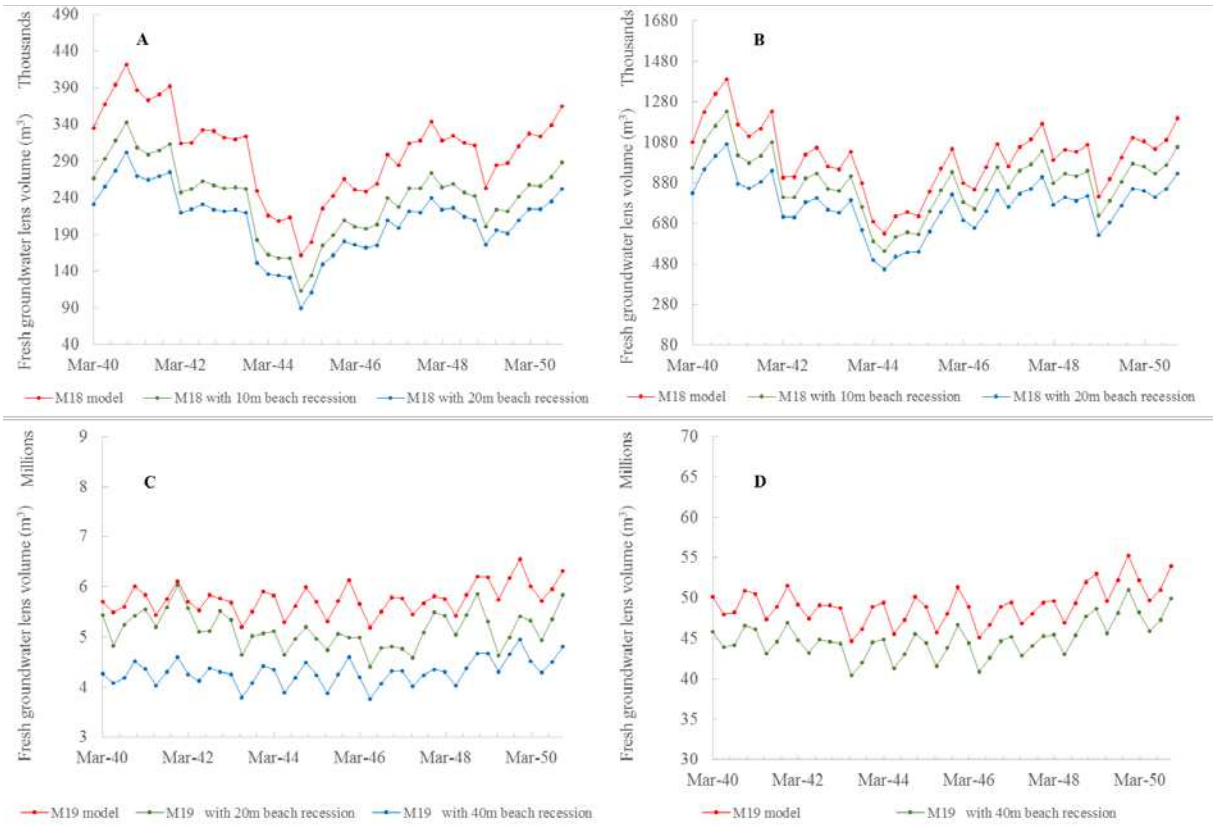

Figure A11 simulated freshwater volume in the four islands in the study area under different sea level rise scenarios coupled with the 2nd ranked climatic model under RCP6.0 scenario; **A**. N. Holhudhoo; **B**. N. Velidhoo; **C**. GDh. Thinadhoo; **D**. L. Gan

Table A11 statistical summary for simulated freshwater lens volume under different sea level rise scenario coupled with 2nd ranked climatic models under RCP6.0

Island	**Average freshwater lens volume w/o SLR (Mm^3)**	**Average freshwater lens volume w/ conservative SLR (Mm^3)**	**Average freshwater lens volume w/ aggressive SLR (Mm^3)**	**% reduction conserv.**	**% reduction Aggres.**
N. Holhudhoo	0.303	0.239	0.208	21.20%	31.45%
N. Velidhoo	1.003	0.886	0.772	11.73%	23.09%
GDh. Thinadhoo	5.760	5.156	4.300	10.50%	25.35%
L. Gan	49.190	44.963	-	8.59%	-

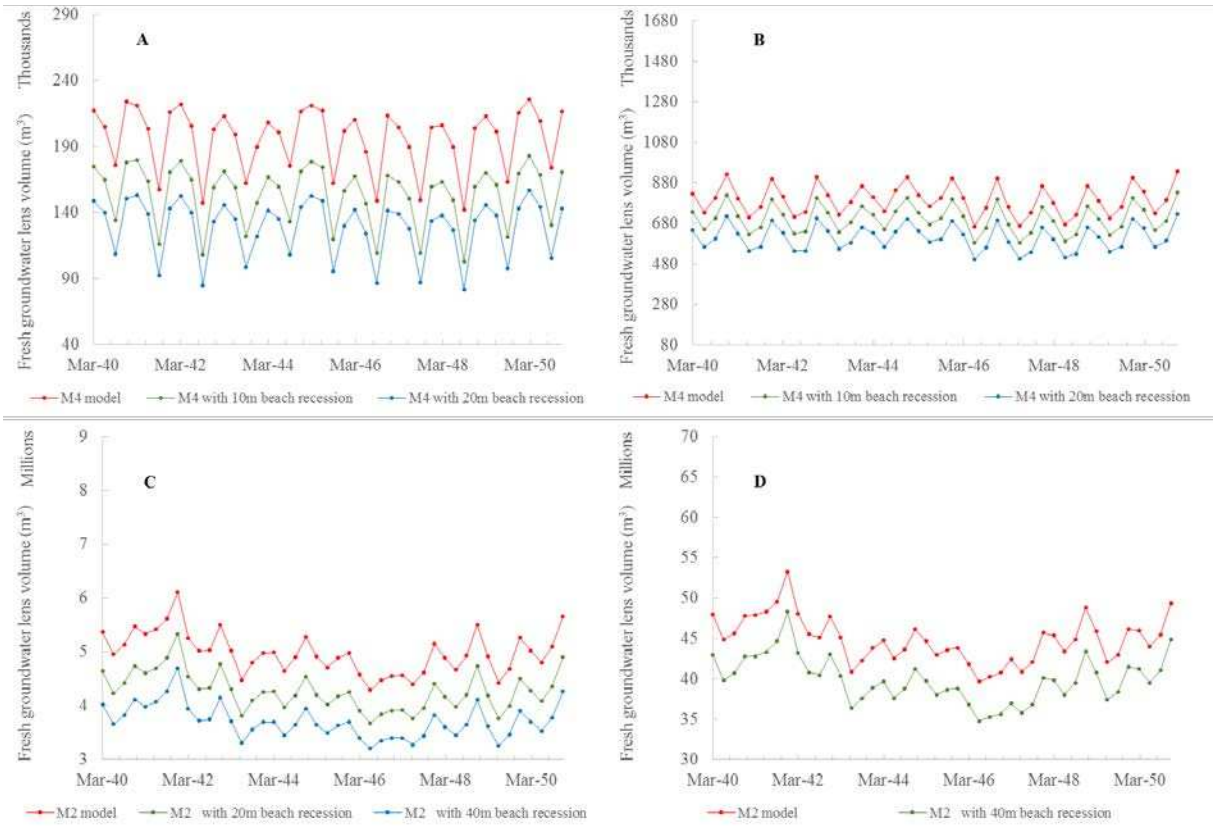

Figure A12 simulated freshwater volume in the four islands in the study area under different sea level rise scenarios coupled with the 3rd ranked climatic model under RCP6.0 scenario; **A**. N. Holhudhoo; **B**. N. Velidhoo; **C**. GDh. Thinadhoo; **D**. L. Gan

Table A12 statistical summary for simulated freshwater lens volume under different sea level rise scenario coupled with 3rd ranked climatic models under RCP6.0

Island	**Average freshwater lens volume w/o SLR (Mm^3)**	**Average freshwater lens volume w/ conservative SLR (Mm^3)**	**Average freshwater lens volume w/ aggressive SLR (Mm^3)**	**% reduction conserv.**	**% reduction Aggres.**
N. Holhudhoo	0.196	0.154	0.129	21.52%	34.18%
N. Velidhoo	0.798	0.704	0.611	11.73%	23.41%
GDh. Thinadhoo	4.986	4.278	3.714	14.21%	25.52%
L. Gan	44.868	39.930	-	11.00%	-

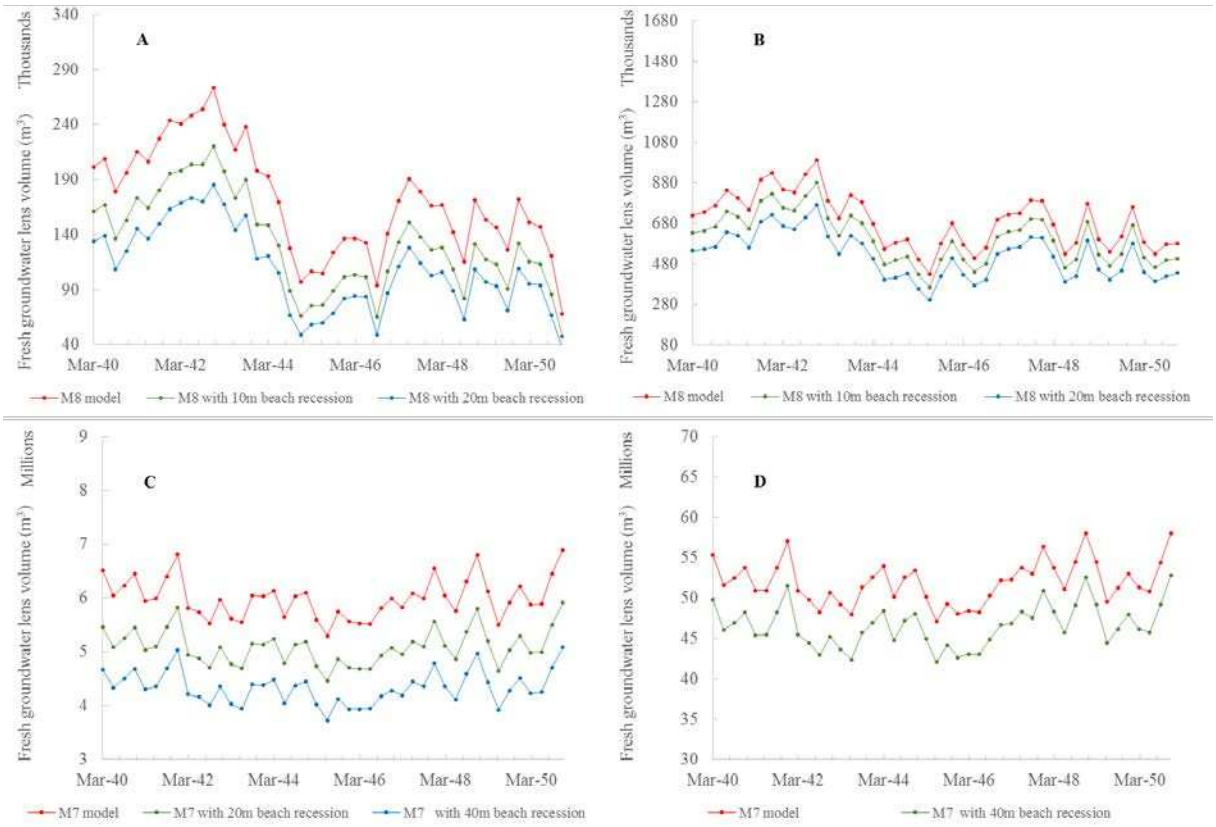

Figure A13 simulated freshwater volume in the four islands in the study area under different sea level rise scenarios coupled with the 2nd ranked climatic model under RCP8.5 scenario; **A**. N. Holhudhoo; **B**. N. Velidhoo; **C**. GDh. Thinadhoo; **D**. L. Gan

Table A13 statistical summary for simulated freshwater lens volume under different sea level rise scenario coupled with 2nd ranked climatic models under RCP8.5

Island	**Average freshwater lens volume w/o SLR (Mm^3)**	**Average freshwater lens volume w/ conservative SLR (Mm^3)**	**Average freshwater lens volume w/ aggressive SLR (Mm^3)**	**% reduction conserv.**	**% reduction Aggres.**
N. Holhudhoo	0.171	0.132	0.109	0.00%	17.93%
N. Velidhoo	0.694	0.608	0.522	12.44%	24.75%
GDh. Thinadhoo	6.000	5.094	5.094	15.09%	15.09%
L. Gan	51.957	46.585	-	10.34%	-

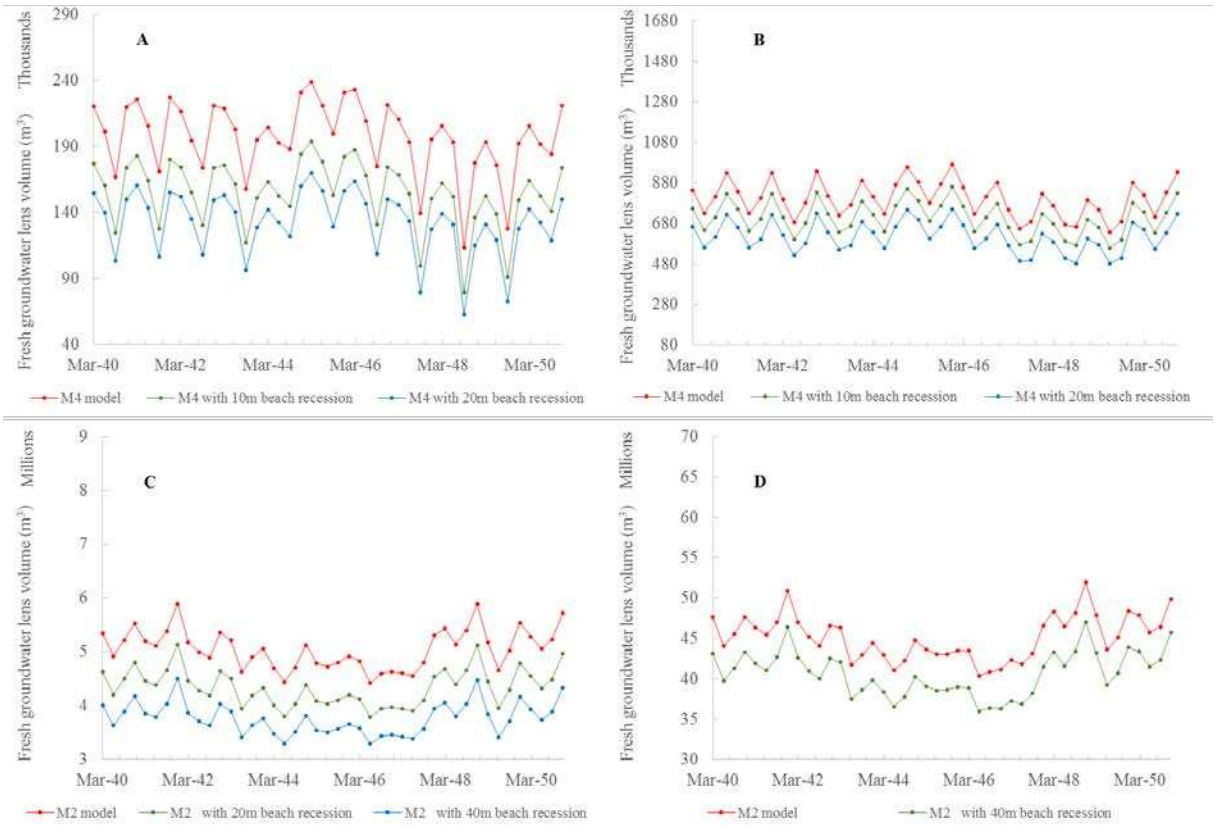

Figure A14 simulated freshwater volume in the four islands in the study area under different sea level rise scenarios coupled with the 3rd ranked climatic model under RCP8.5 scenario; **A**. N. Holhudhoo; **B**. N. Velidhoo; **C**. GDh. Thinadhoo; **D**. L. Gan

Table A14 statistical summary for simulated freshwater lens volume under different sea level rise scenario coupled with 3rd ranked climatic models under RCP8.5

Island	**Average freshwater lens volume w/o SLR (Mm^3)**	**Average freshwater lens volume w/ conservative SLR (Mm^3)**	**Average freshwater lens volume w/ aggressive SLR (Mm^3)**	**% reduction conserv.**	**% reduction Aggres.**
N. Holhudhoo	0.197	0.155	0.133	21.56%	32.69%
N. Velidhoo	0.801	0.708	0.615	11.66%	23.23%
GDh. Thinadhoo	5.057	4.343	3.768	14.11%	25.48%
L. Gan	45.169	40.666	-	9.97%	-

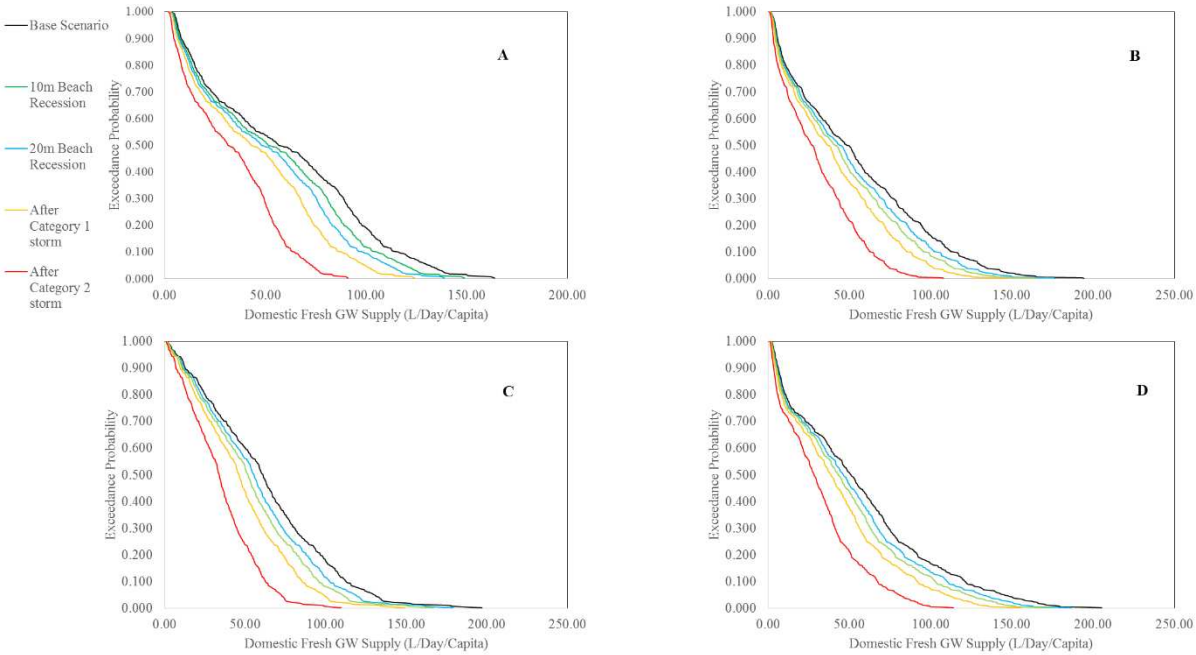

Figure A15 Exceedance probability distribution for monthly groundwater supply average in N. Holhudhoo Island under 2nd ranked GCMs in different climatic RCPs forecasts; **A.** RCP2.6 using model M19; **B.** RCP4.5 using model M8; **C.** RCP6.0 using model M18; **D.** RCP8.5 using model M8

Figure A16 Average annual groundwater supply in N. Holhudhoo Island under 2nd ranked GCMs in different climatic RCPs forecasts; **A.** RCP2.6 using model M19; **B.** RCP4.5 using model M8; **C.** RCP6.0 using model M18; **D.** RCP8.5 using model M8

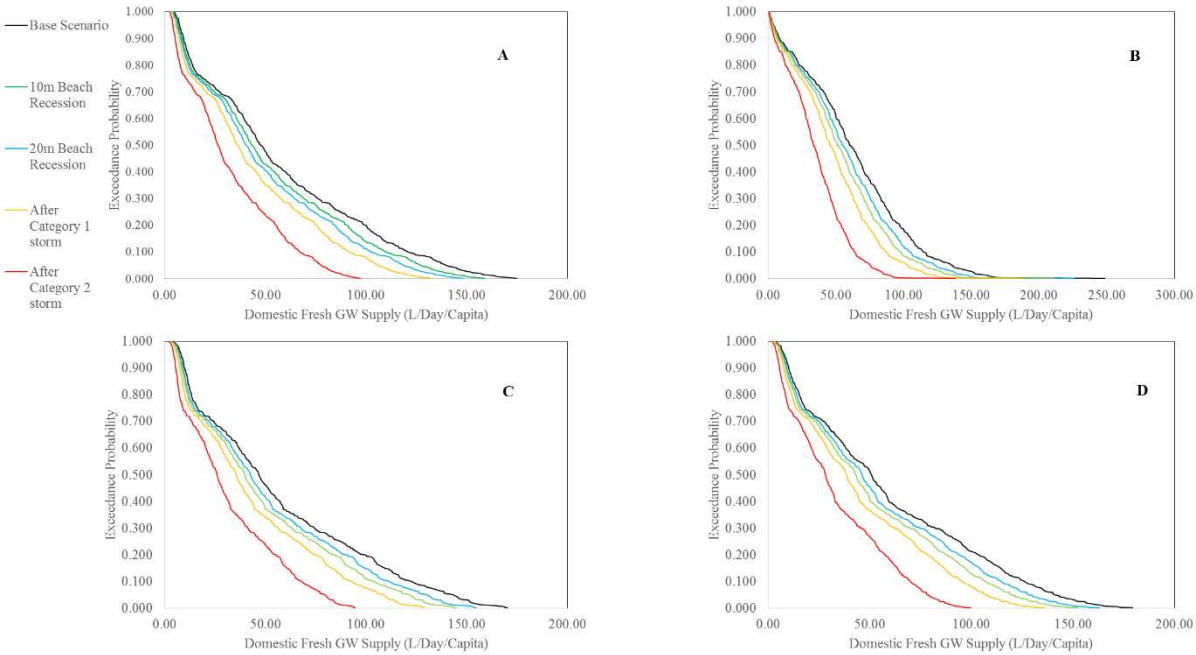

Figure A17 Exceedance probability distribution for monthly groundwater supply average in N. Holhudhoo Island under 3rd ranked GCMs in different climatic RCPs forecasts; **A.** RCP2.6 using model M4; **B.** RCP4.5 using model M18; **C.** RCP6.0 using model M4; **D.** RCP8.5 using model M4

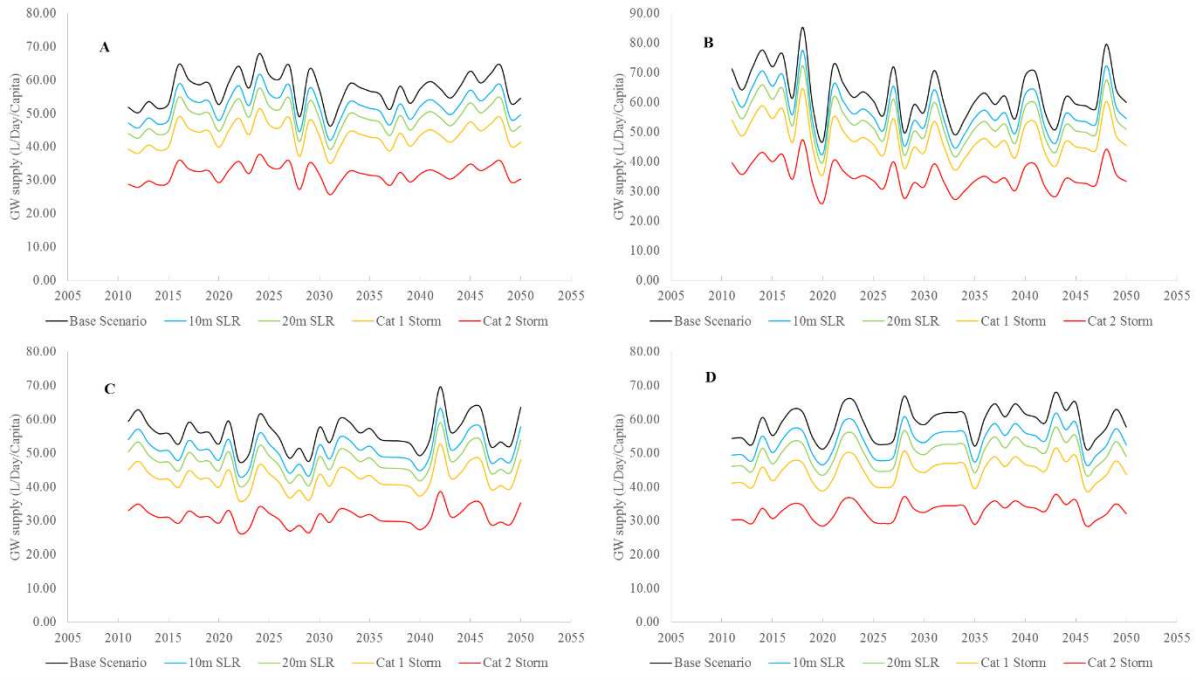

Figure A18 Average annual groundwater supply in N. Holhudhoo Island under 3rd ranked GCMs in different climatic RCPs forecasts; **A.** RCP2.6 using model M4; **B.** RCP4.5 using model M18; **C.** RCP6.0 using model M4; **D.** RCP8.5 using model M4

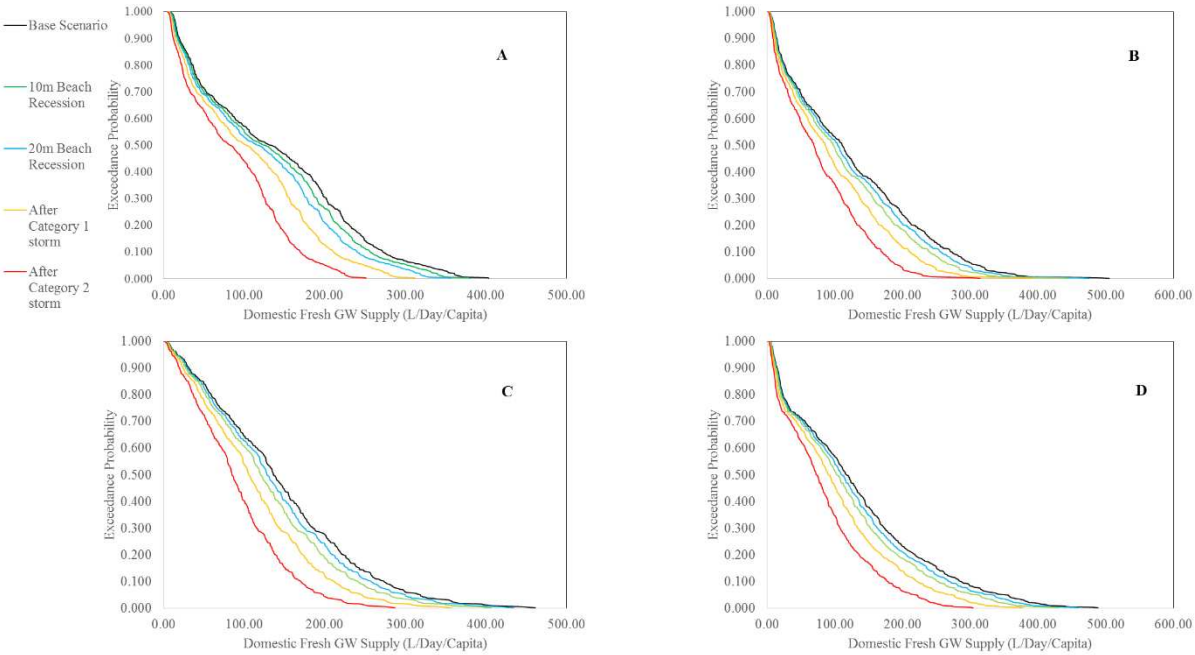

Figure A19 Exceedance probability distribution for monthly groundwater supply average in N. Velidhoo Island under 2nd ranked GCMs in different climatic RCPs forecasts; **A.** RCP2.6 using model M19; **B.** RCP4.5 using model M8; **C.** RCP6.0 using model M18; **D.** RCP8.5 using model M8

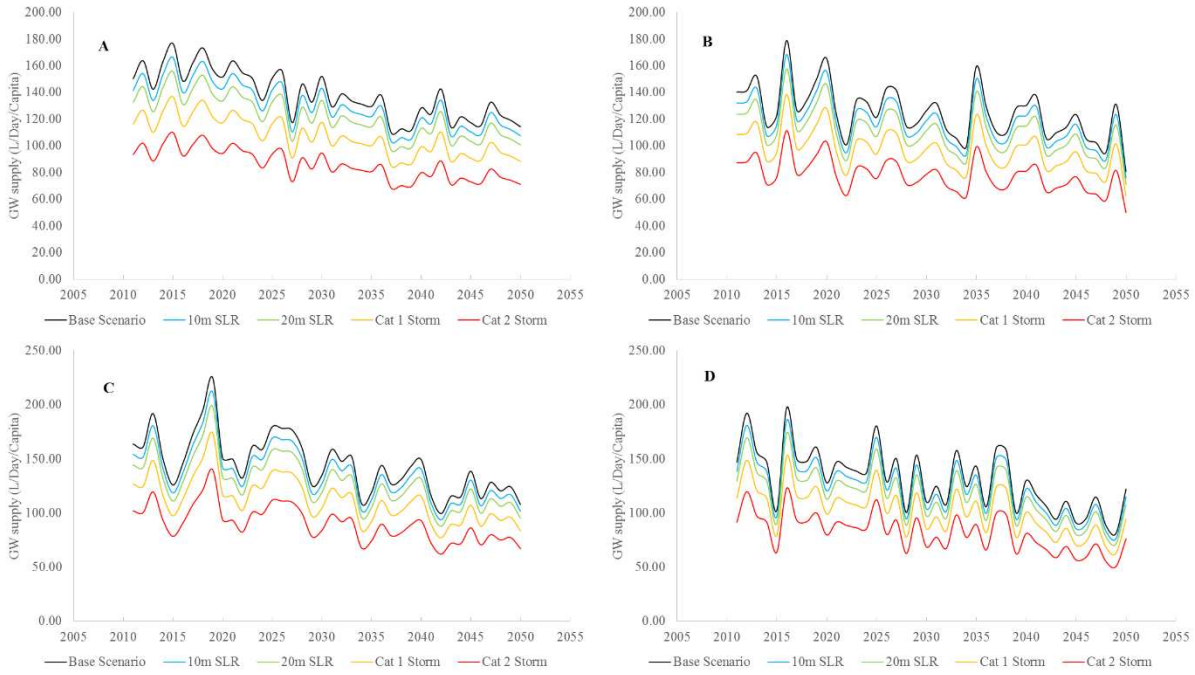

Figure A20 Average annual groundwater supply in N. Velidhoo Island under 2nd ranked GCMs in different climatic RCPs forecasts; **A.** RCP2.6 using model M19; **B.** RCP4.5 using model M8; **C.** RCP6.0 using model M18; **D.** RCP8.5 using model M8

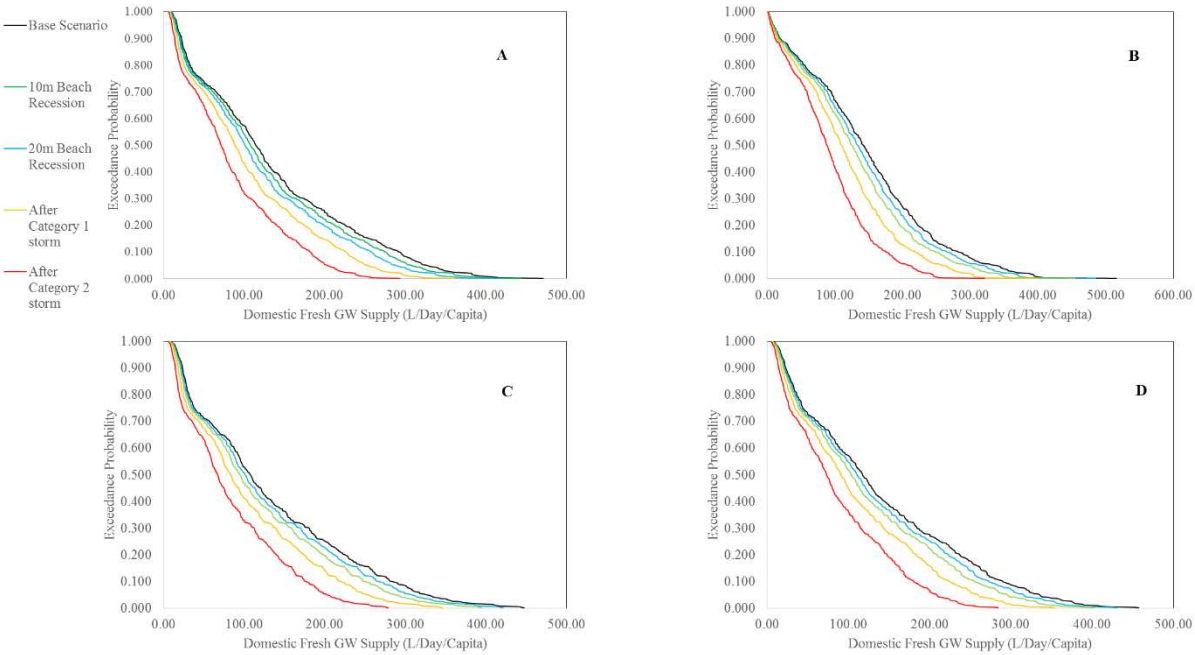

Figure A21 Exceedance probability distribution for monthly groundwater supply average in N. Velidhoo Island under 3rd ranked GCMs in different climatic RCPs forecasts; **A.** RCP2.6 using model M4; **B.** RCP4.5 using model M18; **C.** RCP6.0 using model M4; **D.** RCP8.5 using model M4

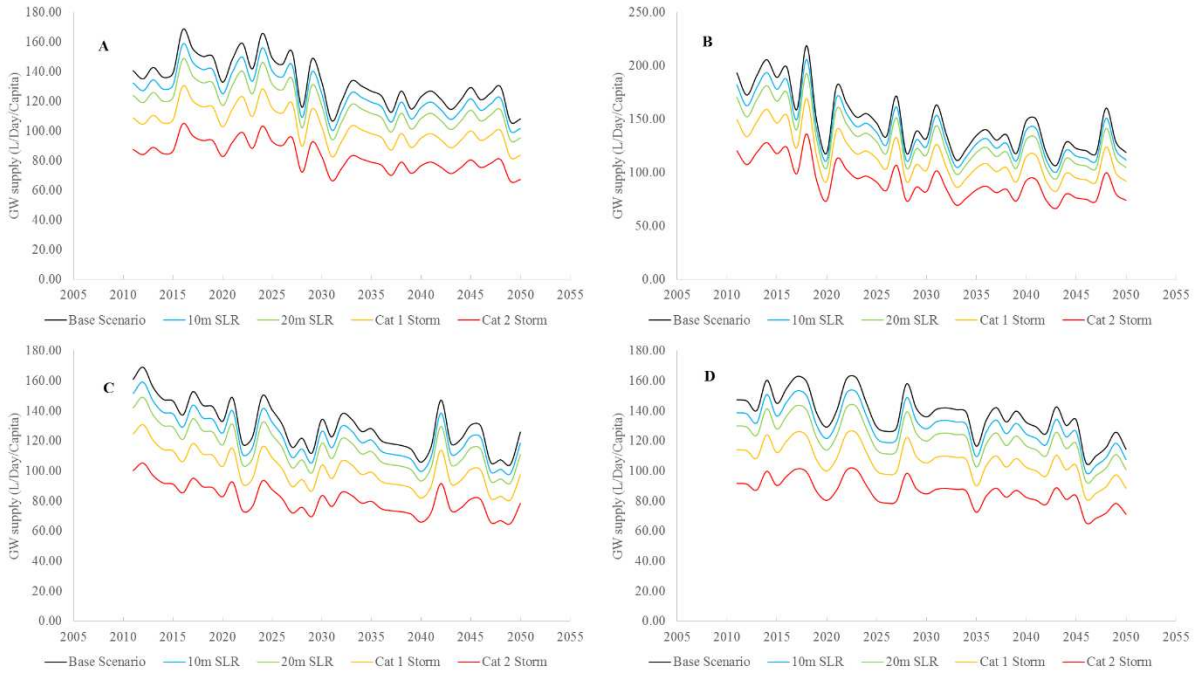

Figure A22 Average annual groundwater supply in N. Velidhoo Island under 3rd ranked GCMs in different climatic RCPs forecasts; **A.** RCP2.6 using model M4; **B.** RCP4.5 using model M18; **C.** RCP6.0 using model M4; **D.** RCP8.5 using model M4

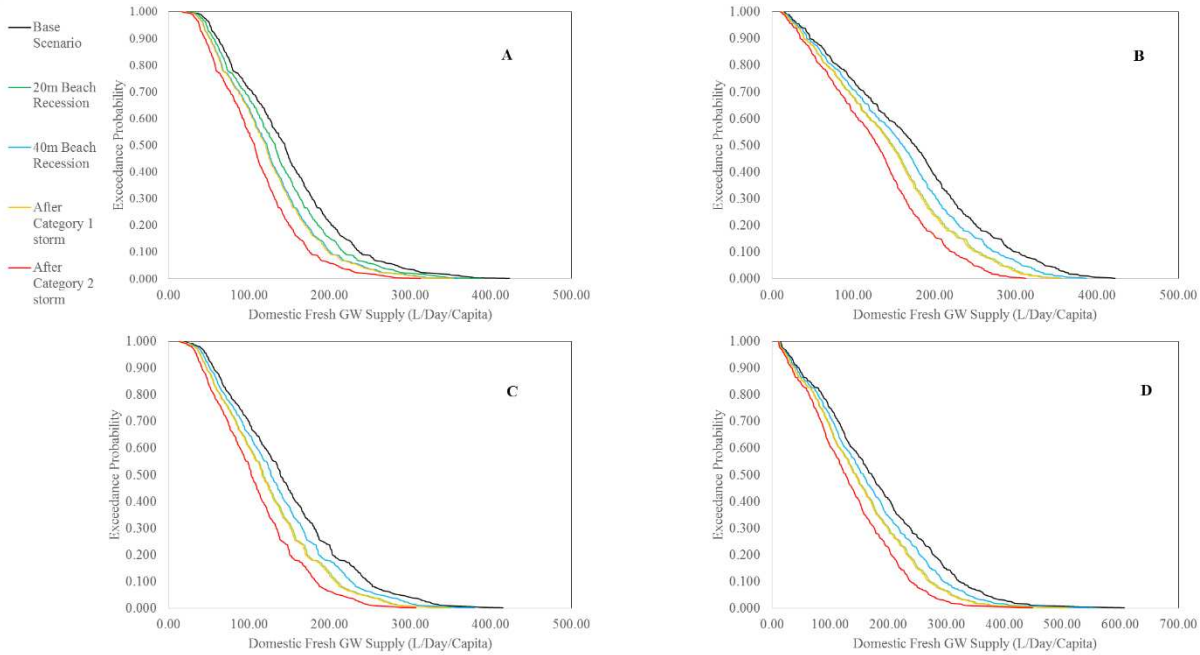

Figure A23 Exceedance probability distribution for monthly groundwater supply average in GDh. Thinadhoo Island under 2nd ranked GCMs in different climatic RCPs forecasts; **A.** RCP2.6 using model M19; **B.** RCP4.5 using model M12; **C.** RCP6.0 using model M19; **D.** RCP8.5 using model M7

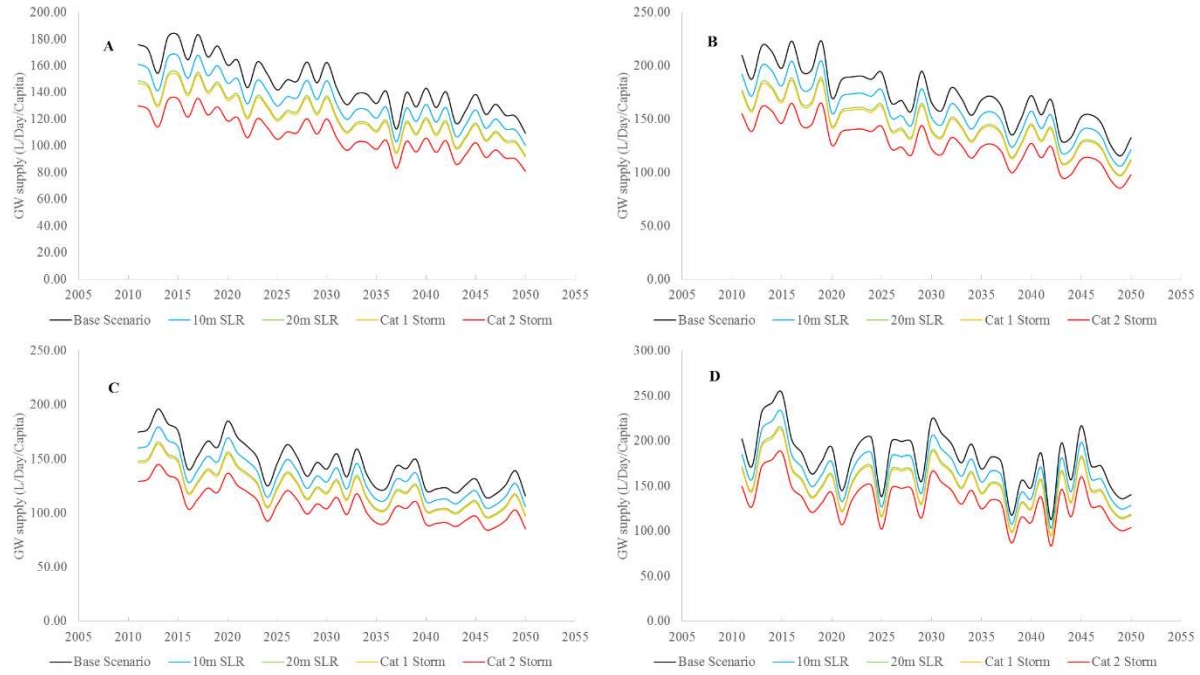

Figure A24 Average annual groundwater supply in GDh. Thinadhoo Island under 2nd ranked GCMs in different climatic RCPs forecasts; **A.** RCP2.6 using model M19; **B.** RCP4.5 using model M12; **C.** RCP6.0 using model M19; **D.** RCP8.5 using model M7

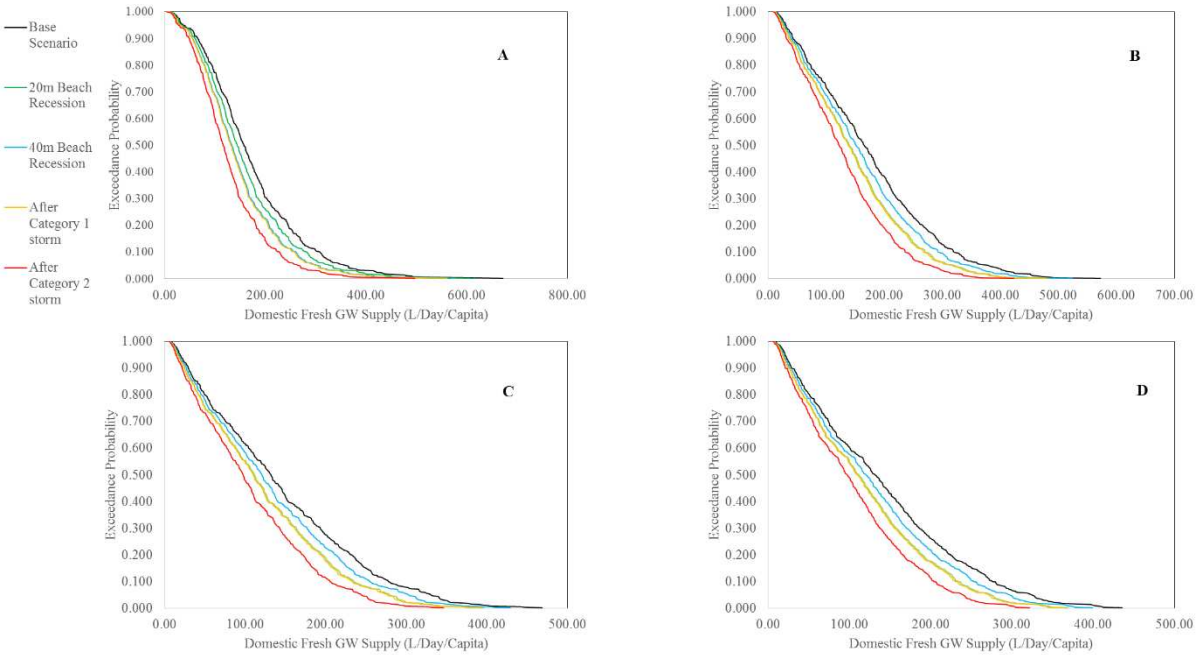

Figure A25 Exceedance probability distribution for monthly groundwater supply average in GDh. Thinadhoo Island under 3rd ranked GCMs in different climatic RCPs forecasts; **A.** RCP2.6 using model M3; **B.** RCP4.5 using model M7; **C.** RCP6.0 using model M2; **D.** RCP8.5 using model M2

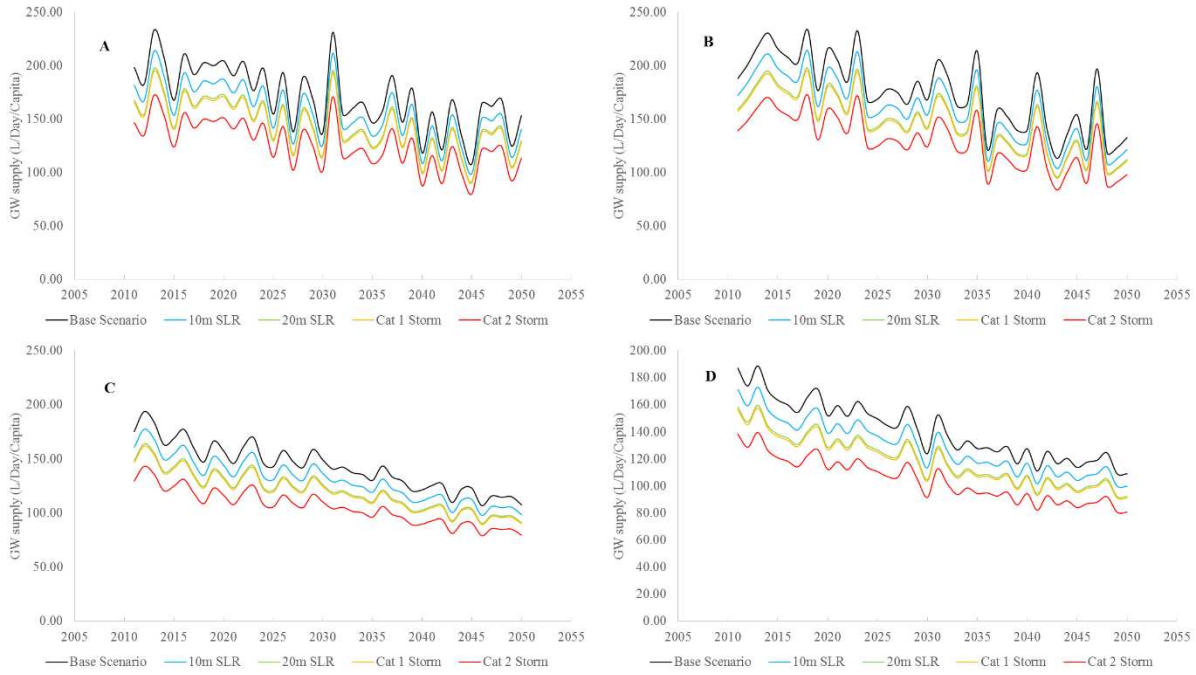

Figure A26 Average annual groundwater supply in GDh. Thinadhoo Island under 3rd ranked GCMs in different climatic RCPs forecasts; **A.** RCP2.6 using model M3; **B.** RCP4.5 using model M7; **C.** RCP6.0 using model M2; **D.** RCP8.5 using model M2

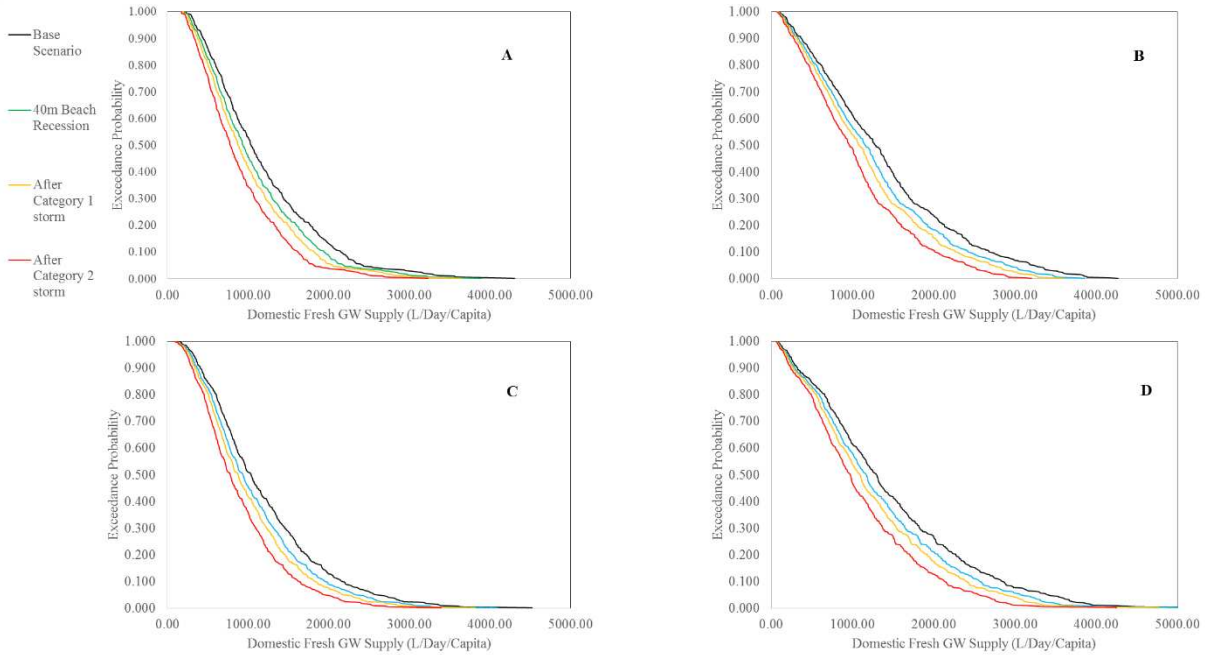

Figure A25 Exceedance probability distribution for monthly groundwater supply average in L. Gan Island under 2nd ranked GCMs in different climatic RCPs forecasts; **A.** RCP2.6 using model M19; **B.** RCP4.5 using model M12; **C.** RCP6.0 using model M19; **D.** RCP8.5 using model M7

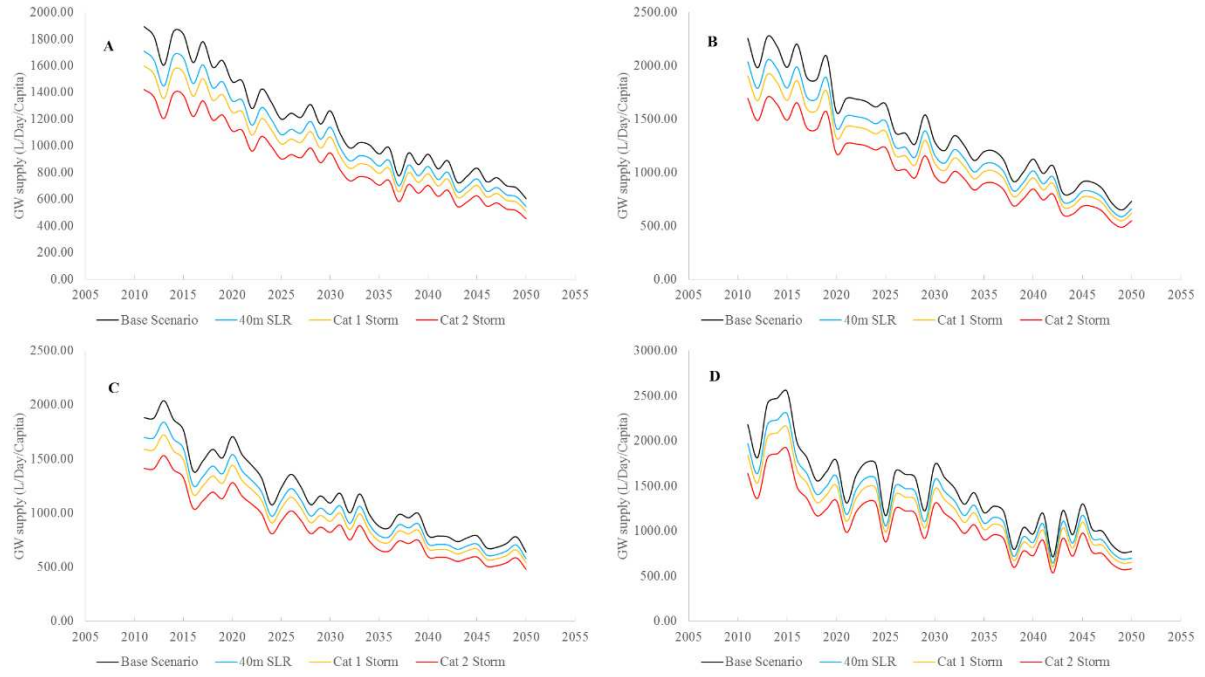

Figure A26 Average annual groundwater supply in L. Gan Island under 2nd ranked GCMs in different climatic RCPs forecasts; **A.** RCP2.6 using model M19; **B.** RCP4.5 using model M12; **C.** RCP6.0 using model M19; **D.** RCP8.5 using model M7

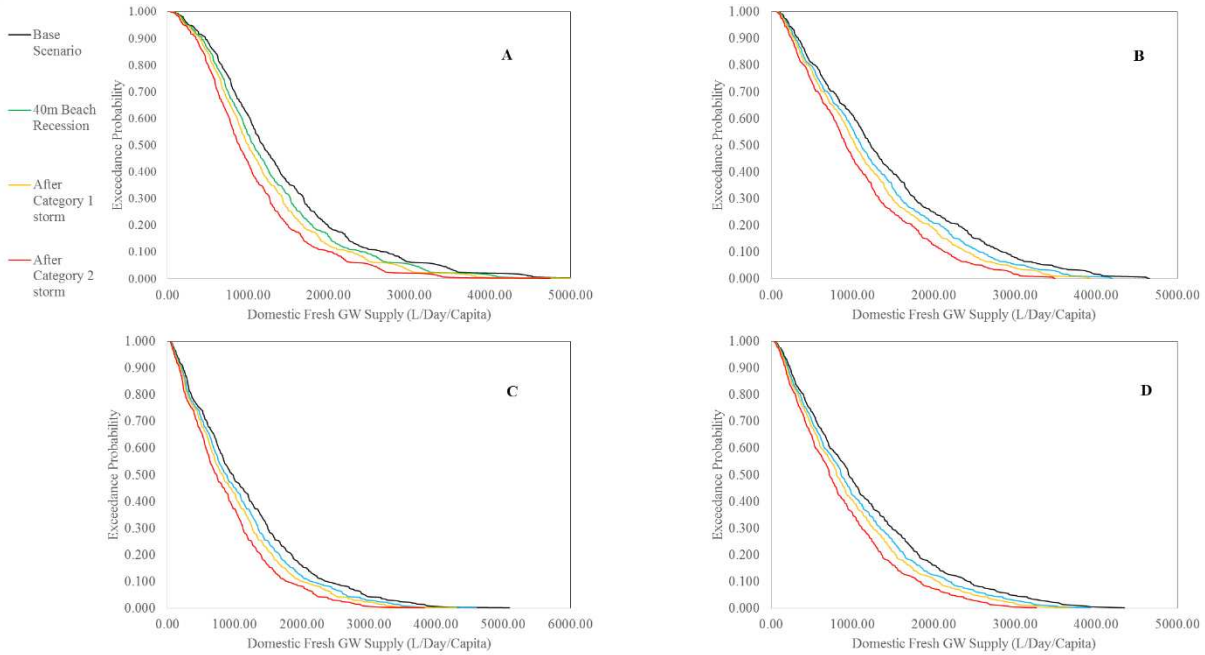

Figure A27 Exceedance probability distribution for monthly groundwater supply average in L. Gan Island under 3rd ranked GCMs in different climatic RCPs forecasts; **A.** RCP2.6 using model M3; **B.** RCP4.5 using model M7; **C.** RCP6.0 using model M2; **D.** RCP8.5 using model M2

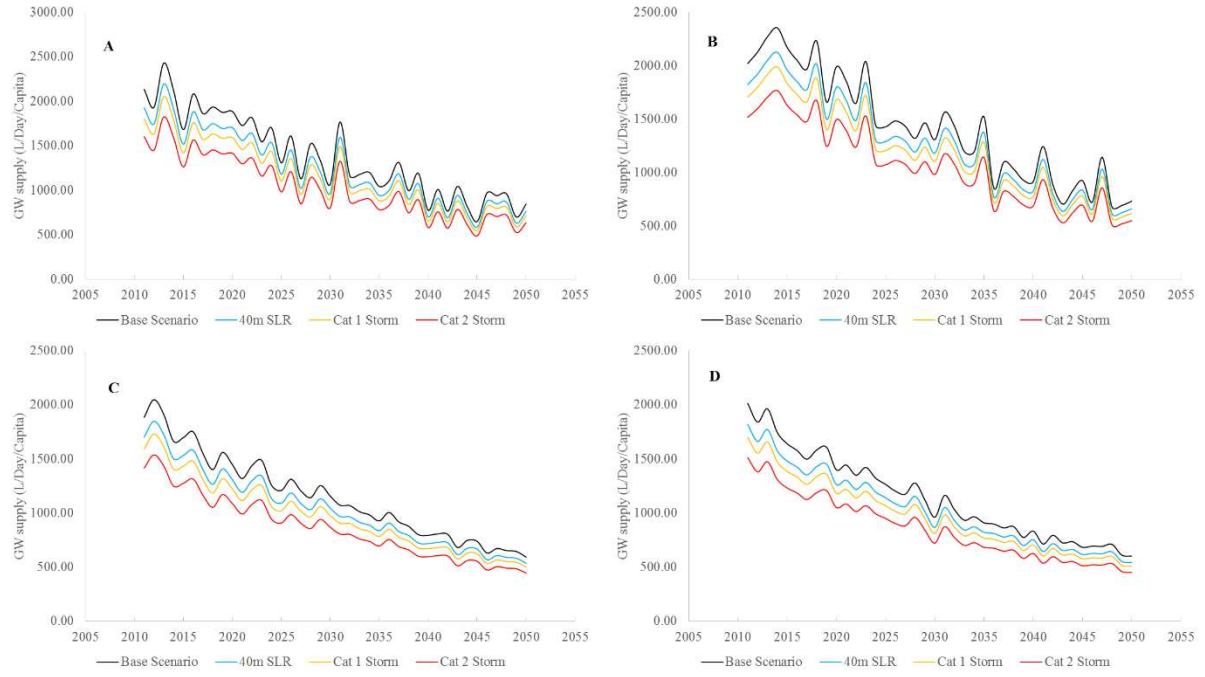

Figure A28 Average annual groundwater supply in L. Gan Island under 3rd ranked GCMs in different climatic RCPs forecasts; **A.** RCP2.6 using model M3; **B.** RCP4.5 using model M7; **C.** RCP6.0 using model M2; **D.** RCP8.5 using model M2